©Copyright 2015

Nicolette A Zhou

Trace organic contaminant degradation by isolated bacteria bioaugmented into lab-scale reactors and identification of associated degradation genes

Nicolette A Zhou

A dissertation
submitted in partial fulfillment of the
requirements for the degree of

Doctor of Philosophy

University of Washington
2015

Reading Committee:
Heidi L. Gough, Chair
H. David Stensel
David A. Stahl

Program Authorized to Offer Degree:
Civil and Environmental Engineering

University of Washington

Abstract

Trace organic contaminant degradation by isolated bacteria bioaugmented into lab-scale reactors and identification of associated degradation genes

Nicolette A Zhou

Chair of the Supervisory Committee:
Professor Heidi L. Gough
Department of Civil and Environmental Engineering

Abstract text

Discharge of trace organic contaminants (TOrCs) with wastewater treatment plant (WWTP) effluents is a surface water quality concern due to their potentially negative effects on aquatic life. TOrCs are currently partially removed during wastewater treatment, though new technologies will be needed if increasingly lower discharge levels are to be achieved. Additionally, removal of TOrCs by sorption to solids is not desirable due to societal concerns about their presence in biosolids has increased substantially in recent years. TOrCs are biologically removed during wastewater treatment and complete mineralization of TOrCs is possible. Therefore, this study hypothesized that Enhanced Biological Trace Organic Contaminant Removal (EBTCR) can be achieved through continuous bioaugmentation with TOrC-degrading bacteria.

Eleven bacteria capable of degrading various TOrCs were isolated from activated sludge, including the first isolated bacteria known to degrade gemfibrozil. The bacteria were characterized for their ability to function under conditions that might be encountered during bioaugmentation in a WWTP. Eight of the isolated bacteria were capable of degrading the TOrCs to below concentrations thought to cause adverse environmental impacts (i.e. low ng/L concentrations). The bacteria grew on a variety different carbon sources, with most bacteria growing best on protein-rich substrates. This suggests that commonly

available materials could be used to grow the bacteria on-site at a WWTP. The bacteria maintained their ability to degrade the contaminant after being grown in the absence of the TOrC, as would be necessary when implementing continuous bioaugmentation at full-scale WWTPs. Eight of bacteria also degraded their TOrC before measurable growth, or during early growth of the bacteria in a nutrient-rich media. This was important because during continuous bioaugmentation the bacteria will bioaugmented in the activated sludge portion of a wastewater treatment, which has many carbon sources at much higher concentrations than the TOrC. Finally, seven of the isolated bacteria were determined to degrade the TOrCs at a rate that predicted potential for improved contaminant removal without increasing the activated sludge biomass by more than 10%.

Continuous bioaugmentation of five bacteria was modeled in two full-scale activated sludge processes, a completely mixed activated sludge (CMAS) process and a 4-stage activated sludge process. The model found that continuous bioaugmentation for EBTCR was a potential solution for all but one of the modeled bacteria in the 4-stage activated sludge process, and was not feasible for a CMAS except with bioaugmentation of one of the isolated bacteria. Next, continuous bioaugmentation for EBTCR was tested in lab-scale sequencing batch reactors with an isolated BPA-degrading bacterium, *Sphingobium* sp. BiD32. This study found that daily bioaugmentation improved the BPA degradation rates, concentrations in the effluent, and concentrations in the waste solids. This study also found that the enhanced BPA removal was lost with time from bioaugmentation, demonstrating that continuous bioaugmentation can be used to overcome bacterial losses as a way to maintain predictably low TOrCs effluent concentrations.

As a part of this study, proteins were identified that are likely involved in the degradation of TOrCs by isolated bacteria. Identification of these proteins and genes can assist in bioaugmentation monitoring by allowing for the production of biomarkers to monitor degradation genes in WWTPs rather than the augmented bacteria specifically. Also, if the gene is known, it can be searched for in other bacteria as a way to identify other similar bacteria capable of degrading TOrCs more rapidly than through the enrichment process. Using genomics, proteomics, and metabolomics, a novel *p*-hydroxybenzoate hydroxylase enzyme and genes previously identified to be involved in protocatechuate degradation were hypothesized to be involved in BPA degradation by *Sphingobium* sp. BiD32. These methods were also used to identify proteins involved in 17β-estradiol (E2) degradation by *Rhodococcus* sp. EsD8, confirming the involvement of proteins related to 3-beta-hydroxysteroid dehydrogenase and estradiol 17beta-dehydrogenase. These findings have identified genes involved in BPA and E2 degradation, which will allow for the creation of qPCR primers to monitor these genes in future studies.

This study demonstrated the potential of continuous bioaugmentation to achieve EBTCR. Bioaugmentation may also be applicable for a variety of other waste streams, including hospital waste, pharmaceutical manufacturing waste, landfill leachate, and prior to reverse osmosis for direct potable reuse. Future work should focus improving the bioaugmentation process. This includes continuous bioaugmentation studies at the pilot-scale with automated bioaugmentation and a continuously stirred tank reactor design instead of a sequencing batch reactor. This will help demonstrate its applicability to full-scale systems. TOrC degradation genes should also be confirmed and used to monitor bacteria augmented into the pilot-scale system. This will allow for monitoring of the TOrC degradation activity, instead of just the bacterial signature. This study identified seven bacteria meeting the bioaugmentation criteria and demonstrated improved TOrCs removal with bioaugmentation.

ACKNOWLEDGEMENTS

First and foremost, I would like to thank my advisor and mentor Heidi Gough for all her support and guidance. You have taught me how to prioritize, be patient, and properly celebrate manuscript acceptations. Thank you for teaching me how to be a better mentor by being a wonderful one. Thank you so much for all of the time and dedication you have put into my education and for making my PhD an enjoyable and productive time.

I would also like to thank John Ferguson for his mentorship and guidance. I am very grateful that I had the opportunity to work with John and that he introduced me to the wonderful world of microbes. I miss him greatly.

To Jeppe Nielsen and Henrik Kjeldal, thank you for welcoming me to Denmark and helping me to have an extremely productive and fun time.

I would also like to thank my PhD committee, David Stensel, David Stahl, and Michael MacCoss, for their time and valuable input throughout this process.

To John Smyth, Bob Bucher, and Pardi Sukapanpotharam, I have greatly appreciated your interest and input over the years. Without it this work would not be where it is today. I am so grateful to have worked with you, advanced this research, and grown as a researcher.

To Kathryn DeBennedetto, Emily Johanning, and Charlton Callender, thank you for helping me become a better mentor, keeping me sane while running reactors, and making lab a brighter place. I miss you all in lab and wish you the best in your future careers.

Thanks to Sean Yeung for all your assistance with finicky instruments and making the lab run smoothly.

Thank you to all my office mates and lab mates throughout the years for your support and laughter. In no particular order: April Lutovsky, Andy Karch, Christa Fagnant, Jenna Forsyth, Songlin Wang, Kyle Shimabuku, Ryan Ziels, Mariko Lust, Bryce Figdore, Tess Young, Lu Fan, James Liu, Yuan Gao, Zhenxiao Cai, Stephany Wei, Bo Li, Lara Pracht, Wei Qin, Nick Waldo, I-Chieh Chien, Ching-Yu Peng, Huan He, Siamak Modarresi, Pepe Mendez, Heidi Danielsen, Marta Nierychlo, Freya Mosbæk, and Vibeke Rudkjøbing.

Finally, I would like to thank my family and friends for all their love, support, and understanding throughout this long process. I would like to thank UW, for introducing me to my husband Peiran Zhou. To Peiran Zhou, thank you for all your support while going through the same process yourself, always being there to bounce ideas off of, and calming me when my bacteria don't cooperate. You have made these last 5 years an adventure and I look forward to many more in the decades to come. To my furry kids Cooper and R2-D2, thank you for all the licks and unconditional love. I also appreciate all of the support from my parents Jon and Lisa Corbin, my sister Joni Corbin, my grandparents Delores Corbin and Stan and Gloria Thorsteinson, and my friends Fahad Pervaiz, Xuezhe Zhou, Cissy Chen, Huy Hong Ta, and Courtney Culbert.

TABLE OF CONTENTS

Acknowledgements i
Table of Contents iii
List of Figures viii
List of Tables x
CHAPTER 1: Introduction 1
CHAPTER 2: Background 3
2.1 Overview of trace organic contaminants studied 3
2.2 Trace organic contaminants in surface waters 4
2.3 Trace organic contaminants in wastewater treatment plants 6
2.3.1 Sources and influent concentration of trace organic contaminants in wastewater treatment plants 6
2.3.2 Fate in wastewater treatment plants 6
2.4 Bioaugmentation as an option to improve trace organic contaminant removal in wastewater treatment plants 8
2.4.1 Previously documented bacteria that degrade trace organic contaminants 8
2.4.2 Early bioaugmentation studies 11
2.5 Trace organic contaminant degradation pathways and associated enzymes and genes 14
2.5.1 Trace organic contaminant biological degradation pathways 14
2.5.2 Potential for biomarker genes 18
2.5.3 Proteomics methods used to identify proteins involved trace organic contaminant degradation 19
CHAPTER 3: Research Hypotheses 20
CHAPTER 4: Cultivation and characterization of bacterial isolates capable of degrading pharmaceutical and personal care products for improved removal in activated sludge wastewater treatment 22
4.1 Chapter summary 22
4.2 Abstract 23
4.3 Introduction 23
4.4 Materials and methods 25
4.4.1 Inocula source 25
4.4.2 Reagents and chemicals 25
4.4.3 Cultivation/culture media 26
4.4.3.1 Liquid media 26
4.4.3.2 Solid media 26
4.4.4 DNA sequencing and phylogeny 26
4.4.5 High pressure liquid chromatography quantification including solid phase extraction and concentration 27
4.4.6 Measure of microbial growth 28
4.4.7 Experimental methods 29
4.4.7.1 Degradation of non-target PPCPs (Experiment 1) 29
4.4.7.2 Degradation to low residual concentrations (Experiment 2) 29
4.4.7.3 Substrate range testing (Experiment 3) 29
4.4.7.4 Growth and degradation in carbon-rich media (Experiment 4) 30
4.4.8 First order growth kinetics 30
4.4.9 First order degradation kinetics 30
4.5 Results 31
4.5.1 Cultivation of bacteria capable of degrading specific PPCPs 31
4.5.2 Description of bacterial isolates 32
4.5.3 Degradation to low ng/L concentrations 35

4.5.4 Growth and degradation in presence of other carbon sources 36
4.6 Discussion 38
4.7 Acknowledgements 41
4.8 Online Resource (Supplementary Information) 42
4.8.1 Materials and Methods 44
4.8.1.1 Reagents and chemicals 44
4.8.1.2 HPLC quantification including solid phase extraction and concentration 45
CHAPTER 5: Kinetics modeling predicts bioaugmentation with Sphingomonad cultures as a viable technology for enhanced pharmaceutical and personal care products removal during wastewater treatment 54
5.1 Chapter summary 54
5.2 Abstract 56
5.3 Introduction 56
5.4 Materials and methods 57
5.4.1 Reagents and chemicals 57
5.4.2 Culture media 58
5.4.3 High pressure liquid chromatography quantification 58
5.4.4 Sources of activated sludge 58
5.4.5 Sorption partitioning coefficients 59
5.4.6 Pure culture degradation kinetics 59
5.4.7 Activated sludge degradation kinetics 60
5.4.8 Modeled continuous bioaugmentation in continuously stirred tank reactors 60
5.4.9 Statistical analyses 63
5.5 Results and discussion 64
5.5.1 Degradation kinetics and sorption coefficients 64
5.5.1.1 Sorption partitioning coefficients 64
5.5.1.2 Pure culture degradation kinetics 65
5.5.1.3 Activated sludge bioaugmentation trials 68
5.5.1.4 Implications of culture work and bioaugmentation tests 70
5.5.2 Modeled full-scale bioaugmentation 71
5.5.2.1 Theoretical bioaugmentation doses 71
5.5.2.2 Influence of activated sludge operating conditions on bioaugmentation modeling 73
5.6 Conclusions 75
5.7 Acknowledgments 75
5.8 Electronic supplementary material 76
CHAPTER 6: Enhanced biological trace organic contaminant removal (EBTCR) during wastewater treatment: a lab scale demonstration with the bisphenol A-degrading bacteria *Sphingobium* sp. BiD32 86
6.1 Chapter summary 86
6.2 Abstract 87
6.3 Introduction 87
6.4 Materials and methods 89
6.4.1 Laboratory reactor set-up 89
6.4.2 Bioaugmentation 90
6.4.3 BPA degradation kinetics testing 91
6.4.4 qPCR 92
6.4.5 Net loss of augmented bacteria 94
6.4.6 Full-scale activated sludge process model 94
6.4.7 Cost estimation for bioaugmentation 95
6.4.8 Induction of BPA degradation 96
6.4.9 Statistical analyses 96

6.5 Results 96
6.5.1 Laboratory reactor operation 96
6.5.2 BPA removal 99
6.5.3 Fate of BPA in the reactors 102
6.5.4 Fate of augmented bacteria under reactor conditions 103
6.5.5 Incorporating calculated biomass loss into the full-scale activated sludge process model 104
6.5.6 Cost estimation for bioaugmentation 104
6.5.7 Induction of BPA degradation 105
6.6 Discussion 105
6.7 Conclusions 108
6.8 Acknowledgements 108
6.9 Supplementary Information 109
CHAPTER 7: Identification of putative genes involved in bisphenol a degradation using differential protein abundance analysis of *Sphingobium* sp. BiD32 118
7.1 Chapter summary 118
7.2 Abstract 119
7.3 Introduction 119
7.4 Materials and methods 120
7.4.1 Chemicals, reagents, and bacterial strain 120
7.4.2 Library preparation, genome sequencing, assembly, and analysis 120
7.4.3 Sample preparation for proteomic analysis 121
7.4.4 LC-MS/MS analyses for proteomics 122
7.4.5 Label-free quantification 122
7.4.6 Functional annotation of proteins 123
7.4.7 Pathway prediction of BPA 123
7.4.8 Sample preparation for metabolomics 123
7.4.9 LC-MS/MS analyses for metabolomics 124
7.5 Results 124
7.5.1 Whole genome sequencing 124
7.5.2 Label-free quantitative MS-based proteomics of *Sphingobium* sp. BiD32 124
7.5.3 Functional annotation of proteins 125
7.5.4 Metabolite identification 131
7.5.5 Catabolic pathway of bisphenol A 131
7.6 Discussion 134
7.7 Acknowledgements 136
7.8 Supporting information 137
7.8.1 Library preparation and genome sequencing 137
7.8.2 Protein extraction 137
7.8.3 In-solution digestion 137
7.8.4 LC/MS analyses for metabolomics 138
CHAPTER 8: Differential protein abundance during 17β-estradiol degradation by *Rhodococcus* sp. EsD8 150
8.1 Chapter summary 150
8.2 Abstract 151
8.3 Introduction 151
8.4 Materials and methods 153
8.4.1 Chemicals, reagents, and bacterial strain 153
8.4.2 Library preparation, genome sequencing, assembly, and analysis 153
8.4.3 Sample preparation for proteomic analysis 153
8.4.4 LC-MS//MS analyses for proteomics 155
8.4.5 Label-free quantification 155

8.4.6 Functional annotation of proteins 156
8.4.7 Pathway prediction of E2 156
8.4.8 Sample preparation for metabolomics 156
8.4.9 LC-MS/MS analyses for metabolomics 156
8.5 Results and discussion 157
8.5.1 Whole genome sequencing 157
8.5.2 Metabolite identification 157
8.5.3 Label-free quantitative MS-based proteomics of *Rhodococcus* sp. EsD8 158
8.5.4 Functional annotation of proteins 159
8.5.5 E2 transformation and associated degradation genes 161
8.6 Conclusions 165
8.7 Acknowledgements 165
8.8 Supplementary Information 166
CHAPTER 9: Conclusions 187
Appendix A: Persistence of *Sphingobium* sp. BiD32 bioaugmented in laboratory reactors A1
10.1 Chapter summary A1
10.2 Introduction A2
10.3 Materials and methods A3
10.3.1 Laboratory reactor operation A3
10.3.2 Bacterial concentrations A3
10.3.3 Kinetics of augmented bacteria A5
10.3.4 Prediction of *Sphingobium* sp. BiD32 and BPA concentrations in reactors A6
10.3.5 Disruption of flocs A6
10.3.6 FISH A7
10.4 Results and discussion A8
10.4.1 Persistence of *Sphingobium* sp. BiD32 in lab scale reactors A8
10.4.2 Predicted *Sphingobium* sp. BiD32 and BPA concentrations in reactors A10
10.4.3 Disruption of flocs A12
10.4.4 FISH method development for visualizing flocs A13
10.5 Conclusions A14
10.6 Supplementary Information A15
Appendix B: Proteomic and metabolomic analysis reveals insight into the degradation of gemfibrozil by *Bacillus* sp. GeD10 B1
11.1 Chapter summary B1
11.2 Abstract B2
11.3 Introduction B2
11.4 Materials and methods B4
11.4.1 Chemicals, reagents, and bacterial strain B4
11.4.2 Library preparation, genome sequencing, assembly, and analysis B4
11.4.3 Sample preparation for proteomic analysis B4
11.4.4 In-gel digestion B5
11.4.5 LC-MS/MS analyses for proteomics B5
11.4.6 Data analysis B6
11.4.7 Functional annotation of proteins B6
11.4.8 Aerobic pathway prediction of gemfibrozil B6
11.4.9 Sample preparation for metabolite identification B7
11.4.10LC/MS analyses for metabolite identification B7
11.5 Results B7
11.5.1 Genome sequencing B7
11.5.2 Cell cultures for MS-based proteomics analysis B8
11.5.3 Label-free quantitative MS-based proteomics of *Bacillus* sp. GeD10 B9

11.5.4 Functional annotation of proteins B9
11.5.5 Proteins related to xenobiotic degradation B10
11.5.6 Metabolite identification B11
11.5.7 Catabolic pathway of gemfibrozil B16
11.6 Discussion B17
11.7 Conclusion B20
11.8 Acknowledgements B21
Appendix C: Growth of *Sphingobium* sp. BiD32 on bisphenol A C1
12.1 Chapter summary C1
12.2 Objective C2
12.3 Materials and methods C2
12.3.1 Chemicals, reagents, and bacterial strain C2
12.3.2 Experimental media C2
12.3.3 Experimental method C3
12.4 Results and conclusions C3

LIST OF FIGURES

Figure 2.1. Proposed triclosan degradation pathway by *Sphingopyxis* sp. KCY1. 15
Figure 2.2. Proposed BPA degradation pathways by *Sphingomonas* sp. MV1, *Sphingomonas* sp. AO1, and *Sphingomonas* sp. TTNP3 and unidentified strain WH1. 16
Figure 2.3. Proposed ibuprofen degradation pathway by *Sphingomonas* sp. Ibu-2. 17
Figure 2.4. Proposed E2 degradation pathway by *S. maltophilia* ZL1. 18
Figure 4.1. Enrichment and isolation process. 31
Figure 4.2. Phylogenetic relationship of the 16S rRNA gene of BiD10, BiD32, TrD22, TrD23, TrD34, TrD1, and IbD51 compared to the sphingomonads. 34
Figure 4.3. Growth of (a) BiD32 during the degradation of bisphenol A and (b) GeD10 during the degradation of gemfibrozil. 38
Figure 4.4. Growth of bacterial isolates during degradation of compound in carbon-rich media. Degradation of bisphenol A by (a) BiD10. Degradation of triclosan by (b) TrD22, (c) TrD23, (d) TrD34, and (e) TrD1. Degradation of ibuprofen by (f) IbD51. Degradation of 17β-estradiol (E2) by (g) EsD8, (h) EsD18, and (i) EsD20. 49
Figure 4.5. Growth of (a) BiD10, (b) BiD32, (c) TrD22, (d) TrD23, (e) TrD34, (f) TrD1, (g) IbD51, (h) EsD8, (i) EsD18, (j) EsD20, and (k) GeD10 on carbon-rich media linearized. 51
Figure 4.6. Degradation of PPCP by (a) BiD10, (b) BiD32, (c) TrD22, (d) TrD23, (e) TrD34, (f) TrD1, (g) IbD51, (h) EsD8, (i) EsD18, (j) EsD20, and (k) GeD10 in carbon-rich media linearized. 53
Figure 5.1. Reactor schematic used to model feasibility of bioaugmentation using experimentally determined degradation kinetics and sorption coefficients. 61
Figure 5.2. Comparison of partitioning for triclosan and BPA as a function of volatile suspended solids (VSS). 64
Figure 5.3. Degradation of pharmaceutical and personal care products. 66
Figure 5.4. Degradation of triclosan or BPA by bacteria augmented to activated sludge. 69
Figure 5.5. Modeling results showing the fate of triclosan and bisphenol A comparing standard treatment to bioaugmentation. 73
Figure 5.6. Effect of a) activated sludge volatile suspended solids (VSS), b) SRT, and c) level of contaminant removal on predicted bioaugmentation dose. 74
Figure 5.7. Degradation and observed sorption coefficients (log K_P) 80
Figure 5.8. Solution to Eq 2 for calculating the degradation rate and lag by a) TrD23, b) TrD1, c) BiD32 (high bisphenol A concentrations), and d) BiD32 (low bisphenol A concentrations) in mineral or minimal media. 81
Figure 5.9. Application of Eq 5.2 to (a, d) activated sludge and (b, c, e, f, g) bioaugmented activated sludge. 83
Figure 6.1. Lab scale sequencing batch reactor cycle operation. 90
Figure 6.2. BPA degradation in the reactors with an initial BPA concentration of approximately 100 µg/L after spiking during the bioaugmentation cycle (cycle 1, squares, n=5), cycle 2 (diamonds, n=3), and cycle 8 (triangles, n=2) in the test reactor and throughout the day in the control reactor (closed circles, n=13) during Phase I (8-day SRT). 101
Figure 6.3. BPA degradation in sequencing batch reactors with an initial BPA concentration of approximately 10 µg/L during operation at (a) an 8-day and (b) a 3-day SRT. 101
Figure 6.4. Total BPA degradation rates in the test reactor (white bars) and control reactor (patterned bars) a) with an initial BPA concentration of 100 µg/L and an 8-day SRT, and b) with an initial BPA concentration of 10 µg/L BPA and an 8-day and 3-day SRT. 102
Figure 6.5. The fate of BPA (~10 µg/L initial concentration) during cycle 1 for Phase I-b (8-day SRT) and Phase II (3-day SRT). 103
Figure 6.6. Natural log of *Sphingobium* sp. BiD32 16S rRNA gene in waste solids vs. time from 8-day SRT reactors. 103
Figure 6.7. Bisphenol A removal in cultures inoculated with bisphenol A pretreated *Sphingobium* sp. BiD32 (open squares) and control (non-pretreated) *Sphingobium* sp. BiD32 (closed circles). 105

Figure 6.8. Overview of bisphenol A additions (bars) and Sphingobium sp. BiD32 augmentation (arrows). 110
Figure 7.1. Growth and harvesting of *Sphingobium* sp. BiD32 for differential proteomics analysis. 122
Figure 7.2. Volcano plot of a) cytosolic and b) membrane quantified proteins. 125
Figure 7.3. Gene organization of the proposed protocatechuate operons (proCBAJ and proRKUI) and close proximity genes on contig 143 (CAVK010000143.1) of *Sphingobium* sp. BiD32.. 130
Figure 7.4. Proposed pathway for BPA degradation by *Sphingobium* sp. BiD32 based on measured metabolites (bold) and metabolites and proteins predicted to be involved in BPA degradation by the EAWAG Biocatalysis/Biodegradation Pathway Prediction System (top panel). The degradation pathway of BPA metabolites (bottom panels) was proposed based upon previous findings (Kamimura et al. 2010b). 133
Figure 7.5. Phylogenetic relationship of *Sphingobium* sp. BiD32 proteins differentially expressed..... 149
Figure 8.1. Growth and harvesting of *Rhodococcus* sp. EsD8 for differential proteomics analysis. 155
Figure 8.2. Volcano plot of cytosolic quantified proteins. 158
Figure 8.3. Orthological assignment of upregulated (black bars) and downregulated (white bars) proteins of *Rhodococcus* sp. EsD8 in response to 17β-estradiol. 160
Figure 10.1. Log of *Sphingobium* sp. BiD32 16S rRNA gene concentrations in the bioaugmented reactor after bioaugmenting (cycle 1; closed squares) and at the end of the cycle prior to bioaugmentation (cycle 8; open circles) when operating at an 8-day SRT. A8
Figure 10.2. Log of *Sphingobium* sp. BiD32 16S rRNA gene concentrations versus time during cycle 1 after daily feeding of *Sphingobium* sp. BiD32 beginning on Day 1. ..... A9
Figure 10.3. *Sphingobium* sp. BiD32 16S rRNA gene concentrations at the end of cycle 8 on day 185 (n=5). A10
Figure 10.4. Natural log of *Sphingobium* sp. BiD32 16S rRNA gene versus time. A11
Figure 10.5. Comparison of predicted bacterial concentrations, and measured and predicted bisphenol A (BPA) removal.. ..... A11
Figure 10.6. Predators in reactor activated sludge. A12
Figure 10.7. Bisphenol A concentrations in untreated waste solids and blended waste solids from both the bioaugmented and control reactors, and during cycle 1 in the bioaugmented reactor (data from Figure 6.2). A13
Figure 10.8. Activated sludge floc from the test reactor using Bacterial FISH probes. A14
Figure 11.1. Workflow for the determination of expressed proteins during gemfibrozil degradation by *Bacillus* sp. GeD10. ..... B8
Figure 11.2. a) Degradation of gemfibrozil (squares) and growth of Bacillus sp. GeD10 in R2B medium in the absence (circles) and presence (triangles) of gemfibrozil. b) Volcano plot of quantified proteins.. B9
Figure 11.3. Proposed catabolic pathway for gemfibrozil by *Bacillus* sp. GeD10. ..... B17
Figure 12.1. Growth of *Sphingobium* sp. BiD32 on 10 mg/L bisphenol A in mineral media (open markers). C4

LIST OF TABLES

Table 2.1. Overview of studied trace organic contaminants 3
Table 2.2. Trace organic contaminants in surface waters and their effects on aquatic life 5
Table 2.3. Summary of trace organic contaminants in wastewater treatment plants 6
Table 2.4. Characterization of previously reported bacteria for their bioaugmentation potential 8
Table 4.1. Representative overview of the bacterial isolates that can degrade various pharmaceutical and personal care products 33
Table 4.2. Range of degradation ability 35
Table 4.3. Growth substrate range for bacterial isolates 36
Table 4.4. Degradation of pharmaceutical and personal care products during growth in R2A medium 38
Table 4.5. Residual concentrations achieved with newly reported bacterial isolates in comparison to previously reported levels 42
Table 4.6. Final concentrations in vitamin solution (Tanner 1997) 46
Table 4.7. PPCP quantification at mg/L, µg/L, and ng/L concentrations 47
Table 5.1. Base conditions used for continuously stirred tank reactor modeling. 62
Table 5.2. First order degradation rate constants determined in mineral media compared to R2A media. 67
Table 5.3. Degradation rates for triclosan and BPA by activated sludge and augmented bacteria. 69
Table 5.4. Predicted bioaugmentation dose and ratio of bioaugmented biomass in reactors to activated sludge biomass needed to obtain effluent concentration goal of 5 ng/L. 72
Table 5.5. Summary of HPLC methods 76
Table 5.6. Sorption coefficient (K_P) determination 77
Table 5.7. Predicted bioaugmentation dose and final concentrations in the reactor needed to obtain effluent concentration goal of 5 ng/L in a single CMAS 84
Table 5.8. Predicted bioaugmentation dose and final concentrations in the reactors needed to obtain effluent concentration goal of 5 ng/L in a 4-stage activated sludge process 85
Table 6.1. Primers used for PCR reactions 93
Table 6.2. Sequencing batch reactor operating conditions (20ºC) 98
Table 6.3. Bisphenol A (BPA) partitioning and removal in sequencing batch reactors (20ºC) 100
Table 6.4. Predicted *Sphingobium* sp. BiD32 bioaugmentation dose and ratio of bioaugmented biomass to activated sludge biomass needed to obtain effluent concentration goal of 5 ng/L 104
Table 6.5. Substrate cost per day in the full-scale activated sludge model 105
Table 6.6. qPCR cycling parameters for 16S rRNA gene concentration quantification 109
Table 7.1. *Sphingobium* sp. BiD32 whole genome assembly. 124
Table 7.2. *Sphingobium* sp. BiD32 proteomic analysis 125
Table 7.3. Proteins upregulated in response to BPA related to xenobiotic degradation and metabolism proteins 127
Table 7.4. Gene cluster containing the protocatechuate transformation genes encoding for proteins upregulated by more than 2-fold in response to bisphenol A and close proximity genes. 129
Table 7.5. BPA metabolites identified during BPA degradation by *Sphingobium* sp. BiD32. 131
Table 7.6. Summary of essential genes in *Sphingobium* sp. BiD32 139
Table 8.1. Identified E2 metabolites from E2 degradation by *Rhodococcus* sp. EsD8. 158
Table 8.2. Identification of proteins upregulated in *Rhodococcus* sp. EsD8 matching to enzymes predicted to be involved in the transformation of E2 to E1 from the EAWAG-BBD PPS in the enzyme classes 1.1.-.-., 1.14.13.- ., and 1.14.12.12. 164
Table 8.3. Summary of essential genes in *Rhodococcus* sp. EsD8 166
Table 10.1. Primers used for PCR reactions A4
Table 10.2. FISH probes for *Sphingobium* sp. BiD32 ..... A7
Table 10.3. Total bisphenol A degradation rates in untreated and blended waste solids A13
Table 11.1. Subset of proteins differentially expressed in response to gemfibrozil B13
Table 11.2. Subset of proteins with no change in expression in response to gemfibrozil B15

CHAPTER 1: INTRODUCTION

Trace organic contaminants (TOrCs) are an emerging concern in surfaces waters due to their potentially negative effects on aquatic life. These effects can include endocrine disruption, stunted growth, and increased mortality. TOrCs include industrial chemicals and by-products, pharmaceuticals, personal care products, hormones, detergents, and pesticides (Schwarzenbach et al. 2006). One source of TOrCs to surface waters is wastewater treatment plant (WWTP) effluent discharge. Current WWTP technologies remove a significant portion of these contaminants (Samaras et al. 2013), though new technologies will be needed if increasingly lower discharge levels are to be achieved. This study examines continuous bioaugmentation as a technological advancement for Enhanced Biological Trace Organic Contaminant Removal (EBTCR) during wastewater treatment. Biological methods have the potential for having lower material costs and requiring less energy than the physical or chemical removal counterparts. The approach is based on the observation that many TOrCs are partially destroyed biologically during the activated sludge process at WWTPs (Bester 2005; Heidler and Halden 2007), and that microbial degradation can result in full contaminant mineralization (Federle et al. 2002). To be practical for bioaugmentation, bacteria must be able to:

(1) remove the TOrCs to levels substantially below typical WWTP effluent concentrations (typically to ng/L concentrations),

(2) grow using common substrates while maintaining the ability to degrade the TOrC,

(3) degrade TOrCs in the presence of higher concentrations of other substrates, and

(4) degrade the TOrCs with degradation rates high enough to be able to reach low TOrC concentrations within a time and with a reactor configuration similar to biological treatment in WWTPs and with low bacteria dosages to activated sludge.

To assist in bioaugmentation monitoring, identification of TOrC degradation genes would be advantageous. This would allow for the production of a gene biomarker, so the degradation gene could be monitored in WWTPs rather than the bacteria specifically. Also, if the gene is known, it can be searched for in other bacteria as a way to identify other bacteria capable of degrading TOrCs more rapidly than through the enrichment process.

The overarching goal of this research is to decrease negative effects on aquatic life by TOrC by decreasing TOrC concentrations in WWTP effluents discharged to surface waters. The background for this work and the research hypotheses are summarized in Chapter 2 and 3, respectively. Chapter 4 discusses the isolation and characterization of eleven bacteria capable of degrading TOrCs and their potential for bioaugmentation. Chapter 5 demonstrates the potential for bioaugmentation to achieve EBTCR through modeling of full scale activated sludge processes. Chapter 6 demonstrates EBTCR in

lab-scale activated sludge reactors with bioaugmentation of a BPA-degrading bacterium. Chapter 7 and 8 document genomics, proteomics, and metabolomics during BPA and E2 degradation as a first step toward identifying genes involved with degradation that may serve as potential activity biomarkers. Overall conclusions and future work are discussed in Chapter 9. The appendices present work on the fate of augmented bacteria in lab-scale reactors and a collaborative study identifying proteins involved in gemfibrozil degradation by an isolated bacterium.

CHAPTER 2: BACKGROUND

2.1 Overview of trace organic contaminants studied

Triclosan, BPA, ibuprofen, E2, and gemfibrozil are described in Table 2.1. These compounds were chosen because they have similar chemical structures, they have range of sorption partitioning coefficients, they may have negative effects on aquatic life, and they are removed to varying degrees in WWTPs. Compounds with similar structures were chosen for ease of analytical methods. By using compounds with a range of sorption partitioning coefficients, effect of sorption on their removal during bioaugmentation can be explored. Finally, compounds with various removal efficiencies in WWTPs were chosen so that more readily degradable and recalcitrant compounds could be compared.

Table 2.1. Overview of studied trace organic contaminants

name and formula	chemical structure	$\log K_{OW}$	source/use
Triclosan $C_{12}H_7Cl_3O_2$	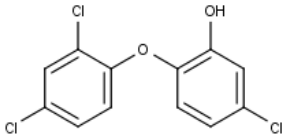	4.76 (Westerhoff et al. 2005)	Consumer product used in antibacterial soaps, toothpaste, deodorant, toys, surgical scrubs, etc. (Thompson et al. 2005)
Bisphenol A $C_{15}H_{16}O_2$	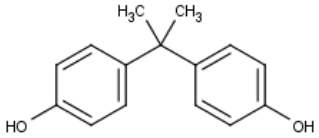	3.4 (Melcer and Klecka 2011a)	Industrial and consumer product used in polycarbonate plastics, epoxy resins, food packaging, etc. ("Bisphenol A (BPA) Action Plan Summary | Existing Chemicals | OPPT | US EPA" 2014)
Ibuprofen $C_{13}H_{18}O_2$	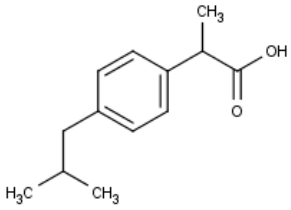	2.48 (Scheytt et al. 2005)	Pharmaceutical used to reduce fever and treat pain or inflammation. Is is a non-steriodal antiinflammatory drug ("Ibuprofen Uses, Dosage & Side Effects - Drugs.com" 2014).
17β-estradiol $C_{18}H_{24}O_2$	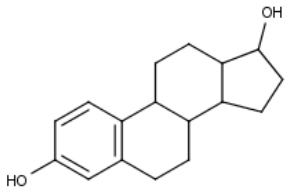	4.01 (Westerhoff et al. 2005)	Natural human hormone produced by females and at lower concentrations by males ("Estradiol - PubChem" 2014).
Gemfibrozil $C_{15}H_{22}O_3$	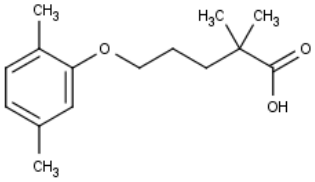	4.77 (Westerhoff et al. 2005)	Pharmaceutical used to treat hypertriglyceridemia and hypercholesterolemia. It is a lipid regulator (Jackevicius et al. 2011).

2.2 Trace organic contaminants in surface waters

TOrCs in surface waters can have a variety of negative effects on aquatic life. TOrCs enter surface waters through many sources including WWTP effluent discharge, industrial effluent discharge, runoff of biosolids from croplands, runoff of animal husbandry pharmaceuticals, and aquaculture (Daughton 2007). Some negative effects TOrCs have on aquatic life include endocrine disruption, increased mortality, and slowed development.

Endocrine disrupting compounds (EDCs) interfere with the endocrine system by mimicking a natural hormone, blocking the effects of a hormone from specific receptors, or stimulating or inhibiting the endocrine system directly ("What Are Endocrine Disruptors?| Endocrine Disruptor Screening Program | US EPA" 2014). Some common effects include increased vitellogenin production, production of intersex fish, and feminization of genetic males (Sumpter 2005). Vitellogenin is a yolk protein that is required at very high concentrations in female fish so they can grow ovaries with many yolky oocytes. It is barely detected, if at all, in males. However, with exposure to EDCs, vitellogenin production can be increased in males (Sumpter and Jobling 1995). Increased vitellogenin production can lead to intersex fish and feminization of fish. Generally, intersex fish are males with female oocytes. In some cases with exposure to high concentrations of WWTP effluents, genetically male fish gonads contain only oocytes, so they appear to be fully female (Sumpter 2005).

The five TOrCs studied in this research are all potential EDCs (Dann and Hontela 2011; Caliman and Gavrilescu 2009) and are present in surface waters at concentrations shown to have effects on aquatic life (Table 2.2). Triclosan has been shown to cause changes in the alga community structure at 120 ng/L (Wilson et al. 2003), decrease tadpoles activity at 230 ng/L (Fraker and Smith 2004), and cause earlier and higher rate of mortality of American Toad tadpoles at the maximum detected concentration of 2,300 ng/L (Smith and Burgett 2005). Triclosan also bioaccumulates in both algae and marine mammals (Fair et al. 2009; Coogan et al. 2007). BPA has also been shown to have effects on aquatic life at environmentally relevant concentrations. Gonad morphology of female *Gasterosteus aculeatus* was affected with an exposure of 1,000 ng/L BPA (de Kermoysan et al. 2013). The gonadosomatic index in male minnows increased with exposure to 5,000 ng/L BPA (Zhang et al. 2013). Exposure of medaka to 10,000 ng/L BPA resulted in some intersex fish (Metcalfe et al. 2001). Most effects on aquatic life by ibuprofen occurs at concentrations higher than have been detected in aquatic samples (Corcoran et al. 2010). However, changes in medaka reproduction patterns were seen at concentrations ranging from 1,000 to 100,000 ng/L. Increasing concentrations of ibuprofen caused medaka to spawn eggs less frequently and to spawn

more each time (Flippin et al. 2007). E2, which has been better studied than other TOrC compounds, can cause a variety of negative effects on aquatic life at concentrations commonly detected in waterways. For example, it causes vitellogenin induction in brown trout at 2 ng/L and effects their fertility at 10 ng/L (Burkhardt-Holm et al. 2008). It caused an increase in hepatic vitellogenin in male medaka at 55.7 ng/L (Kang et al. 2002), and at 100 ng/L E2 caused an increase in phenotypic female medaka resulting in many male medaka expressing intersex characteristics (Metcalfe et al. 2001). At the upper end of environmentally relevant concentrations (1,000 and 1,000,000 ng/L), gemfibrozil has been shown to effect aquatic life by inducing stress, damage, and reproduction biomarkers in marine mussels (Schmidt et al. 2011). There is evidence that gemfibrozil may be an EDC as it has been found to reduce testosterone levels in the goldfish, *Carassius auratus* (Bulloch et al. 2012; Mimeault et al. 2005). Also, its high partitioning coefficient causes it to be a concern due to bioaccumulation potential. It has been taken up and concentrated in goldfish at 1500 ng/L (Mimeault et al. 2005) and was detected in the livers of common carp and White sucker (Ramirez et al. 2009).

Table 2.2. Trace organic contaminants in surface waters and their effects on aquatic life

trace organic contaminant	frequency in surface waters tested (%)	median concentration (ng/L)	maximum concentration (ng/L)	lowest concentration with effect and observed effect (ng/L)
Triclosan	57.6[a]	0.4 - 1023[bc]	2,300[a]	120; alga community structure[d]
BPA	41.2[a]	2.1 - 881[bc]	12,000[a]	5,000; increase in GSI of male minnows[e]
Ibuprofen	9.5 - 12.5[af]	11.3 - 200[af]	1,000[a]	1,000; changes in medaka reproduction pattern[g]
E2	85[a]	1.1 - 160[ah]	200[a]	2; vitellogenin induction in brown trout[i]
Gemfibrozil	3.6[a]	1.9 - 48[aj]	1,500 - 17,036[kl]	1,000; induction of stress biomarkers in mussels[m]

GSI, gonadosomatic index

[a]Kolpin et al. 2002; [b]Kleywegt et al. 2011; [c]Peng et al. 2008; [d]Wilson et al. 2003; [e]Zhang et al. 2013; [f]Wu et al. 2014; [g]Flippin et al. 2007; [h]Kim et al. 2009; [i]Burkhardt-Holm et al. 2008; [j]Lin et al. 2011; [k]Sanderson et al. 2003; [l]Spongberg et al. 2011; [m]Schmidt et al. 2011

Endocrine disrupting effects are cumulative when multiple compounds are present (Caliman and Gavrilescu 2009). The concentrations at which TOrCs have effects on aquatic life may be lower due the additive nature of the compounds (Jin et al. 2012; Petersen et al. 2013). For example, a high concentration (12.5 μg/L) of an EDC mixture including E2, 17α-ethinylestradiol, permethrin, atrazine, and nonylphenol had a greater effect on innate immune-related gene transcription in zebrafish than the same concentration of each compound individually (Jin et al. 2010). Also, exposure of minnows to a mixture of E2, diethylstilbestrol, and nonylphenol at environmentally relevant concentrations resulted in an significant increase in VTG concentrations compared to the concentrations in minnows exposed to individual compounds (Jin et al. 2012). The mixture also induced the reduction change of testis somatical index and

GSI and the feminization of fish, unlike the single compound exposed minnows. This makes it important to try to decrease the concentrations of many compounds in surface waters rather than just the compounds known to individually have effects.

2.3 Trace organic contaminants in wastewater treatment plants

2.3.1 Sources and influent concentration of trace organic contaminants in wastewater treatment plants

TOrCs can enter WWTPs following post-consumer use through excretion with urine or feces, bathing, washing, improper disposal of medication, cleaning, swimming, urban runoff, etc. (Luo et al. 2014). Their influent concentrations range widely among compounds and WWTPs (Table 2.3). While the TOrCs are typically found at low µg/L concentrations in the influent, they are also detected at high concentrations in some WWTPs. For example, a review of triclosan concentrations in untreated wastewater found a median concentration of 3,130 ng/L (n=218), and a maximum concentration of 393,000 ng/L (Perez et al. 2013). Also, BPA has been detected in influent at concentrations up to 37,000 ng/L (Melcer and Klecka 2011), ibuprofen at concentrations up to 373,000 ng/L (Santos et al. 2007), E2 at concentrations up to 3000 ng/L (Foster 2007), and gemfibrozil at concentrations up to 17,100 ng/L (Rosal et al. 2010). The minimum detected influent concentrations are very low (<113 ng/L) for all of the compounds, and frequent they are not detected in the influent.

Table 2.3. Summary of trace organic contaminants in wastewater treatment plants

trace organic contaminant	average influent concentrations (ng/L)	average effluent concentrations range (ng/L)	removal efficiencies (%)	biological removal efficiencies (%)
Triclosan	<1 - 3,130[abcd]	<0.2 - 440[abcde]	46 - 99[bcde]	48 - 81[bd]
BPA	80 - 2,500[bfyz]	4 - 1,600[bgh]	55 - 96[b]	54 - 85[b]
Ibuprofen	<112.9 - 12,000[bci]	5 - 3,400[cjk]	26 - 100[bclj]	50 - 100[bm]
E2	<0.3 - <80[fn]	0.1 - 19[go]	21.8 - 99.9[pq]	75 - 95[rs]
Gemfibrozil	<60.5 - 2,200[di]	4 - 200[dtu]	46 - 100[dw]	32 - 100[mx]

[a]Perez et al. 2013; [b]Samaras et al. 2013; [c]Nakada et al. 2006; [d]Snyder et al. 2007; [e]Bester 2005; [f]Yu et al. 2011; [g]Duong et al. 2010; [h]Ballesteros-Gomez et al. 2007; [i]Kosma et al. 2014; [j]Ternes 1998; [k]Gross et al. 2004; [l]Tauxe-Wuersch et al. 2005; [m]Yan et al. 2014; [n]Foster 2007; [o]Zhang et al. 2011; [p]Ternes et al. 1999; [q]Zorita et al. 2009; [r]Zhou et al. 2012; [s]Ifelebuegu 2011; [t]Khan and Ongerth 2005; [u]Kim et al. 2007; [v]Rosal et al. 2010; [w]Stumpf et al. 1999; [x]Huang et al. 2011; [y]Guerra et al. 2015; [z]Melcer and Klecka 2011

2.3.2 Fate in wastewater treatment plants

Documented TOrC effluent concentrations and removals are shown in Table 2.3. Average effluent concentrations range from low ng/L concentrations to low µg/L concentrations for all five studied TOrCs, though maximum concentrations detected can be higher (Munoz et al. 2010; Santos et al. 2007; Rosal et al. 2010; Karnjanapiboonwong et al. 2011). Reported removal efficiencies also are reported over a broad range; some are efficiently removed in WWTPs with many removals reported above 90% for triclosan

(Lozano et al. 2013; Foster 2007; Snyder et al. 2007), BPA (Samaras et al. 2013; Clara et al. 2005; Drewes et al. 2005; Nakada et al. 2006), ibuprofen (Zorita et al. 2009; Snyder et al. 2007; Lishman et al. 2006; Samaras et al. 2013), and E2 (Foster 2007; Joss et al. 2004; Ternes et al. 1999; Baronti et al. 2000), whereas gemfibrozil generally has moderate removal (Lishman et al. 2006; Paxeus 2004; Stumpf et al. 1999; Ternes 1998).

A range of removals exist for the same compound between different WWTPs (Table 2.3; Onesios et al. 2009). Even in conventional activated sludge (CAS) treatment processes with similar operating conditions the removal rates can vary. For example, in a CAS with a 9 hour hydraulic retention time (HRT) and a 8 day SRT the removal efficiency of triclosan is 52% (Samaras et al. 2013) and in another CAS with a 8.9 hour HRT and a 8.4 day SRT the average removal efficiency of triclosan is 65% (Nakada et al. 2006). Different activated sludge bacterial communities are able to remove TOrCs with different efficiencies, likely due to the acclimation of the community to the TOrC (A. Layton et al. 2000). The removal efficiencies also depend on operating conditions such as HRT and SRT (Ying and Kookana 2007).

TOrCs are removed primarily through sorption and biological degradation. Primary treatment is ineffective at removing most TOrCs (Carballa et al. 2005), though removal through sorption onto primary sludge can be high for compounds with high partitioning coefficients, such as the fragrances, galaxolide and tonalide (Carballa et al. 2004). TOrC removal in secondary treatment by sorption and their subsequent transfer to biosolids is also important for very hydrophobic compounds (Heidler and Halden 2007). For example, Lozano et al. (2013) found that 64% of the triclosan was transferred to the solid phase. However, significant removal by biological degradation has been demonstrated (Onesios et al. 2009). Estimations of biological removals have been documented by evaluating the mass balance of the TOrC on the secondary treatment systems, with lost components attributed to biological removal. A summary of these results is shown in Table 2.3, with removal efficiencies above 50% for all compounds.

Studies showing mineralization of triclosan, ibuprofen, and E2 further support hypotheses for microbial degradation (Federle et al. 2002; Kimura et al. 2010; Layton et al. 2000). Triclosan fate in activated sludge was studied using a continuous activated sludge system with ^{14}C-labeled triclosan. Greater than 94% of the triclosan was degraded with between 81 and 92% of the triclosan mineralized or incorporated into the activated sludge biomass and the remaining triclosan transformed into metabolites (Federle et al. 2002). Ibuprofen biodegradation was studied using ^{14}C-labeled ibuprofen. Biosolids from an activated sludge plant and a membrane bioreactor were used as the inocula in batch tests. When the biosolids were collected from the activated sludge plant, approximately 15% of the radioactivity was incorporated into

the biomass and 40% of the radioactivity was gone. When the biosolids were collected from the membrane bioreactor, approximately 20% of the radioactivity was incorporated into the biomass and 55% of the radioactivity was gone (Kimura et al. 2010). E2 biodegradation was studied using ^{14}C-labeled E2 and biosolids from municipal WWTPs. Between 70 and 80% of the ^{14}C-labeled E2 was mineralized to CO_2 by municipal WWTP biosolids (A. Layton et al. 2000).

2.4 Bioaugmentation as an option to improve trace organic contaminant removal in wastewater treatment plants

2.4.1 Previously documented bacteria that degrade trace organic contaminants

Many bacteria have been isolated that are capable of degrading TOrCs (Table 2.4). Seven (7) of the previously isolated bacteria are capable of degrading E2 to very low concentrations (<0.5 and 1.8 ng/L) (Hashimoto et al. 2010; Pauwels et al. 2008). Other bacteria either are not able to achieve low residual concentrations or were not tested. For the six E2-degrading bacteria, E1 was found to be the primary transformation product of E2 (Pauwels et al. 2008). The TOrC-degrading bacteria are all within phylum typically found in WWTPs (Ye and Zhang 2013). A majority of the bacteria are proteobacteria, gram-negative, and aerobic. Some of the TOrC-degrading bacteria are amongst bacterial genera known for their degradation of contaminants, including *Sphingomonas* (Aylward et al. 2013), *Sphingopyxis* (Aylward et al. 2013), *Pseudomonas* (Mrozik et al. 2003), and *Rhodococcus* (Solyanikova and Golovleva 2011).

Table 2.4. Characterization of previously reported bacteria for their bioaugmentation potential

organism	lowest reported degradation level (ng/L)	citation
Bacteria degrading triclosan		
Pseudomonas putida TriRY	10,000	Meade et al. 2001
Alcaligenes xylosoxidans subsp. *denitrificans* TR1	20,000	Meade et al. 2001
Sphingomonas sp. PH-07	7,500,000	Kim et al. 2011
Sphingomonas sp. RD1	325,000,000	Hay et al. 2001
Nitrosomonas europaea	not reported	Roh et al. 2009
Sphingopyxis sp. KCY1	not reported	Lee et al. 2012
Bacteria degrading bisphenol A		
Achromobacter xylosoxidans B-16	<13,000	Zhang et al. 2007
Pseudomonas sp. KA4	89,000	Kang and Kondo 2002
Streptomyces sp.	<100,000	Kang et al. 2004
Pseudomonas putida KA5	112,000	Kang and Kondo 2002
Sphingomonas sp. WH1	<890,000	Ronen and Abeliovich 2000
Sphingomonas bisphenolicum AO1	<1,000,000	Oshiman et al. 2007
Cupriavidus basilensis JF1	3,900,000	Fischer et al. 2010

Table 2.4. (continued)

organism	lowest reported degradation level (ng/L)	citation
Pseudomonas sp. KU1	5,000,000	Kamaraj et al. 2014
Pseudomonas sp. KU2	7,500,000	Kamaraj et al. 2014
Bacillus sp. KU3	1×10^7	Kamaraj et al. 2014
Enterobacter sp. HA18	9.51×10^7	Matsumura et al. 2009
HN8	1.161×10^8	Matsumura et al. 2009
Enterobacter sp. H19	1.179×10^8	Matsumura et al. 2009
Bacillus sp. NO15	1.209×10^8	Matsumura et al. 2009
Serratia sp. HI110	1.221×10^8	Matsumura et al. 2009
Pseudomonas sp. FU12	1.269×10^8	Matsumura et al. 2009
Klebsiella sp. SU5	1.29×10^8	Matsumura et al. 2009
Pseudomonas sp. NAR11	1.299×10^8	Matsumura et al. 2009
Bacillus sp. NO13	1.32×10^8	Matsumura et al. 2009
Pseudomonas sp. FU20	1.341×10^8	Matsumura et al. 2009
Alcaligenes sp. OIT7	1.359×10^8	Matsumura et al. 2009
Pseudomonas sp. SU19	1.389×10^8	Matsumura et al. 2009
Pseudomonas sp. SU1	1.449×10^8	Matsumura et al. 2009
Pandoraea sp. HYO6	1.461×10^8	Matsumura et al. 2009
Klebsiella sp. NE2	1.47×10^8	Matsumura et al. 2009
Pseudomonas sp. SU4	1.509×10^8	Matsumura et al. 2009
Pseudomonas sp. NO14	1.53×10^8	Matsumura et al. 2009
Pseudomonas sp. KA16	1.689×10^8	Matsumura et al. 2009
Bordetella sp. OS17	1.77×10^8	Matsumura et al. 2009
Sphingomonas sp. SO11	1.851×10^8	Matsumura et al. 2009
Sphingomonas sp. SO4a	1.95×10^8	Matsumura et al. 2009
Sphingomonas sp. SO1a	1.98×10^8	Matsumura et al. 2009
Bacillus sp. YA27	2.019×10^8	Matsumura et al. 2009
Klebsiella sp. SU3	2.211×10^8	Matsumura et al. 2009
Pseudomonas sp. HUK21	2.267×10^8	Matsumura et al. 2009
Pseudomonas sp. HUK22	2.769×10^8	Matsumura et al. 2009
Bacillus sp. GZB	not reported	Li et al. 2012
Sphingomonas sp. MV1	not reported	Lobos et al. 1992
Pseudomonas paucimobilis FJ-4	not reported	Ike et al. 1995
Sphingomonas sp. TTNP3	not reported	Kolvenbach et al. 2007
Pseudomonas monteilii N-502	not reported	Masuda et al. 2007
Nitrosomonas europaea	not reported	Roh et al. 2009
Bacillus cereus BPW4	not reported	Saiyood et al. 2010
Enterobacter sp. BPR1	not reported	Saiyood et al. 2010
Enterobacter sp. BPW5	not reported	Saiyood et al. 2010
Sphingomonas sp. BP-7	not reported	Sakai et al. 2007

. . . . . .

Table 2.4. (continued)

organism	lowest reported degradation level (ng/L)	citation
Pseudomonas sp. LBC1	not reported	Telke et al. 2009
Novosphingobium sp. TYA-1	not reported	Toyama et al. 2009
Bacillus pumilus BP-2CK	not reported	Yamanaka et al. 2007
Bacillus pumilus BP-21DK	not reported	Yamanaka et al. 2007
Bacillus pumilus BP-22DK	not reported	Yamanaka et al. 2007
Sphingomonas yanoikuyae BP-11R	not reported	Yamanaka et al. 2008
Enterobacter gergoviae BYK-7	not reported	Badiefar et al. 2015
Klebsiella pneumoniae BYK-9	not reported	Badiefar et al. 2015
Bacteria degrading ibuprofen		
Patulibacter sp. I11	65,000	Almeida et al. 2013
Gordonia sp. I2	74,000	Almeida et al. 2013
Paracoccus sp. I5	83,800	Almeida et al. 2013
Acinetobacter sp. I4	87,200	Almeida et al. 2013
Nocardia sp. NRRL 5646	$< 4 \times 10^8$	Chen and Rosazza 1994
Variovorax sp. Ibu-1	not reported	Murdoch and Hay 2015
Sphingomonas sp. Ibu-2	not reported	Murdoch and Hay 2005
Bacteria degrading 17β-estradiol		
Novosphingobium sp. JEM-1	<0.5	Hashimoto et al. 2010
Acinetobacter sp. BP 10	1.8±0.4	Pauwels et al. 2008
Phyllobacterium myrsinacearum BP 1	1.8±0.4	Pauwels et al. 2008
Ralstonia pickettii BP 2	1.8±0.4	Pauwels et al. 2008
Pseudomonas aeruginosa BP 3	1.8±0.4	Pauwels et al. 2008
Pseudomonas sp. BP 7	1.8±0.4	Pauwels et al. 2008
Acinetobacter sp. BP 8	1.8±0.4	Pauwels et al. 2008
Rhodococcus zopfii Y 50158	<1,000	Yoshimoto et al. 2004
Rhodococcus equi Y 50155	<1,000	Yoshimoto et al. 2004
Rhodococcus equi Y 50156	<1,000	Yoshimoto et al. 2004
Rhodococcus equi Y 50157	<1,000	Yoshimoto et al. 2004
Novosphingobium tardaugens ARI-1	<1,000	Fujii et al. 2002
Rhodococcus sp. KC4	<5,000	Yu et al. 2007
Sphingomonas sp. KC8	<5,000	Yu et al. 2007
Stenotrophomonas maltophilia ZL1	20,000	Li et al. 2012
Mycobacterium sp. MI21.2	60,000	Isabelle et al. 2011
Aminobacter sp. KC7	100,000	Yu et al. 2007
Ochrobactrum sp. MI9.3	140,000	Isabelle et al. 2011
Pseudomonas sp. MI14.1	300,000	Isabelle et al. 2011
Ochrobactrum sp. MI6.1B	610,000	Isabelle et al. 2011
Aminobacter sp. KC6	750,000	Yu et al. 2007
Sphingomonas sp. KC14	800,000	Yu et al. 2007

. . . . . .

Table 2.4. (continued)

organism	lowest reported degradation level (ng/L)	citation
Novosphingobium sp. EDB-LI1	<5,000,000	Iasur-Kruh et al. 2011
Rhodococcus sp. ED6	<20,000,000	Kurisu et al. 2010
Rhodococcus sp. ED7	<20,000,000	Kurisu et al. 2010
Rhodococcus sp. ED10	<20,000,000	Kurisu et al. 2010
Sphingomonas sp. ED8	<20,000,000	Kurisu et al. 2010
Sphingomonas sp. ED9	<20,000,000	Kurisu et al. 2010
Flavobacterium sp. KC1	not reported	Yu et al. 2007
Terrimonas sp. KC2	not reported	Yu et al. 2007
Nocardioides sp. KC3	not reported	Yu et al. 2007
Microbacterium sp. KC5	not reported	Yu et al. 2007
Sphingomonas sp. KC9	not reported	Yu et al. 2007
Sphingomonas sp. KC10	not reported	Yu et al. 2007
Sphingomonas sp. KC11	not reported	Yu et al. 2007
Brevundimonas sp. KC12	not reported	Yu et al. 2007
Escherichia sp. KC13	not reported	Yu et al. 2007
Nitrosomonas europaea	not reported	Shi et al. 2004
Bacillus sp. E2Y1	not reported	Jiang et al. 2010
Acinetobacter sp. LHJ1	not reported	Ke et al. 2007
Agromyces sp. LHJ3	not reported	Ke et al. 2007
Sphingomonas sp. CYH	not reported	Ke et al. 2007

2.4.2 Early bioaugmentation studies

Bioaugmentation involves the addition of a specific bacteria, an enrichment of bacteria, or specific genes to an existing microbial community (Semrany et al. 2012). This technique has been used extensively for groundwater bioremediation (Gentry et al. 2004; Tyagi et al. 2011) and was recently studied for its application to water treatment (Semrany et al. 2012). Many lab-scale bioaugmentation studies have been completed with many resulting in little benefit to the system (Qasim and Stinehelfer 1982; Stephenson and Stephenson 1992) and some resulting in improved COD removal (Yeh and Hung 1988), improved startup (Wilderer et al. 1991; Stephenson and Stephenson 1992), and improved TOC removal and nitrification (Abllah and Lee 1991). Bioaugmentation has also been applied to a few full scale WWTPs resulting in improved BOD removal (Stephenson and Stephenson 1992) and a reduced sludge blanket (Hung et al. 1986).

Bioaugmentation with nitrifiers has resulted in improved nitrification efficiencies and allowed for lower SRTs to be used (Salem et al. 2003; Wett et al. 2011; Bartrolí, Carrera, and Pérez 2011; Cui et al. 2014). Different strategies have been explored including the parallel-plants, enricher-reactor, and enricher-

reactor return activated sludge approaches (Leu and Stenstrom 2010). These strategies all utilize a side reactor in which the bacteria to be augmented are enriched using reactor centrate as the feed source. In the parallel-plants approach, the enrichment is grown in a side continuously mixed activated sludge system that is fed influent wastewater and centrate, allowing the enrichment to acclimate in a long SRT reactor before augmentation into a low SRT system. The enricher-reactor approach uses a side sequencing batch reactor fed centrate to grow the bacteria prior to bioaugmentation. Finally, in the enricher-reactor return activated sludge approach, the enrichment reactor is fed centrate and receives some recycle activated sludge. These strategies differ greatly from the bioaugmentation strategy that would likely work best for TOrCs removal because the bacteria to be augmented for TOrCs removal are pure cultures, rather than an enrichment. This strategy would involve growing an isolated bacteria that degrades the TOrC in a side chemostat reactor using an inexpensive, readily available carbon source, rather than reactor centrate.

Bioaugmentation for improved removal of recalcitrant compounds has previously been proposed, though its testing has been limited (Van Limbergen et al. 1998) and it has also been proposed as option for removal TOrCs during drinking water treatment (Benner et al. 2013). An early bioaugmentation study focused on the enhanced removal of polyaromatic hydrocarbons (PAH; naphthalene and phenanthrene) (Cardinal and Stenstrom 1991). During this study, enricher reactors were used to enrich for bacteria capable of degrading PAHs. Three different enricher reactors were tested and they were fed different concentrations of naphthalene. Enhanced PAH removal was seen when bacteria were augmented from the enricher reactor into the continuous flow reactor. However, the degradation ability of the bacteria in the enricher reactor was lost when the naphthalene was removed from the influent to the reactor. This demonstrates the importance of bioaugmentation criterion 2, which states that bacteria must be able to grow on common substrates while maintaining the ability to degrade the contaminant. Therefore, bacteria to be augmented will be tested for this ability.

More recent studies for enhanced TOrCs removal have involved bioaugmentation of pure cultures rather than enrichments. Three studies have bioaugmented single organisms to improve E2 removal during wastewater treatment and one study has bioaugmented a single organism to improve triclosan removal. Starting with an equal biomass of the E2-degrading bacterium *Sphingomonas* sp. KC8, Roh and Chu (2011) demonstrated removal of 1 mg/L E2 in lab scale sequencing batch reactors, though contributions by *Sphingomonas* sp. KC8 were obscured by high background degradation rates by the activated sludge. This study was important in demonstrating the rapid loss of the bioaugmented *Sphingomonas* sp. KC8, which decreased by over 1 to 2.5 orders of magnitude within one solids retention time (SRT). Iasur-Kruh (2011) used a different approach by demonstrating that the integration of an E2-degrading bacteria, EDB-

LI1, into a wetland pond biofilm resulted in enhanced removal of 40 mg/L E2 over 24 hours. Hashimoto et al. (2010) bioaugmented the E2-degrading bacteria, *Novosphingobium* sp. JEM-1, in lab scale reactors consisting of aeration and settling tanks with an SRT of 5 days. Improved E2 and E1 removal was seen in the experimental reactor, compared to the control reactor (residual of 1 vs. 2.9 ng/L). Similar to the Roh and Chu (2011) study, the bioaugmented bacterial concentrations decreased by almost two orders of magnitude in two days, so that after seven days the E2 effluent concentrations and the *Novosphingobium* sp. JEM-1 concentrations were approximately the same in both the experimental and control reactors. Lee et al. (2015) bioaugmented the triclosan-degrading bacteria, *Sphingopyxis* sp. KCY1, into batch reactors with nitrifying activated sludge. No improvement in triclosan removal was seen with bioaugmentation, potentially due to grazing of the augmented bacteria by protozoa, lack of preferential degradation of triclosan by *Sphingopyxis* sp. KCY1, or slow degradation rates.

Future studies should focus on continuous bioaugmentation with bacteria that meet bioaugmentation criteria. Many challenges remain for successful implementation of bioaugmentation for improved TOrC removal during wastewater treatment, including the rapid loss of augmented bacteria and the extreme low TOrC concentrations in WWTPs. Predators favor grazing on dispersed bacteria, which may be a contributing factor to the rapid loss of bacteria following bioaugmentation into activated sludge, as demonstrated by protozoan grazing of bioaugmented denitrifying bacteria (Bouchez et al. 2000). Continuous or periodic bioaugmentation would compensate for losses and help maintain improved TOrCs removal, and will be tested to account for the rapid loss seen during *Sphingomonas* sp. KC8 and *Novosphingobium* sp. JEM-1 bioaugmentation. Bioaugmentation will also be done with a bacterium that preferentially degrades its TOrC and has practical degradation rates to account for the issues seen with *Sphingopyxis* sp. KCY1. Also, because the TOrCs concentrations are too low to sustain bacterial growth, the bacteria to be augmented must grow using other carbon sources. Therefore, pure cultures with known TOrCs degradation capabilities would be cultured in a side growth reactor on a common carbon source. This differs from nitrification bioaugmentation techniques, which utilize the higher concentration of ammonia in anaerobic digester centrate to enrich for nitrifiers in a side stream reactor. But the low TOrCs concentrations preclude this type of in-line enrichment approach. Bioaugmentation has not previously been studied for many TOrCs, and in only one study were the augmented bacteria capable of degrading the TOrC to low ng/L concentrations.

2.5 Trace organic contaminant degradation pathways and associated enzymes and genes

2.5.1 Trace organic contaminant biological degradation pathways

Biological degradation pathways have been proposed for triclosan, BPA, ibuprofen, and E2 degradation by isolated bacteria. Intermediates were observed during triclosan degradation by *Sphingomonas* sp. PH-07 (Kim et al. 2011). Two of the metabolites identified during triclosan degradation by *Sphingomonas* sp. PH-07 (monohydroxy-triclosan and 2,4-dichlorophenol) were also seen during triclosan degradation by *Sphingopyxis* sp. KCY1 and a triclosan degradation pathway was proposed (Figure 2.1; Lee et al. 2012). A commercially available standard was used to identify 2,4-dichlorophenol. Other metabolites were tentatively identified based on mass spectrometry and their fragmentation patterns. This pathway proposed a *meta*-cleavage, as the addition of 3-flurocatechol, a *meta*-cleavage inhibitor, caused the inhibition of triclosan degradation. Also, catechol 2,3-dioxygenase was detected in the bacteria grown on triclosan. Transformation by *Sphingopyxis* sp. KCY1 results in the complete dechlorination of triclosan, as demonstrated by the release of chloride ions. These experiments were completed with an initial triclosan concentration of 5 mg/L and have not been documented within the concentration ranges observed in wastewater or natural waters (Lee et al. 2012).

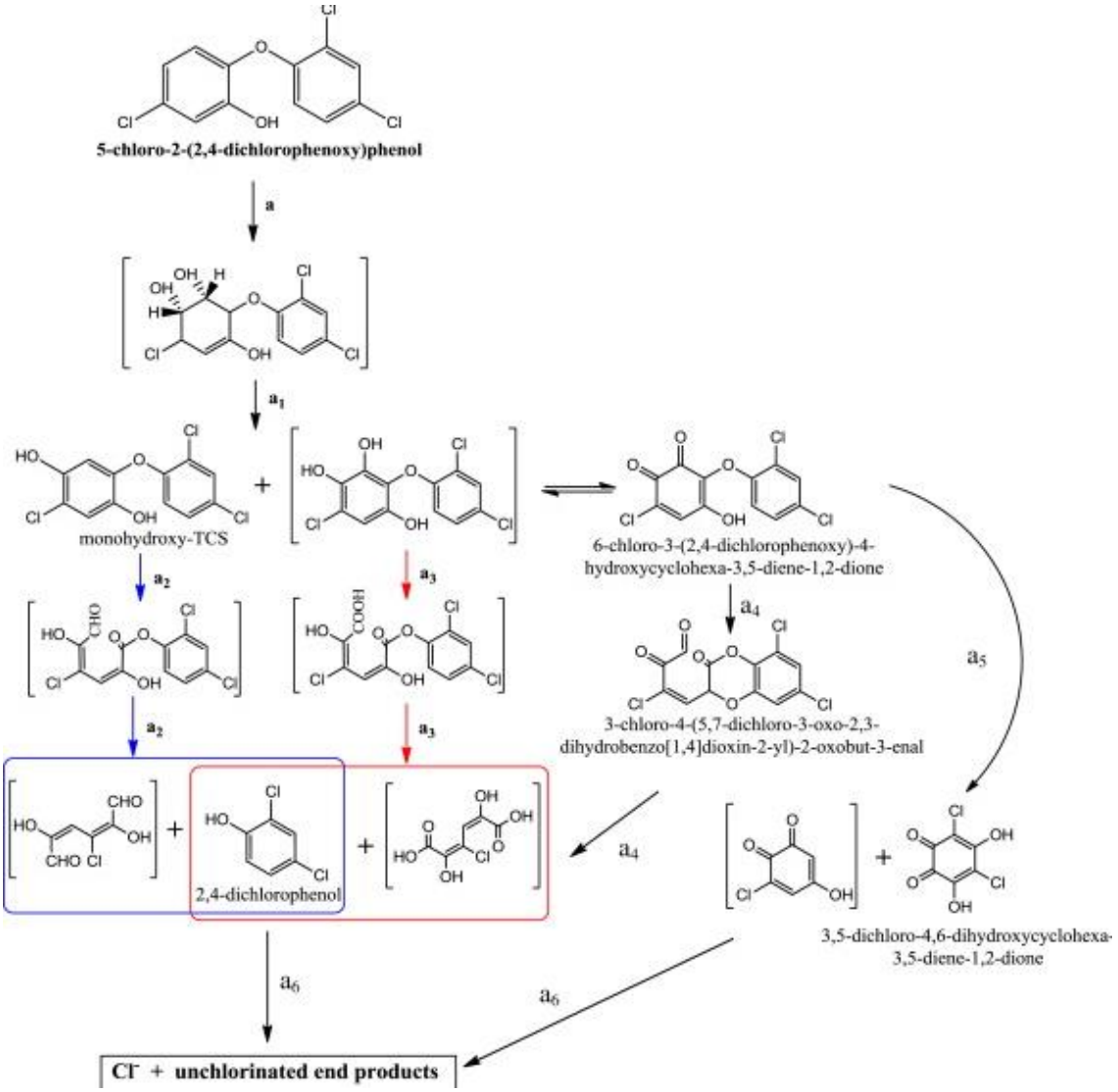

Figure 2.1. Proposed triclosan degradation pathway by *Sphingopyxis* sp. KCY1. Figure reprinted from Water Research, 46, Lee et al., Biodegradation of triclosan by a wastewater microorganism, 4226-4234, (2012), with permission from Elsevier. Metabolites boxed in blue result from the blue pathway and metabolites boxed in red result from the red pathway, with the detected metabolite, 2,4-dichlorophenol, a metabolite of both pathways. Metabolites not in brackets were identified through mass spectra and fragmentation patterns.

BPA degradation by isolated bacteria is shown in Figure 2.2 (Zhang et al. 2013a). Three of these four bacteria initially followed a similar degradation path, with 1,2-bis(4-hydroxyphenyl)-2-propanol (metabolite II, Figure 2.2. circled in red) as the first or second metabolite in BPA transformation. BPA degradation by *Sphingomonas* sp. MV1 resulted in the transformation of 85% of the BPA to metabolite II and only 15% to metabolite I. Metabolite II is further degraded and finally mineralized to carbon dioxide and cell biomass, as determined by HPLC. A majority of metabolite I (90%) is then transformed to metabolite VI, which is further degraded, and 10% of metabolite I is transformed into metabolite X,

which is not degraded any further (Spivack et al. 1994). Metabolites I and II were detected during BPA by *Sphingomonas* sp. AO1. Further investigation of the degradation products was completed as it was not the focus of the study (Sasaki et al. 2005). BPA degradation by *Sphingomonas* sp. TTNP3 followed a different pathway than proposed for the other bacteria. BPA was initially transformed into metabolite III through an *ipso* substitution and metabolite III was further transformed through a cleavage of the carbon-carbon bond between the isopropyl and phenolic groups and through the hydrogenation of the hydroxylated or quinol ring (Kolvenbach et al. 2007). BPA degradation by unidentified bacterial strain WH1 was predicted to follow the degradation pathway proposed for *Sphingomonas* sp. MV1 due to the detection of the metabolites, HBA and HAP (Ronen and Abeliovich 2000).

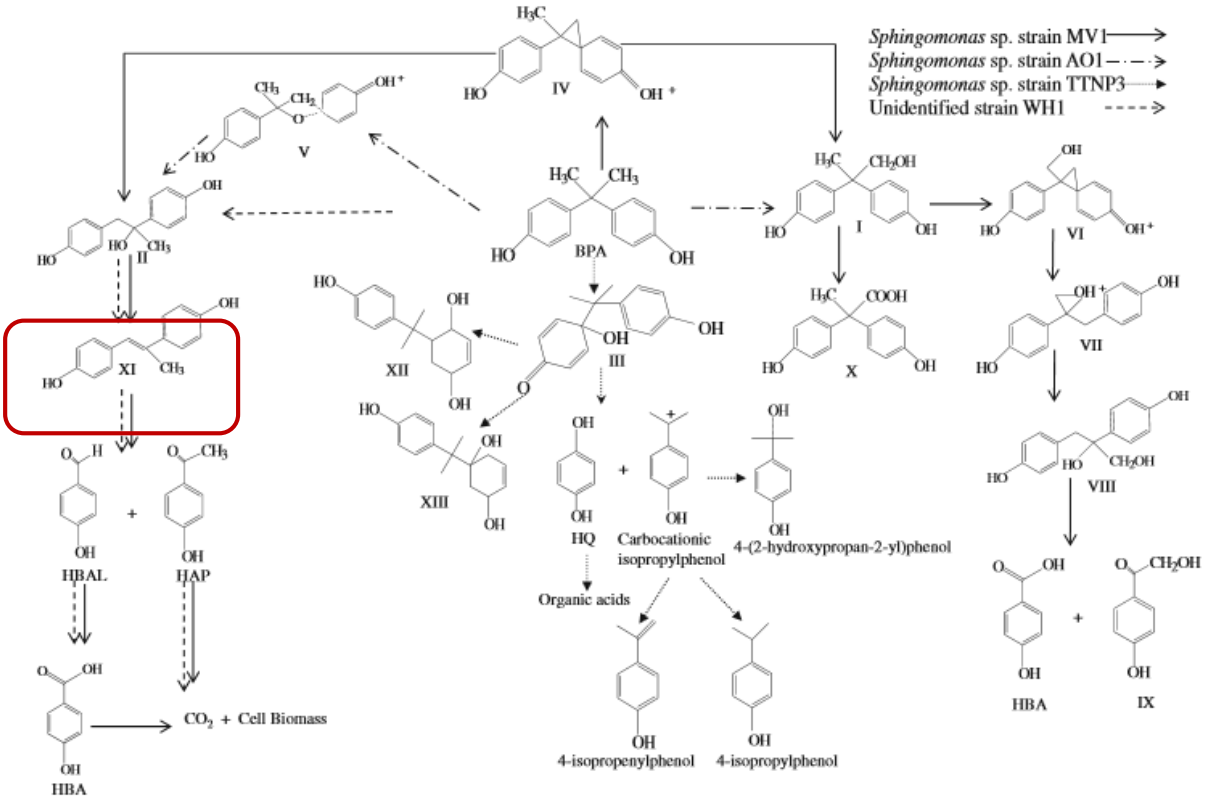

Figure 2.2. Proposed BPA degradation pathways by *Sphingomonas* sp. MV1, *Sphingomonas* sp. AO1, and *Sphingomonas* sp. TTNP3 and unidentified strain WH1. Figure reprinted from Springer and Applied Microbiology and Biotechnology, 97, 2013, pg. 5684, Bacteria-mediated bisphenol A degradation, Zhang, Figure 1, with kind permission from Springer Science and Business Media.

Ibuprofen degradation by *Sphingomonas* sp. Ibu-2 is proposed to proceed through a *meta*-cleavage of the aromatic ring. GC-MS analysis of ibuprofen-grown Ibu-2 confirmed the production of metabolites b, c, and d (Figure 2.3; Murdoch and Hay 2005). Knockout of the *ipfF* gene, a coenzyme A ligase, resulted in no transformation of ibuprofen. This suggests that *ipfF* is necessary for that first step in ibuprofen degradation by *Sphingomonas* sp. Ibu-2 (Murdoch and Hay 2013).

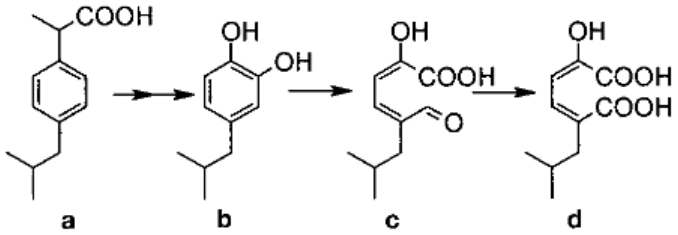

Figure 2.3. Proposed ibuprofen degradation pathway by *Sphingomonas* sp. Ibu-2. Figure reprinted from Applied and Environmental Microbiology, Murdoch and Hay, Formation of catechols via removal of acid side chaings from ibuprofen and related aromatic acids, 6121-25, (2005) with permission from American Society of Microbiology.

The current understanding for E2 biological degradation indicates that the first transformation product is estrone (E1). Some bacteria are not capable of degrading it further including E2Y2, E2Y3, and E2Y5 (Jiang et al. 2010), though others are able to degrade E1 (Pauwels et al. 2008; Kurisu et al. 2010). *S. maltophilia* is proposed to initially transform E2 to E1 and then eventually to tyrosine (Figure 2.4; Li et al. 2012). The gray arrow represents an enzyme identified in the genome and the black arrow represents an enzyme identified in the proteome. The degradation of E1 through a *meta*-cleavage by *Sphingomonas* sp. ED8 was proposed (Kurisu et al. 2010).

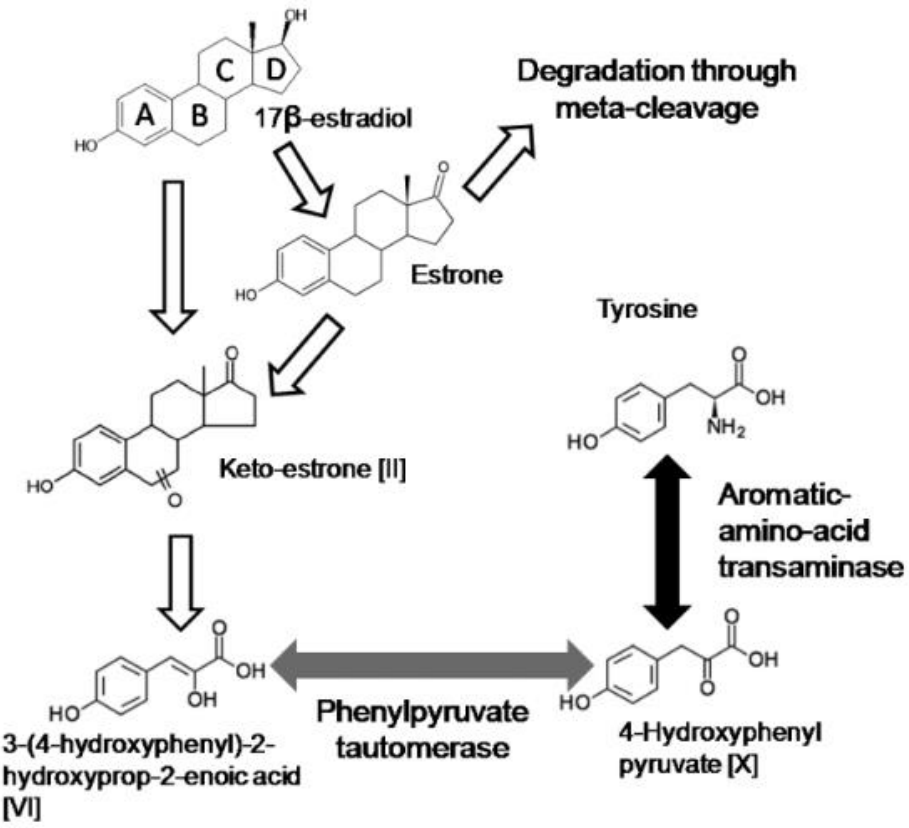

Figure 2.4. Proposed E2 degradation pathway by *S. maltophilia* ZL1. Figure reprinted from Environmental Science and Technoloyg, Li et al., Proteomic analysis of 17 beta-estradiol degradation by *Stenotrophomonas Maltophilia*, 5947-55, (2012) with permission from American Chemical Society.

2.5.2 Potential for biomarker genes

Identification of proteins involved in TOrC degradation can lead to the identification of genes involved in TOrC degradation that might serve as biomarkers for this functional ability. These biomarker genes would be useful because the degradation genes could be monitored during bioaugmentation rather than the 16S rRNA gene and the degradation genes could be searched for in other bacteria, possibly allowing for the identification of other bacteria capable of degrading TOrCs. The 16S rRNA gene may be insufficient to monitor augmented bacteria because the bacteria may lose their ability to degrade the TOrC resulting in an overestimation of TOrC degradation. Also, the degradation genes may transfer to other bacteria resulting in an underestimation of TOrC degradation. An example of this was shown by Gedalanga et al. (2014). The degradation of 1,4-dioxane by *Pseudonocardia dioxanivorans* CB1190 in activated sludge was predicted better by monooxygenase-based biomarkers than by *P. dioxanivorans* 16S rRNA genes (Gedalanga et al. 2014). Monard et al. (2013) also showed that *atzD*, the atrazine-degrading gene, may be a suitable biomarker to monitor atrazine biodegradation in soils.

2.5.3 Proteomics methods used to identify proteins involved trace organic contaminant degradation

Quantitative proteomics is a valuable tool to study the physiological response of a bacteria to a specific compounds, such as TOrCs. This aids in the identification of degradation pathways, as well as the development of biomarker genes. The expression of proteins involved in TOrC degradation, as well as stress proteins and efflux pumps amongst others, are induced in many bacteria when they are grown in the presence of the TOrC. Comparison of proteomes in the presence and absence of the TOrC may allow for identification of proteins involved in TOrC degradation (Kim et al. 2007; Kim et al. 2009). Label-free quantitative proteomics allows for faster and less expensive measurement of protein expression levels than previous proteomic techniques (Zhu et al. 2010). Also, label-free proteomics results in more proteins identified and less proteins identified based on a single peptide (Patel et al. 2009). Label-free quantitative proteomics has some disadvantages however. Even the same sample can have differences in the peak intensities, which can be corrected for by normalization amongst the samples. Also, drifts in retention time and the mass to charge ratio can complicate the analysis extremely. The use of a highly reproducible LC-MS and careful peak alignments are necessary (Zhu et al. 2010).

Proteomics has been used to study the degradation of several aromatic hydrocarbons (Kim et al. 2009), though the degradation of TOrCs has been less extensively studied (Li et al. 2012; Almeida et al. 2013). Ibuprofen degradation by *Sphingomonas* sp. I11 was studied using quantitative proteomics (Almeida et al. 2013). 251 proteins upregulated in the presence of ibuprofen were identified. The *Sphingomonas* sp. I11 genes were compared to the *Sphingomonas* sp. Ibu-2 *ipf* genes previously proposed to be involved in ibuprofen degradation (Kagle et al. 2009) and four (4) upregulated genes matched to *Sphingomonas* sp. Ibu-2 *ipf* genes (Almeida et al. 2013). This study confirmed genes potentially involved in the degradation of ibuprofen by *Sphingomonas* sp. Ibu-2 are also potentially involved in the degradation of ibuprofen by *Sphingomonas* sp. I11 and demonstrated the usefulness of proteomics to study TOrC degradation. Protein expression during E2 degradation by *S. maltophilia* ZL1 was studied over time using quantitative proteomics (Li et al. 2012). For this study a protein was considered upregulated if the expression level increase by more than a 100% from hour zero to hour sixteen. One of the identified, upregulated protein, aromatic-amino-acid transaminase, is known to be responsible for the transformation from 4-hydroxyphenyl pyruvate to tyrosine. This study proposed that E2 was transformed into tyrosine (Figure 2.4). This study furthers the knowledge of the E2 degradation pathway and provides genomic and proteomic support.

CHAPTER 3: RESEARCH HYPOTHESES

Biological degradation of trace organic contaminants has been established as an important removal mechanism during wastewater treatment (Onesios et al. 2009; Luo et al. 2014). This leads to the over-arching hypothesis that *bioaugmentation of TOrC-degrading bacteria into the activated sludge portion of a WWTP can improve the removal efficiencies of the TOrC*. The overarching goal of this research is to decrease negative effects on aquatic life by TOrC by decreasing TOrC concentrations in WWTP effluents discharged to surface waters while also minimizing the transfer of TOrCs to biosolids. To progress towards this goal the following objectives were completed.

Hypothesis I: Bacteria suitable for bioaugmentation can be isolated from activated sludge.

Objective I: Isolate and characterize bacteria that have potential for successful bioaugmentation

Approach: Bacterial cultures from activated sludge were enriched for bacteria capable of degrading TOrCs, with the TOrC as the sole carbon and energy source. TOrCs used included triclosan, BPA, ibuprofen, E2, and gemfibrozil. These contaminants were chosen for their different sorption potentials and their similar chemical structures for ease of measuring. Isolated bacteria were evaluated for their ability to *(1)* degrade TOrCs below ng/L concentrations, *(2)* grow using readily available, common substrates, *(3)* preferentially degrade TOrCs in the presence of higher concentrations of other substrates, and *(4)* degrade the TOrCs with high enough degradation rates that bioaugmentation is practical. TOrC degradation kinetics by isolated bacteria were determined in nutrient rich media, in nutrient poor media, and when bioaugmented activated sludge. To better account for the bio-degradable fraction during evaluation of TOrC degradation kinetics in activated sludge, sorption partitioning coefficients were determined.

Hypothesis II: Continuous bioaugmentation is a sustainable and practical technique to enhance trace organic contaminant removal in activated sludge.

Objective II: Model bioaugmentation of isolated bacteria in full scale activated sludge processes

Approach: BPA and triclosan degradation was modeled in a completely mixed activated sludge reactor (CMAS) and in a 4-staged activated sludge process (ASP). The model included BPA/triclosan degradation by bioaugmented bacteria (*Sphingopyxis* sp. BiD10, *Sphingobium* sp. BiD32, *Sphingopyxis* sp. TrD1, *Sphingomonas* sp. TrD23, and *Sphingomonas* sp. TrD34) and by activated sludge using measured degradation rates. Also, sorption of BPA/triclosan was included using measured sorption coefficients. The required bioaugmentation doses to reach a desired BPA/triclosan effluent concentration were calculated and compared to the total system VSS, with

increases of less than 10% considered practical. The bioaugmentation doses were also calculated over a range of activated sludge VSS, SRT, and level of contaminant removal.

Objective III: Test the feasibility of bioaugmentation to improve TOrC removal in lab scale reactors

Approach: Lab-scale sequencing batch reactors were operated with BPA in the feed and periodic additions of higher concentrations of BPA to determine degradation kinetics. One reactor received regular doses of a BPA-degrading bacteria, *Sphingobium* sp. BiD32, to simulate continuous bioaugmentation. The control reactor was bioaugmented with a closely related, non-BPA-degrading bacteria, *Sphingopyxis* sp. TrD1, to account for potential changes caused by addition of biomass or from incidental spent media. BPA removal was compared between the bioaugmented and control reactors.

Objective IV: Calculate the degradation and survival kinetics parameters of augmented bacteria

Approach: BPA degradation kinetics associated with and normalized to the augmented *Sphingobium* sp. BiD32 (k_c') were determined by monitoring BPA degradation in the bioaugmented and control reactor. Bioaugmented bacterial concentrations were monitored in batch experiments completed with blended reactor waste sludge to inactivate protozoa and rotifers and with untreated waste sludge as a control. This allowed for differentiation between losses to endogenous respiration (k_d) and predation (k_p). *Sphingobium* sp. BiD32 was grown using reactor waste sludge that had been autoclaved and sonicated to remove effects of predation and competing bacteria, allowing for determination of growth kinetics (k_g).

Hypothesis III: TOrCs degradation is achieved through activity of specialized enzymes and degradation pathways.

Objective V: Identify proteins potentially involved in trace organic contaminant degradation

Approach: Label-free quantitative proteomics was completed with *Sphingobium* sp. BiD32, *Rhodococcus* sp. EsD8, and *Bacillus* sp. GeD10 (collaboratively) to determine the proteins present during TOrCs degradation compared to proteins present in the absence of these compounds. The whole genomes of the bacterial isolates were sequenced to increase the confidence in the proteins identified. Metabolites produced during the degradation of the compound by the bacterial isolate were determined to assist in the identification of proteins involved in the degradation.

CHAPTER 4: CULTIVATION AND CHARACTERIZATION OF BACTERIAL ISOLATES CAPABLE OF DEGRADING PHARMACEUTICAL AND PERSONAL CARE PRODUCTS FOR IMPROVED REMOVAL IN ACTIVATED SLUDGE WASTEWATER TREATMENT

Reproduced with permission from:
Zhou, NA, AC Lutovsky, GL Andaker, HL Gough, JF Ferguson. 2013. "Cultivation and Characterization of Bacterial Isolates Capable of Degrading Pharmaceutical and Personal Care Products for Improved Removal in Activated Sludge Wastewater Treatment." *Biodegradation* 24 (6): 813–27. doi:10.1007/s10532-013-9630-9.

4.1 Chapter summary

This chapter documents the results of Objective I: the isolation and characterization of bacteria that have potential for successful bioaugmentation. An approach for isolating bacteria from activated sludge capable of degrading TOrCs was developed and demonstrated using triclosan, BPA, ibuprofen, E2, and gemfibrozil. The bacteria were screened for their bioaugmentation practicality. Eleven bacteria were isolated for their ability to degrade a specific TOrC, and eight of these bacteria were capable of degrading the TOrCs to low ng/L concentrations. These were the first bacteria reported to degrade triclosan, BPA, and ibuprofen to low ng/L concentrations. This was also the first documented bacterial isolate known to degrade gemfibrozil. The bacteria grew using a variety of readily available carbon sources with protein-rich substrates supporting the best growth results for the widest range of bacteria. The bacteria were able to maintain the ability to degrade TOrCs after being grown in the absence of the TOrCs, which is important so that the contaminant need not be introduced prior to initiating degradation. Eight of the bacteria degraded the TOrC before growth or during the early growth phase in the presence of higher concentrations of other substrates, suggesting that the compound may be used as a preferred secondary substrate. When the bacteria are bioaugmented into the activated sludge portion of the WWTP where there will be many carbon sources at much higher concentrations then the TOrCs. Therefore, it is important that the bacteria are able to degrade the TOrC in complex media. It is also important to note that bacteria with similar evolutionary history (based on 16S rRNA gene similarity) could not degrade the same TOrCs, nor was there a pattern such that degrading one TOrC automatically indicated the ability to degrade a second. This combined evidence suggests that the degradation is mediated by specialized genes, and is therefore not co-metabolic in these organisms. Finally, eight of the bacteria degraded the TOrCs with first order specific degradation rates greater than 0.06 L/mg-hr. This study identified bacteria suitable for bioaugmentation to improve TOrCs removal efficiencies.

4.2 Abstract

Pharmaceutical and personal care products (PPCPs) discharged with wastewater treatment plant (WWTP) effluents are an emerging surface water quality concern. Biological transformation has been identified as an important removal mechanism during wastewater treatment. The aim of this research was the identification of bacteria with characteristics for potential bioaugmentation to enhance PPCP removal. We report here the cultivation and characterization of bacteria capable of degrading PPCPs to ng/L concentrations. An isolation approach was developed using serial enrichment in mineral medium containing 1 mg/L of an individual PPCP as the sole organic carbon source available to heterotrophs until the original activated sludge inocula was diluted to approximately 10^{-8} of its initial concentration, followed by colony growth on solid R2A agar. Eleven bacteria were isolated, eight that could remove triclosan, bisphenol A, ibuprofen, or 17β-estradiol to below 10 ng/L, one that could remove gemfibrozil to below 60 ng/L, and two that could remove triclosan or E2, but not to ng/L concentrations. Most bacterial isolates degraded contaminants during early growth when grown utilizing rich carbon sources and were only able to degrade the PPCPs on which they were isolated. Seven of the bacterial isolates were sphingomonads, including all the triclosan and bisphenol A degraders and the ibuprofen degrader. The study results indicate that the isolated bacteria may have a positive influence on removal in WWTPs if present at sufficient concentrations and may be useful for bioaugmentation.

4.3 Introduction

Pharmaceuticals and personal care products (PPCPs) that enter the environment through wastewater treatment plant (WWTP) effluents (Daughton and Ternes 1999) are an emerging concern in surface waters (Kolpin et al. 2002). PPCPs encompass several categories of contaminants including fragrances, cosmetics, prescription drugs, and many more compounds that are detected in wastewater and surface water systems (Kolpin et al. 2002; US EPA 2012). Low concentrations of PPCPs may impact aquatic life, including changes in growth and mortality of algae and amphibians and changes in the community structure (Wilson et al. 2003; Fraker and Smith 2004; Brausch and Rand 2011). Endocrine disrupting compounds, such as estrone (E1), 17β-estradiol (E2), 17α-ethinylestradiol (EE2), and bisphenol A, are implicated in changes in fertility and vitellogenin production and increases in the number of intersex fish and the female to male phenotype ratio (Metcalfe et al. 2001; Burkhardt-Holm et al. 2008). Other compounds, such as triclosan, are suspected to impact the survivability of aquatic life (Fraker and Smith 2004), and bioaccumulation has been reported both in algae and marine mammals (Fair et al. 2009; Coogan et al. 2007). The impacts of many other PPCPs remain as yet unknown.

There is evidence that biological degradation plays a role in PPCP removal (Onesios et al. 2009). PPCPs are removed to varying levels during conventional wastewater treatment with final effluent concentrations generally in the µg/L to ng/L ranges (Daughton and Ternes 1999). For example, mass balance calculations completed on WWTPs showed biological removal of triclosan (48-65%, Bester 2003), ibuprofen (80%, Heidler and Halden 2007), naproxen (60%, Carballa et al. 2004), E2 (93%, Andersen et al. 2003), and EE2 (85%, Andersen et al. 2003). Research showing mineralization of triclosan, ibuprofen, and E2 further supports the hypotheses for microbial degradation (Federle et al. 2002; Quintana et al. 2005; Layton et al. 2000). Removal by sorption and transfer to biosolids may be important for very hydrophobic compounds (Heidler and Halden 2007) and removal by chemical oxidation can possibly transform compounds to by-products of unknown toxicity (Westerhoff et al. 2005). These processes may be less desirable than removal and possible mineralization of PPCPs by microbial activity.

Bacteria capable of degrading select PPCPs are isolated and characterized for the potential bioaugmentation of WWTPs for improved PPCP removal. An advantage of bioaugmentation is that it can be implemented in existing WWTPs with the addition of a side stream reactor to produce the bacteria. To be practical for bioaugmentation, identified bacteria must be able to *(1)* remove the PPCPs to levels substantially below typical WWTP effluent concentrations (typically to ng/L concentrations), *(2)* grow using common substrates while maintaining the ability to degrade the PPCP, *(3)* degrade PPCPs in the presence of higher concentrations of other substrates, and *(4)* degrade the PPCPs with degradation rates high enough to be able to reach low PPCP concentrations in a time and with a reactor configuration similar to biological treatment in WWTPs and with low bacteria dosages to activated sludge.

PPCPs explored in this study include triclosan, bisphenol A, ibuprofen, E2, EE2, gemfibrozil, and carbamazepine. These compounds represent a variety of PPCPs, including an antimicrobial, plasticizer, non-steroidal antiinflammatory drug, natural and synthetic hormones, cholesterol lowering drug, and anticonvulsant with a range of partitioning coefficients (log K_{OW}) from 1.51 for carbamazepine (Scheytt et al. 2005) and up to 4.8 for triclosan (Westerhoff et al. 2005b). Sorption to activated sludge solids will affect the removal efficiencies of these compounds. They have a broad range of reported removals from WWTPs; some are efficiently removed in WWTPs with many removals reported above 90% for triclosan, bisphenol A, ibuprofen, E2, and EE2, whereas gemfibrozil has moderate removal and carbamazepine has little removal (Onesios et al. 2009; Chimchirian et al. 2007; Joss et al. 2004; Froehner et al. 2011). Also, a range of removals exists for the same compound between different WWTPs (Onesios et al. 2009). These PPCPs are present at a range of effluent concentrations with averages over time at WWTPs reaching up to 0.37 µg/L for triclosan (Paxeus 2004), 1.6 µg/L for bisphenol A (Ballesteros-Gomez et al. 2007), 10.2

µg/L for ibuprofen (Santos et al. 2007), 0.019 µg/L for E2 (Zhang et al. 2011), <0.01 µg/L for EE2 (Yang et al. 2011), 0.73 µg/L for gemfibrozil (Paxeus 2004), and 2.1 µg/L for carbamazepine (Dickenson et al. 2011). Previously isolated bacteria capable of degrading the PPCPs tested in this study have not been reported to degrade to final concentrations comparable to those in WWTP effluents, with the exception of six E2 degraders (Online Resource Table 4.5) (Pauwels et al. 2008).

4.4 Materials and methods

4.4.1 Inocula source

Activated sludge obtained from five wastewater treatment plants in the greater Seattle area was used as inocula in the enrichment process. Samples (1 L or larger) were taken and stored on ice while transported to the University of Washington. Samples were then aerated and mixed if not refrigerated. Samples were generally used the same day. West Point Treatment Plant (West Point) in Seattle, Washington, USA is a non-nitrifying secondary treatment facility that treats stormwater and residential, commercial, and industrial wastewater (average flow of 378,500 m^3/day and a SRT of 2 to 3 days). Quilceda Village Wastewater Treatment Plant (Tulalip) in Tulalip, Washington, USA is a membrane bioreactor facility that treats casino, hotel, and commercial wastewater (average flow of 950 m^3/day and a SRT of 25 to 30 days). Carnation Treatment Plant (Carnation) in Carnation, Washington, USA is a membrane bioreactor facility that treats residential and commercial wastewater (average flow of 380 m^3/day and a SRT of 20 to 35 days). Snoqualmie Wastewater Facility (Snoqualmie) is a carousel oxidation ditch configured for anaerobic/anoxic/aerobic treatment (average flow of 11,400 m^3/day and a SRT of 25 to 30 days). South Treatment Plant (South Plant) in Renton, Washington, USA is an activated sludge plant that treats residential, commercial, and industrial wastewater (average flow of 265,000 m^3/day and a SRT of 2.5 to 3.5 days).

4.4.2 Reagents and chemicals

PPCPs, deuterated PPCPs, media components, alternative carbon sources, and analytical reagents used are listed in the Online Resource. Organic solvents and water used for PPCP sample extraction and analysis were high-pressure liquid chromatography (HPLC) grade.

Aqueous stocks of individual PPCPs were prepared at concentrations between 2 and 35 mg/L. The stock was prepared by adding the PPCPs dissolved in acetonitrile (1000 mg/L) to a bottle, evaporating the acetonitrile at 105ºC for at least one hour, adding water (18Ω, MilliQ Plus Ultra Pure Water Systems; Millipore, Billerica, MA, USA) or media, and autoclaving to sterilize the solution. The final concentrations of the stocks were then determined analytically. Stocks were stored in amber glass bottles

to minimize potential photodegradation (Yu et al. 2006; Lin and Reinhard 2005). Aqueous stocks were stored at room temperature.

4.4.3 Cultivation/culture media

4.4.3.1 Liquid media

Two nutrient-poor media were used. Mineral medium consisted of mineral solution (Tanner 1997) modified to decrease the ammonia (0.2 g/L) and with potassium phosphate (2 mM) and sodium bicarbonate (2 mM) added as pH buffer and sodium nitrate (5 mg/L) as a nitrogen source. Potassium phosphate and sodium nitrate stock solutions were autoclaved. Other mineral salts and sodium bicarbonate stock solutions were filter sterilized (0.22 µm surfactant-free cellulose acetate membrane; Nalgene, Rochester, NY, USA), as was the final mineral medium. Mineral medium stock was made at 5x concentration and stored at 4ºC. Minimal medium, which was used for isolation of one triclosan degrader, consisted of the mineral medium with the addition of vitamin and trace elements according to the *Manual of Environmental Microbiology* (Tanner 1997) and no ammonia present. The total vitamin mass added to the medium was approximately 0.54 mg/L (Online Resource Table 4.6). It was also made at 5x concentration and stored at 4ºC. Vitamin and trace element stock solutions were filter sterilized.

Two nutrient-rich media were used. R2A medium (autoclave sterilized) was made based on the composition of R2A agar (Reasoner and Geldreich 1979) and contained 0.5 g/L yeast extract, 0.5 g/L proteose peptone, 0.5 g/L casamino acid, 0.5 g/L sucrose, 0.5 g/L soluble starch, 0.3 g/L pyruvic acid, 0.3 g/L dipotassium phosphate, and 0.05 g/L magnesium sulfate. Luria-Bertani broth (LB; autoclave sterilized; Fisher Scientific, Pittsburgh, PA, USA) contained 5 g/L yeast extract, 10 g/L tryptone, and 10 g/L NaCl.

4.4.3.2 Solid media

R2A agar was purchased commercially (BD Difco R2A Agar; Franklin Lakes, NJ, USA) and prepared according to manufacturer instructions. It was used alone or augmented with aqueous PPCPs stock to a final concentration of 1 mg/L and was autoclaved before use.

4.4.4 DNA sequencing and phylogeny

DNA was isolated from single colonies using modifications to a previously published protocol (Frothingham et al. 1991). Briefly, a single colony picked using a sterile loop was suspended in 250 µL sterile phosphate buffered saline (PBS). After brief vortexing, the bacteria were pelleted by centrifugation (10 minutes at 10,000 ×g), and the PBS was decanted. An aliquot (70 µl) of molecular biology-grade

water (Hyclone; Thermo Scientific, Pittsburgh, PN, USA) and a small scoop of 0.10 μm glass beads (Sigma-Aldrich, St. Louis, MO, USA) was added to the pellet, and the tube was agitated for 20 seconds at speed 4.0 in a cell homogenizer (FastPrep®-24 Instrument; MP Biomedicals, Inc, Solon, OH, USA). The solution was centrifuged (5 minutes at 10,000 ×g) and 50 μL was removed to a clean tube and stored at −20°C pending PCR.

PCR was conducted using 0.2 mM each of a Bacterial-domain primer (8F (Delong 1992)) and a Universal primer (1492R (Fry et al. 1997)), PCR 2× Master Mix (Fermentas Molecular Biology Tools; Thermo Scientific, Pittsburgh, PN, USA), and 0.1 mg/ml bovine serum albumin (BSA). A 96-well thermocycler (EppendorfMastercyclerep realplex, Hauppauge, NY, USA) was programmed for 3 minutes at 94°C followed by 34 cycles of 94°C for 30 seconds, 52°C for 45 seconds, and 72°C for 1 minute. It finished with 4 minutes at 72°C and was held at 4°C until sample removal. PCR products were cleaned either by ethanol precipitation or using an UltraClean PCR clean up DNA Purification kit (Mo Bio Laboratories, Inc; Carlsbad, CA, USA). Cleaned PCR products were transformed into pCR™ 4-TOPO® plasmid vector using a TOPO TA cloning for sequencing kit (Invitrogen Corporation; Carlsbad, CA, USA). Plasmids were purified using the Invitrogen PureLink (K2100-10, Carlsbad, CA, USA) plasmid prep kit. Sequencing was completed using the SimpleSeq DNA Sequencing Service (Eurofins MWG Operon, Huntsville, AL, USA) or sequence reactions were conducted using BigDye 3.1 Ready Reaction Mix (Applied Biosystem, Foster City, CA, USA) at the Comparative Genomics Center at the University of Washington using a 3130xl Genetic Analyzer (Applied Biosystems; Foster City, CA, USA). Sequencing primers were 8F, 1492R, and, when needed for full coverage, 907R (Teske et al. 1996) in separate reactions.

16S rRNA gene sequence information was obtained using the three primers and was compiled using Sequencher software (version 4.9, Gene Codes Corporation, Ann Arbor, MI, USA). The sequences were submitted to the NCBI BLAST database (National Center for Biotechnology Information (NCBI); http://www.ncbi.nlm.nih.gov/BLAST/) to identify close relatives. Alignment was done using ARB alignment software version 5.1 (Ludwig et al. 2004). These sequences are stored in GenBank under accession numbers JX879736 to JX879745 and JN940802.

4.4.5 High pressure liquid chromatography quantification including solid phase extraction and concentration

Samples from various bacterial degradation experiments were analyzed for total PPCP (triclosan, bisphenol A, naproxen, ibuprofen, gemfibrozil, carbamazepine, E1, E2, or EE2) concentrations. Samples

from the well-mixed flask or bottle were taken and preserved by mixing with an equal volume of acetonitrile, which also extracted the sorbed PPCP from bacterial solids, followed by centrifugation for 10 minutes at 10,000 ×g. Decanted samples were stored at 4ºC and analyzed within a month. A high pressure liquid chromatography instrument with ultraviolet detector (HPLC-UV, DionexUltiMate 3000; Sunnyvale, CA, USA) was used to measure PPCP concentrations in the mg/L range. A liquid chromatography tandem mass spectrometer instrument (LC-MS/MS) comprised of a Shimadzu HPLC equipped with a 4000 Q Trap Tandem Mass Spectrometer (Applied Biosystems Inc; Carlsbad, CA, USA) was used to measure PPCP concentrations in the µg/L and ng/L range. Methods were optimized for each PPCP, using a C8 or C18 column with a mobile phase comprised of acetonitrile or methanol. Further details are provided in Online Resource Table 4.7. Levels of quantification were determined by Standard Methods 1-10 (AWWA 1998).

$$LLD = 3.3s \quad \text{(Eq 4.1)}$$

Where LLD is the lower level of detection and s is the standard deviation of the lowest standard.

$$LOQ = 5LLD \quad \text{(Eq 4.2)}$$

Where LOQ is the level of quantification and the ratio of LLD: LOQ is 1:5.

Solid phase extraction (SPE) followed by measurement on the LC-MS/MS was used to determine triclosan, bisphenol A, ibuprofen, and gemfibrozil concentrations in the ng/L range. Details of this method are in the Online Resource.

E1, E2, and EE2 samples in the µg/L and ng/L concentration ranges were processed using the following method (Anari et al. 2002). Internal standards (50 pg of each d_4E1, d_4E2, and d_4EE2) were added to 500 µL samples. Liquid-liquid extraction was performed with 3 mL of ethyl acetate, and the organic fraction was transferred to a clean tube (8 mL overflow volume) and evaporated to dryness with a gentle stream of nitrogen gas while suspended in a water bath at 40°C. Samples were reconstituted with 100 µL of $NaHCO_3$ buffer (pH 10.5) and 100µL of 1 mg/mL dansyl chloride in acetonitrile and heated at 60°C for 30 minutes.

4.4.6 Measure of microbial growth

Two methods of measuring microbial growth were used. Optical density (OD) measurements were taken when frequent growth measurements were needed and were used in modeling growth of the bacteria. Volatile suspended solids (VSS) concentrations were determined for inocula concentrations and final biomass concentrations and were used in modeling degradation.

The OD at 600 nm was used to monitor active microbial growth in R2A medium and LB broth (Hach DR/4000U Spectrophotometer, Loveland, CO, USA). The path length was 1 cm. ODs over 1.0 were diluted 1:1 with deionized (DI) water and remeasured. The limit of quantification (LOQ) in both R2A medium and LB broth was approximately 0.01.

VSS concentrations were measured using Standard Method 2540E (AWWA 1998). Briefly, VSS concentrations were determined by vacuum filtering samples through prepared glass microfiber filters (Whatman, Piscataway, NJ, USA) and then drying the filters at 105ºC (oven weight) and 500ºC (furnace weight). The VSS concentration was calculated by the difference in the oven weight (in mg) and the furnace weight (in mg) divided by the volume filtered (in L).

4.4.7 Experimental methods

4.4.7.1 Degradation of non-target PPCPs (Experiment 1)

Isolates were tested to see if they could degrade PPCPs other than the one used in their isolation (non-target PPCPs). This was investigated using 1 mg/L of an individual PPCP in R2A medium. Headspace to solution volumes were maintained at 1:1. An aliquot (10 µL) of culture actively growing in R2A was inoculated into 5 mL of fresh medium containing the test PPCP. PPCP concentrations were measured after growth of the bacteria was observed. If degradation was seen, tests were repeated to confirm results. Uninoculated sterile controls contained 1 mg/L of the test PPCP in R2A medium.

4.4.7.2 Degradation to low residual concentrations (Experiment 2)

Experiments to determine PPCP residual concentrations were completed in mineral medium, 10% R2A medium, 100% R2A medium, or LB broth. Bacteria were grown using R2A medium or LB broth prior to batch tests. Aliquots of bacteria inocula were pelleted by centrifugation (4000 ×g for 30 minutes at 4ºC) and resuspended in a small portion of the experimental medium as a way to start experiments with a known biomass concentration. Uninoculated sterile controls were prepared the same as the experiments. At the end of the test, samples were concentrated by solid phase extraction (SPE) and quantified by LC-MS/MS. TrD22, EsD8, EsD18, EsD20, and GeD10 experiments were duplicated. Multiple experiments were completed for TrD23, TrD34, BiD10, BiD32, and IbD51. Multiple experiments and duplicates were completed for TrD1.

4.4.7.3 Substrate range testing (Experiment 3)

The range of substrates on which the isolates could grow was studied. The substrates tested include casamino acid, proteose peptone, tryptone, whey protein, yeast extract, molasses, dextrose, fructose,

lactose, starch, acetate, ethanol, glycerol, and pyruvic acid. Mineral and R2A media were used as negative and positive controls, respectively. High concentration stock solutions of the substrates were prepared gravimetrically and autoclaved. They were then combined with filter sterilized mineral medium to obtain an initial calculated concentration of 0.5 g/L substrate. Headspace to solution volumes were maintained at 1:1. An aliquot (10 µL) of culture actively growing in R2A was inoculated into 5 mL of fresh medium containing the test PPCP. Bacterial growth was measured using OD.

4.4.7.4 Growth and degradation in carbon-rich media (Experiment 4)

Growth of isolates and degradation of PPCPs in the presence of other carbon sources was completed in R2A medium or LB broth with approximately 1 mg/L of the target PPCP. Bacteria were grown using R2A medium or LB broth prior to batch tests. Aliquots of bacteria inocula were pelleted by centrifugation (4000 ×g for 30 minutes at 4ºC) and resuspended in a small portion of the experimental medium. Sequential inoculations were completed to allow for ease of monitoring the experiments over several days. Flasks were inoculated in the morning, in the afternoon in some cases, and in the evening. Uninoculated sterile controls contained 1 mg/L of the target PPCP in R2A medium or LB broth. OD and HPLC-UV samples were collected approximately each hour. Initial VSS concentrations were determined from measurements of the inocula and final VSS concentrations were measured directly for the experiments.

4.4.8 First order growth kinetics

Growth rates of the bacterial isolates were determined by first order kinetics.

$$\frac{dX_{OD}}{dt} = k_G X_{OD} \qquad \text{(Eq 4.3)}$$

Where dX_{OD}/dt is the rate of growth of the bacteria over time (OD/hr), k_G is the growth rate constant (hr^{-1}), and X_{OD} is the amount of bacterial isolate (OD). The integrated and linearized form was solved graphically to find k_G.

4.4.9 First order degradation kinetics

In a batch reaction, the rate of degradation is:

$$\frac{dc_t}{dt} = -k_c' X f_L c_t \qquad \text{(Eq 4.4)}$$

Where dc_t/dt is the rate of change in concentration over time (mg/L-hr), k_c' is the first order reaction coefficient normalized to biomass (L/mg-hr), X is the bacterial biomass (mg/L), c_t is the total concentration of the PPCP (mg/L), and f_L is the fraction of dissolved PPCP (assumed to be 1 at low

biomass levels). Biomass measurements corresponding to observations of degradation were used in the models. Assuming constant biomass, the integrated and linearized form was solved graphically to find k_c'.

4.5 Results

4.5.1 Cultivation of bacteria capable of degrading specific PPCPs

A method for isolating bacteria from activated sludge that degrade PPCPs was developed (Figure 4.1). Mineral medium containing 1 mg/L of an individual PPCP as the sole organic carbon and energy source was inoculated with municipal activated sludge (1% and/or 10% by volume). For one triclosan enrichment, minimal medium containing 1 mg/L triclosan was used. When PPCP degradation was observed, cultures were transferred (10% by volume) to fresh mineral medium containing 1 mg/L of the individual PPCP. When rapid degradation of the compound was observed, 1% by volume was transferred. After the activated sludge inoculum was diluted to approximately 10^{-8} of its original concentration by successive transfers, the enrichment was spread plated on R2A agar augmented with the individual PPCP. Colonies representing different morphologies were picked and tested for their ability to degrade the PPCP in R2A medium. Using this approach, the ratio of isolates obtained that degraded the PPCP to isolates with no degradation abilities was approximately 1:20. Attempts to obtain colonies in cultures without sufficient activated sludge dilution resulted in obtaining no isolates with degradation capabilities.

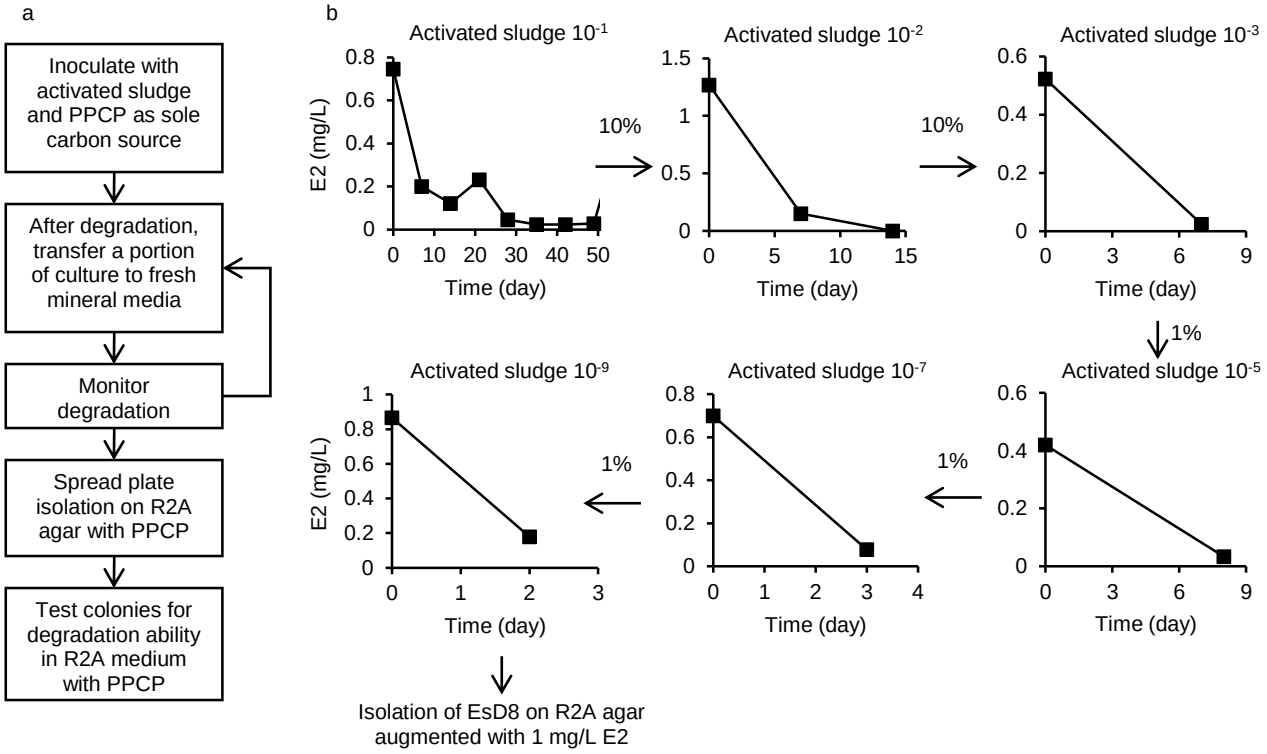

Figure 4.1. Enrichment and isolation process. (a) Overall process and (b) example isolation of a 17β-estradiol (E2) degrading bacteria

An example of the isolation process is shown for bacterium designated EsD8, an E2 degrading bacteria, isolated from Snoqualmie wastewater facility's activated sludge (Figure 4.1). The original enrichment was transferred five times until the activated sludge was diluted to 10^{-9} of the original concentration. The final transfer degraded E2 within 3 days, and it was spread plated on solid R2A augmented with 1 mg/L E2. Ten colonies were tested for their degradation ability in R2A medium with 1 mg/L E2. Two colonies (EsD7 and EsD8) were initially able to degrade E2 below the LOD of the HPLC. The E2 degradation ability of ED7 was lost in the next round of transfers however. Five other colonies were able to degrade E2 by greater than 50%, and three colonies were not able to degrade E2. This cultivation and isolation process was completed in 10 weeks. Other cultivation and isolation procedures took longer; for example, the isolation of BiD10 was completed in 19 weeks and the isolation of BiD32 was completed in 15 weeks.

4.5.2 Description of bacterial isolates

Eleven bacteria were isolated (Table 4.1) including two bisphenol A, four triclosan, one ibuprofen, three E2, and one gemfibrozil degrading bacteria. One of the triclosan degrading bacteria, TrD1, isolated on minimal medium, requires a vitamin mixture to grow and to degrade triclosan. Bacteria capable of degrading EE2 and carbamazepine have yet to be isolated. EE2 degradation is seen in early transfers in several enrichments but has not been maintained long enough to attempt isolation. No evidence of carbamazepine biodegradation has yet been seen. 16S rRNA genes sequences showed that a diverse group of bacteria were isolated, but with a preponderance of sphingomonads (Figure 4.2). Seven of the eleven bacterial isolates were sphingomonads, one was a *Nubsella* sp. and the others, EsD8, EsD20, and GeD10, were Gram positive bacteria. The bacteria isolated in this manuscript have 97% or greater similarity to known species (with the exception of one) (Table 4.1).

Table 4.1. Representative overview of the bacterial isolates that can degrade various pharmaceutical and personal care products

Bacterial ID	Lowest reported degradation level (ng/L)	Number of: experiments (this study) bacterial isolates (previously reported)	Identification, Max Identity BLAST Score	Citation
Bacteria degrading triclosan				
TrD22	8340	2	*Novosphingobium* sp., 98%	This study
TrD23	2.1	6	*Sphingomonas* sp., 98%	This study
TrD34	4.3	2	*Sphingomonas* sp., 99%	This study
TrD1	0.5	9	*Sphingopyxis* sp., 99%	This study
TriRY	10000	6	*Pseudomonas putida*	Meade et al. 2001
Bacteria degrading bisphenol A				
BiD10	<2.5	5	*Sphingopyxis* sp., 98%	This study
BiD32	4.2	4	*Sphingobium* sp., 98%	This study
B-16	<13000	22	*Achromobacter xylosoxidans*	Zhang et al. 2007
Bacteria degrading ibuprofen				
IbD51	0.2	3	*Sphingobium* sp., 97%	This study
Ibu-2	Not reported	1	*Sphingomonas* sp.	Murdoch and Hay 2005
Bacteria degrading 17β-estradiol				
EsD8	5.9	2	*Isoptericola* sp., 98%	This study
EsD18	3240	2	*Nubsella* sp., 95%	This study
EsD20	8.6	2	*Rhodococcus* sp., 99%	This study
BP 10	1.8	38	*Acinetobacter* sp.	Pauwels et al. 2008
Bacteria degrading gemfibrozil				
GeD10	57	2	*Bacillus* sp., 99%	This study

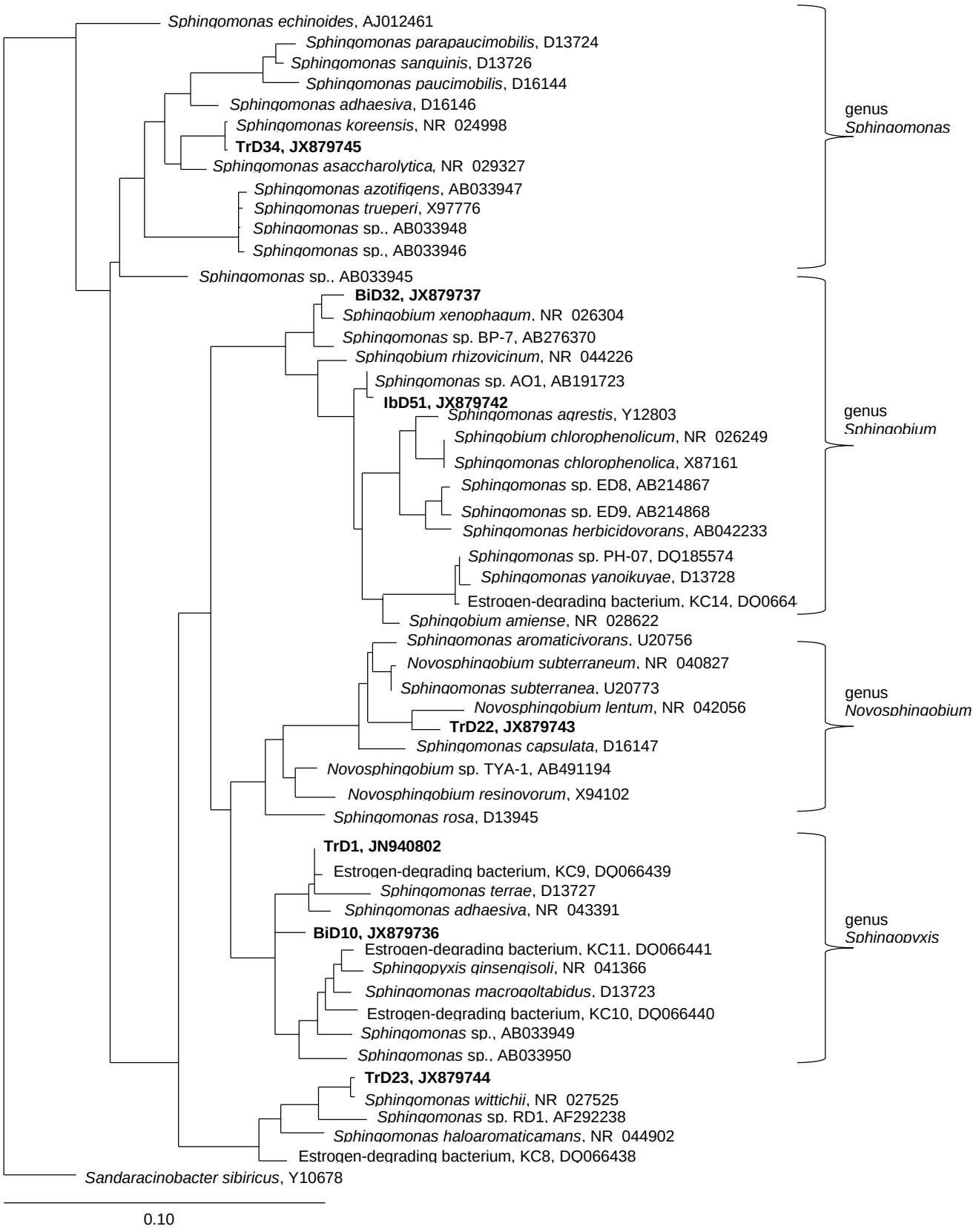

Figure 4.2. Phylogenetic relationship of the 16S rRNA gene of BiD10, BiD32, TrD22, TrD23, TrD34, TrD1, and IbD51 compared to the sphingomonads. Genus designations correspond to those recommended by Takeuchi et al. 2001.

Most bacteria were able to degrade some PPCPs other than the one used for isolation (Experiment 1, Table 4.2). Exceptions included BiD32, TrD34, and EsD8. Generally, isolates degraded two to three of the PPCPs tested. However, IbD51 and GeD10 were able to degrade most PPCPs tested with the exception of bisphenol A for IbD51 and carbamazepine for both. No isolates were able to degrade carbamazepine. Of interest, TrD23 degraded naproxen below the LOQ, TrD1 degraded ibuprofen and E2 below the LOQ, and GeD10 degraded ibuprofen below the LOQ. BiD10 was not able to grow in the presence of triclosan or naproxen and BiD32 was not able to grow in the presence of triclosan. Uninoculated sterile controls showed no degradation of the PPCPs. The ability of the bacteria to degrade PPCPs other than the one used for isolation could be due to similarity in the chemical structures of the PPCPs. All PPCPs studied have at least one aromatic ring and some having the same functional groups; for example, gemfibrozil, ibuprofen, and naproxen all have a carboxylic acid group.

Table 4.2. Range of degradation ability

	BiD10	BiD32	TrD22	TrD23	TrD34	TrD1	IbD51	EsD8	EsD20	GeD10
Triclosan	0%[a]	0% [a]	100%	100%	100%	100%	>50%	0%	0%	<50%
Ibuprofen	<50%	0%	<50%	0%	0%	100%	100%	0%	100%	100%
Bisphenol A	100%	100%	0%	0%	0%	0%	0%	0%	<50%	<50%
Naproxen	0% [a]	0%	0%	100%	0%	0%	<50%	0%	0%	<50%
Gemfibrozil	0%	0%	0%	0%	0%	0%	<50%	0%	0%	100%
Carbamazepine	0%	0%	0%	0%	0%	nt	0%	0%	nt	nt
Estrone	0%	0%	<50%	<50%	0%	0%	>50%	0%	<50%	>50%
17β-estradiol	0%	0%	0%	0%	0%	100%	<50%	100%	100%	>50%
17α-ethinylestradiol	0%	0%	0%	0%	0%	0%	<50%	0%	0%	<50%

100%, to LOQ; >50%, >50% degradation; <50%, <50% degradation; 0%, no degradation detected; nt, not tested
[a] No growth occurred

4.5.3 Degradation to low ng/L concentrations

The lowest PPCP concentrations the bacteria were able to degrade to were determined (Experiment 2, Table 4.1). Three isolates (TrD22, EsD18, and GeD10) were not able to degrade the PPCPs in mineral medium alone, but could in R2A medium. Eight of the eleven isolated bacteria degraded PPCPs from µg/L concentrations to low ng/L concentrations, one bacterial isolate, GeD10, degraded gemfibrozil to <60 ng/L from µg/L concentrations, and two bacterial isolates were only able to degrade to µg/L concentrations, TrD22 and EsD18. Uninoculated sterile controls showed no degradation of the PPCPs. Values reported were the lowest residual concentrations from several experiments and/or replicates. All values were less than 30 ng/L with the exception of those from TrD22, EsD18, and GeD10 experiments.

4.5.4 Growth and degradation in presence of other carbon sources

The ability of the bacterial isolates to grow on a range of carbon sources is shown in Table 4.3 (Experiment 3). A variety of substrates were tested to determine which inexpensive, readily available carbon sources the bacteria could use for growth and to understand which constituents of the R2A medium were being used for growth. The bacteria did not grow using mineral medium (negative control) and all grew utilizing R2A medium (positive control). Of the components of R2A medium, casamino acids and proteose peptone were utilized by all bacterial isolates. All bacteria were able to grow using yeast extract except for TrD1. Glucose was used by BiD32, TrD22, TrD1, EsD8, and EsD20. Six of the bacteria used sodium pyruvate as a growth substrate, but only two of them were able to grow to a high OD. Soluble starch was the component of R2A medium least able to be utilized by the isolated bacteria; only three bacteria were able to partly grow using it. Sugars were most able to be used by BiD10, BiD21, TrD1, EsD8, and EsD20. Molasses, which contains sucrose, glucose, and fructose, was the only sugar tested that TrD23, TrD34, and IbD51 were able to utilize for growth. GeD10 was only able to grow slightly on starch out of the sugars tested. All bacteria were able to use substrates high in proteins. IbD51 was not able to use carbon sources other than protein-rich substrates. TrD23 and TrD34 also mainly used protein-rich substrates, with the exception of also utilizing acetate and pyruvic acid. TrD1 was able to partially grow on all substrates tested except ethanol and glycerol.

Table 4.3. Growth substrate range for bacterial isolates

		BiD10	BiD32	TrD22	TrD23	TrD34	TrD1	IbD51	EsD8	EsD20	GeD10
Protein-rich	Casamino acid	++	++	++	++	++	++	++	++	++	++
	Proteose Peptone	++	++	++	++	++	++	++	++	++	++
	Tryptone	++	++	++	++	++	++	++	++	++	++
	Whey protein	++	++	++	++	++	++	++	++	-	++
	Yeast Extract	++	++	++	++	++	-	++	++	++	++
	Molasses	-	++	nt	++	++	+	++	++	++	-
Sugars	Dextrose	-	+	++	-	-	++	-	++	++	-
	Fructose	++	+	-	-	-	++	-	++	++	-
	Lactose	++	++	-	-	-	+	-	-	-	-
	Starch	-	-	+	-	-	+	-	-	-	+
Other	Acetate	+	+	+	+	+	++	-	-	++	+
	Ethanol	+	-	-	-	-	-	-	++	++	-
	Glycerol	-	-	+	-	-	-	-	-	+	+
	Pyruvic acid	+	+	-	+	-	++	-	++	-	+
Controls	Mineral Medium	-	-	-	-	-	-	-	-	-	-
	R2A	++	++	++	++	++	++	++	++	++	++

-, no growth; +, growth below 0.1 optical density; ++, growth above 0.1 optical density; nt, not tested

PPCP degradation experiments at mg/L concentrations with concurrent growth of bacteria in R2A medium were completed (Experiment 4, Table 4.4, Online Resource Figure 4.4). Experiments were completed to determine if the bacteria would degrade the PPCP before growth on a nutrient-rich medium

and to obtain estimates of growth and degradation rates. Uninoculated sterile controls showed no degradation of the PPCPs. Example experiments are shown in Figure 4.3. When the sequential inoculations overlapped the replication was good. BiD32 degraded bisphenol A by 4.2 hours with no apparent degradation lag. Growth had begun by 11 hours when 10% of final OD was reached and was completed in 40 hours (Figure 4.3). BPA degradation was completed before measurable OD changes. In contrast, GeD10 completed degradation of gemfibrozil during late growth of GeD10 (Figure 4.3b). The degradation was completed after 14.3 hours whereas GeD10 had reached 75% of its final OD by 8.5 hours. Generally, bacteria followed the BiD32 pattern with PPCP degradation occurring before OD changes or during the early growth phase of the bacteria (before OD reached 25% of final OD). Exceptions include TrD22, EsD18, and GeD10, which degraded during late growth or after growth was completed and EsD8 and EsD20, which completed degradation before the bacteria reached 50% of its final OD. The growth rates of the bacteria were estimated using OD data and ranged from 0.06 to 0.61 hr^{-1}, with GeD10 having the fastest growth rate and TrD22 the slowest. Early and mid growth data points were chosen to calculate growth rates (Online Resource Figure 4.5), and data points before OD changes and after OD began leveling off were excluded. Bacterial isolates grew to final OD in 2 days or less with the exception of TrD22, which took 63 hours to grow. Degradation rates of the PPCP (k_c') by the bacteria were determined by linearization of PPCP concentrations versus time normalized to biomass with f_L assumed to be 1 (Online Resource Figure 4.6). Degradation rates were normalized to initial biomass, except for TrD22, EsD18, and GeD10 degradation rates, which were normalized to final biomass as degradation occurred during late growth or after growth was completed.

Table 4.4. Degradation of pharmaceutical and personal care products during growth in R2A medium

Bacterial ID	VSS added (mg/L)	Time to 25% of final OD (hour)	Time to final OD (hour)	Growth rate[a] (hr^{-1})	Apparent degradation lag[b] (hour)	Time to degradation below LLD (hour)	Degradation constant (k'_c)[c] (L/mg-hr)
BiD10	0.73	19.6	46	0.15	0	nd	0.21
BiD32	5.1	15.7	40	0.14	0	4.2	0.20
TrD22	8	33.9	63	0.06	30	80	8.5E-05
TrD23	5.9	17.9	24	0.13	0	8	0.17
TrD34	2.9	15.8	34	0.15	2	11.3	0.38
TrD1[d]	2.6	13.7	20	0.21	4	7	0.42
IbD51	4.3	8.7	18	0.20	0	6.2	0.13
EsD8	3.2	20.6	37	0.22	7	23	0.06
EsD18	10.9	8.9	17	0.12	20	120	2.3E-04
EsD20	6.7	9.6	22	0.23	2	10	0.11
GeD10	5.8	5.5	22	0.61	3.25	14.3	1.2E-03

LLD, lower level of detection
[a] Growth rate was calculated by Eq 4.3
[b] Apparent degradation lag was the time when the first change in concentration was observed
[c] Degradation constant was calculated by Eq 4.4
[d] Completed in 10% LB broth

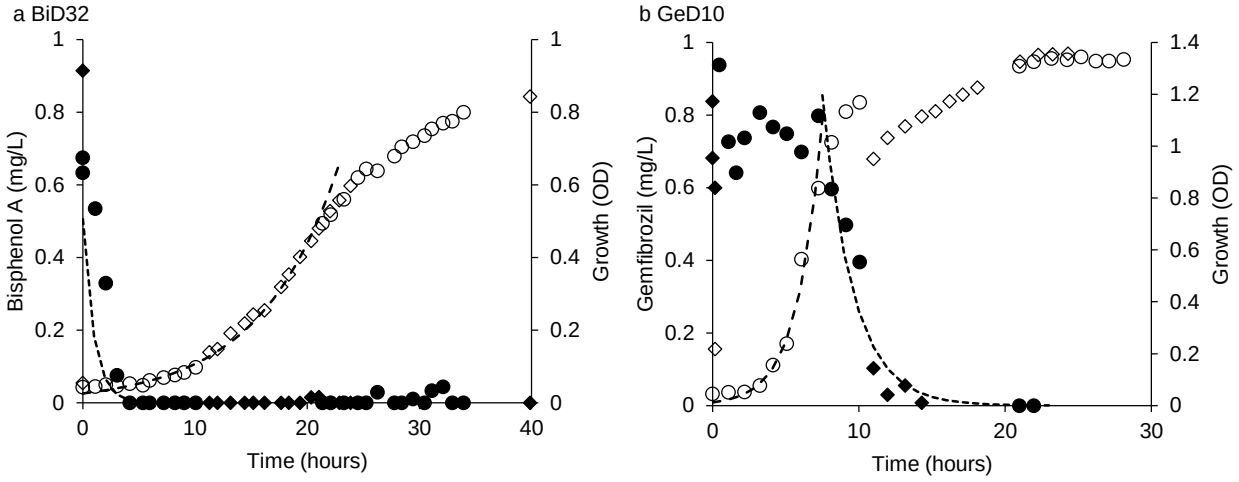

Figure 4.3. Growth of (a) BiD32 during the degradation of bisphenol A and (b) GeD10 during the degradation of gemfibrozil. Open markers represent growth of isolate and closed markers represent degradation. Circles and diamonds represent separate bottles. Dashed lines represent growth and degradation based on kinetic constants extracted from the data. Other bacteria and graphs showing fitted kinetic constants are shown in Online Resource Figure 4.4.

4.6 Discussion

This study reports an approach for isolating bacteria from activated sludge to meet requirements of bioaugmentation, and provides data on eleven isolated bacteria capable of degrading five different PPCPs.

Eight of these bacteria degraded PPCPs to concentrations less than 10 ng/L, suggesting that they can have a positive influence on removal in WWTPs if present at sufficient concentrations (Table 4.1). Currently, PPCPs studied have a range of average effluent concentrations from <10 to 1100 ng/L for triclosan (Yang et al. 2011; Stasinakis et al. 2008), 4 to 1600 ng/L for bisphenol A (Ballesteros-Gomez et al. 2007; Duong et al. 2010), 7 to 10160 ng/L for ibuprofen (Gross et al. 2004; Santos et al. 2007), 0.1 to 19 ng/L for E2 (Duong et al. 2010; Zhang et al. 2011), and 4 to 730 ng/L for gemfibrozil (Gross et al. 2004; Paxeus 2004). In many cases, the addition of these bacteria could potentially reduce effluent concentrations in WWTPs.

Eight of the isolated bacteria met the criteria for bioaugmentation including BiD10, BiD32, TrD23, TrD34, TrD1, IbD51, EsD8, and EsD20. Three isolated bacteria do not meet the criteria for bioaugmentation, and bacteria that degrade EE2 and carbamazepine have yet to be isolated. For successful bioaugmentation, it is necessary for the bacteria to degrade PPCPs to levels substantially below typical WWTP effluent concentrations to cause an effect when bioaugmented (criterion 1). Eight bacteria degraded PPCPs to less than 10 ng/L; however three other bacteria, TrD22, EsD18, and GeD10, did not reach these low levels. Bacteria must be able to grow using readily available carbon sources and maintain the ability to degrade the PPCP (criterion 2), since in a bioaugmentation application, bacteria will be grown up in a side stream reactor on a carbon source before addition to a biological treatment process. These isolated bacteria grew using a variety of carbon sources (Table 4.3) with protein-rich substrates supporting the best growth results for the widest range of bacteria. All isolated bacteria were able to maintain the ability to degrade PPCPs after being grown up in the absence of the PPCP, which is important as the PPCP may or may not be present in the side reactor when grown. Eight of the bacteria were able to degrade the PPCP preferentially in the presence of higher concentrations of other substrates (criterion 3). When the bacteria are grown they will then be fed into the activated sludge portion of the WWTP where there will be many carbon sources at much higher concentrations then the PPCP. Therefore, it is important that the bacteria are able to degrade the PPCP in complex media (Table 4.4). Eight of the isolated bacteria met this criterion with the PPCP degradation completed before bacteria reached 50% of final OD, and in most cases even before 25% or 10% of final OD. Degradation of the PPCP before growth could be due to the PPCP being the preferred growth substrate or, in the case of an antimicrobial such as triclosan, the PPCP being inhibitory to the growth of the bacteria. Finally, the bacteria must degrade the PPCP with favorable kinetics so the bioaugmentation of these isolates can result in low PPCP concentrations (criterion 4). Degradation rates by the bacterial isolates are greater than 0.06 L/mg-hr with the exception of TrD22, EsD18, and GeD10, which had very low specific degradation rates. Eight of the bacteria met all criteria for bioaugmentation, and three of the bacteria did not meet the

criteria for bioaugmentation: TrD22, EsD18, and GeD10, and were excluded from further bioaugmentation studies as they did not degrade to ng/L concentrations, degrade before growth in complex media, and have favorable degradation kinetics.

The bacteria identified as capable of degrading PPCPs were diverse representing four phyla including proteobacteria, firmicutes, bacteroidetes, and actinobacteria (Figure 4.2). Others have reported PPCP degradation abilities among the same phyla (Hay et al. 2001; Kim et al. 2011; Kurisu et al. 2010; G. Li et al. 2012; Z. Li et al. 2012; Oshiman et al. 2007; Pauwels et al. 2008; Roh and Chu 2010; Sakai et al. 2007; Toyama et al. 2009; Yu et al. 2007). The diversity of isolated bacteria with PPCP degradation ability might also be explained by the transfer of these genes by mobile genetic units such as plasmids that have been associated with xenobiotic degradation by the sphingomonads (Stolz 2009). Seven of the ten bacterial isolates were sphingomonads. Several sphingomonads have been previously isolated which biodegrade various xenobiotics including triclosan (Hay et al. 2001; Kim et al. 2011), bisphenol A (Oshiman et al. 2007; Sakai et al. 2007; Toyama et al. 2009), ibuprofen (Murdoch and Hay 2005), and E2 (Kurisu et al. 2010; Yu et al. 2007). Figure 4.2 shows the relations of this study's sphingomonad bacterial isolates and previously isolated bacteria. The relation of the 16S rRNA gene does not predict degradation ability with IbD51 related to a bisphenol A degrading bacteria, AO1 (Oshiman et al. 2007), TrD1 and BiD32 related to an E2 degrading bacteria, KC9 (Yu et al. 2007), and KC14, an E2 degrading bacteria, related to a triclosan degrading bacteria, PH-07 (Yu et al. 2007; Kim et al. 2011).

The bacterial isolates reported in this study represent the first bacteria capable of degrading specific PPCPs to ng/L concentrations, with the exception of six E2 degraders (Online Resource Table 4.5). BP 1, 2, 3, 7, 8, and 10 were capable of degrading E2 to 1.8 ±0.4 ng/L (Pauwels et al. 2008), lower than the concentrations reached by the E2 degraders reported in this study. All other previously isolated E2 degraders reported concentrations of <1000 ng/L or greater though. The lowest reported concentration of triclosan is 10,000 ng/L by *Pseudomonas putida* TriRY (Meade et al. 2001) compared to <5 ng/L concentration by three of the triclosan degraders from this study. The bisphenol A degrading bacteria, *Achromobacter xylosoxidans* B-16, reached a residual concentration of <13,000 ng/L (Zhang et al. 2007) compared to <5 ng/L concentration by both bisphenol A degraders from this study. While GeD10 does not reach low ng/L concentrations, it is of interest as the first reported gemfibrozil degrading bacteria. Many other previously isolated PPCP degrading bacteria resulted in higher residual concentrations reported or no reported concentrations due to limitations of the analytical methods used.

Future work should focus on further determining the suitability for bioaugmentation, including experiments with bacteria doses in activated sludge to determine degradation rates in a complex microbial community where sorption affects availability of the PPCPs and competition and predation may affect the viability of the added bacteria. This knowledge, with degradation rates determined in this study, could then be used to model biological reactors to determine the needed dosage of bacterial isolates to reach desired PPCP effluent concentrations.

4.7 Acknowledgements

Funding was provided by the National Science Foundation (CBET 0829132) and the King County Fellowship Program. We thank Venkateswarlu Nanaboina for his assistance developing LC-MS/MS methods.

4.8 Online Resource (Supplementary Information)

Table 4.5. Residual concentrations achieved with newly reported bacterial isolates in comparison to previously reported levels

Organism	Lowest reported degradation level (ng/L)	Citation
Bacteria degrading triclosan		
Sphingopyxis sp. TrD1	0.5	This study
Sphingomonas sp. TrD23	2.1	This study
Sphingomonas sp. TrD34	4.3	This study
Novosphingobium sp. TrD22	8340	This study
Pseudomonas putida TriRY	10,000	Meade et al. 2001
Alcaligenes xylosoxidans subsp. *denitrificans* TR1	20,000	Meade et al. 2001
Sphingomonas sp. PH-07	7,500,000	Kim et al. 2011
Sphingomonas sp. Rd1	325,000,000	Hay et al. 2001
Nitrosomonas europaea	not reported	Roh et al. 2009
KCY1	not reported	Lee et al. 2012
Bacteria degrading bisphenol A		
Sphingopyxis sp. BiD10	2.6	This study
Sphingobium sp. BiD32	4.2	This study
Achromobacter xylosoxidans B-16	<13,000	Zhang et al. 2007
Pseudomonas sp. KA4	89,000	Kang and Kondo 2002
Streptomyces sp.	<100,000	Kang et al. 2004
Pseudomonas putida KA5	112,000	Kang and Kondo 2002
Sphingomonas sp. WH1	<890,000	Ronen and Abeliovich 2000
Sphingomonas bisphenolicum AO1	<1,000,000	Oshiman et al. 2007
Cupriavidus basilensis JF1	3,900,000	Fischer et al. 2010
Bacillus sp. GZB	not reported	Li et al. 2012
MV1	not reported	Lobos et al. 1992
Pseudomonas paucimobilis FJ-4	not reported	Ike et al. 1995
Pseudomonas monteilii N-502	not reported	Masuda et al. 2007
Sphingomonas sp. SO11	not reported	Matsumura et al. 2009
Sphingomonas sp. SO1a	not reported	Matsumura et al. 2009
Sphingomonas sp. SO4a	not reported	Matsumura et al. 2009
Bacillus sp. YA27	not reported	Matsumura et al. 2009
Nitrosomonas europaea	not reported	Roh et al. 2009
Sphingomonas sp. BP-7	not reported	Sakai et al. 2007
Novosphingobium sp. TYA-1	not reported	Toyama et al. 2009
Bacillus pumilus BP-2CK	not reported	Yamanaka et al. 2007
Bacillus pumilus BP-21DK	not reported	Yamanaka et al. 2007
Bacillus pumilus BP-22DK	not reported	Yamanaka et al. 2007
Sphingomonas yanoikuyae BP-11R	not reported	Yamanaka et al. 2008
Bacteria degrading ibuprofen		
Sphingobium sp. IbD51	0.7	This study
Sphingomonas sp. Ibu-2	not reported	Murdoch and Hay 2005
Bacteria degrading 17β-estradiol		
Acinetobacter sp. BP 10	1.8±0.4	Pauwels et al. 2008

Phyllobacterium myrsinacearum BP 1	1.8±0.4	Pauwels et al. 2008
Ralstonia pickettii BP 2	1.8±0.4	Pauwels et al. 2008
Pseudomonas aeruginosa BP 3	1.8±0.4	Pauwels et al. 2008
Pseudomonas sp. BP 7	1.8±0.4	Pauwels et al. 2008
Acinetobacter sp. BP 8	1.8±0.4	Pauwels et al. 2008
Isoptericola sp. EsD8	5.9	This study
Rhodococcus sp. EsD20	8.6	This study
Rhodococcus zopfii Y 50158	<1,000	Yoshimoto et al. 2004
Rhodococcus equi Y 50155	<1,000	Yoshimoto et al. 2004
Rhodococcus equi Y 50156	<1,000	Yoshimoto et al. 2004
Rhodococcus equi Y 50157	<1,000	Yoshimoto et al. 2004
Novosphingobium tardaugens ARI-1	<1,000	Fujii et al. 2002
Nubsella sp. EsD18	3240	This study
Rhodococcus sp. KC4	<5,000	Yu et al. 2007
Sphingomonas sp. KC8	<5,000	Yu et al. 2007
Stenotrophomonas maltophilia ZL1	20,000	Li et al. 2012
Mycobacterium sp. MI21.2	60,000	Isabelle et al. 2011
Aminobacter sp. KC7	100,000	Yu et al. 2007
Ochrobactrum sp. MI9.3	140,000	Isabelle et al. 2011
Pseudomonas sp. MI14.1	300,000	Isabelle et al. 2011
Ochrobactrum sp. MI6.1B	610,000	Isabelle et al. 2011
Aminobacter sp. KC6	750,000	Yu et al. 2007
Sphingomonas sp. KC14	800,000	Yu et al. 2007
Rhodococcus sp. ED6	<20,000,000	Kurisu et al. 2010
Rhodococcus sp. ED7	<20,000,000	Kurisu et al. 2010
Rhodococcus sp. ED10	<20,000,000	Kurisu et al. 2010
Sphingomonas sp. ED8	<20,000,000	Kurisu et al. 2010
Sphingomonas sp. ED9	<20,000,000	Kurisu et al. 2010
Flavobacterium sp. KC1	not reported	Yu et al. 2007
Terrimonas sp. KC2	not reported	Yu et al. 2007
Nocardioides sp. KC3	not reported	Yu et al. 2007
Microbacterium sp. KC5	not reported	Yu et al. 2007
Sphingomonas sp. KC9	not reported	Yu et al. 2007
Sphingomonas sp. KC10	not reported	Yu et al. 2007
Sphingomonas sp. KC11	not reported	Yu et al. 2007
Brevundimonas sp. KC12	not reported	Yu et al. 2007
Escherichia sp. KC13	not reported	Yu et al. 2007
Nitrosomonas europaea	not reported	Shi et al. 2004
Acinetobacter sp. LHJ1	not reported	Ke et al. 2007
Agromyces sp. LHJ3	not reported	Ke et al. 2007
Sphingomonas sp. CYH	not reported	Ke et al. 2007
Bacteria degrading gemfibrozil		
Bacillus sp. GeD10	57	This study

4.8.1 Materials and Methods

4.8.1.1 Reagents and chemicals

4.8.1.1.1 PPCP

Triclosan (99.8% purity) was obtained from EMD Chemicals, Inc. (Calbiochem, Gibbstown, NJ). Bisphenol A (>99% purity), naproxen (meets USP specifications), ibuprofen (meets USP specifications), gemfibrozil (suitable for 1694 per US EPA), carbamazepine (meets USP specifications), E1 (>99% purity), E2 (>99% purity), and EE2 (>99% purity) were obtained from Sigma Aldrich (St. Louis, MO, USA). Estrone-2,4,16,16-d_4 (d_4E1) (>98% purity), 17β-estradiol-2,4,16,16-d_4 (d_4E2) (>98% purity), and 17α-ethynylestradiol-2,4,16,16-d_4 (d_4EE2) (>98% purity) were purchased from C/D/N Isotopes, Inc. (Quebec, Canada).

4.8.1.1.2 Media

Components of mineral media were obtained from the following companies. Potassium phosphate was obtained from EMD Chemicals, Inc. (Calbiochem, Gibbstown, NJ, USA). Sodium bicarbonate was obtained from Fisher Scientific (Pittsburgh, PA, USA). Sodium nitrate was obtained from Sigma Aldrich (St. Louis, MO, USA).

Components of R2A media were obtained from the following companies. Yeast extract, sodium pyruvate, and dipotassium phosphate were obtained from Sigma Aldrich (St. Louis, MO, USA). Proteose peptone was obtained from HIMEDIA Laboratories (Mumbai, India). Casamino acid was obtained from BD (Franklin Lakes, NJ, USA). Sucrose and magnesium sulfate were obtained from JT Baker (Phillipsburg, NJ, USA). Soluble starch was obtained from Fisher Scientific (Pittsburgh, PA, USA).

4.8.1.1.3 Alternative carbon sources

Alternative carbon sources used for testing the range of substrates the bacteria could utilize for growth were obtained from the following companies. Fructose and lactose were obtained from Now Foods (Bloomingdale, IL, USA). Tryptone was obtained from BD (Franklin Lakes, NJ, USA). Whey protein was obtained from Nature's Best (Hauppauge, NY, USA). Glycerol was obtained from JT Baker (Phillipsburg, NJ, USA). Molasses was obtained from B&G Foods, Inc. (Parsippany, NJ, USA). Acetate was obtained from Fisher Scientific (Pittsburgh, PA, USA). Ethanol was obtained from Decon Laboratories, Inc. (King of Prussia, PA, USA).

4.8.1.1.4 Analytical reagents

Sodium bicarbonate ($NaHCO_3$) was obtained from EMD Chemicals, Inc. (Calbiochem, Gibbstown, NJ, USA). Dansyl chloride (≥99% purity) was obtained from Sigma Aldrich (St. Louis, MO, USA).

4.8.1.2 HPLC quantification including solid phase extraction and concentration

To quantify PPCP concentrations below the limit of quantification of the LC-MS/MS, samples were concentrated using either solid phase extraction (SPE) to assess liquid-phase PPCP or centrifugation followed by solid-liquid extraction to assess solid-bound PPCP. Samples were centrifuged (4000 ×g for 30 minutes at 4ºC). The supernatant was processed using an AutoTrace SPE Workstation (Caliper LifeSciences, now sold by Dionex, Sunnyvale, CA, USA) using C_{18} columns (Thermo Scientific 1000 mg/ 6 mL; Waltham, MA, USA). The columns were sequentially conditioned with 5 mL MTBE, 5 mL methanol, and 5 mL 18Ω Milli Q water. 180 mL of sample supernatant was pumped through the column, followed by a rinse with 5 mL of 5% methanol in water. The columns were then dried under nitrogen for 20 minutes, and the PPCP was eluted off of the columns using 4 mL of MTBE, followed by 5 mL of methanol. The eluent was evaporated under nitrogen, and the dried samples were dissolved in 1:1 acetonitrile:water. PPCP associated with the centrifuge pellet was quantified by resuspending the pellet in 10 mL MTBE followed by rapid vortexing and centrifugation (4000 ×g for 30 minutes at 4ºC). 8 mL of the MTBE was recovered, evaporated under nitrogen, and the dried samples were dissolved in 1:1 acetonitrile:water. The resuspended samples were analyzed by LC-MS/MS as described above. Percentage recovered in the liquid phase was determined by controls with known PPCP concentrations in 18Ω water and included in each SPE run with values >90%. Percentage recovered in the solid phase was determined by known PPCP concentrations added to bacterial isolate pellets and processed through with MTBE with values 60-100%, depending on compound.

Table 4.6. Final concentrations in vitamin solution (Tanner 1997)

Component	Concentration in final solution (mg/L)
Pyridoxine-HCl	0.10
Thymidine-HCl	0.05
Riboflavin	0.05
Calcium pantothenate	0.05
Thioctic acid	0.05
p-aminobenzoic acid	0.05
Nicotinic acid	0.05
Vitamin B_{12}	0.05
Mercaptoethanesulfonic acid	0.05
Biotin	0.02
Folic acid	0.02
Total concentration of vitamins	0.54

Table 4.7. PPCP quantification at mg/L, µg/L, and ng/L concentrations

PPCP	Triclosan	Bisphenol A	Ibuprofen	Naproxen	Gemfibrozil	Carbamazepine	Estrone	17β-estradiol	17α-ethinylestradiol
mg/L concentration range									
Column	A	A	A	A	A	B	C	C	C
Flow rate (ml/min)	0.5	0.5	0.5	0.5	0.5	1	1	1	1
Run time (minute)	15	15	15	15	15	10	6	6	6
Wavelength	280	275	220	230	280	285	200	200	200
Elution time (minute)	8.79	7	10.57	9.26	8.3	4.2	2.97	2.35	2.63
Injection volume (µL)	100	100	50	50	100	20	50	50	50
Lower level of detection (LLD, µg/L)	50	30	85	20	2.5	130	15	6	15
Level of quantification (LOQ, µg/L)	260	150	425	100	130	640	65	30	70
µg/L and ng/L concentration range									
Column	A	A	A	NA	A	NA	D	D	D
Flow rate (ml/min)	0.3	0.3	0.3	NA	0.3	NA	0.5	0.5	0.5
Run time (minute)	15	15	15	NA	15	NA	8	8	8
Detention time (minute)	7.9	6.36	6.95	NA	7.8	NA	3.58	3.29	3.38
Injection volume (µL)	10	10	10	NA	10	NA	20	20	20
LLD (ng/L)	100	150	150	NA	25	NA	1[a]	1[a]	1[a]
LOQ (ng/L)	460	750	750	NA	125	NA	5[b]	5[b]	5[b]
m/z, parent>product	287> 35	227> 212	205> 161	NA	249> 121	NA	504.2> 171.3	506.2> 171.3	530.0> 171.3

A is a Intersil ODS-3 C18 column (150 x 2 mm inner diameter, 5 µm particle size) from GL Sciences (Torrance, CA, USA)
B is an Alltima C18 column (250 x 4.6 mm inner diameter, 5 µm particle size) from W.R. Grace & Co. (Deerfield, IL, USA)
C is a Nova-Pak C8 column (150 x 3.9 mm inner diameter, 4 µm particle size) from Waters Co. (Milford, ME, USA)
D is a Phenomenex Luna Phenyl-Hexyl column (50 x 3 mm inner diameter, 3 µm particle size) from Phenomenex (Torrance, CA, USA)
NA, not applicable
[a] Limit of detection (signal to noise ratio of 3:1)
[b] Limit of quantification (signal to noise ratio of 10:1)

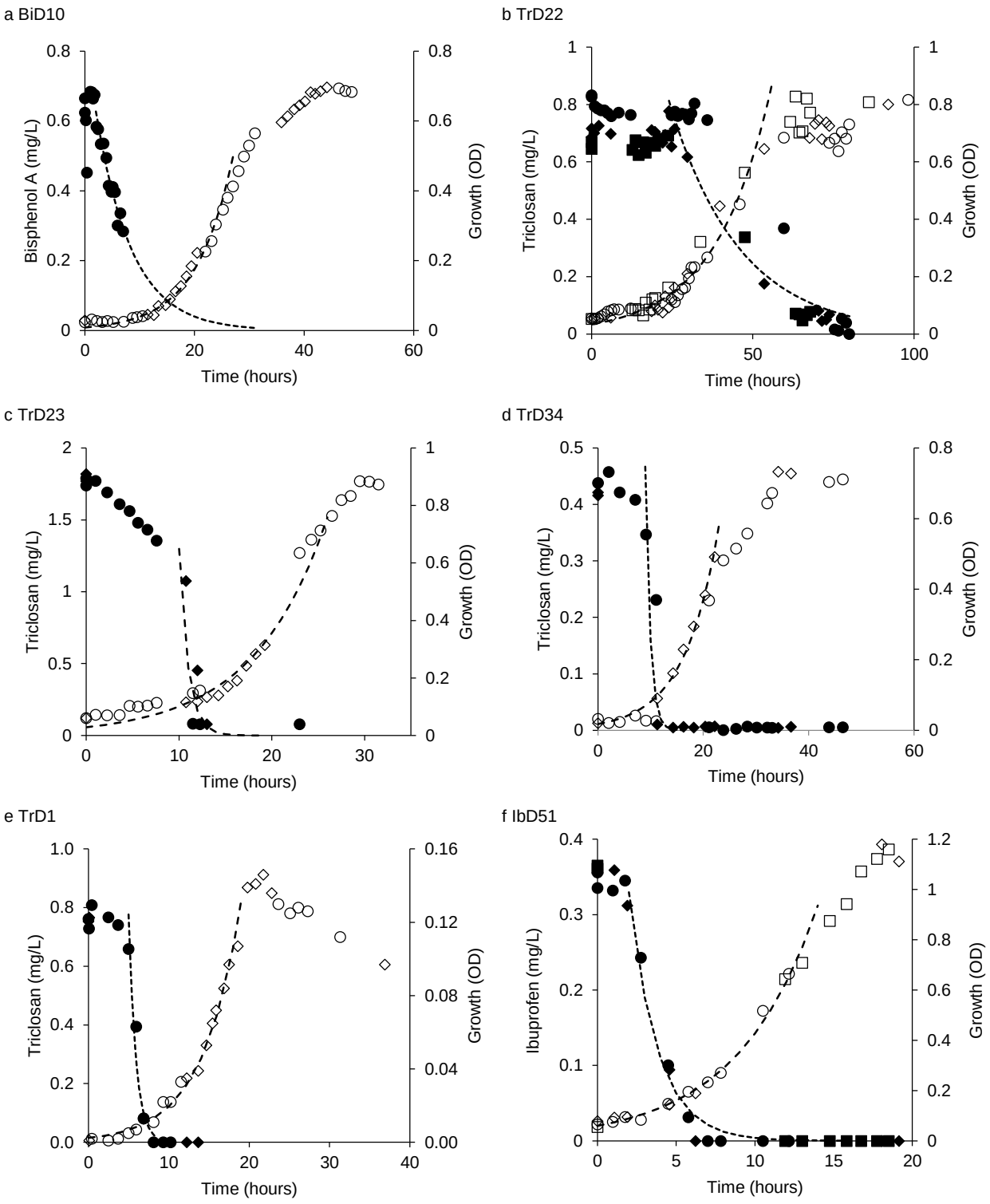
a BiD10
Bisphenol A (mg/L)
Growth (OD)
Time (hours)
b TrD22
Triclosan (mg/L)
Growth (OD)
Time (hours)
c TrD23
Triclosan (mg/L)
Growth (OD)
Time (hours)
d TrD34
Triclosan (mg/L)
Growth (OD)
Time (hours)
e TrD1
Triclosan (mg/L)
Growth (OD)
Time (hours)
f IbD51
Ibuprofen (mg/L)
Growth (OD)
Time (hours)

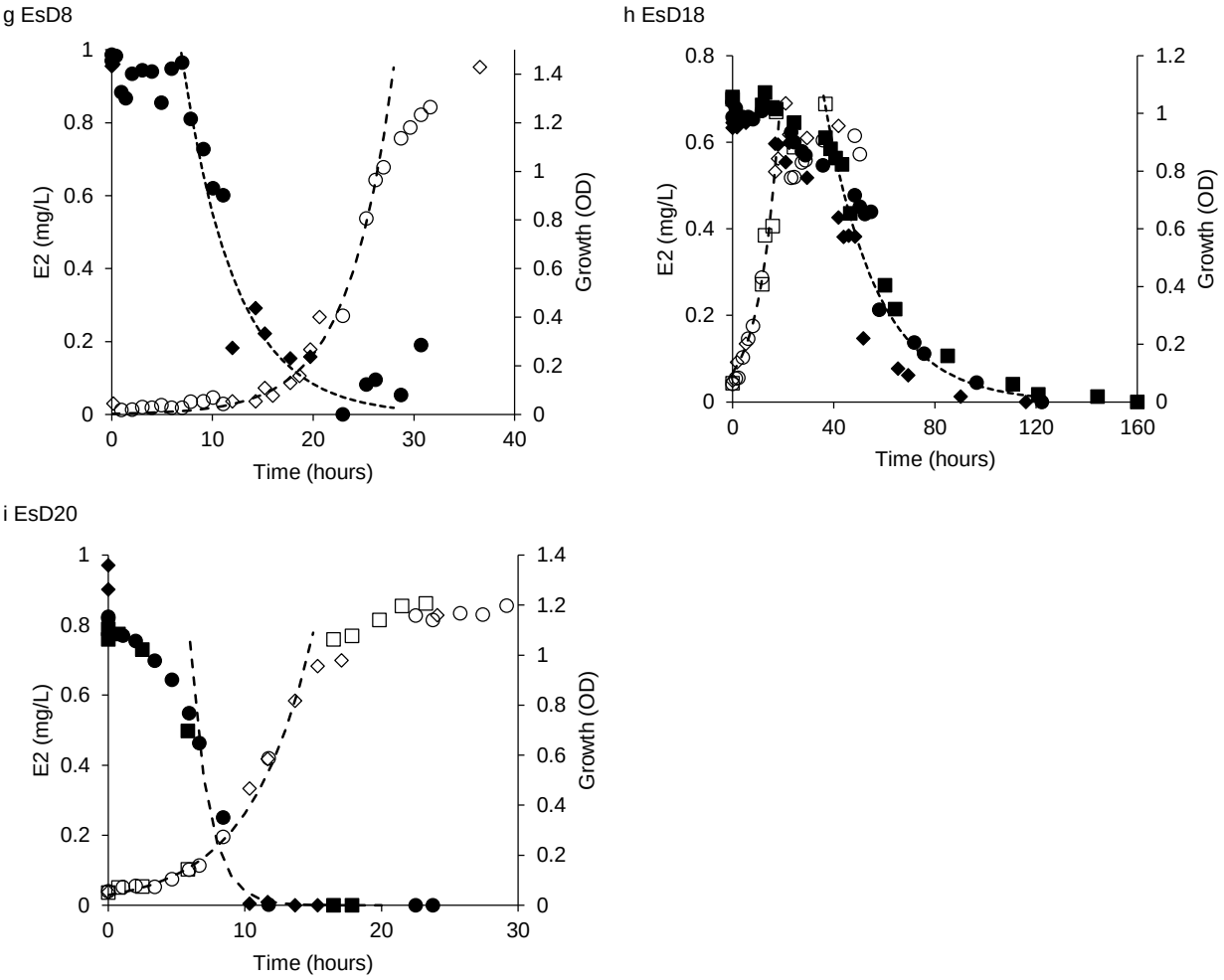

Figure 4.4. Growth of bacterial isolates during degradation of compound in carbon-rich media. Degradation of bisphenol A by (a) BiD10. Degradation of triclosan by (b) TrD22, (c) TrD23, (d) TrD34, and (e) TrD1. Degradation of ibuprofen by (f) IbD51. Degradation of 17β-estradiol (E2) by (g) EsD8, (h) EsD18, and (i) EsD20. Open markers represents growth and closed markers represents degradation. Circles, diamonds and squares represent separate bottles. Dashed lines represent degradation and growth models.

a BiD10

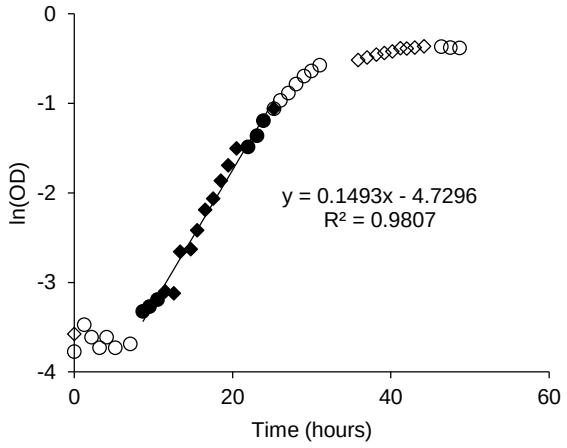

b BiD32

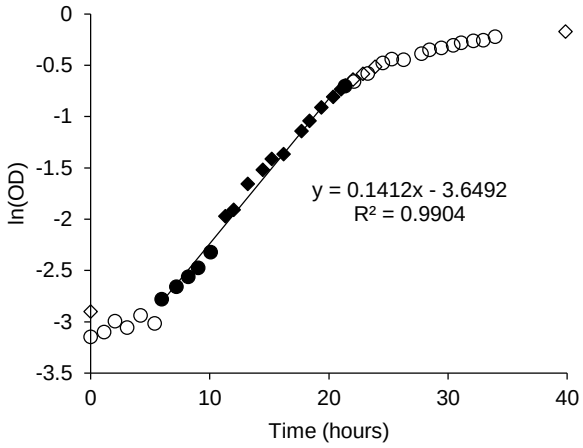

c TrD22

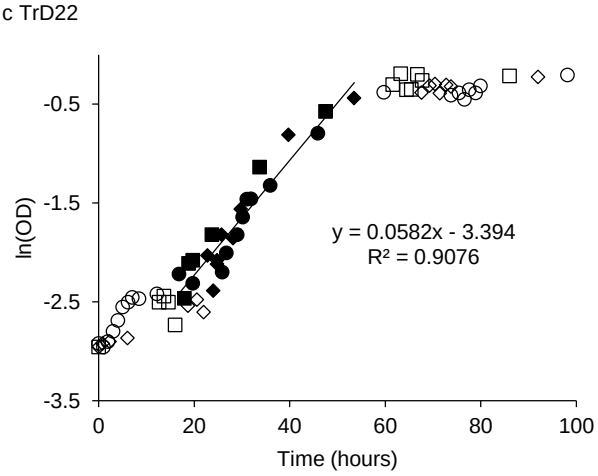

d TrD23

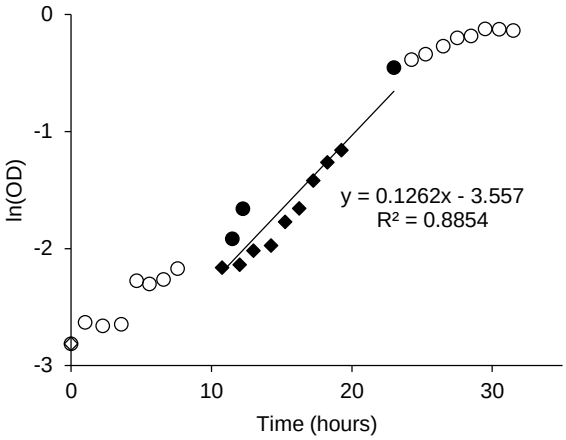

e TrD34

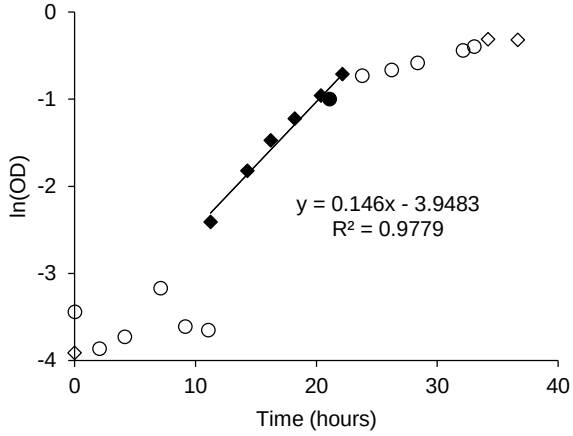

f TrD1

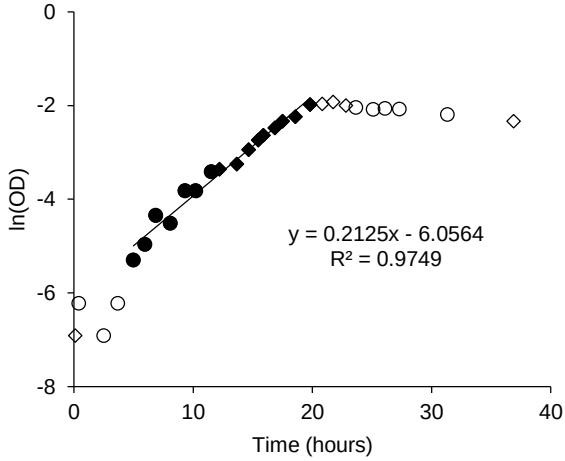

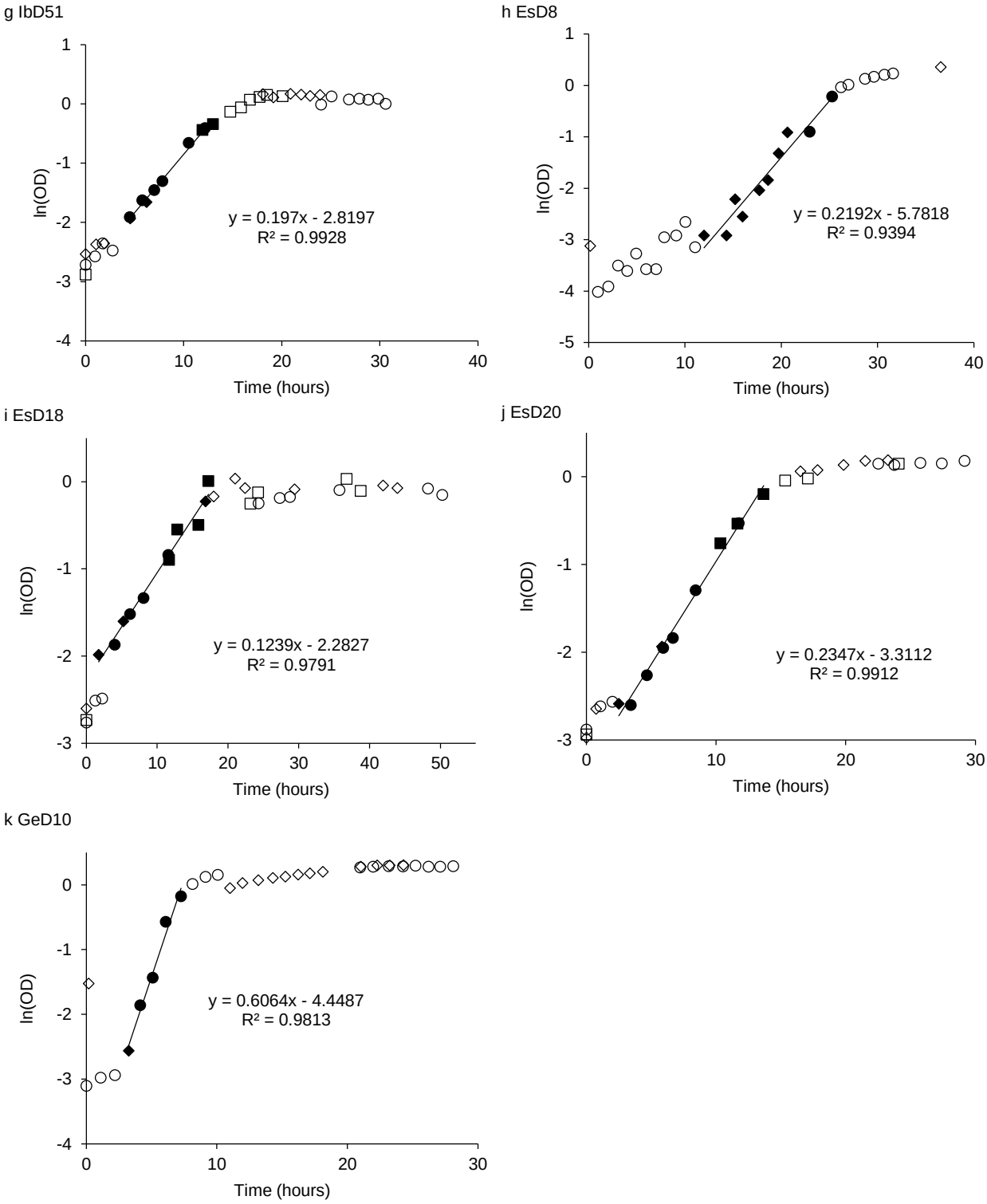

Figure 4.5. Growth of (a) BiD10, (b) BiD32, (c) TrD22, (d) TrD23, (e) TrD34, (f) TrD1, (g) IbD51, (h) EsD8, (i) EsD18, (j) EsD20, and (k) GeD10 on carbon-rich media linearized. Open markers represent data excluded from growth rate calculation and closed markers represent data used to calculate growth rates. Circles, diamonds and squares represent separate bottles.

a BiD10

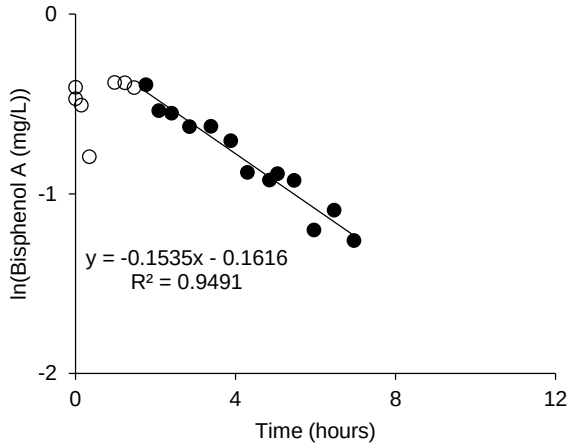

b BiD32

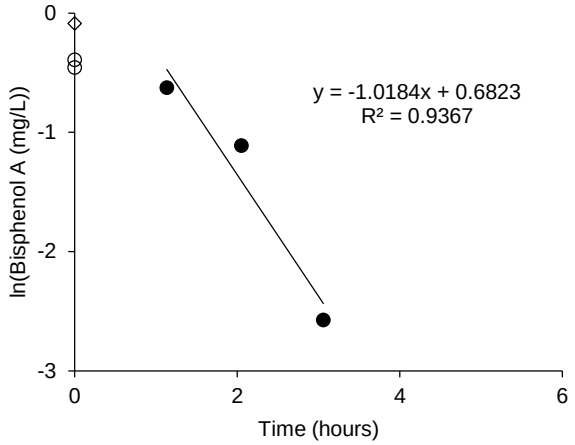

c TrD22

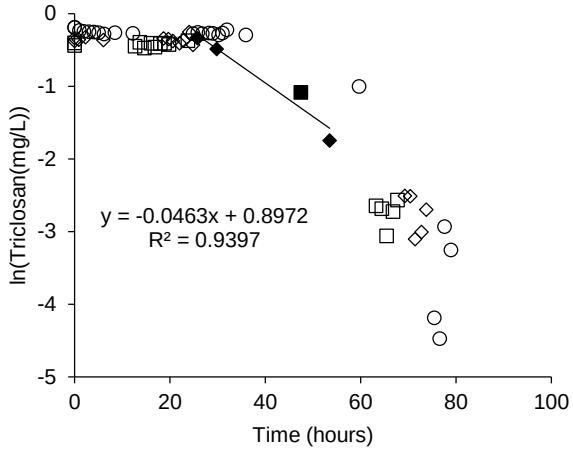

d TrD23

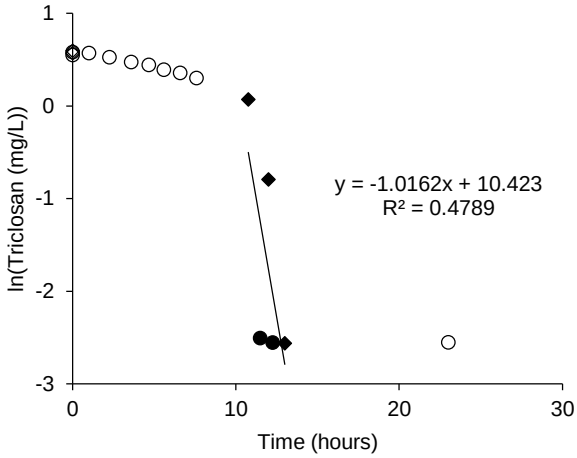

e TrD34

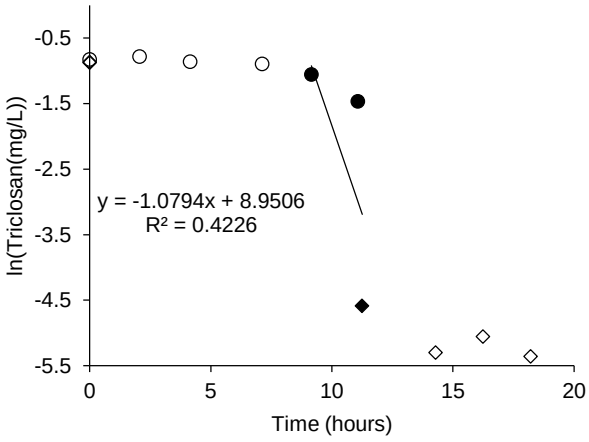

f TrD1

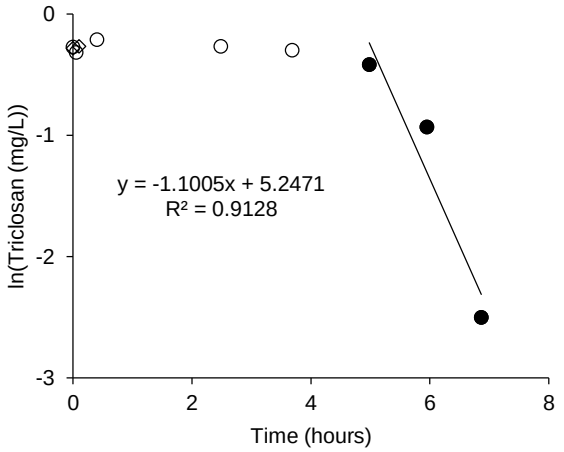

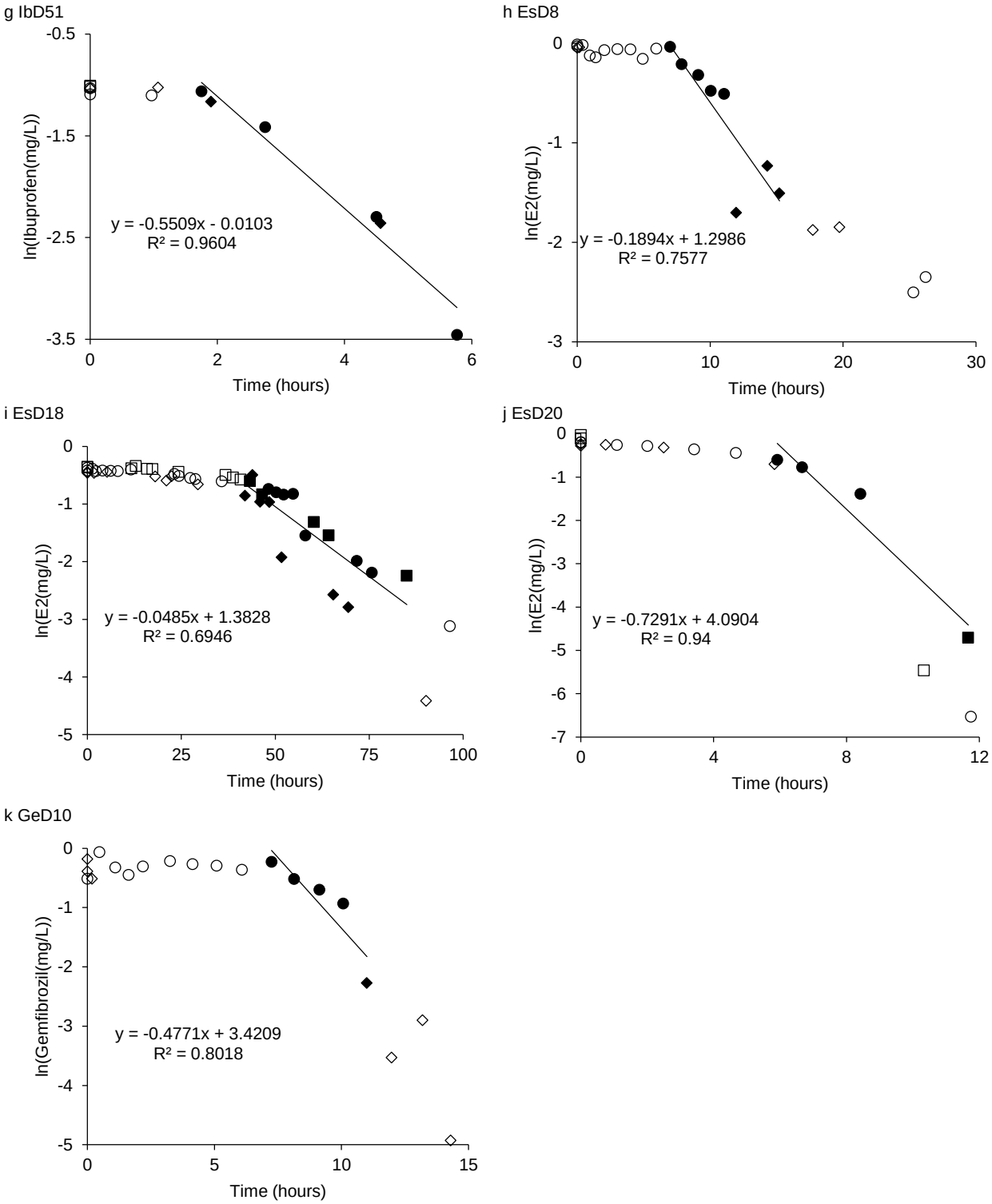

Figure 4.6. Degradation of PPCP by (a) BiD10, (b) BiD32, (c) TrD22, (d) TrD23, (e) TrD34, (f) TrD1, (g) IbD51, (h) EsD8, (i) EsD18, (j) EsD20, and (k) GeD10 in carbon-rich media linearized. Open markers represent data excluded from degradation rate calculation and closed markers represent data used to calculate degradation rates. Circles, diamonds and squares represent separate bottles. E2 is 17β-estradiol.

CHAPTER 5: KINETICS MODELING PREDICTS BIOAUGMENTATION WITH SPHINGOMONAD CULTURES AS A VIABLE TECHNOLOGY FOR ENHANCED PHARMACEUTICAL AND PERSONAL CARE PRODUCTS REMOVAL DURING WASTEWATER TREATMENT

Reproduced with permission from:
Zhou, Nicolette A., April C. Lutovsky, Greta L. Andaker, John F. Ferguson, and Heidi L. Gough. 2014. "Kinetics Modeling Predicts Bioaugmentation with Sphingomonad Cultures as a Viable Technology for Enhanced Pharmaceutical and Personal Care Products Removal during Wastewater Treatment." *Bioresource Technology* 166 (August): 158–67. doi:10.1016/j.biortech.2014.05.028

5.1 Chapter summary

This chapter focuses on Objective I: the isolation and characterization of bacteria that have potential for successful bioaugmentation and Objective II: the modeling of bioaugmentation of isolated bacteria in full scale activated sludge processes. The objectives were demonstrated using triclosan and BPA as model compounds. These were selected based on the drastic difference in their sorption affinity. During this study, TOrC degradation kinetics by the isolated bacteria were determined in pure culture (described in Chapter 4) and in activated sludge. Sorption partitioning coefficients were determined in activated sludge as part of determining the specific first order degradation rates. Addition of the bacteria into activated sludge resulted in a temporary improvement in triclosan and BPA degradation. Determined specific degradation rates by the augmented bacteria and the activated sludge were incorporated into full scale activated sludge process models. The model predicted that bioaugmentation of TOrC-degrading bacteria into a 4-stage activated sludge process resulted in a less than 10% increase in total system VSS to reach an effluent concentration of 5 ng/L, for all but one of the modeled bacteria. Based on this result, seven of the isolated bacteria were determined to be practical for bioaugmentation, with one bacteria requiring too much biomass to be dosed to reach an effluent concentration of 5 ng/L. The required bioaugmentation doses needed to reach a desired effluent concentration were determined over a range of activated sludge VSS, SRT, and level of contaminant removal. With increasing activated sludge VSS, an increase in bioaugmentation dose was required. Decreasing the SRT resulted in an increase in the required bioaugmentation dose. Increasing the desired level of contaminant removal increased the required bioaugmentation dose. These results indicated that bioaugmentation is a practical solution for improving TOrCs removal in WWTPs or potentially from other waste streams and in other treatment facilities. These results also led to a study that investigated bioaugmentation in lab reactors and compared the results.

5.2 Abstract

Pharmaceutical and personal care products (PPCPs) discharged with wastewater treatment effluents are a surface water quality concern. PPCPs are partially removed during wastewater treatment and biological transformation is an important removal mechanism. To investigate the potential for enhanced PPCP removal using bioaugmentation, bacteria were previously isolated from activated sludge capable of degrading PPCPs to ng/L concentrations. This study examined the degradation kinetics of triclosan and bisphenol A by five of these bacteria, both in pure culture and when augmented to activated sludge. Sorption coefficients were determined to account for the influence of partitioning during bioremoval. When the bacteria were added to activated sludge, degradation increased. Experimentally determined kinetic parameters were used to model a full-scale continuous treatment process, showing that low biomass could achieve reduced effluent PPCP concentrations. These results demonstrated that bioaugmentation may improve PPCP removal using established wastewater infrastructure under conditions of high solids partitioning.

5.3 Introduction

Recent recognition that pharmaceuticals and personal care products (PPCPs) are discharged with wastewater treatment plant (WWTP) effluents (Yang et al., 2011; Paxeus, 2004; Duong et al., 2010) has raised concerns that this contaminant source may contribute to deleterious environmental effects (Thorpe et al., 2009; Brausch and Rand, 2011). While current WWTP technologies remove a significant portion of these contaminants (Samaras et al., 2013), new technologies will be needed if increasingly lower discharge levels are to be achieved. This study is part of a larger effort to examine the potential for continuous bioaugmentation as a technological advancement for improved PPCP removal during wastewater treatment. The approach is based on the observation that many PPCPs are partially destroyed biologically during the activated sludge process at WWTPs (Bester, 2005; Heidler and Halden, 2007), and that microbial degradation can result in full contaminant mineralization (Federle et al., 2002). An important first step towards development of bioaugmentation as a viable technology was achieved when bacteria were isolated from activated sludge that were each capable of degrading a range of PPCPs within a complex carbon environment, such as would be found at a WWTP (Zhou et al., 2013; Lee et al., 2012; Ike et al., 1995). Here, as a next step, degradation kinetics were measured and kinetics modeling was used to evaluate the potential for bioaugmentation within the realistic constraints of typical WWTP operations.

Testing of bioaugmentation for PPCP removal has been very limited. Two studies have reported examination of bioaugmentation for 17β-estradiol (E2) removal (Roh and Chu 2011; Iasur-Kruh et al. 2011). Starting with an equal biomass of the E2-degrading bacterium KC8, Roh and Chu (2011)

demonstrated removal of 1 mg/L E2 in lab scale sequencing batch reactors led to high levels of removal, though contributions by KC8 were obscured by high background degradation rates by the activated sludge. This study was important in demonstrating the rapid loss of the bioaugmented KC8, which decreased by over 1 to 2.5 orders of magnitude within one solids retention time (SRT). Iasur-Kruh (2011) used a different approach by demonstrating that the integration of an E2-degrading bacteria, EDB-LI1, into a wetland pond biofilm resulted in enhanced removal of 40 mg/L E2 for 24 hours. This study builds upon this existing research by focusing on the concept of continuous bioaugmentation using pure cultures demonstrated to degrade two PPCP (triclosan and bisphenol A (BPA)) to compensate for rapid removal such as seen with the single dose bioaugmentation of KC8. Bioaugmentation has not previously been studied for these PPCPs and the cultures used have the documented capability to degrade these contaminants to below the ng/L concentration ranges (Zhou et al. 2013) typically associated with WWTP effluents (Yang et al. 2011; Paxeus 2004; Duong et al. 2010; Ballesteros-Gomez et al. 2007).

Bacteria likely to be successful for PPCP removal during continuous bioaugmentation should exhibit four specific characteristics (Zhou et al., 2013), which include the ability of the bacteria to *(1)* remove the PPCPs to levels below typical WWTP effluent concentrations, *(2)* grow using common substrates while maintaining their ability to degrade PPCPs, *(3)* degrade PPCPs in the presence of higher concentrations of other substrates, and *(4)* degrade the PPCPs at practical degradation rates. Three triclosan degrading bacteria and two BPA degrading bacteria that were reported in Zhou et al. (2013) met the first three criteria. This study focused on obtaining data to evaluate the fourth criteria. The objective was to model the potential influence of continuous bioaugmentation on resulting effluent concentrations by applying experimentally measured PPCP degradation kinetics and sorption partitioning coefficients to a completely mixed activated sludge (CMAS) and a multi-staged activated sludge model.

5.4 Materials and methods

5.4.1 Reagents and chemicals

Organic solvents and water used for PPCP sample extraction and analysis were high-pressure liquid chromatography (HPLC) grade. Triclosan (99.8% purity) was obtained from EMD Chemicals, Inc. (Calbiochem, Gibbstown, NJ, USA). BPA (>99% purity) was obtained from Sigma Aldrich (St. Louis, MO, USA). BPA-2,2',6,6'-d_4 (d_4-BPA) (>98% purity) and (±)ibuprofen-d_3 (d_3-ibuprofen) (99% purity) were purchased from C/D/N Isotopes, Inc. (Quebec, Canada).

Stock solutions of triclosan (5 mg/L) and BPA (35 mg/L) were prepared by adding triclosan or BPA dissolved in acetonitrile (1000 mg/L) to a glass bottle, evaporating the acetonitrile at 105ºC for at least

one hour, adding water (18Ω, MilliQ Plus Ultra Pure Water Systems; Millipore, Billerica, MA, USA), and autoclaving to sterilize the solution. Stock solutions were stored at room temperature in amber glass bottles to minimize potential photodegradation (Yu et al., 2006).

5.4.2 Culture media

Two low nutrient media were used: mineral media and minimal media. They were prepared as described in the *Manual of Environmental Microbiology* (Tanner, 1997) with modifications to reduce the ammonia concentrations as previously described (Zhou et al., 2013). Two nutrient-rich media were used (autoclave sterilized). R2A media was prepared based on the composition of R2A agar (Reasoner and Geldreich, 1979; Zhou et al., 2013). Luria-Bertani broth (LB) was purchased from Fisher Scientific (Pittsburgh, PA, USA).

5.4.3 High pressure liquid chromatography quantification

Triclosan and BPA concentrations in the mg/L range were measured using a HPLC with a ultraviolet detector (HPLC-UV, DionexUltiMate 3000; Sunnyvale, CA, USA) and triclosan and BPA concentrations in the µg/L and ng/L range were measured by liquid chromatography tandem mass spectrometry (LC-MS/MS, Shimadzu HPLC with a 4000 Q Trap Tandem Mass Spectrometer; Applied Biosystems Inc; Carlsbad, CA, USA). Details for the optimized method used for triclosan and BPA, including levels of quantification (LOQ) are provided in Table 5.5.

Samples to determine total PPCP concentrations (c_T) were preserved by adding an equal volume of acetonitrile, vortexing, and centrifuging for 10 minutes at 10,000 ×g to remove particles. Aqueous phase PPCP concentrations (c_L) were preserved by centrifuging for 10 minutes at 10,000 ×g to remove the particles prior to adding an equal volume of acetonitrile. Preserved samples were stored at 4ºC in sealed glass vials and analyzed within one month. Samples analyzed by LC-MS/MS were amended with an internal standard: 10 µg/L d_3-ibuprofen for triclosan samples and 10 µg/L d_4-BPA for BPA samples.

5.4.4 Sources of activated sludge

Activated sludge was obtained from three wastewater treatment plants. West Point Treatment Plant (West Point) in Seattle, Washington, USA is a non-nitrifying secondary treatment facility that treats stormwater and residential, commercial, and industrial wastewater (average flow is 378,500 m^3/day and SRT is 2 to 3 days). Carnation Treatment Plant (Carnation) in Carnation, Washington, USA is a membrane bioreactor facility that treats residential and commercial wastewater (average flow is 380 m^3/day and SRT is 20 to 35 days). Snoqualmie Wastewater Facility (Snoqualmie) is a carousel oxidation ditch configured for

anaerobic/anoxic/aerobic treatment (average flow is 11,400 m^3/day and SRT is 25 to 30 days). Samples were collected and stored on ice during transportation. Samples were refrigerated or aerated during storage and used within one day.

5.4.5 Sorption partitioning coefficients

Volatile suspended solids (VSS) were measured in accordance with Standard Method 209E (AWWA, 1998). The sorbed mass of PPCP per unit volume (c_s) was calculated as:

$$c_s = c_T - c_L \quad \text{(Eq 5.1)}$$

The sorption partitioning coefficient (K_P) was calculated as (Piwoni and Keeley, 1990):

$$K_P = \frac{c_s/_{VSS}}{c_L} \quad \text{(Eq 5.2)}$$

where K_P has the units L/kg VSS and VSS was the activated sludge concentration (kg VSS/L).

The fraction of PPCP in the aqueous phase, f_L, was calculated as:

$$f_L = \frac{1}{1 + K_P VSS} \quad \text{(Eq 5.3)}$$

To compare K_P values to octanol-water partition coefficients (K_{ow}), organic carbon-water partition coefficients (K_{oc}) were estimated using an empirical correlation relating $\log K_{ow}$ to $\log K_{oc}$ for polycyclic aromatics, and K_{oc} was corrected for the organic carbon content (Karickhoff et al., 1979).

$$log\ K_{oc} = log\ K_{ow} - 0.21 \quad \text{(Eq 5.4)}$$

$$K_P = f_{oc} K_{oc} \quad \text{(Eq 5.5)}$$

where f_{oc} was the fraction of organic carbon in the solids (assumed to be 0.5 kg organic carbon/kg VSS).

5.4.6 Pure culture degradation kinetics

Bacterial strains were previously isolated from activated sludge and shown capable of degrading either triclosan (*Sphingomonas* sp. TrD23, *Sphingopyxis* sp. TrD1, and *Sphingomonas* sp. TrD34) or BPA (*Sphingopyxis* sp. BiD10 and *Sphingobium* sp. BiD32) to low ng/L concentrations (Zhou et al., 2013). Bacterial inocula were grown in R2A media without triclosan or BPA and harvested during active growth as measured by optical density changes at 600 nm (OD_{600}). The cells were pelleted by centrifugation (4000 ×g for 30 minutes at 4ºC), the R2A media was decanted, and the cells were resuspended in minimal media (TrD1) or mineral media (all other cultures). PPCP concentrations were measured over time. The rate of degradation was calculated as:

$$\frac{dc_T}{dt} = -k_c' X f_L c_T \quad \text{(Eq 5.6)}$$

where dc_T/dt was the rate of change (mg/L-hr), k_c' was the specific first order degradation rate (L/mg-hr), and X was the augmented biomass (mg/L). f_L was assumed to be 1 in pure culture experiments with low biomass. In studies with mineral and minimal media, biomass (X) was assumed to be constant (i.e. no growth), and Eq 5.6 was integrated and linearized as:

$$\ln c_T = -k_c' X f_L t + ln c_{T,0} \quad \text{(Eq 5.7)}$$

where $c_{T,0}$ was the initial concentration. The equation was solved graphically and the y-intercept was ln $c_{T,0}$ and the slope was $k_c' X f_L$ (hr^{-1}). k_c' was calculated by dividing the slope by measured values for X and f_L. The lag time prior to start of degradation (t_L) was estimated as the time (t) when the predicted c_T in Eq 5.7 equaled the measured initial c_T.

5.4.7 Activated sludge degradation kinetics

Experiments to determine degradation kinetics were completed using West Point activated sludge augmented with initial triclosan or BPA concentrations ranging from 2.1 to 24 µg/L. Bacterial inocula were grown using R2A media and harvested during active growth as described above. Activated sludge VSS was diluted with mineral media to obtain initial experimental VSS. Controls included activated sludge diluted in mineral media without bioaugmentation, and autoclaved activated sludge. Batch reactors were continuously stirred and aerated. Total PPCP and aqueous phase PPCP were measured over time.

Degradation by activated sludge (k_{AS}) was determine by applying data from the control reactor to Eq 5.7. The degradation rate attributable to the bioaugmentation was calculated by subtracting the degradation associated with activated sludge:

$$k_c' = \frac{k_{cT} - k_{AS}}{f_L X} \quad \text{(Eq 5.8)}$$

where k_{cT} was the total degradation rate in the reactor (hr^{-1}), and k_c' was the specific degradation rate for augmented bacteria normalized to augmented biomass (X) and bioavailable contaminant concentrations (f_L from Eq 5.3). The specific degradation rate by the activated sludge (k_{AS}') was also determined for use in modeling (L/mg-hr).

$$k_{AS}' = \frac{k_{AS}}{f_L VSS} \quad \text{(Eq 5.9)}$$

5.4.8 Modeled continuous bioaugmentation in continuously stirred tank reactors

The efficacy of bioaugmentation for PPCP removal was modeled to represent two commonly used activated sludge configurations; CMAS (Figure 5.1a) and a 4-stage process (Figure 5.1b). Multi-staged activated sludge processes have been endorsed by the US EPA for nitrification because they greatly

reduces reactor volume requirements in comparison to single reactor CMAS (U.S. EPA 2010). Base conditions used for modeling are summarized in Table 5.1. Assuming steady state and constant active biomass, c_T, was solved as (Metcalf & Eddy et al., 2003):

$$c_T = \frac{c_{in}^*}{1 + (k\frac{\tau}{N})^N} \quad \text{(Eq 5.10)}$$

where c_{in}^* was the PPCP concentration entering the first reactor (ng/L), k was the total PPCP degradation rate (hr^{-1}), N=1 for the CMAS and N=4 for the 4-stage reactor system, and τ was the hydraulic retention time (hour).

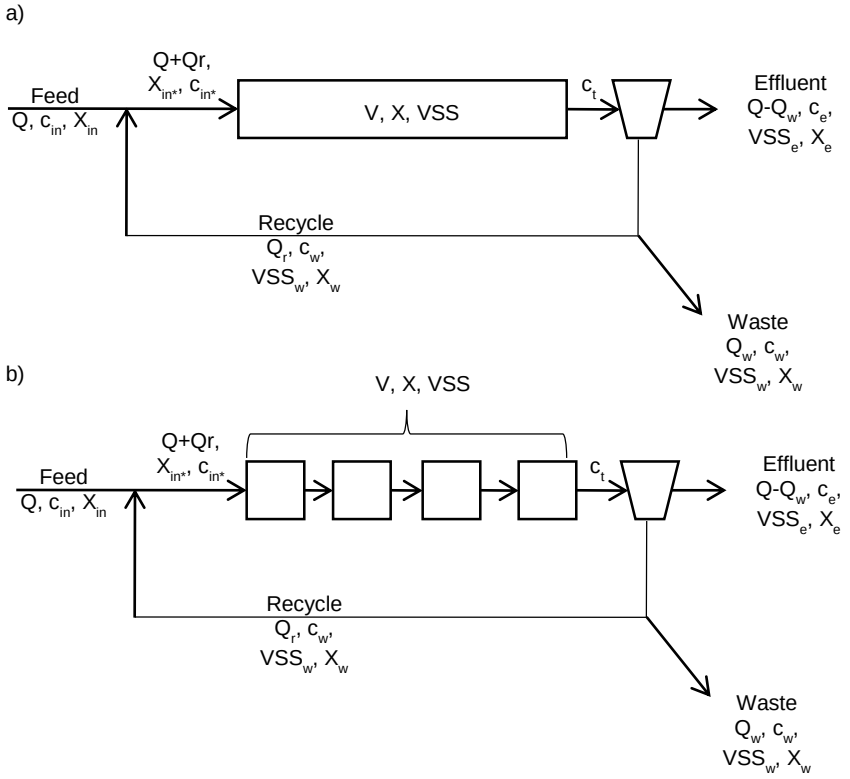

Figure 5.1. Reactor schematic used to model feasibility of bioaugmentation using experimentally determined degradation kinetics and sorption coefficients.

Table 5.1. Base conditions used for continuously stirred tank reactor modeling.

Parameter	Value
Initial PPCP concentration (c_{in}, µg/L)	3[a]
Effluent PPCP concentration goal (c_e, ng/L)	5
Activated sludge volatile suspended solids (VSS, mg/L)	2000
Hydraulic retention time (τ, hour)	4[b]
Solids retention time (SRT, day)	5
Influent flowrate (Q, m^3/d)	300,000
Recycle flow ratio (%)	50
Solids in the effluent (VSS_e+X_e, mg/L)	20

PPCP, pharmaceuticals and personal care products
[a]typical WWTP primary effluent concentrations (Bester, 2005; Wang et al., 2010)
[b]determined to maintain an effluent BOD ≤ 25 mg/L at all conditions modeled

In the modeled scenario, the total PPCP degradation rate (k) was calculated as:

$$k = (k_c'\mathrm{X} + k_{AS}'\mathrm{VSS})f_L \quad \text{(Eq 5.11)}$$

where the PPCP degradation constants k_c' and k_{AS}' was determined experimentally as described above. f_L was calculated based on experimentally determined K_P (Eq 5.3) and VSS was set as experimental conditions (Table 5.1). X was the experimental unknown.

The c_{in}^* was calculated starting with a PPCP mass balance on the clarifier to determine the PPCP concentration in waste and recycle stream (c_w, ng/L):

$$c_w = \frac{c_T(Q + Q_r) - c_e(Q - Q_w)}{Q_w + Q_r} \quad \text{(Eq 5.12)}$$

where Q was the influent flow rate (m^3/d), Q_r was the recycle flow rate (m^3/d), c_e was the PPCP concentration in the effluent (ng/L), and Q_w was the waste stream flow rate (m^3/d) (Figure 5.1). The blending of influent and recycle stream was used to calculate c_{in}^*:

$$c_{in}^* = \frac{c_{in}Q + c_wQ_r}{Q + Q_r} \quad \text{(Eq 5.13)}$$

The simultaneous solution of Eq 5.10, 5.12, and 5.13 with the values used in Table 5.1 were combined to solve for c_{in}^* as a function of X.

The Q_w was calculated by combining the definition for SRT (Eq 5.14) with the activated sludge mass balance around the clarifier (Eq 5.15).

$$SRT = \frac{V(VSS + X)}{(Q - Q_w)(VSS_e + X_e) + Q_w(VSS_w + X_w)} \quad \text{(Eq 5.14)}$$

where the sum of VSS_e and X_e was the total biomass in the effluent (mg/L), VSS_w was the activated sludge biomass in the waste stream (mg/L), and X_w was the augmented biomass retained in the waste stream (mg/L).

$$VSS_w = \frac{(Q + Q_r)VSS - (Q - Q_w)VSS_e}{Q_w + Q_r} \quad \text{(Eq 5.15)}$$

where VSS_e was the activated sludge biomass in the effluent (mg/L), which was calculated by assuming that the settlability of the X and VSS were similar so that the two biomasses remained in the same proportional concentrations in the effluent as in the activated sludge.

$$X_e = X\frac{VSS_e + X_e}{VSS + X} \quad \text{(Eq 5.16)}$$

The PPCP concentration in the effluent (c_e, ng/L) was the sum of the liquid concentration and the concentration associated with effluent suspended solids, and was calculated as:

$$c_e = c_T f_L + c_T(1 - f_L)\frac{VSS_e + X_e}{VSS + X} \quad \text{(Eq 5.17)}$$

The augmented biomass in the feed (X_{in}, mg/L) required to maintain targeted activity in the reactor, was calculated by a mass balance around the clarifier (Eq 5.18) and substituting the solved value for X_w into the equation for the mass balance of the augmented bacteria mass balance around the whole system (Eq 5.19).

$$X_w = \frac{(Q + Q_r)X - (Q - Q_w)X_e}{Q_w + Q_r} \quad \text{(Eq 5.18)}$$

where X can be solved using Eq 5.16.

$$X_{in} = \frac{(Q - Q_w)X_e - Q_w X_w}{Q} \quad \text{(Eq 5.19)}$$

The biomass from augmented bacteria was assumed to be constant at steady state.

5.4.9 Statistical analyses

Average deviation from the mean was used to estimate error when the number of replicates (n) was too low to assume a normal distribution as required when calculating standard deviation (Panneerselvam, 2004):

$$AD = \frac{\Sigma|x - \bar{x}|}{n} \quad \text{(Eq 5.20)}$$

Error on regression slopes were calculated as the 95% confidence intervals as previously described (Gough et al. 2013; Hayter 1996). Analysis of variance (ANOVA) was used to test for differences among groups of data.

5.5 Results and discussion

5.5.1 Degradation kinetics and sorption coefficients

5.5.1.1 Sorption partitioning coefficients

Partitioning coefficients were determined using Eq 5.2 by comparing total and liquid PPCP concentrations during activated sludge experiments. A total of 78 triclosan and 21 BPA measurements were made (Table 5.6). Triclosan K_P were measured using activated sludge from West Point with three VSS concentrations (136, 870, and 1,100 mg/L), resulting in an average logK_P of 4.3±0.23. BPA K_P were determined using three different activated sludge sources, Carnation (6130 mg/L VSS), Snoqualmie (1170 mg/L VSS), and West Point (2140 mg/L VSS), resulting in an average logK_P of 2.3±0.15. BPA logK_P from the three different plants were statistically equivalent (ANOVA p>0.05). Variation among logK_P was not observed during degradation of triclosan or BPA (Figure 5.7), indicating that the sorption/desorption kinetics were faster than degradation kinetics. In the literature, logK_{ow} values have been reported for triclosan and BPA as 4.8 and 3.4, respectively (Westerhoff et al., 2005; Melcer and Klecka, 2011). Conversion of these logK_{ow} using Eq 5.4 and 5.5 showed estimated logK_P of 4.3 (triclosan) and 2.9 (BPA), which were similar to the experimental values determined in this study.

The effect of sorption on the biologically available concentration (i.e. $c_L=f_L c_T$) was calculated over a range of VSS (Figure 5.2). When VSS concentrations were between 2000 and 5000 mg/L (typical ranges for activated sludge processes (Metcalf & Eddy et al., 2003)), triclosan would be very highly sorbed (>95%) while 18-50% of the BPA would be sorbed.

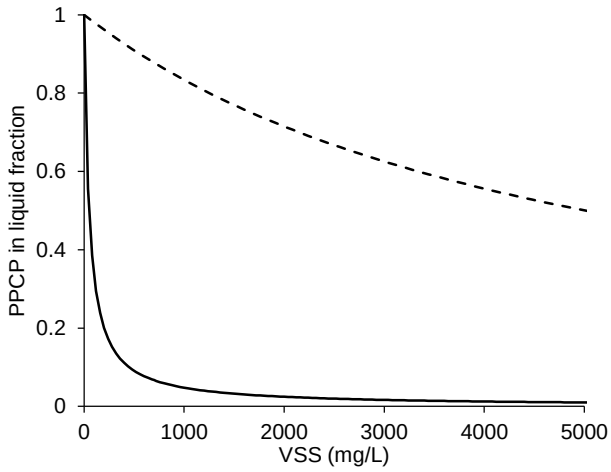

Figure 5.2. Comparison of partitioning for triclosan and BPA as a function of volatile suspended solids (VSS).

5.5.1.2 Pure culture degradation kinetics

Triclosan and BPA were removed to below the LOQ when incubated in mineral or minimal media (Figure 5.3). Calculations for lag prior to the onset of degradation and specific degradation rates (k_c') using Eq 5.7 are shown in Figure 5.8, and the results are presented in Table 5.2. For each bacterial strain, degradation was observed earlier in cultures with higher biomass additions. This observation was numerically confirmed by the higher degradation rate constants (k_c) and decreased lag times observed with higher biomass (Table 5.2). As an exception, the measured k_c were similar when either 9.6 or 19 mg/L TrD23 were tested. This might indicate that inactive biomass was present in the higher biomass incubations.

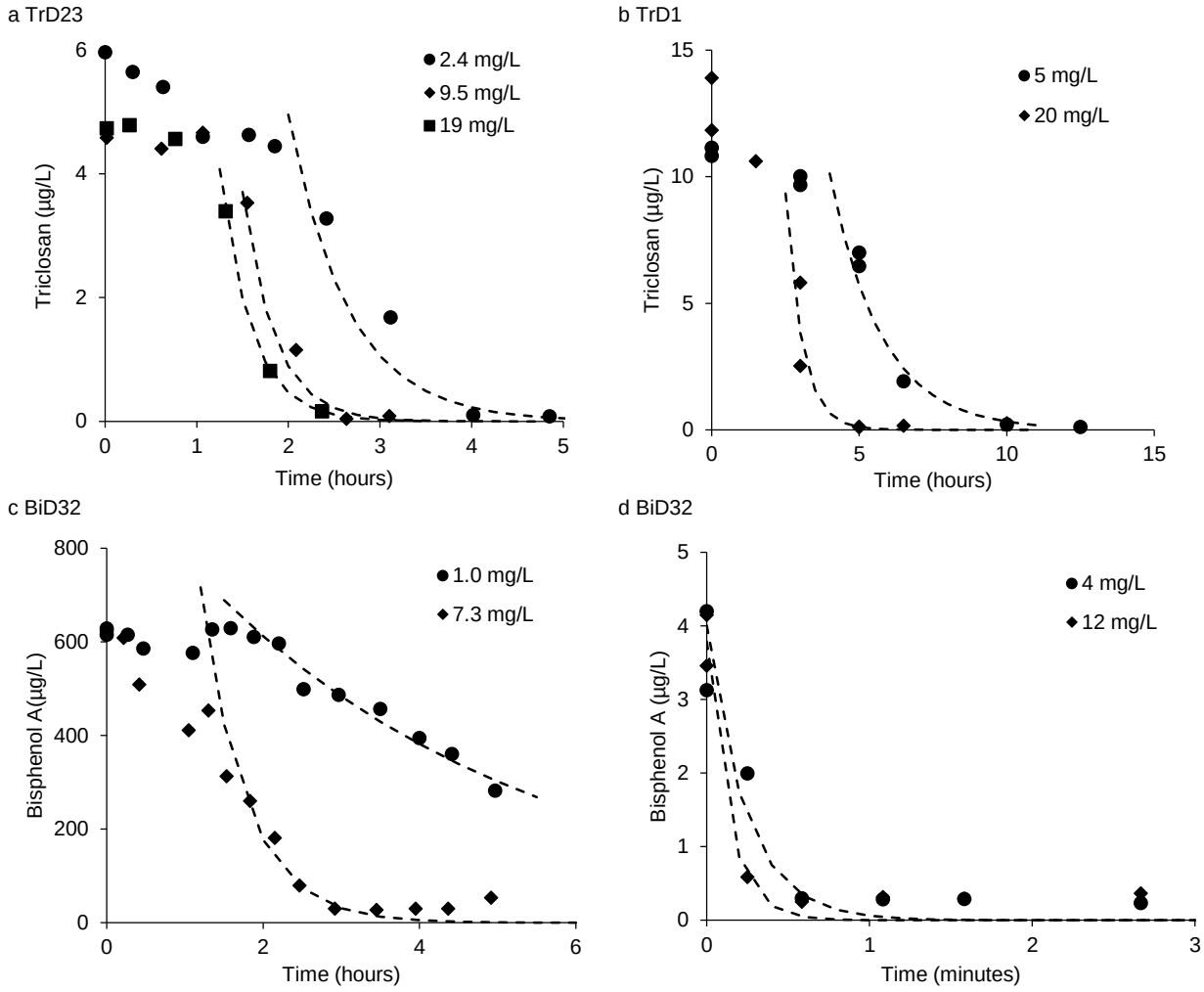

Figure 5.3. Degradation of pharmaceutical and personal care products by a) Sphingomonas TrD23, b) Sphingopyxis TrD1, c) Sphingobium BiD32 (at high µg/L concentrations), and d) Sphingobium BiD32 (at low µg/L concentrations) in mineral or minimal media. Data shown for later time points for (c) and (d) were below the limit of quantification of 150 µg/L and 0.75 µg/L, respectively.

Table 5.2. First order degradation rate constants determined in mineral media compared to R2A media.

Bacterial ID	Mineral media						R2A media[a]				
	initial PPCP (c_o, µg/L)	biomass (X, mg/L)	lag time (t_L, hr)	degradation rate (k_c, hr^{-1})	specific degradation rate[b] (k_c', L/mg-hr)	average k_c'[c] (L/mg-hr)	initial PPCP (co, µg/L)	biomass (X, mg/L)	lag time (t_L, hr)	degradation rate (k_c, hr^{-1})	specific degradation rate[b] (k_c', L/mg-hr)
					Triclosan degradation						
TrD23	6	2.4	2.1	1.7	0.7±0.5		1800	5.9	9.7	1.02	0.17[d]
	4.5	9.6	1.4	2.8	0.3[d]						
	4.5	19	1.2	2.9	0.15±0.0005						
TrD1[e]	10	5	4.0	0.57	0.11±0.01	0.1 ±0.01	800	2.6	5.0	1.1	0.42[d]
	10	20	2.5	1.8	0.09±0.02						
TrD34	not measured						450	2.9	9.0	1.08	0.37[d]
					BPA degradation						
BiD32	600	1.04	2.1	0.24	0.23±0.004	0.23 ±0.005	900	5.1	0.8	1.02	0.20[d]
	600	7.27	1.3	1.75	0.24±0.02						
	4.2	4	0	4.2	1.0±0.2	0.84 ±0.18					
	4.2	12	0	7.5	0.62±0.09						
BiD10	not measured						700	0.7	1.3	0.15	0.21±0.002

PPCP, pharmaceutical and personal care products

[a]data from R2A is summarized from (Zhou et al. 2013); [b]95% confidence interval; [c]average deviation; [d]insufficient data to determine 95% confidence intervals; [e]minimal media used instead of mineral media and 10% LB broth used instead of R2A media

Specific degradation rates (k_c'), which were normalized to biomass concentrations, were similar for the two experiments conducted with TrD1 at different biomass concentrations, but showed variation for other bacterial isolates. The most apparent of these differences was for TrD23, which stemmed from the similarity of the k_c as discussed above. BPA degradation kinetics appeared to be dependent on the initial BPA concentration and not on the growth conditions. Specific degradation rates (k_c') were lower when higher initial BPA concentrations were used (Figure 5.3 c, d and Table 5.2). Interestingly, kinetics by BiD32 were similar in both nutrient-poor and nutrient-rich media for experiments with comparable initial BPA concentrations, suggesting that carbon availability in WWTPs may not effect PPCP degradation and that PPCPs are preferentially utilized before other substrates. This corroborates with earlier observations of PPCP degradation before or during early growth by these bacteria (Zhou et al., 2013) and observations that additional organic carbon did not affect estrone degradation during substrate competition experiments (Tan et al., 2013).

5.5.1.3 Activated sludge bioaugmentation trials

Background degradation rates by activated sludge and the influence of bioaugmentation were tested in batch experiments (Figure 5.4). Graphical solutions for degradation rates (Eq 5.7) are shown in Figure S5.3 and the resulting k_c' and k_{AS}' are presented in Table 5.3. Triclosan was degraded by the activated sludge to below 2 µg/L within 9 hours (Figure 5.4a). k_{AS}' values (Table 5.3) were similar among the tests, including when tested at different VSS and using activated sludge collected on different dates (i.e. WP1 compared to WP2, Table 5.3), demonstrating that f_L (a function of both K_P and VSS, Eq 5.3) had a strong influence in predicting degradation rates. During bioaugmentation, improved degradation was observed. Higher bioaugmentation levels resulted in both faster triclosan degradation and lower residual triclosan concentrations. The specific degradation rate (k_c') was lower when higher TrD23 biomass was applied (Table 5.3), similar to the observations made during pure culture testing (Table 5.2). However, the specific degradation rate for TrD23 was an order of magnitude higher than the rates measured for activated sludge biomass, confirming a specialized degradation by TrD23 in comparison the mixed activated sludge community.

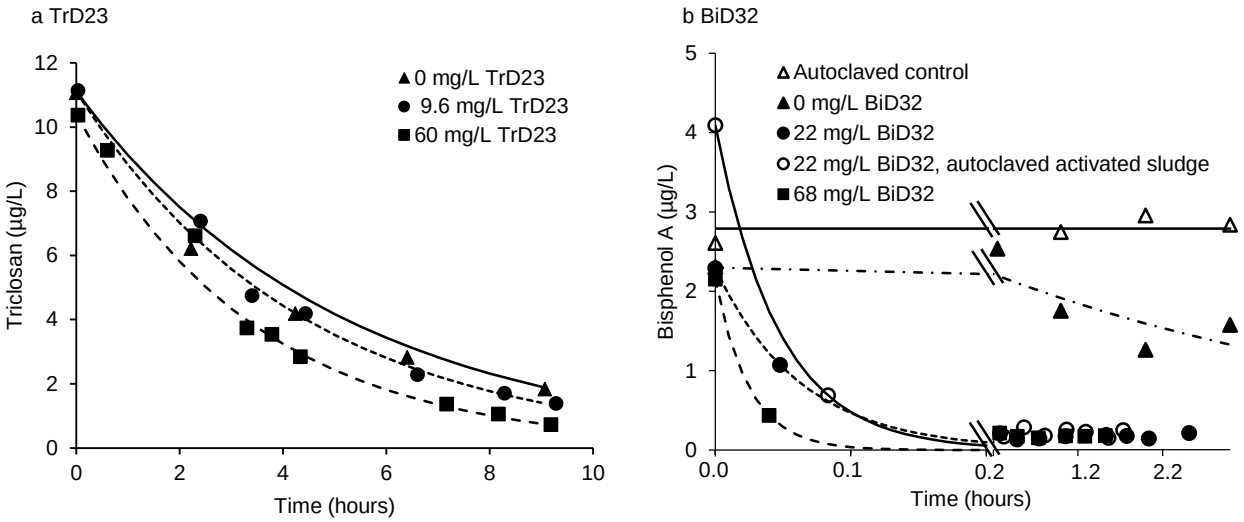

Figure 5.4. Degradation of triclosan or BPA by bacteria augmented to activated sludge. a) 870 mg/L volatile suspended solids (VSS) activated sludge bioaugmented with TrD23 and b) 2140 mg/L VSS activated sludge bioaugmented with BiD32 (later time points were below the limit of quantification of 0.75 µg/L). Solid line shows live activated sludge and dashed line shows autoclaved activated sludge.

Table 5.3. Degradation rates for triclosan and BPA by activated sludge and augmented bacteria.

Bacteria ID	initial triclosan or BPA (c_o, µg/L)	augmented biomass (X, mg/L)	Source of activated sludge	activated sludge biomass (VSS, mg/L)	degradation rate[a] (k_c or k_{AS}, hr^{-1})	specific degradation rate[bc] (k_c' or k_{AS}', L/mg-hr)	average[d] (k_c', L/mg-hr)
				Triclosan degradation			
Activated sludge	24		WP 1	136	0.108±0.016	0.0029±0.0005	0.0033 ±0.0005
	11.1		WP 2	870	0.196±0.003	0.0041±0.0001	
	15		WP 1	1100	0.145±0.007	0.0030±0.0001	
TrD23	11.1	10	WP 2	870	0.229±0.001	0.065±0.003	0.05 ±0.02
	10.4	60	WP 2	870	0.291±0.002	0.031±0.001	
				BPA degradation			
Activated sludge	0.9		S	1172	0.063±0.008	0.00007±0.00001	0.00008 ±0.00003
	2.3		WP 3	2140	0.183±0.048	0.00012±0.00003	
	0.9		C	6130	0.137±0.011	0.000050±0.000004	
BiD32	2.5	22	WP 3	2140	16	1.0[f]	1.08 ±0.21
	2.2	68	WP 3	2140	40	0.9[f]	
	4.1	22	WP 3	2140[e]	21	1.4[f]	

WP 1, West Point activated sludge sampling time 1; WP 2, West Point activated sludge sampling time 2; WP 3, West Point activated sludge sampling time 3; S, Snoqualmie activated sludge; C, Carnation activated sludge. [a]solved graphically with Eq 5.7 as shown in Figure S5.3; [b]k_c' was calculated using Eq 5.8 and k_{AS}' was calculated using Eq 5.9, using f_L calculated using Eq 5.3, logK_P 4.3 for triclosan and logK_P 2.3 for BPA; [c]error represents the 95% confidence interval of the slope in Figure S5.3; [d]average deviation; [e]autoclaved; [f]insufficient data to determine 95% confidence intervals

Bioaugmentation for BPA degradation showed a clearer influence than observed for triclosan. The was largely due to the slower background degradation of BPA by the activated sludge, which degraded less than half of the BPA over 3 hours (Figure 5.4b) leaving residual concentrations between 1.3 and 1.6 µg/L. Autoclaved controls showed no change in BPA concentration, confirming that the observed degradation was biologically mediated. Graphical determination of the BPA degradation rates using Eq 5.7 are shown in Figure S5.3, and the resulting values are shown in Table 5.3. Activated sludge obtained from different WWTPs had different degradation rates, which was not associated with VSS concentrations (k_{AS}', Table 5.3). During bioaugmentation with BiD32, BPA concentration declined to below the LOQ within 3 minutes. As observed with triclosan, higher bioaugmentation levels resulted in faster BPA degradation. However, because of the rapid decline, only two data points above the LOQ were obtained for kinetics calculations (Figure 5.9) so statistical evaluation of the degradation rates was not possible. Still, bioaugmentation showed a clear impact resulting in an average estimated specific degradation rate of 1.08 L/mg-hr for BiD32 (Table 5.3).

5.5.1.4 Implications of culture work and bioaugmentation tests

This work identified three main observations that are important for selecting kinetic parameters appropriate for modeling bioaugmentation for enhanced PPCP removal. Firstly, during triclosan degradation when higher concentrations of bacteria were bioaugmented lower specific degradation rates were obtained. This pattern was most apparent when comparing the k_c' measured for TrD23 in mineral media at three biomass concentrations (X, Table 5.2) and during activated sludge bioaugmentation (Table 5.3), but was also apparent by comparing k_c' in the nutrient-rich R2A media between the three tested triclosan-degrading strains (Table 5.2). This finding suggests that at higher concentrations not all of the biomass was actively degrading triclosan. Additional research will be needed to determine if the biomass becomes less active due to activity suppression in live cells or to loss of the cells due to predation.

Secondly, for BPA two distinct specific degradation rates (k_c') were observed that were independent of the culture conditions (i.e. compare Tables 5.2 and 5.3). These differences instead were related to the initial BPA concentration such that at higher BPA concentrations (600 to 900 µg/L) the average k_c' was 0.22 L/mg-hr and when BPA concentrations were lower (2.1 and 4.2 µg/L) the average k_c' was 1.0 L/mg-hr. Patterns showing lower degradation rates at higher concentrations have been associated with partial inhibition by the contaminant (Almeida et al., 2013; Kim et al., 2011), though this has not previously been reported for BPA.

The third observation critical to accurate modeling was determination of the fraction of the PPCP dissolved in the liquid phase. Measures of f_L for BPA were highly variable (Table 5.6), likely due to decreased accuracy when quantifying low concentrations. Thus K_p and the resulting f_L used for modeling should be obtained using an average of multiple analyses, as shown in Figure S5.3 and presented in Table 5.6, to obtain more robust values.

5.5.2 Modeled full-scale bioaugmentation

5.5.2.1 Theoretical bioaugmentation doses

Success of continuous bioaugmentation of PPCP-degrading bacteria to activated sludge (e.g. Figure 5.1) as a means to improve PPCP removal is a function of a combination of multiple variables including the hydraulic retention time, working concentration of the PPCP-degrading bacteria (itself a function of dose and solids retention time), and the bioavailable PPCP concentration (itself a function of partitioning and solids content). Thus, the specific degradation rates, which were substantially higher for individual bacterial species than for mixed sludge communities (Table 5.3), were applied to a model simulating full-scale municipal wastewater treatment to test if there is support for the potential for enhanced removal. Using the operating conditions provided in Table 5.1 and the modeled schematics in Figure 5.1, the amount of biomass dose needed during bioaugmentation (X) was calculated. While ecological data is not yet complete for identifying appropriate targets for WWTP effluent discharges, 5 ng/L was selected as an aggressive target (99.83% removal when influents are 3 μg/L) as a way to evaluate potential for bioaugmentation. By solving Eq 5.10 through 5.19 simultaneously, a required bioaugmentation dose was calculated that ranged from 3.1 to 15.9 mg/L for BPA removal and from 10.5 to 88 mg/L for triclosan removal with a single CMAS and from 0.13 to 0.67 mg/L for BPA removal and from 2.6 to 26 mg/L for triclosan removal with a 4-stage activated sludge process (Table 5.4, 5.7, and 5.8). BPA degradation kinetics alone did not predict the lower doses for degradation, which for BiD10 were less kinetically favorable than for TrD1 and TrD34. This observation highlighted the importance of the higher triclosan K_P in predicting PPCP removal, and the potential challenges for bioaugmentation of strongly sorbed contaminants. Uncertainty introduced into the models by the experimental k_c' and k_{AS}' was evaluated using the upper and lower 95% confidence interval values or the average deviation of replicate experiments for k_c' and k_{AS}'. The largest impact was indicated for TrD23, which predicted up to a 2-fold dose increase due to the uncertainty of the experimental parameters. For the other bacteria, the range of the bioaugmented dose did not vary considerably.

Table 5.4. Predicted bioaugmentation dose and ratio of bioaugmented biomass in reactors to activated sludge biomass needed to obtain effluent concentration goal of 5 ng/L.

bacterial ID	specific degradation rate (k_c', L/mg-hr)	single CMAS		4-stage activated sludge process	
		bioaugmentation dose (X_{in}, mg/L)	ratio of bioaugmented biomass to activated sludge biomass (X:VSS)	bioaugmentation dose (X_{in}, mg/L)	ratio of bioaugmented biomass to activated sludge biomass (X:VSS)
TrD23	0.05	88	1.3	26	0.40
TrD34	0.37	11.9	0.18	3.0	0.045
TrD1	0.42	10.5	0.16	2.6	0.040
BiD10	0.21	15.9	0.24	0.67	0.010
BiD32	1.08	3.1	0.046	0.13	0.0019

Calculated using operating conditions shown in Table 1 using a single completely mixed activated sludge (CMAS) and a 4-stage activated sludge process (Figure 5.1); VSS, activated sludge biomass in the reactors.

The increase in total system VSS introduced by continuous bioaugmentation was considered, as effluent VSS is a regulated parameter at WWTPs. Increases in system VSS is presented as the ratio of X to VSS (Table 5.4). For a single CMAS the bioaugmented VSS increased total system VSS by less than 5% for BiD32, but by over 15% for all other organisms, making bioaugmentation of a single CMAS impractical under modeled conditions for most of the bacteria considered. However, for a 4-stage activated sludge process the total system VSS increased by less than 4% of the activated sludge VSS for four of the modeled organisms. As an exception, a much higher TrD23 dose was predicted resulting in a 40% increase and as a consequence would make bioaugmentation of TrD23 impractical under modeled conditions. Further results focus on the 4-stage activated sludge process model, whose results suggested greater potential than the single stage CMAS.

Modeling results were used to compare the predicted final fate of the PPCPs (Figure 5.5). In a 4-stage activated sludge process addition of BPA-degrading bacteria improved degradation by 87.6%, and addition of triclosan-degrading bacteria improved degradation by 4.3%. The lower increase with triclosan was due partially to the higher background triclosan degradation potential of the tested activated sludge, and could vary if an activated sludge with lower inherent triclosan degradation capacity was used. Analysis of the contaminant fate showed a decreased in the PPCP mass discharged with waste activated sludge, demonstrating the potential of bioaugmentation to reduce contaminants rather than shifting them from one phase to another and improving the quality of the recovered biosolids.

5.5.2.2 Influence of activated sludge operating conditions on bioaugmentation modeling

Values for the activated sludge VSS (Figure 5.6a), system SRT (Figure 5.6b) and the level of contaminant removal (Figure 5.6c) were varied in the 4-stage activated sludge process model to assess the influence of these parameters on predicted bioaugmentation doses. Predicted doses remained below 2 mg/L for BPA removal and below 10 mg/L for triclosan removal for all scenarios considered (Figure 5.6; TrD23 was not tested based on observations discussed in section 5.3.2.1). Increased activated sludge VSS had a more pronounced impact for triclosan removal than for BPA, reflecting the lower predicted bioavailability (i.e. f_L) for triclosan due to its higher solids partitioning coefficient than BPA (Section 5.3.1.1). SRT can cause two effects on contaminant degradation; first, the bioaugmented bacteria are retained in the system longer so that lower doses can result in higher reactor concentrations of these bacteria; second, reaction time is increased for contaminants sorbed to the recycled activated sludge (Stringfellow and Alvarez-Cohen, 1999). These influences were evident in the increased dosing required when SRT was decreased (Figure 5.6b). Not included in the current model are the potential increases of endogenous respiration (k_r) and predation by protozoa (k_p) at higher SRT (Metcalf & Eddy et al., 2003), and these were assumed to balance with cellular growth (k_g) for the current model. Experimental data to determine k_r, k_p, and k_g for the bioaugmented species will be needed in the future to confirm assumptions and refine the model. Finally, as expected increasing the desired level of contaminant removal increased the required bioaugmentation dose (Figure 5.6c). The dose for triclosan-degrading bacteria increased much more than for the BPA-degrading bacteria though for all evaluated removal levels the dose stayed within the acceptable range.

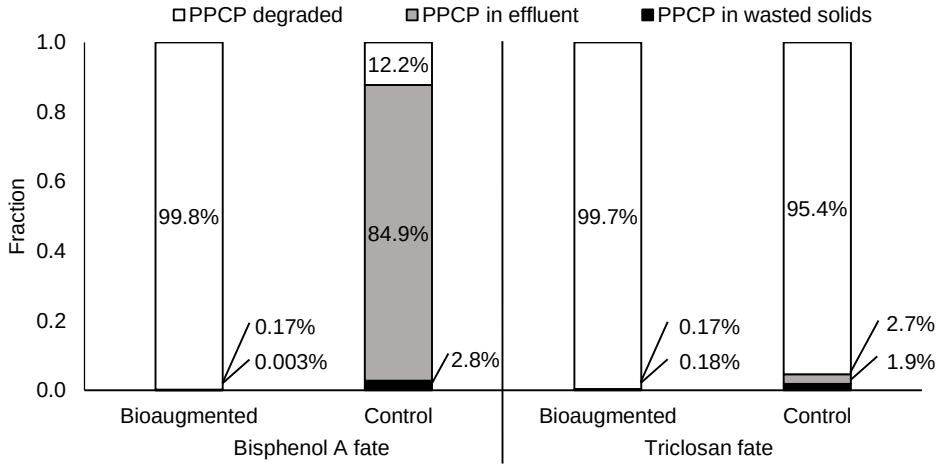

Figure 5.5. Modeling results showing the fate of triclosan and bisphenol A comparing standard treatment to bioaugmentation. Concentration in effluent included contaminants associated with effluent solids (i.e. Eq 5.16).

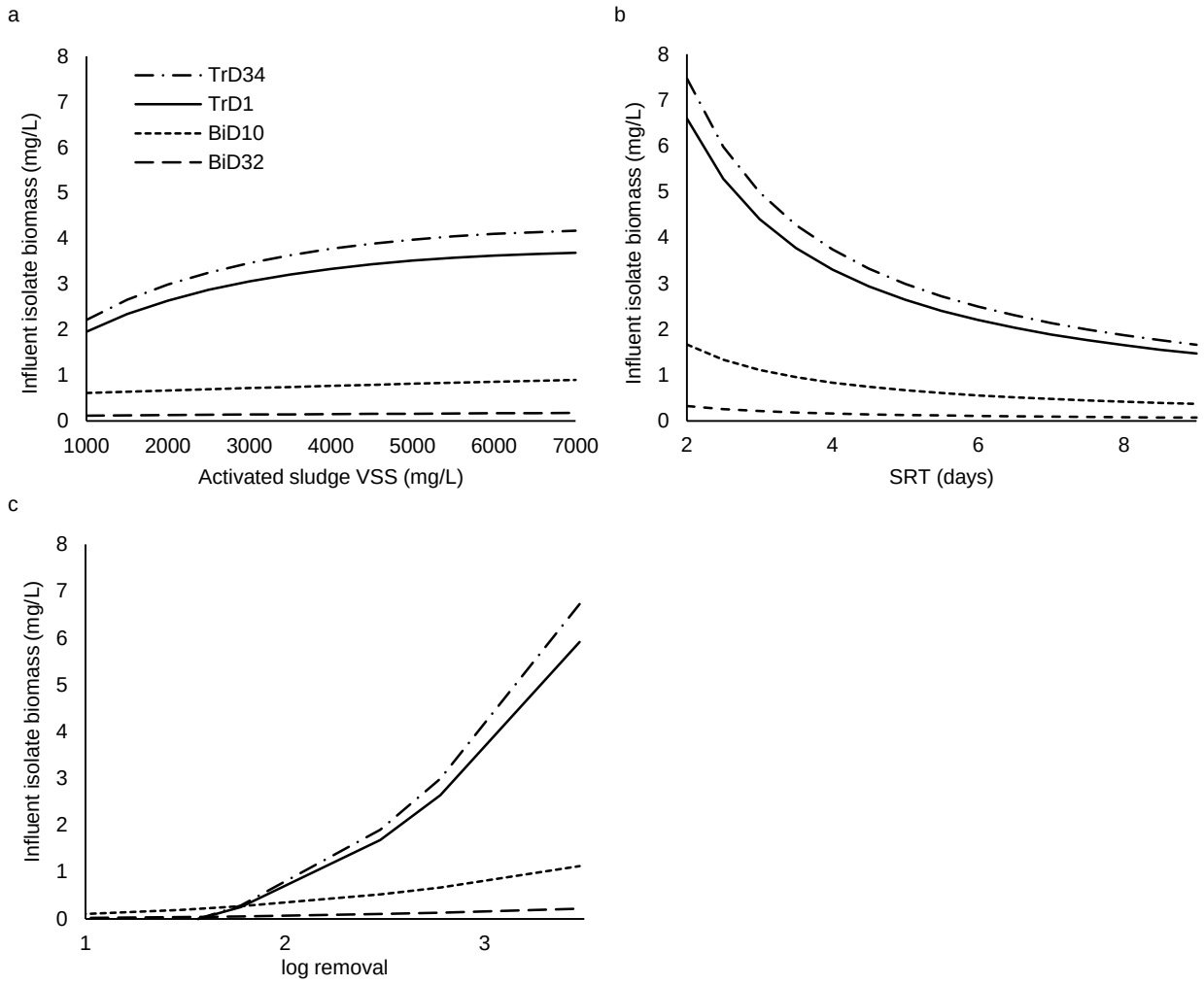

Figure 5.6. Effect of a) activated sludge volatile suspended solids (VSS), b) SRT, and c) level of contaminant removal on predicted bioaugmentation dose. Operating parameters are shown in Table 5.1. Bacteria TrD1 and TrD34 were modeled for triclosan removal, and BiD10 and BiD32 were modeled for bisphenol A (BPA) removal.

5.6 Conclusions

This research demonstrated that PPCP-degrading bacteria enhanced degradation when added to activated sludge. Degradation kinetics were found to vary when determined using differing biomass and contaminant concentrations. Lower specific degradation rates with higher biomass during triclosan degradation suggested loss of activity at high biomass concentrations. Lower BPA degradation rates at higher BPA concentrations suggested a potentially inhibitory response. Application of experimental results to a full-scale model predicted that bioaugmentation may be a feasible technology for enhanced PPCP removal. Lab-scale reactor experiments are needed to confirm modeling and determine if additional parameters will affect the long-term applicability of measured kinetics.

5.7 Acknowledgments

Funding was provided by the National Science Foundation (CBET 0829132). The King County Wastewater Treatment Division Graduate Student Research Fellowship Program provided support to GLA and NAZ.

5.8 Electronic supplementary material

Table 5.5. Summary of HPLC methods

PPCP	Triclosan	Bisphenol A
HPLC-UV		
Column	C18	C18
Flow rate (mL/min)	0.5	0.5
Elution time (minute)	8.79	7
Wavelength	280	275
Injection volume (µL)	100	100
LLD (µg/L)	50	30
LOQ (µg/L)	260	150
LC-MS/MS		
Column	C18	C18
Flow rate (mL/min)	0.3	0.3
Detention time (minute)	7.9	6.36
m/z, parent>product	287> 35	227> 212
Injection volume (µL)	10	10
LLD (µg/L)	0.10	0.15
LOQ (µg/L)	0.46	0.75

C18, Intersil ODS-3 C18 column (150 x 2 mm inner diameter, 5 µm particle size) from GL Sciences (Torrance, CA, USA)
LLD, Lower level of detection (determined according to Standard Method 1-10 (AWWA 1998))
LOQ, Limit of quantification (determined according to Standard Method 1-10 (AWWA 1998))

Table 5.6. Sorption coefficient (K_P) determination

Total PPCP concentration (μg/L)	Liquid phase PPCP concentration (μg/L)	Fraction of PPCP in liquid phase (f_L)	Partitioning coefficient (K_P, L/kg)	log K_P
		Triclosan		
		136 mg/L West Point activated sludge		
0.35[a]	0.09[b]	0.25	22037	4.34
23.66	3.25	0.14	46119	4.66
2.37	0.71	0.30	17029	4.23
1.85	0.55	0.30	17177	4.23
1.82	0.60	0.33	14774	4.17
1.52	0.51	0.34	14409	4.16
1.30	0.34[a]	0.26	20614	4.31
1.20	0.39[a]	0.32	15297	4.18
1.05	0.30[a]	0.29	18088	4.26
0.90	0.36[a]	0.40	11021	4.04
0.90	0.21[a]	0.23	24717[c]	4.39
0.74	0.28[a]	0.38	12235[c]	4.09
0.13[a]	0.06[b]	0.45	9068[c]	3.96
28.46	6.28	0.22	24246[c]	4.38
2.29	0.83	0.36	11999[c]	4.08
2.08	0.75	0.36	12254[c]	4.09
1.37	0.40[a]	0.29	16741[d]	4.22
0.40[a]	0.09[b]	0.23	23297[d]	4.37
0.16[a]	0.02[b]	0.15	38989[d]	4.59
25.67	14.27	0.56	4075[d]	3.61
15.57	8.09	0.52	4718[d]	3.67
3.18	0.82	0.26	14574[d]	4.16
2.86	0.86	0.30	11854[d]	4.07
0.47	0.04[b]	0.09	53431	4.73
0.13[a]	0.04[b]	0.31	11193	4.05
0.10[b]	0.01[b]	0.09	52764	4.72
		870 mg/L West Point activated sludge		
11.08	0.85	0.08	13863	4.14
6.22	0.40[a]	0.06	16933[c]	4.23
4.19	0.33[a]	0.08	13468[c]	4.13
1.84	0.15[a]	0.08	13106[c]	4.12
11.15	0.36[a]	0.03	34102[c]	4.53
7.08	0.24[a]	0.03	32955[c]	4.52
4.19	0.25[a]	0.06	17961[d]	4.25
2.29	0.15[a]	0.07	15910[d]	4.20
1.40	0.12[a]	0.08	12434[d]	4.09
10.38	0.72	0.07	14421[d]	4.16

Table 5.6. (*continued*)

Total PPCP concentration (μg/L)	Liquid phase PPCP concentration (μg/L)	Fraction of PPCP in liquid phase (f_L)	Partitioning coefficient (K_P, L/kg)	log K_P
6.62	0.37[a]	0.06	18145[d]	4.26
3.55	0.28[a]	0.08	12512[d]	4.10
2.85	0.22[a]	0.08	12710	4.10
1.37	0.11[a]	0.08	12439	4.09
0.74	0.07[b]	0.09	10548	4.02
	1100 mg/L West Point activated sludge			
14.58	0.26[a]	0.02	49477	4.69
9.65	0.26[a]	0.03	33248	4.52
4.77	0.14[a]	0.03	31124	4.49
3.74	0.17[a]	0.05	19226	4.28
3.48	0.17[a]	0.05	17202	4.24
2.66	0.08[b]	0.03	28023	4.45
2.25	0.10[b]	0.04	19819	4.30
1.85	0.06[b]	0.03	28107	4.45
1.58	0.05[b]	0.03	27711[c]	4.44
2.12	0.09[b]	0.04	20814[c]	4.32
1.26	0.10[b]	0.08	10689[c]	4.03
28.65	1.29	0.05	19078[c]	4.28
19.95	1.14	0.06	14879[c]	4.17
5.36	0.16[a]	0.03	28611[c]	4.46
4.51	0.13[a]	0.03	29388[c]	4.47
4.47	0.14[a]	0.03	27482[c]	4.44
3.68	0.15[a]	0.04	20524[c]	4.31
4.01	0.11[a]	0.03	31072[c]	4.49
2.43	0.10[b]	0.04	21339[c]	4.33
3.15	0.07[b]	0.02	37309[c]	4.57
1.76	0.11[a]	0.06	13342[c]	4.13
1.52	0.09[b]	0.06	14843[d]	4.17
1.31	0.05[b]	0.04	22406[d]	4.35
0.38[a]	0.04[b]	0.11	7357[d]	3.87
15.70	1.18	0.08	10626[d]	4.03
18.70	1.04	0.06	14626[d]	4.17
8.18	0.20[a]	0.02	35131[d]	4.55
6.21	0.16[a]	0.03	32417[d]	4.51
7.08	0.34[a]	0.05	16879[d]	4.23
4.69	0.11[a]	0.02	36655[d]	4.56
2.43	0.08[b]	0.03	25431[d]	4.41
2.07	0.08[b]	0.04	21855[d]	4.34
2.14	0.07[b]	0.03	25923[d]	4.41

Table 5.6. (*continued*)

Total PPCP concentration (μg/L)	Liquid phase PPCP concentration (μg/L)	Fraction of PPCP in liquid phase (f_L)	Partitioning coefficient (K_P, L/kg)	log K_P
1.72	0.06[b]	0.03	24007[d]	4.38
1.47	0.06[b]	0.04	20696	4.32
0.89	0.06[b]	0.06	12890	4.11
0.27[a]	0.04[b]	0.14	5404	3.73
			triclosan average[g]	**4.27±0.22**
		Bisphenol A		
		2140 mg/L West Point activated sludge		
2.31	1.47	0.64	267	2.43
2.29	1.52	0.66	234[e]	2.37
0.21[a]	0.15[b]	0.72	176[e]	2.24
2.15	1.69	0.78	125[f]	2.10
0.21[a]	0.11[b]	0.52	424[f]	2.63
			West Point average[h]	2.35±0.15
		1172 mg/L Snoqualmie activated sludge		
0.94	0.79	0.84	158	2.20
0.65[a]	0.49[a]	0.75	279	2.45
0.63[a]	0.54[a]	0.86	136	2.13
0.67[a]	0.50[a]	0.75	282	2.45
0.65[a]	0.51[a]	0.78	240	2.38
0.64[a]	0.52[a]	0.82	189	2.28
0.62[a]	0.47[a]	0.76	272	2.43
0.58[a]	0.44[a]	0.76	263	2.42
			Snoqualmie average[h]	2.34±0.10
		6130 mg/L Carnation activated sludge		
0.92	0.36[a]	0.40	249	2.40
0.59[a]	0.18[a]	0.31	359	2.56
0.54[a]	0.26[a]	0.47	181	2.26
0.54[a]	0.25[a]	0.46	190	2.28
0.48[a]	0.22[a]	0.45	198	2.30
0.50[a]	0.26[a]	0.53	146	2.16
0.42[a]	0.24[a]	0.57	121	2.08
0.41[a]	0.24[a]	0.58	119	2.08
			Carnation average[h]	2.26±0.12
			bisphenol A average[g]	**2.32±0.15**

[a] Below LOQ; [b] Below LLD; [c] Bioaugmented with 9.6 mg/L TrD23; [d] Bioaugmented with 60 mg/L TrD23; [e] Bioaugmented with 22 mg/L BiD32; [f] Bioaugmented with 68 mg/L BiD32; [g] standard deviation; [h] average deviation

a Triclosan

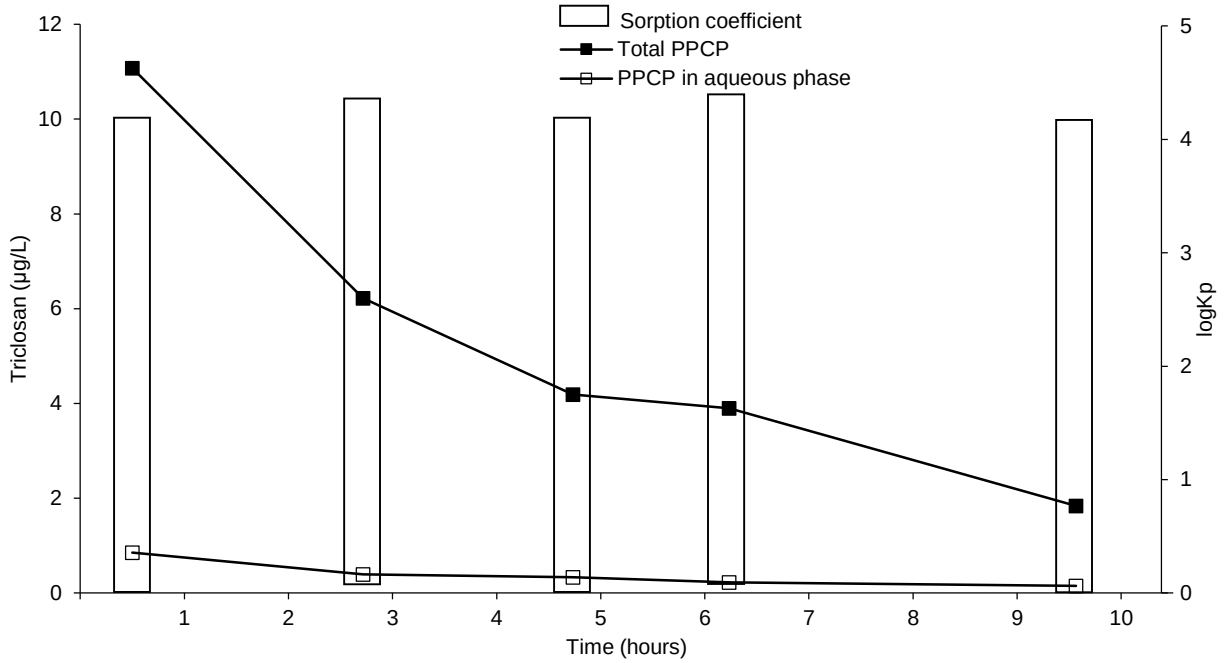

b Bisphenol A

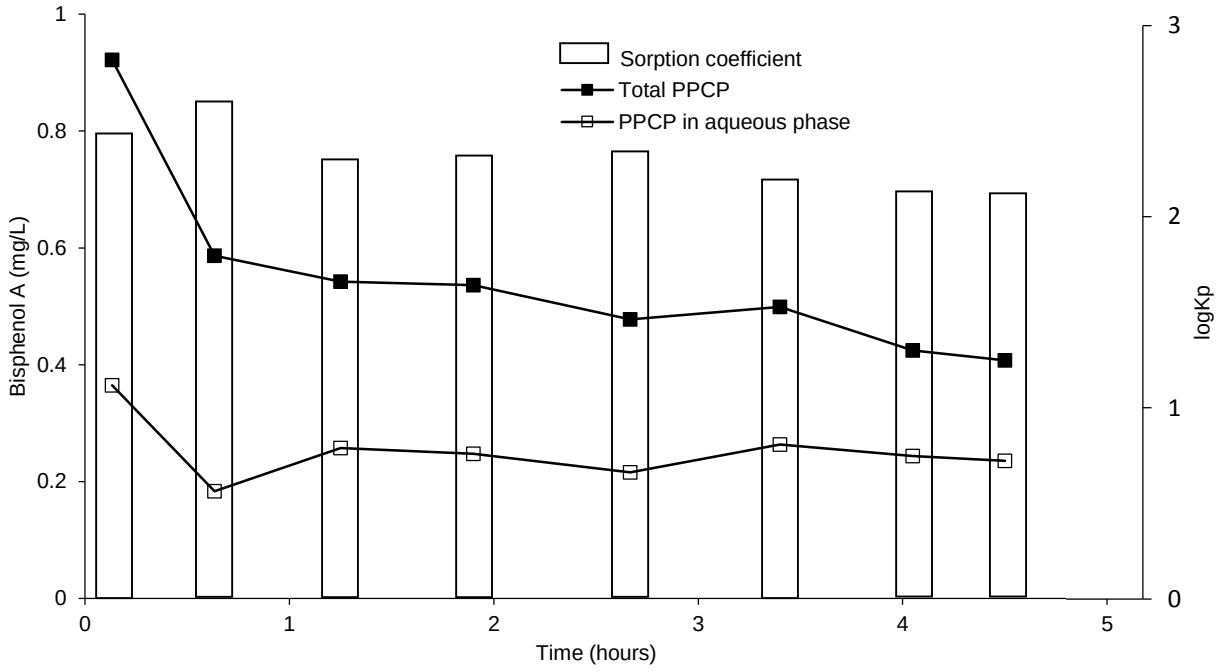

Figure 5.7. Degradation and observed sorption coefficients (log K_P) for a) triclosan in activated sludge from West Point wastewater treatment plant and b) bisphenol A in activated sludge from Carnation wastewater treatment plant. Open squares show PPCP in the aqueous phase, closed squares show total PPCP, and bars show calculated log K_P values. LogKp remained consistent in this dynamic system, suggesting that sorption and desorption kinetics were not rate limiting during PPCP degradation in these experiment

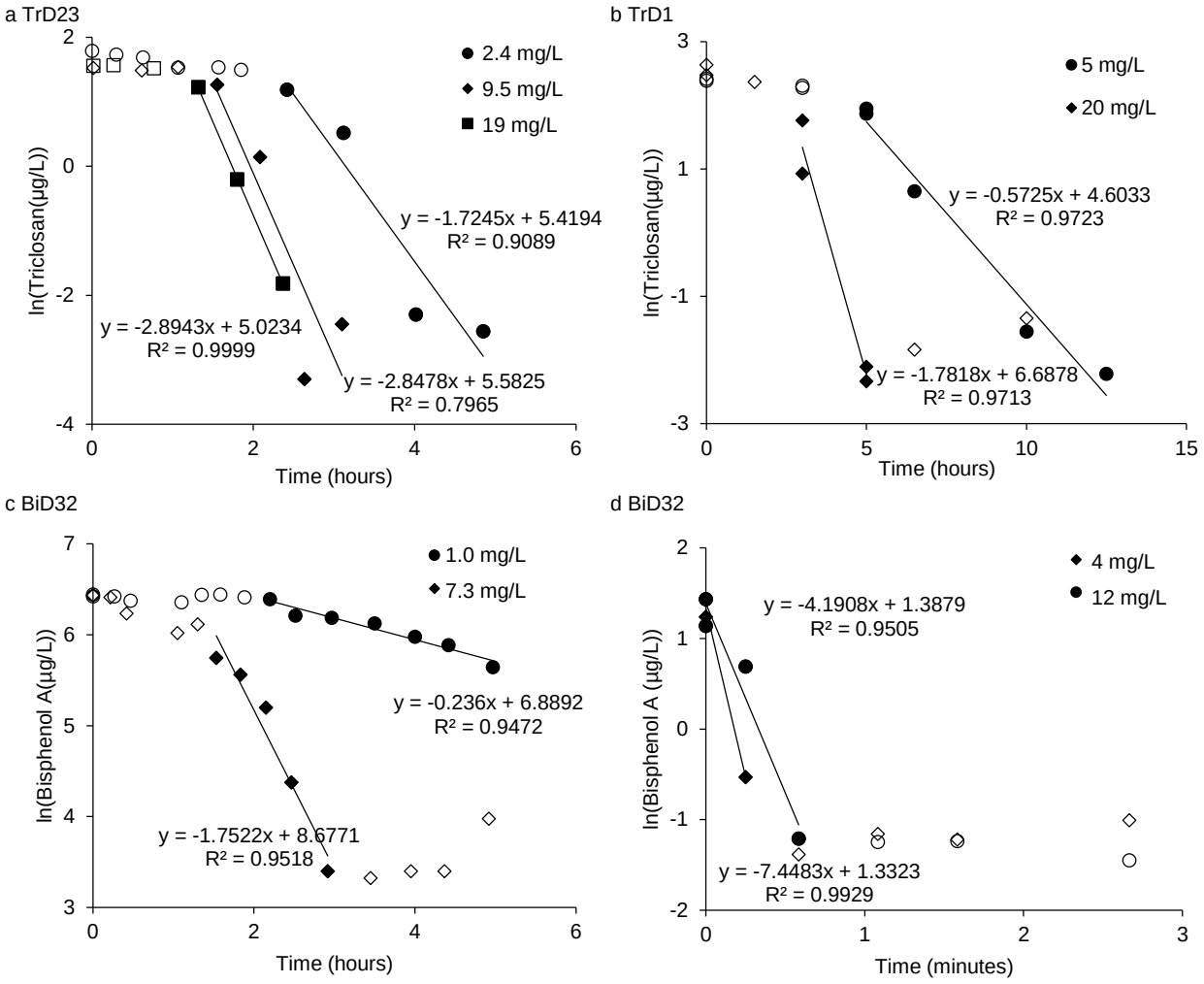

Figure 5.8. Solution to Eq 2 for calculating the degradation rate and lag by a) TrD23, b) TrD1, c) BiD32 (high bisphenol A concentrations), and d) BiD32 (low bisphenol A concentrations) in mineral or minimal media. Closed markers show data used to calculate degradation rates. Data points on graphs c and d at later time points were below the limit of quantification of 150 µg/L and 0.75 µg/L, respectively.

a 0 mg/L TrD23, 136 mg/L West Point activated sludge

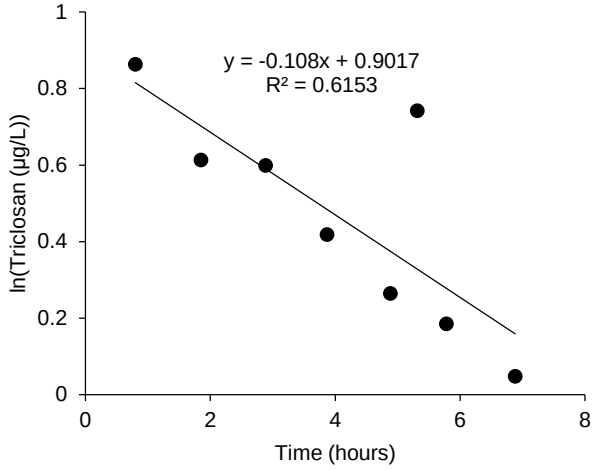

b 0 mg/L TrD23, 870 mg/L West Point activated sludge

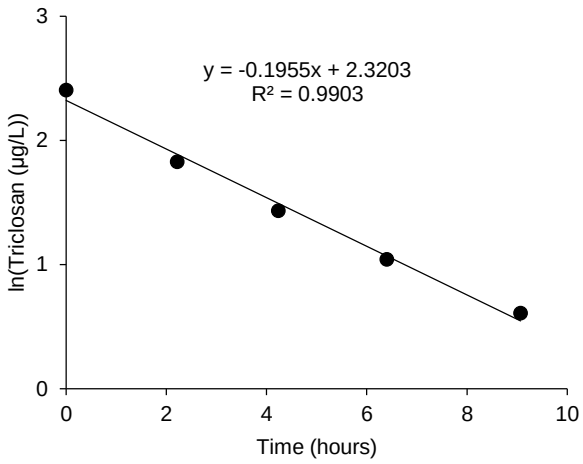

c 0 mg/L TrD23, 1100 mg/L West Point activated sludge

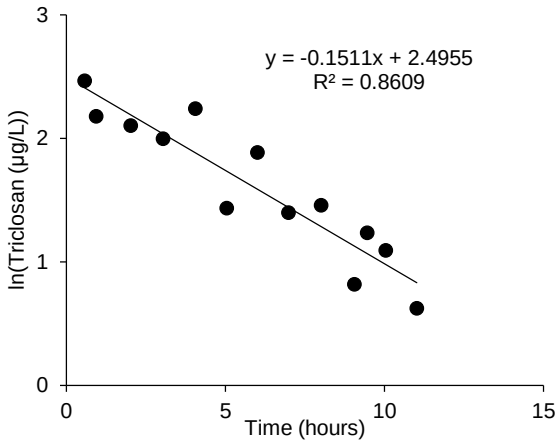

d 9.6 mg/L TrD23, 870 mg/L West Point activated sludge

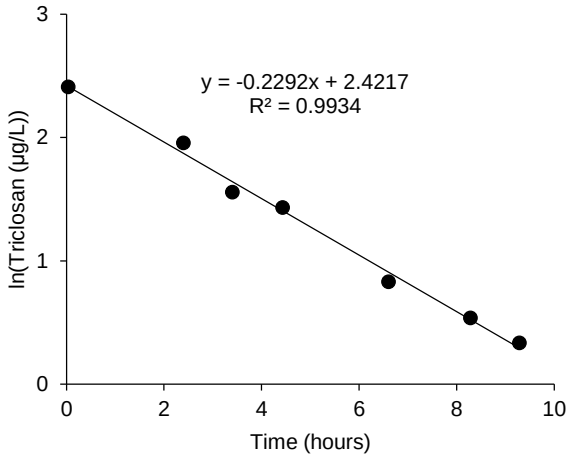

e 60 mg/L TrD23, 870 mg/L West Point activated sludge

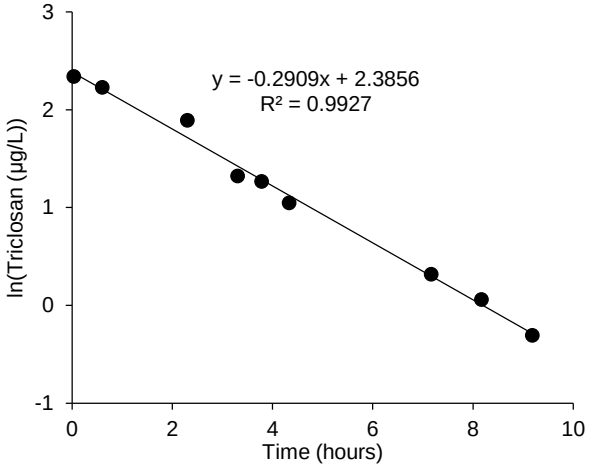

f 0 mg/L BiD32, 1172 mg/L Snoqualmie activated sludge

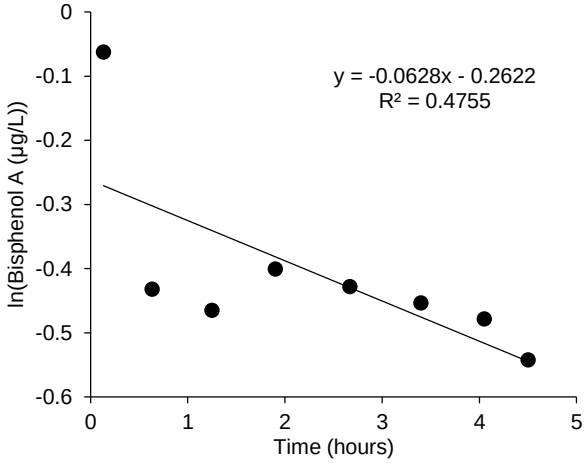

g 0 mg/L BiD32, 2140 mg/L West Point activated sludge

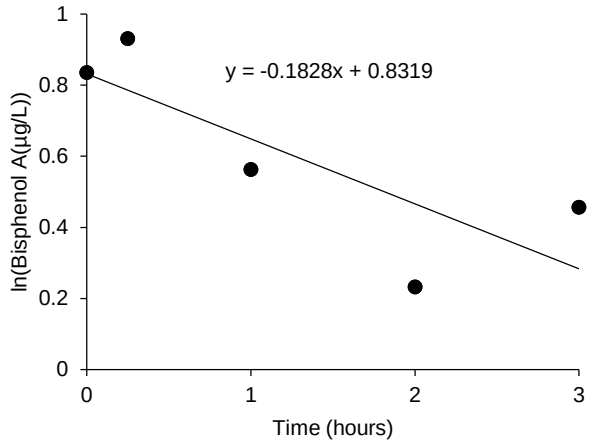

h 0 mg/L BiD32, 6130 mg/L Carnation activated sludge

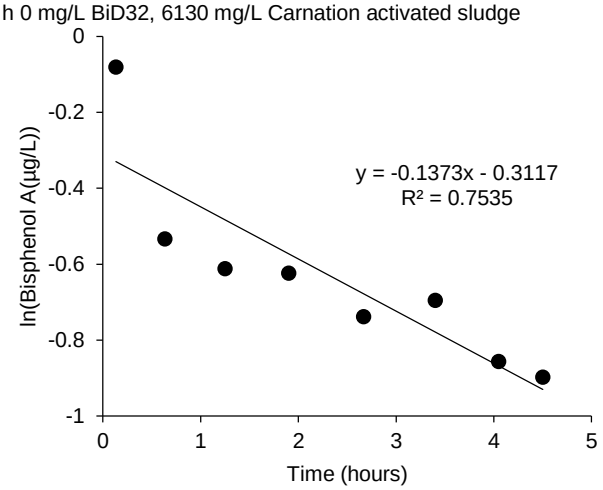

i 22 mg/L BiD32, 2140 mg/L West Point activated sludge

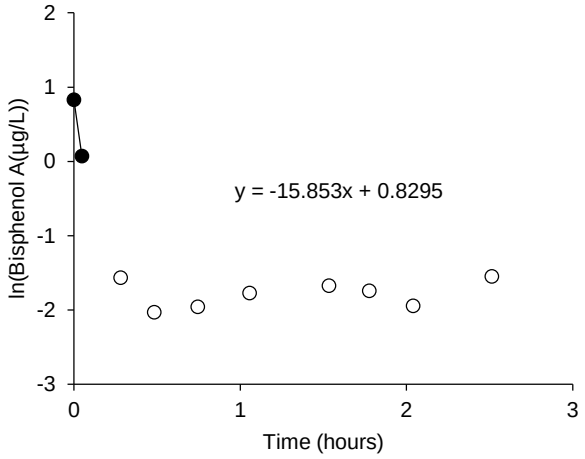

j 22 mg/L BiD32, 2140 mg/L autoclaved West Point activated sludge

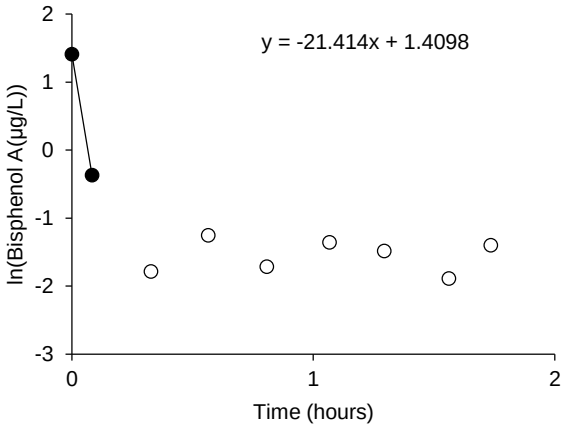

k 68 mg/L BiD32, 2140 mg/L West Point activated sludge

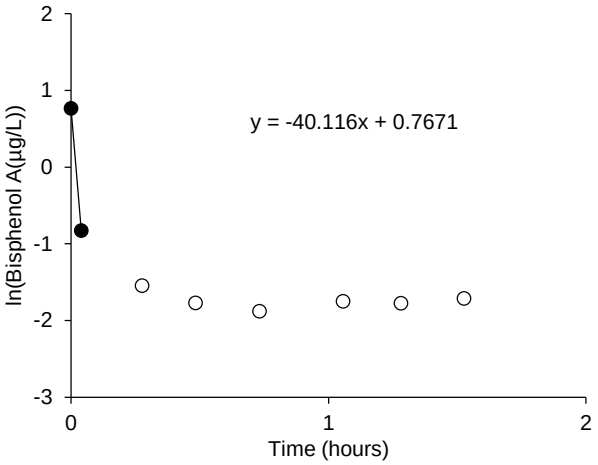

Figure 5.9. Application of Eq 5.2 to (a, d) activated sludge and (b, c, e, f, g) bioaugmented activated sludge. Open markers were below the LOQ, and were not used for determining the graphical slope.

Table 5.7. Predicted bioaugmentation dose and final concentrations in the reactor needed to obtain effluent concentration goal of 5 ng/L in a single CMAS

bacterial ID	specific degradation rate (k_c', L/mg-hr)	degradation rate in the reactor (k_c'*X, hr^{-1})	bioaugmentation dose (X_{in}, mg/L)		bioaugmented biomass in the reactors (X, mg/L)		ratio of bioaugmented biomass to activated sludge biomass (X:VSS)
			average	range	average	range	
TrD23	0.05	130	88	63 - 150	2700	1900 - 4450	1.3
TrD34	0.37	130	11.9	11.8 - 12.0	357	355 – 360	0.18
TrD1	0.42	130	10.5	10.5 - 10.6	316	314 – 319	0.16
BiD10	0.21	100	15.9	15.7 - 16.1	477	472 – 481	0.24
BiD32	1.08	100	3.1	2.6 – 3.8	93	78 – 120	0.046

Calculated using operating conditions shown in Table 5.1 using a single CMAS (Fig. 5.1a); VSS, activated sludge biomass in the reactors.

Table 5.8. Predicted bioaugmentation dose and final concentrations in the reactors needed to obtain effluent concentration goal of 5 ng/L in a 4-stage activated sludge process

bacterial ID	specific degradation rate (k_c', L/mg-hr)	degradation rate in the reactor (k_c'*X, hr^{-1})	bioaugmentation dose (X_{in}, mg/L)		bioaugmented biomass in the reactors (X, mg/L)		ratio of bioaugmented biomass to activated sludge biomass (X:VSS)
			average	range	average	range	
TrD23	0.05	40	26	17 - 51	790	520 - 1500	0.40
TrD34	0.37	33	3.0	2.9 - 3.1	90	87 - 93	0.045
TrD1	0.42	33	2.6	2.6 - 2.7	79	77 - 82	0.040
BiD10	0.21	4.2	0.67	0.65 - 0.68	20	20 - 21	0.010
BiD32	1.08	4.2	0.13	0.11 - 0.16	3.9	3.2 - 4.9	0.0019

Calculated using operating conditions shown in Table 5.1 using a 4-stage activated sludge process (Fig. 5.1b); VSS, activated sludge biomass in the reactors.

CHAPTER 6: ENHANCED BIOLOGICAL TRACE ORGANIC CONTAMINANT REMOVAL (EBTCR) DURING WASTEWATER TREATMENT: A LAB SCALE DEMONSTRATION WITH THE BISPHENOL A-DEGRADING BACTERIA *SPHINGOBIUM* SP. BID32

6.1 Chapter summary

This chapter documents testing using lab scale reactors to evaluate the use of bioaugmentation to improve trace organic contaminant (TOrC) removal (Objective III). The hypothesis "continuous bioaugmentation is a sustainable and practical technique to enhance trace organic contaminant removal in activated sludge" was tested using BPA as a model compound. In Chapter 5, the model used to assess EBTCR assumed that the growth and loss of the augmented bacteria were equal because actual data was not yet available. Thus, the survival of the augmented bacteria was tested (Objective IV) as part of the reactor study. *Sphingobium* sp. BiD32 (described in Chapter 4) were bioaugmented into the test reactor. A control reactor was bioaugmented with a closely related, non-BPA-degrading bacteria, *Sphingopyxis* sp. TrD1, to test if improved BPA degradation could be explained by addition of non-specific bacterial biomass or from residual growth media transferred with the augmented bacteria. BPA removal and BPA degradation rates were 2 to 4 times greater in the test reactors compared to the control reactor during cycle 1 (the bioaugmentation cycle) when operated with both an 8 and 3-day SRT, though the enhanced removal was lost over time. BPA was lower in the effluent and wasted solids, in the test reactor, demonstrating that this technology protects both the biosolids and the effluent from TOrCs contamination. This is important for use of biosolids as a fertilizer and the public perception of their use. A net loss of augmented bacteria was measured. This differs from the assumptions made in Chapter 5 (i.e. that growth and loss of the augmented bacteria were equal), suggesting that higher augmentation rates that previously determined may be needed to compensate for the measured loss. Additionally, testing showed that BPA degradation by *Sphingobium* sp. BiD32 was partially inducible, suggesting that future modifications could be made to the side growth reactor to improve BPA degradation when bioaugmented. In conclusion, the feasibility of achieving EBTCR with bioaugmentation was demonstrated in lab scale reactors and supported by theoretical modeling.

6.2 Abstract

Discharge of trace organic contaminants (TOrCs) from wastewater treatment plants (WWTPs) may contribute to deleterious effects on aquatic life. Release to the environment is both through direct WWTP effluent and also from runoff following land applications of biosolids. This study introduces Enhanced Biological TOrCs Removal (EBTCR), which uses continuous bioaugmentation of TOrC-degrading bacteria, to improve TOrC destruction during wastewater treatment. The study investigated the degradation of bisphenol A (BPA) in two parallel lab-scale sequencing batch reactors (SBRs). The reactors were fed primary effluent from a municipal WWTP. The reactors were operated with 8 cycles per day and operation at 8-day and 3-day solids retention times (SRTs) were compared. The test reactor was bioaugmented with *Sphingobium* sp. BiD32 daily in cycle 1. BPA degradation was 2 to 4 times higher in the test reactor than in a control reactor for all the tested conditions (i.e. initial BPA concentrations of 100 µg/L and 10 µg/L; $p<0.05$) during cycle 1. Improved BPA removal persisted for greater than 15 hours (5 cycles) following bioaugmentation. By the 8th cycle (the cycle just prior to bioaugmentation), the degradation rates were not statistically different between the test and the control reactors, though the enchanced removal returned with the bioaugmentation at the beginning of the next day. Removal of the TOrC was demonstrated to reduce concentrations in both the reactor effluent and in the wasted solids. There was a net loss of *Sphingobium* sp. BiD32 following bioaugmentation, supporting the original hypothesis that continuous bioaugmentation (rather than single dose bioaugmentation) would be required to improve removal of TOrCs during wastewater treatment. This study demonstrates a biologically-based approach for enhanced removal of TOrCs that reduces concentrations in both the wastewater effluent and prevents transfer to the biosolids.

6.3 Introduction

While trace organic contaminants (TOrC) are known to be degraded by biologic action during wastewater treatment (Samaras et al. 2013; Bester 2005; Yan et al. 2014), their residual concentrations in effluent and biosolids remain an environmental concern (Paxeus 2004; Topp et al. 2008). A wide range of TOrCs effluent concentrations (Duong et al. 2010a; Ballesteros-Gomez et al. 2007; Gross et al. 2004; Perez et al. 2013) and removal rates (Samaras et al. 2013b; Snyder et al. 2007; Nakada et al. 2006; Ternes et al. 1999) are reported at wastewater treatment plants (WWTP) operating with traditional secondary treatment. As a result, the TOrCs that should be targeted for enhanced treatment will differ among WWTPs. Variation in effluent concentrations are speculated to result from a combination of multiple factors such as operational conditions (e.g. retention times and reactor configurations), influent concentrations, and microbial communities (Lubliner et al. 2010). Because bacteria are capable of degrading TOrCs, potential exists for engineering their degradation abilities to improve TOrCs removal during wastewater treatment.

Bioaugmentation with bacteria capable of degrading TOrCs has theoretical potential to enhance removal of TOrC from WWTPs. Many bacteria have been identified in activated sludge that are capable of degrading TOrCs in a complex carbon environment (Lee et al. 2012; Ike et al 1995; Zhou et al. 2013), and studies of the transfer of labeled carbon have suggested that mineralization of some TOrCs (e.g. triclosan (Federle et al. 2002), ibuprofen (Kimura et al. 2010), testosterone (Layton et al. 2000), and 17β-estradiol (Layton et al. 2000)) can be achieved by activated sludge communities. A proposed approach to bioaugmentation, Enhanced Biological TOrC Removal (EBTCR), involves augmenting TOrCs-degrading bacteria into the activated sludge of a WWTP. Improved TOrCs removal by EBTCR was theoretically demonstrated in Chapter 5 by modeling of a full-scale activated sludge process (Zhou et al. 2014). Because the treatment occurs in activated sludge, this approach additionally reduces the sorbed TOrCs in waste activated sludge and potentially reduces the amount of TOrCs in biosolids. EBTCR could represent a low-impact option for increasing TOrCs removal without requiring extensive capital and maintenance costs.

Many challenges remain for successful implementation of bioaugmentation for improved TOrC removal during wastewater treatment. Among these are the rapid loss of augmented bacteria (over one order of magnitude in one day (Hashimoto et al. 2010) and over 1-2.5 orders of magnitude in one SRT (Roh and Chu 2011)). For example, predators favor grazing on dispersed bacteria, which may be a contributing factor to the rapid loss of bacteria following bioaugmentation into activated sludge, as demonstrated by protozoan grazing of bioaugmented denitrifying bacteria (Bouchez et al. 2000). Continuous or periodic bioaugmentation would compensate for losses and help maintain improved TOrCs removal during EBTCR (Zhou et al. 2014).

Another challenge for successful bioaugmentation is the extreme low TOrC concentrations in WWTPs. Because the TOrCs concentrations are too low to sustain bacterial growth, the bacteria to be augmented must grow using other carbon sources. Therefore during EBTCR, pure cultures with known TOrCs degradation capabilities would be cultured in a side growth reactor on a common carbon source (Zhou et al. 2014). This differs from nitrification bioaugmentation techniques, which utilize the higher concentration of ammonia in anaerobic digester centrate to enrich for nitrifiers in a side stream reactor. But the low TOrCs concentrations preclude this type of in-line enrichment approach.

The primary goal of this study was to test EBTCR in activated sludge fed municipal wastewater with a common TOrCs concentration. The study was conducted in lab-scale sequencing batch reactors. The

hypothesis was that low dose, continuous bioaugmentation with specific organisms will improve TOrCs removal and reduce the TOrCs transferred to solids. BPA was used as a model TOrC compound and *Sphingobium* sp. BiD32 as a model organism. BPA was chosen as the model compound because it is a TOrC commonly detected in WWTP effluents (Duong et al. 2010a; Ballesteros-Gomez et al. 2007) and surface waters (Kolpin et al. 2002; Kleywegt et al. 2011; Peng et al. 2008) at concentrations found to have negative effects on aquatic life (low µg/L) (Zhang et al. 2013). *Sphingobium* sp. BiD32 was chosen as the model organism as it is capable of: *(1)* degrading BPA to <5 ng/L, *(2)* degrading BPA after it was grown in the absence of BPA, *(3)* degrading BPA before growth on other carbon sources, and *(4)* degrading BPA with reasonable degradation rates for bioaugmentation (Zhou et al. 2013; Zhou et al. 2014). In this study, BPA degradation kinetics was determined under operation at an 8-day and 3-day solids retention time (SRT). The fate of the removed BPA was determined under operation at a 3-day SRT. These values were determined in both the test reactor (augmented with *Sphingobium* sp. BiD32) and in the control reactor (augmented with a bacteria that does not degrade BPA). The loss of *Sphingobium* sp. BiD32 was measured under reactor conditions and these results were applied to the previously created model (Zhou et al. 2014) to assess the practicality of bioaugmentation to improve BPA removal.

6.4 Materials and methods

6.4.1 Laboratory reactor set-up

Two (2) lab scale sequencing batch reactors (SBR, a test reactor and a control reactor) were operated. Each had a working volume of 950 mL and were maintained in a temperature controlled chamber (20ºC). The SBRs were seeded with activated sludge from a municipal WWTP (West Point WWTP; Seattle, Washington). The reactors were fed effluent from the primary clarifiers at West Point WWTP that was amended with 100 mg/L $NaHCO_3$ and 100 mg/L NaOAc (77 mg/L COD) to adjust for the low alkalinity and soluble COD (sCOD) at this facility. The feed was collected from the WWTP weekly, and stored at 4ºC until used. sCOD of the feed was measured when collected and on the final day of use to ensure that changes did not impact reactor operation. The average background BPA concentration in the feed was 0.9 µg/L ± 0.7 (n=17). Additional BPA (0.8 µg/L) was added to the reactors with the feed during the first step resulting in an initial BPA concentration of 1.7 µg/L ± 0.7 each cycle, which is within the mean range of influents for WWTPs (Nie et al. 2012; Melcer and Klecka 2011b).

The SBRs were operated with a 3-hour cycle consisting of 5 steps, as shown in Figure 6.1. The reactors were mixed during the feeding (step 1), anoxic (step 3), and reaction (step 3) steps; and were quiescent for settling (step 4) and effluent decantation (step 5). During Step 1 (feeding), 237.5 mL of feed and BPA solution was added to the reactors resulting in a nominal 12 hour hydraulic retention time (HRT).

Aeration during Step 3 was provided with an aquarium pump and a ceramic stone sparger. The SBRs were manually wasted at the end of step 3 once each day. Solids wasting was conducted when the SBRs were fully mixed to ensure a consistent solids concentrations in the waste activated sludge (WAS), which is more difficult to obtain from the settled zone in step 5 when using lab-scale reactors. The waste volume of WAS was adjusted to maintain an 8-day and 3-day SRT in Phase I and Phase II of the experiment, respectively. Bulk liquid (from WAS) and effluent (from step 5) were monitored for total suspended solids/volatile suspended solids (TSS/VSS; Standard Method 2540E (AWWA 1998)), pH (Beckman Coulter, Inc., Brea, CA, USA), sCOD (0.45 µm cellulose acetate filtered and determined using a low range Hach COD kit (Standard Method 5220D (AWWA 1998); Hach Company, Loveland, CO, USA)), and rotifers and protozoan concentrations (Standard Methods 10300C (AWWA 1998)) at least once a week.

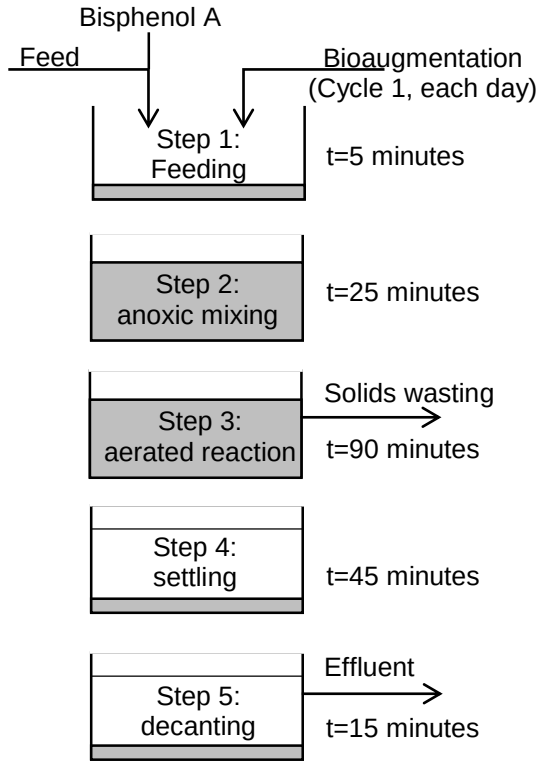

Figure 6.1. Lab scale sequencing batch reactor cycle operation. The steps were continuous and automated; 8 cycles were run each day.

6.4.2 Bioaugmentation

Both reactors were bioaugmented each day at the start of cycle 1. The test reactor received *Sphingobium* sp. BiD32 and the control reactor received *Sphingopyxis* sp. TrD1. *Sphingopyxis* sp. TrD1 was selected for the control reactor because it is phylogenetically related and had a similar growth rate to *Sphingobium* sp. BiD32, but does not degrade BPA (Zhou et al. 2013). The cultures were grown in 2X R2B. R2B is a

nutrient-rich broth with a sCOD of approximately 5.5 g/L (at 2X strength) whose composition is based on R2 Agar (Reasoner and Geldreich 1979) and is composed of 1 g/L yeast extract, 1 g/L proteose peptone, 1 g/L casamino acids, 1 g/L glucose, 1 g/L soluble starch, 0.6 g/L sodium pyruvate, 0.6 g/L dipotassium phosphate, and 0.1 g/L magnesium sulfate (at 2X strength). The concentration of the cultures was measured using optical density at 600 nm (OD_{600}) prior to addition to the reactors and biomass equivalency of the measured OD was confirmed by measuring VSS on a regular basis. 25 mL of the grown cultures were added to the reactors each day to achieve an approximate concentration of 15 mg/L of *Sphingobium* sp. BiD32 (15.1 mg/L ± 2.7, n=76) and *Sphingopyxis* sp. TrD1 (17.5 mg/L ± 3.7, n=75). The sCOD associated with the spent media added with the cultures to the test and control reactors was 118 and 105 mg/L sCOD, respectively. Each day, the cultures were transferred into fresh 2X R2B for an approximate initial biomass concentration of 5 mg/L. These cultures were grown overnight and used for bioaugmentation the next day.

6.4.3 BPA degradation kinetics testing

Total BPA removal rates were measured by tracking single spike additions of 100 µg/L (at an 8-day SRT) and 10 µg/L (at both an 8-day and a 3-day SRT) (at step 1, Figure 6.8) while keeping all other parameters (including the bioaugmentation dose) the same. Whole sample extractions (Zhou et al. 2013) allowed both the dissolved and the sorbed BPA to be quantified in a single sample. These higher single dose additions allowed for detection of BPA in smaller volume samples collected at multiple time points during the aerated reaction step without necessitating larger volume samples that would compromise the reactors. BPA concentrations were monitored in both reactors during step 3 for two cycles after the BPA spike. BPA was quantified as previously described using a high performance liquid chromatography tandem mass spectrometer (LC-MS/MS) (Zhou et al. 2013, Chapter 4). The lower level of detection was 0.15 µg/L and the level of quantification was 0.75 µg/L (Zhou et al. 2013; AWWA 1998).

The rate of degradation was as assumed to fit a first-order model:

$$\frac{dc_T}{dt} = -k_{cT}c_T \qquad \text{(Eq 6.1)}$$

where dc_T/dt is the rate of change of the total BPA concentration (aqueous and sorbed, µg/L-h), k_{cT} is the total degradation rate (hr^{-1}, Eq 6.4), and c_T is the total BPA concentration (aqueous and sorbed, µg/L). Eq 6.1 was integrated and linearized as:

$$lnc_T = -k_{cT}t + lnc_{T,0} \qquad \text{(Eq 6.2)}$$

where $c_{T,0}$ is the initial BPA concentration and t is reaction time (hr). k_{cT} was solved graphically by plotting $\ln_{cT}$ versus t and the y-intercept was $\ln c_{T,0}$ and the slope was k_{cT}. The BPA degradation in the reactors could then be modeled using the average k_{cT} from replicate experiments:

$$\frac{c_T}{c_{T,0}} = exp(-k_{cT}t) \quad \text{(Eq 6.3)}$$

The total degradation rate (k_{cT}) was a combination of the degradation by *Sphingobium* sp. BiD32 and the background degradation of the activated sludge:

$$k_{cT} = (k_c'\mathrm{X} + k_{AS}'\mathrm{VSS})f_L \quad \text{(Eq 6.4)}$$

where k_c' is the specific degradation rate by *Sphingobium* sp. BiD32 (L/mg-hr), X is the augmented *Sphingobium* sp. BiD32 concentration (mg/L), k_{AS}' is the specific degradation rate by the background activated sludge (L/mg-hr), and VSS is the activated sludge concentration (mg/L). f_L is the BPA in the liquid fraction, which was assumed to be more bioavailable than the sorbed fraction. f_L was calculated as:

$$f_L = \frac{1}{1 + K_P(VSS + X)} \quad \text{(Eq 6.5)}$$

where K_p is the adsorption coefficient of BPA measured in activated sludge (L/kg VSS; Zhou et al. 2014, Chapter 5). Data from the control reactors (i.e. $k_c'\mathrm{X} = 0$) was used to calculate k_{AS}'. The k_c' in the test reactor was then solved by applying the calculated k_{AS}' term into Eq 6.4.

6.4.4 qPCR

Sphingobium sp. BiD32 16S rRNA gene concentrations were measured by qPCR. DNA was extracted using the MO BIO UltraClean Microbial DNA Isolation Kit (MO BIO Laboratories, Inc., Carlsbad, CA, USA). The manufacturer's instructions were followed with two modifications: the samples were heated (65ºC, 10 min) to increase the yield (an optional step suggested by the manufacturer) and the samples were agitated for 20 seconds at speed 4.0 in a cell homogenizer (FastPrep®-24 Instrument; MP Biomedicals, Inc, Solon, OH, USA). Extracts were evaluated using a NanoDrop 1000 spectrophotometer (NanoDrop Technologies, Wilmington, DE, USA) to determine the quality and concentration of the DNA. A 260:280 ratio between 1.7 and 1.9 was considered to be acceptable, and the concentration was determined at 260 nm.

Primers for detection of *Sphingobium* sp. BiD32 16S rRNA gene concentrations were designed using NCBI Primer-BLAST (http://www.ncbi.nlm.nih.gov/tools/primer-blast/) and purchased from Invitrogen (Invitrogen, Carlsbad, CA, USA). The primers are summarized in Table 6.1. The primers matched 100% to *Sphingobium* sp. BiD32 and to five closely related sequences including uncultured soil bacterium

clones, *Sphingomonas* sp. B1-105, and *Sphingomonas* sp. A1-13. The forward primer had greater than 6 mismatches, insertions, or deletions compared to *Sphingopyxis* sp. TrD1 and the reverse primer had one mismatch.

Table 6.1. Primers used for PCR reactions

Target Organisms	Primer	Sequence	Tm	GC (%)
Primers used for qPCR				
Sphingobium sp. BiD32[1]	65F	5'-AACGATCCCTTCGGGGATA-3'	60.2	52.6
	268R	5'-TAAGGATCGTTGCCTTGGTGA-3'	60.6	47.6
Primers used for cloning reactions				
Bacteria[2]	8F	5'-AGAGTTTGATCCTGGCTAG-3'		
	1492R	5'-TTCCGGTTGATCCYGCCGGA-3'		

[1]These primers were designed for this study

[2] Delong, EF. 1992. "Archaea in Coastal Marine Environments." *Proceedings of the National Academy of Sciences of the United States of America* 89 (12): 5685–89. doi:10.1073/pnas.89.12.5685.

Standards were prepared using the PCR product of 16S rRNA genes of *Sphingobium* sp. BiD32 using Bacterial Domain primers (Table 6.1). These PCR products were cloned using a TOPO TA Cloning Kit (Invitrogen Molecular Probes, Grand Island, NY, USA). Plasmids were isolated by QIAprep Spin Miniprep Kit (Qiagen, Valencia, CA, USA), quantified using a NanoDrop 1000 spectrophotometer (NanoDrop Technologies, Wilmington, DE, USA), and linearized by the restriction enzyme EcoRI (R6011, Promega Corporation, Madison, WI, USA).

qPCR analysis was performed using an Eppendorf MasterCycler Realplex (Eppendorf North America, Inc., Westbury, NY, USA) and GoTaq qPCR Master Mix (Promega Corporation, Madison, WI, USA). The PCR program to determine *Sphingobium* sp. BiD32 16S rRNA gene concentrations was as follows: hot-start activation (95ºC for 10 minutes), 50 cycles of denaturation (95ºC for 15 seconds), annealing (65ºC for 1 minute), and extension (60ºC for 1 minute), and dissociation (95ºC for 15 seconds). Each DNA extract was processed at a tenfold and hundredfold dilution to monitor for PCR inhibition effects.

A standard curve was generated using tenfold dilutions of the linearized plasmids (Figure 6.9, supplemental). The resulting standard curve for *Sphingobium* sp. BiD32 had an average efficiency of 0.70 (R^2=0.958) with a method detection limit of $6.7x10^3$ 16S rRNA gene copies per PCR reaction (cycle threshold ~31.5, n=15). Negative controls included the closely related organisms *Sphingobium* sp. BiD10 (cycle threshold ~32.3, n=17), *Sphingopyxis* sp. TrD1 (cycle threshold ~31.7, n=14), and a water blank (rarely amplified, cycle threshold ~38.1, n=8).

6.4.5 Net loss of augmented bacteria

Loss kinetics of the augmented bacteria were measured. The rate of change in augmented bacterial concentrations was calculated as:

$$\frac{dX}{dt} = -k_X X \quad \text{(Eq 6.6)}$$

where dX/dt is the rate of change of the augmented bacteria (mg/L-hr), k_X is the net loss rate coefficient (hr^{-1}), and X is the augmented bacterial concentration (mg/L).

To determine the net loss, a batch experiment was completed where *Sphingobium* sp. BiD32 was inoculated into reactor waste sludge collected from the control reactor (to minimize bias from background readings in the bioaugmented reactor). *Sphingobium* sp. BiD32 concentrations were monitored using qPCR. Eq 6.7 was solved graphically and the y-intercept was $\ln X_0$ and the slope was k_X. In this case the k_X represented the overall fate of the augmented bacteria, including growth and death. The losses could be due to predation, endogenous decay, or loss in the effluent due to differential settling.

To determine the maximum possible growth kinetics under reactor conditions, approximately 15 mg/L *Sphingobium* sp. BiD32 was inoculated into a 3:1 mixture of reactor waste sludge:feed and *Sphingobium* sp. BiD32 concentrations were monitored using qPCR while mixing and aerating over 17 hours. The waste sludge collected from the control reactor and the feed was autoclaved, sonicated (35 minutes) to release cell lysis debris, filtered (0.2 µm SCFA), and autoclaved to remove competing bacteria and to include cell lysis debris. Eq 6.6 was integrated and linearized as:

$$lnX = -k_X t + lnX_0 \quad \text{(Eq 6.7)}$$

where k_X is assumed to represent the maximum bacterial growth only under these conditions. The equation was solved graphically and the y-intercept was $\ln X_0$ and the slope was k_X.

6.4.6 Full-scale activated sludge process model

The loss of *Sphingobium* sp. BiD32 over time was added to a previously described 4-stage activated sludge model that demonstrated the theorectial feasilibity of bioaugmentation for BPA removal (Zhou et al. 2014). When accounting for the change in *Sphingobium* sp. BiD32 in the reactors and assuming steady state, the BPA concentrations were calculated by:

$$c_1 = \frac{c_{in}^*}{1 + \frac{k_1 \tau}{4}} \quad \text{(Eq 6.8)}$$

where c_1 is the BPA concentration in reactor 1 (ng/L), c_{in}* is the BPA concentration entering reactor 1 (ng/L), τ is the total hydraulic retention time (hr), and k_1 is the total BPA degradation rate in reactor 1 calculated by:

$$k_1 = (k_c' X_1 + k_{AS}' \text{VSS}) f_L \quad \text{(Eq 6.9)}$$

where X_1 is the augmented biomass in reactor 1 (mg/L).

The BPA concentration and the total BPA degradation rate in each of the four reactors were calculated using the *Sphingobium* sp. BiD32 concentration in each reactor. The *Sphingobium* sp. BiD32 concentration in reactor 1 was calculated by:

$$X_1 = \frac{X_{in}^*}{1 + \frac{k_X \tau}{4}} \quad \text{(Eq 6.10)}$$

where X_{in}* is the augmented biomass entering reactor 1 (mg/L). The concentrations in reactor 2, 3, and 4 were calculated similarly.

Other calculations were completed as previously described (Zhou et al. 2014) with the exception of the calculation for c_{in}*. The BPA entering reactor 1 was calculated by:

$$c_{in}^* = \frac{\frac{Q c_{in}}{Q + Q_r} - \frac{Q_r c_e (Q - Q_w)}{(Q_w + Q_r)(Q + Q_r)}}{1 - \frac{Q_r}{Q_w + Q_r} / (1 + \frac{k_1 \tau}{4}) / (1 + \frac{k_2 \tau}{4}) / (1 + \frac{k_3 \tau}{4}) / (1 + \frac{k_4 \tau}{4})} \quad \text{(Eq 6.11)}$$

where Q is the influent flow rate (m^3/d), c_{in} is the influent BPA concentration (ng/L), Q_r is the recycle flow rate (m^3/d), c_e is the effluent BPA concentration (ng/L), and Q_w is the waste stream flow rate (m^3/d).

6.4.7 Cost estimation for bioaugmentation

The costs were estimated for purchase of feed stocks needed to grow *Sphingobium* sp. BiD32 sufficient to treat the modeled full-scale system. The cost per day was calculated as:

$$\frac{substrate\ cost}{day} = \frac{X_{in} Q}{450 \frac{mg\ Sphingobium\ sp. BiD32}{g\ substrate\ oxidized}} \times \frac{cost}{g\ substrate} \quad \text{(Eq 6.12)}$$

where 450 mg *Sphingobium* sp. BiD32 per g substrate oxidized was assumed based on the yield of 0.45 g VSS per g substrate oxidized (Tchobanoglous et al. 2014)

Costs for feed stocks were estimated as: whey protein ($2.8/kg), tryptone ($1/kg), yeast extract ($1/kg), molasses ($0.12/kg), and lactose ($1/kg). These substrates were selected for consideration based on their ability to sustain *Sphingobium* sp. BiD32 growth (Zhou et al. 2013) and their relatively low costs.

6.4.8 Induction of BPA degradation

To determine if BPA degradation by *Sphingobium* sp. BiD32 was inducible, degradation of BPA was compared between *Sphingobium* sp. BiD32 cultures previously exposed and not exposed to BPA. Parallel cultures of *Sphingobium* sp. BiD32 was grown in R2B with and without adding 2 mg/L BPA. To ensure that BPA was still actively being degraded when the culture was transferred, BPA was re-spiked during active growth. When the cultures were grown (OD_{600} of approximately 0.36, 9.5 hours after inoculation, ~170 mg/L), the cultures were transferred into fresh R2B containing either 1, 2, or 10 mg/L BPA. To measure BPA degradation in the absence of continued growth, the same cultures were transferred into buffered mineral salts media (solution described in Chapter 4 and Tanner 1997) containing 2 mg/L BPA. BPA was monitored using a high pressure liquid chromatography instrument with a UV detector as previously described (Zhou et al. 2013). Growth was monitored by change in optical density (OD_{600}). The specific degradation rate by *Sphingobium* sp. BiD32 (k_c', $hr^{-1}OD_{600}^{-1}$) was determined by:

$$\frac{lnc_T}{X} = -k_c' t \qquad \text{(Eq 6.13)}$$

where X is biomass concentration (OD_{600}). The equation was solved graphically and the slope was k_c'.

6.4.9 Statistical analyses

Average deviation from the mean was used to estimate error when the number of replicates (n) was too low to meet the assumption of a normal distribution as required when calculating standard deviation (Panneerselvam 2004):

$$AD = \frac{\Sigma|x - \bar{x}|}{n} \qquad \text{(Eq 6.14)}$$

Unpaired student t-tests were used to compare replicate BPA degradation rates obtained for the test and control reactors.

6.5 Results

6.5.1 Laboratory reactor operation

The reactors operated stably during the experiments (Figures 6.10 and 6.11, supplemental). Reactor performance is shown in Table 6.2. Reactor pH was between 7.2 and 7.9, and no trends were indicated between the reactors or with operational SRT. Reactor VSS and TSS were higher with a higher SRT, as is typical for higher SRT systems. Effluent VSS was more variable within single reactors, but was consistent between reactors. Bioaugmentation dosing to the control reactor was slightly higher than to the test reactor; this difference was statistically significant when operated with an 8-day SRT (p=9.5x10^{-6}, t-test), but was not statistically significant when operated with a 3-day SRT (p=0.19, t-test). During Phase I

(8-day SRT), the bioaugmented *Sphingobium* sp. BiD32 represented approximately 1.2% of the total VSS (Table 6.2). During Phase II (3-day SRT), the bioaugmented *Sphingobium* sp. BiD32 represented approximately 1.9% of the total VSS (Table 6.2). sCOD at the start of the aeration period varied, mirroring the differences in the feed. Despite the initial sCOD variation, the test and control reactors consistently removed sCOD to a final concentration of 22.4 and 24.3 mg/L, respectively, during the aeration period (Table 6.2). Experiments were initiated after operation for a minimum of 3 SRTs following start-up or change in system operation.

Table 6.2. Sequencing batch reactor operating conditions (20ºC)

	SRT (day)	HRT (hour)	Bioaugmentation dose* (mg/L)	Reactor TSS (mg/L)	Reactor VSS (mg/L)	Effluent VSS (mg/L)	pH	sCOD	
								Start of aeration (mg/L)	End of aeration (mg/L)
				Phase I					
Test reactor	8	12	15.1 ± 2.7	1614 ± 336	1270 ± 192	9 ± 7	7.44 ± 0.19	46.4 ± 38.6	22.4 ± 7.8
Control reactor	8	12	17.5 ± 3.7	1440 ± 217	1221 ± 190	19 ± 15	7.73 ± 0.19	47.9 ± 38.6	24.3 ± 7.4
				Phase II					
Test reactor	3	12	13.9 ± 2.8	856 ± 264	715 ± 188	14 ± 6	7.48 ± 0.17	59.0 ± 24.7	26.9 ± 3.8
Control reactor	3	12	18.1 ± 5.0	838 ± 232	741 ± 192	10 ± 4	7.66 ± 0.10	57.7 ± 25.6	25.1 ± 7.4

SRT, solids retention time; HRT, hydraulic retention time; TSS, total suspended solids; VSS, volatile suspended solids; sCOD, soluble chemical oxygen demand

* "Test reactor" was bioaugmented with *Sphingobium* sp. BiD32; "Control reactor" was bioaugmented with *Sphingopyxis* sp. TrD1

6.5.2 BPA removal

The extent of BPA removal and the total removal rate were greater in the test reactor than in the control under all conditions tested during cycle 1 (Table 6.3, Figure 6.2, Figure 6.3; $p<0.05$, t-test). Enhanced BPA removal lasted for up to 5 cycles after bioaugmentation (Figure 6.4a). The differences in the BPA removal in the test reactor compared to the control reactor were statistically significant in the first two cycles after bioaugmentation (cycles 1 and 2; $p=1.5\text{x}10^{-5}$ and 0.004, respectively, t-test). The enhanced BPA degradation activity was lost by cycle 8 (last cycle each day before bioaugmentation), when the measured k_{cT} in the test reactor was 0.19 ± 0.01 h^{-1} (n=2), which was significantly equivalent to the control reactor (t-test, $p=0.76$). Values in the control reactor were statistically equivalent for all cycles during Phase I-a (not tested for Phase I-b or Phase II), which confirmed that the addition of the non-BPA degrading *Sphingopyxis* sp. TrD1 at cycle 1 did not affect removal efficiencies.

The BPA degradation rate coefficient was similar over the range of tested concentrations, but differed when the SRT was changed (Table 6.3). The percent of BPA removal and degradation rates were statistically similar in Phase I-a and Phase I-b testing in the test reactor, which considered different initial BPA concentrations with the same reactor SRT. When the SRT was lowered in Phase II, the percent removal was significantly different, but the degradation rate attributed to the bioaugmented bacteria (k_c', Table 6.3) remained the same. This difference in removal may be attributable to the higher k_{AS}' at lower BPA concentrations (i.e. Phase I-b and Phase II, Table 6.3), suggesting that higher BPA concentration may induce a stress-response within the background activated sludge and confirming previous findings (Zhou et al. 2014). This also illustrates that the higher background VSS levels at higher SRTs (i.e. Phase I) contributed measurably to degradation. During operation Phase I-b, there was an apparent lag in the BPA removal in the control reactor (Figure 6.3a), which may be an induction period.

Table 6.3. Bisphenol A (BPA) partitioning and removal in sequencing batch reactors (20ºC)

	Removal (%)	Degradation rate			number of replicates	Fraction of BPA in liquid phase (f_L)	initial BPA (µg/L)	SRT (day)	reactor VSS (mg/L)
		Total (k_{cT}, hr^{-1})	By activated sludge (k_{AS}', L/mg-hr)	By augmented bacteria in Cycle 1 (k_c', L/mg-hr)*					
				Phase I-a					
Test reactor	70.2 ± 3.8 [a]	0.88 ± 0.10 [c]	assumed same as control	0.057 ± 0.010 [gh]	5	0.81 ± 0.01 [jkl]	100	8	1270 ± 192
Control reactor**	24.3 ± 7.2 [b]	0.20 ± 0.05 [d]	0.00023 ± 0.00006	0	13	0.83 ± 0.01 [jl]	100	8	1221 ± 190
				Phase I-b					
Test reactor	68.5 ± 2.5 [a]	0.75 ± 0.03 [ce]	assumed same as control	0.052 ± 0.009 [gi]	2	0.77 ± 0.03 [km]	10	8	1270 ± 192
Control reactor	40.7 ± 0.2	0.37 ± 0.003	0.00037 ± 0.00006 [f]	0	2	0.79 ± 0.03 [lmn]	10	8	1221 ± 190
				Phase II					
Test reactor	51.7 ± 2.5	0.58 ± 0.05 [e]	assumed same as control	0.046 ± 0.0002 [hi]	2	0.89 ± 0.005 [o]	10	3	715 ± 188
Control reactor	17.2 ± 2.6 [b]	0.17 ± 0.03 [d]	0.00033 ± 0.00002 [f]	0	2	0.89 ± 0.02 [no]	10	3	741 ± 192

* specific degradation rates are calculated normalized to the amount of *Sphingobium* sp. BiD32 added and using the specific degradation rate by the activated sludge from the control reactor as there was no enhancement in BPA removal during cycle 8

** values presented are average for all SBR cycles, as these showed no statistical differences (p<0.05, t-test)

lower case letters in the same column indicate that the values were statistically equivalent

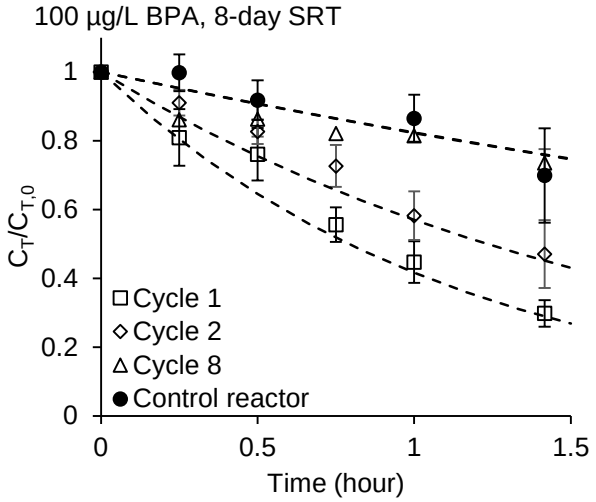

Figure 6.2. BPA degradation in the reactors with an initial BPA concentration of approximately 100 µg/L after spiking during the bioaugmentation cycle (cycle 1, squares, n=5), cycle 2 (diamonds, n=3), and cycle 8 (triangles, n=2) in the test reactor and throughout the day in the control reactor (closed circles, n=13) during Phase I (8-day SRT). Error bars show the deviation from the mean of replicate experiments. The time when replicate experiments were conducted is shown in Figure 6.8. Dashed lines model the BPA degradation based on the average k_{cT} from the replicate experiments. BPA concentrations shown in Figure 6.12. Effluent concentrations were <10 µg/L after 2 cycles from spiking in the test reactor and approximately 30 µg/L in the control reactor.

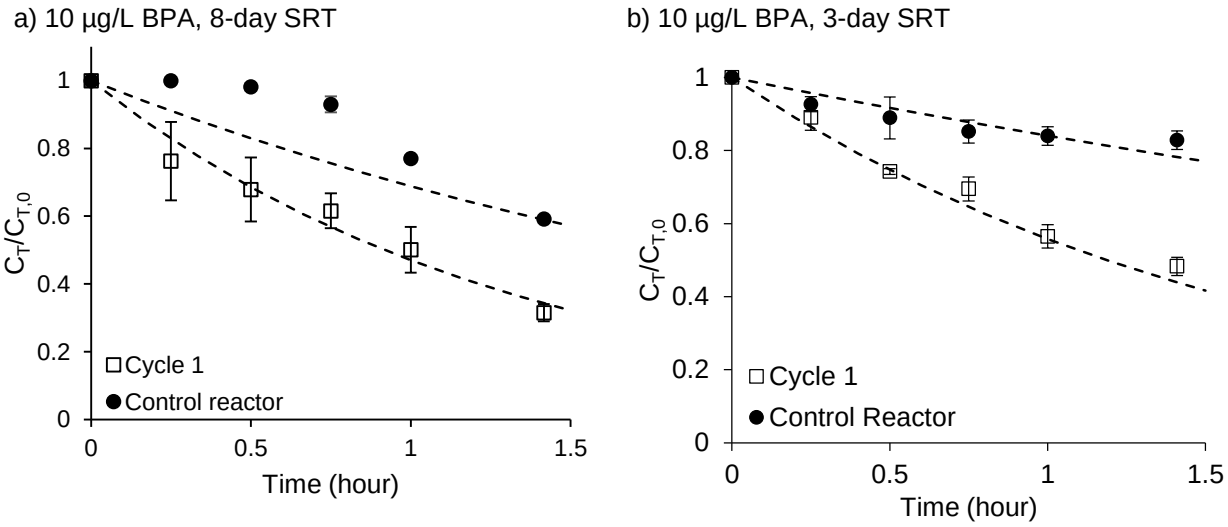

Figure 6.3. BPA degradation in sequencing batch reactors with an initial BPA concentration of approximately 10 µg/L during operation at (a) an 8-day and (b) a 3-day SRT. The open squares show BPA remaining in the test reactor recorded for the cycle immediately after bioaugmentation (cycle 1). Closed circles show the BPA remaining in the control reactor. Error bars show the deviation from the mean of replicate experiments (n=2). Dashed lines show modeled BPA degradation using the average k_{cT} from the replicate experiments, as calculated by Equations 6.2 and 6.3.

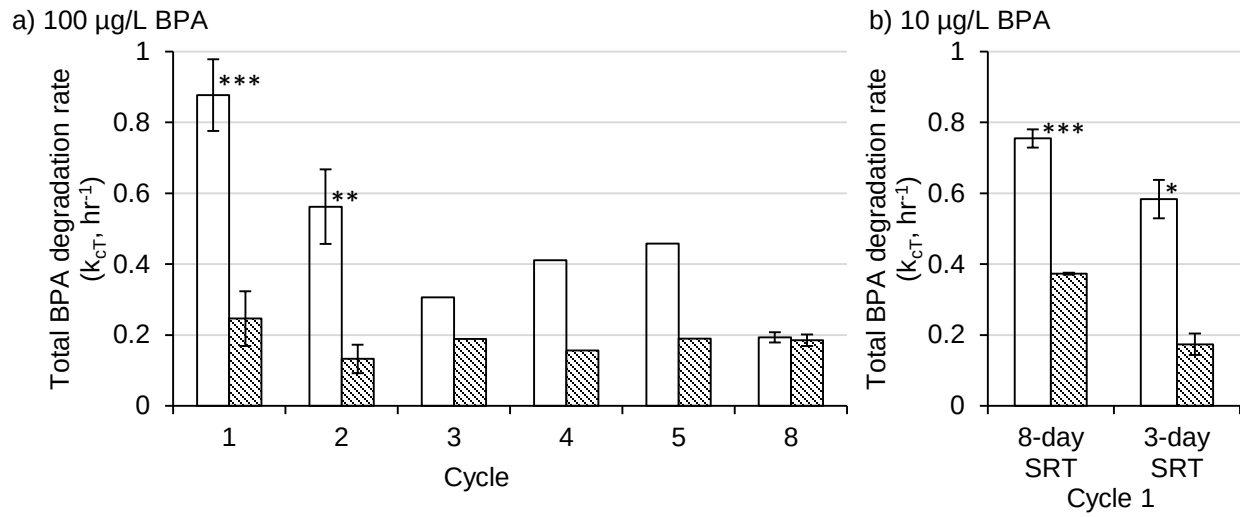

Figure 6.4. Total BPA degradation rates in the test reactor (white bars) and control reactor (patterned bars) a) with an initial BPA concentration of 100 µg/L and an 8-day SRT, and b) with an initial BPA concentration of 10 µg/L BPA and an 8-day and 3-day SRT. Error bars show the deviation from the mean of replicate experiments (the time when replicate experiments were conducted is shown in Figure 6.8); replicate testing were not conducted for cycles 3-5. Total BPA degradation rates in the test reactor significantly different from the control reactor are marked (*, $p<0.05$; **, $p<0.01$; ***, $p<0.005$, t-test).

Specific BPA degradation rates by *Sphingobium* sp. BiD32 in pure culture batch experiments were statistically equivalent to the specific degradation rates by the augmented *Sphingobium* sp. BiD32 in the test reactor (p=0.15, t-test). The specific degradation rates were statistically equivalent when beginning with an initial BPA concentration of 100 µg/L and 10 µg/L (p=0.74, t-test; 0.07 L/mg-hr ± 0.02 (n=4) and 0.07 L/mg-hr ± 0.02 (n=4), respectively).

6.5.3 Fate of BPA in the reactors

Bioaugmentation of the test reactor resulted in a lower BPA effluent concentration, less BPA in the wasted solids, and less BPA remaining in the reactor compared to the control reactor when 10 µg/L BPA was added to the reactors during cycle 1 when operated with an 8-day and 3-day SRT (Figure 6.5). BPA added to the reactors was either degraded, sorbed, or dissolved. Both dissolved and sorbed BPA was removed from the reactors with the effluent and the solids wasting, in different proportions depending on the VSS of each waste stream. Additionally, sorbed and dissolved BPA was retained in the reactor, again in proportion to the amount of liquid and VSS retained. Testing the BPA concentration in each waste stream demonstrated that the BPA sorbed to the waste activated sludge in the test reactor was lower than in the control reactor at both SRTs, reflecting desorption that would be expected with higher rates of degradation in the dissolved phase. A greater fraction of the BPA that was removed was sorbed to the wasted solids with a 3-day SRT, than with an 8-day SRT, as would be expected as more solids were

wasted each day with a 3-day SRT. A decrease in the fraction of BPA discharged with effluent in the bioaugmented reactor was also observed compared to the control reactor (18.9% with an 8-day SRT; 24.9% with a 3-day SRT). The fraction of BPA residual in the reactors was also lower in the test reactor than the control reactor, and lower with a 3-day SRT than with an 8-day SRT.

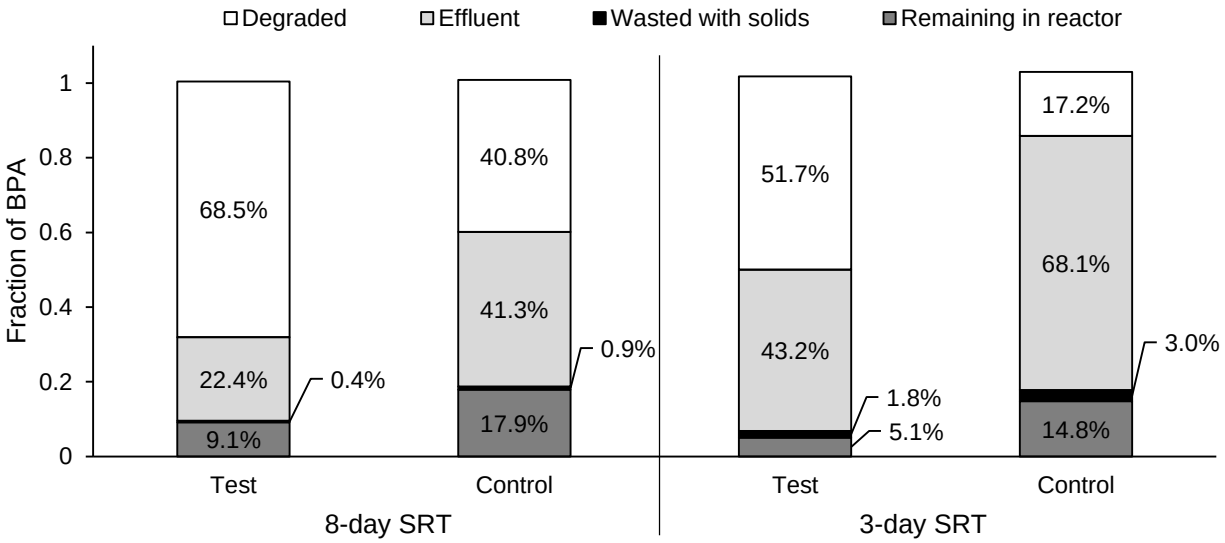

Figure 6.5. The fate of BPA (~10 µg/L initial concentration) during cycle 1 for Phase I-b (8-day SRT) and Phase II (3-day SRT).

6.5.4 Fate of augmented bacteria under reactor conditions

There was a net loss of *Sphingobium* sp. BiD32 when added to reactor sludge. Under the maximum possible growth condition, the growth rate was 0.059 hr^{-1} ± 0.0003 (n=2) (Figure 6.13). The average net loss rate was determined to be 0.16 hr^{-1} ± 0.05 (n=2) (Figure 6.6). Raw qPCR data is shown in Figures 6.14 and 6.15.

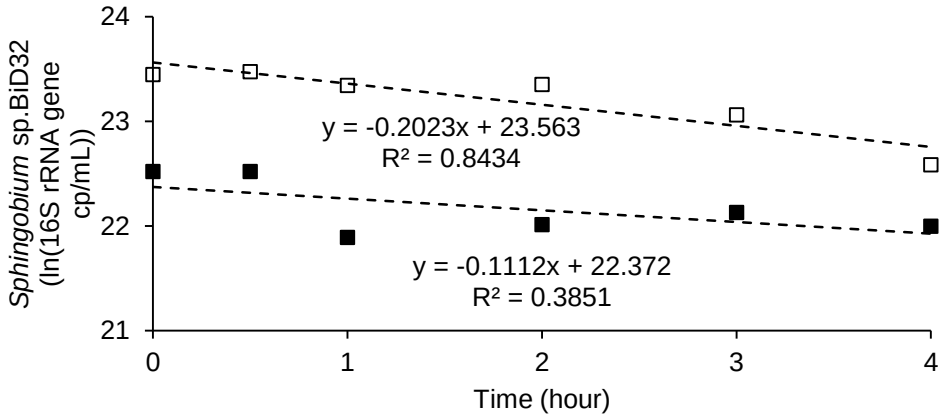

Figure 6.6. Natural log of *Sphingobium* sp. BiD32 16S rRNA gene in waste solids vs. time from 8-day SRT reactors. y-axis is shown as a ln so that the regression lines represent Eq 6.7. The closed and open markers show samples from replicate experiments.

6.5.5 Incorporating calculated biomass loss into the full-scale activated sludge process model

Incorporation of the loss term into the previously described model (Zhou et al. 2014) showed that the higher bioaugmentation dose required to achieve a BPA effluent concentration of 5 ng/L did not result in excess total system VSS (i.e. an increase of less than 10%). With the loss of 0.16 hr^{-1} added into the model, the bioaugmentation dose required increased from 0.13 mg/L (Zhou et al. 2014) to 3.7 mg/L (Table 6.4) to achieve a BPA effluent concentration of 5 ng/L with an influent concentration of 3000 ng/L. Further model modification involved using degradation kinetics determined from the reactor experiments (0.06 L/mg-hr, Table 6.3). With this modification, the bioaugmentation dose required increase to 64 mg/L *Sphingobium* sp. BiD32. These changes resulted in a less than 10% increase in the total system VSS, however, suggesting that bioaugmentation is a feasible technology.

Table 6.4. Predicted *Sphingobium* sp. BiD32 bioaugmentation dose and ratio of bioaugmented biomass to activated sludge biomass needed to obtain effluent concentration goal of 5 ng/L.

degradation rates based on	specific degradation rate by *Sphingobium* sp. BiD32 (k_c', L/mg-hr)	specific degradation rate by activated sludge (k_{AS}', L/mg-hr)	Bioaugmented biomass					ratio of augmented biomass in reactor 1 to activated sludge biomass (X:VSS)
			feed (X_{in}, mg/L)	reactor 1 (X_1, mg/L)	reactor 2 (X_2, mg/L)	reactor 3 (X_3, mg/L)	reactor 4 (X_4, mg/L)	
Zhou et al. 2014	1.08	0.00008	3.7	4.6	4.0	3.5	3.0	0.002
reactor experiments	0.06	0.00023	64.0	81.2	70.2	60.7	52.5	0.041

6.5.6 Cost estimation for bioaugmentation

The primary cost of EBTCR will be the cost of the feed stock for growing the bioaugmentation bacteria. These costs depend substantially on the feed stock used (Table 6.5). Costs were calculated assuming the required *Sphingobium* sp. BiD32 influent concentrations from Table 6.4.

Table 6.5. Substrate cost per day in the full-scale activated sludge model

	cost of substrate per day				substrate cost ($/kg)[a]
	80 MGD WWTP		10 MGD WWTP		
	X_{in}=3.7 mg/L	X_{in}=64 mg/L	X_{in}=3.7 mg/L	X_{in}=64 mg/L	
whey protein	$6,907	$119,467	$871	$15,073	2.8
tryptone	$2,467	$42,667	$311	$5,383	1
yeast extract	$2,467	$42,667	$311	$5,383	1
lactose	$2,467	$42,667	$311	$5,383	1
molasses	$296	$5,120	$37	$646	0.12

Costs were calculated for the two bioaugmentation doses predicted in Table 6.4.
[a] Prices found on alibaba.com

6.5.7 Induction of BPA degradation

BPA degradation by *Sphingobium* sp. BiD32 was determined to be partially inducible. The removal of BPA by cultures pre-conditioned with BPA was faster than the removal by control cultures (Figure 6.7). The pretreated cultures degraded BPA below the limit of detection in 4 hours, compared to the 7.5 hours required for the control cultures to degrade the BPA. The BPA specific degradation rate (k_c', $hr^{-1}OD_{600}^{-1}$) in cultures inoculated with BPA-pretreated *Sphingobium* sp. BiD32 was 13.0 $hr^{-1}OD_{600}^{-1}$, compared to the BPA specific degradation rate in control cultures (4.8 $hr^{-1}OD_{600}^{-1}$) (n=4, p=0.005, t-test). Thus, while pre-conditioning improved the rates, cultures not receiving pre-conditioning were also able to rapidly degrade the BPA contaminant.

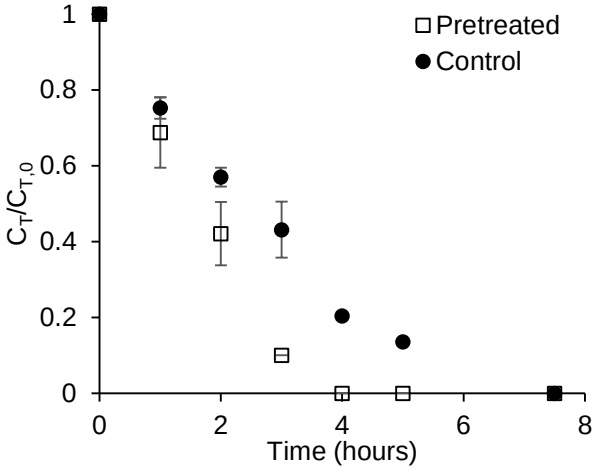

Figure 6.7. Bisphenol A removal in cultures inoculated with bisphenol A pretreated *Sphingobium* sp. BiD32 (open squares) and control (non-pretreated) Sphingobium sp. BiD32 (closed circles).

6.6 Discussion

This study demonstrated the applicability of Enhanced Biological Trace Organic Contaminant Removal (EBTCR) through enhanced removal of BPA with daily bioaugmentation of *Sphingobium* sp. BiD32 in lab scale sequencing batch reactors. The bioaugmentation cycle, cycle 1, is the condition that would be

seen when implementing continuous bioaugmentation at WWTPs. During cycle 1, the removal of BPA was improved significantly compared to the control reactor for all conditions tested. However, the enhancement in BPA removal was lost after greater than five cycles from bioaugmentation. This is similar to results seen by other researchers who saw loss of enhanced TOrCs removal (four days after bioaugmentation (Hashimoto et al. 2010)) and loss of the augmented bacteria (over one order of magnitude in a day (Hashimoto et al. 2010) and over 1-2.5 orders of magnitude in one SRT, depending on the SRT (Roh and Chu 2011)). This loss in BPA removal activity supports the original hypothesis that continuous bioaugmentation, rather than single dose bioaugmentation, is a potential solution to improve the removal efficiencies of TOrCs in WWTPs.

The improvement in BPA removal was completed without a significant increase in the reactor VSS (Table 6.2). As effluent VSS is a regulated parameter at WWTPs, an increase in total system VSS of less than 10% was considered practical for bioaugmentation (N. A. Zhou et al. 2014). In this study, the average increase in system VSS with bioaugmentation was less than 2% when operated with both an 8-day and 3-day SRT. This confirms the potential for bioaugmentation to improve TOrC removal in WWTPs without requiring significantly changes in operation.

SRT had a large effect on BPA removal in the reactors. First, the BPA removal in the control reactor was greater with a longer SRT (Figure 6.3a vs. Figure 6.3b), which agrees with previous studies that found high TOrCs removal with long SRTs (Roh and Chu 2011; Clara et al. 2005; Servos et al. 2005). However, in this study the improved TOrCs removal with the longer SRT was likely due greater activated sludge biomass present, rather than a different microbial community. This is supported by the measured specific BPA degradation rates by the background activated sludge, which are statistically equivalent when operated at an 8-day and 3-day SRT. Second, BPA removal in the test reactor was greater when operated with an 8-day SRT than operated with a 3-day SRT. This is due to greater BPA removal by the background activated sludge, rather than by accumulation of *Sphingobium* sp. BiD32 in the test reactor over time as previously predicted (Zhou et al. 2014). Third, the enhancement in BPA removal with bioaugmentation was greater at the lower SRT. As the BPA removal by the background activated sludge was less in the reactors when operated with a lower SRT, the addition of *Sphingobium* sp. BiD32 resulted in a greater improvement in BPA removal compared to the 8-day SRT. This suggests that bioaugmentation may be especially helpful for WWTPs with low SRTs and, therefore, typically low TOrC removal rates.

The specific degradation rate by the activated sludge is 3 to 4.5 times greater in this study than in a previous study using activated sludge directly from local wastewater treatment plants (Zhou et al. 2014). This is possibly to due reactor operation or adjustment of the system to a continuous low concentration of BPA. However, even with much higher BPA degradation rates by the background activated sludge, bioaugmentation of *Sphingobium* sp. BiD32 still improved the removal of BPA. This suggests that bioaugmentation will improve BPA removal in WWTPs with high TOrC degradation rates, but will be especially helpful for systems with low TOrC degradation rates by the activated sludge.

As the augmented bacteria had a net loss under reactor conditions (Figure 6.6), the *Sphingobium* sp. BiD32 would likely not accumulate as previously modeled (Zhou et al. 2014). Under the maximum possible growth conditions, the growth of the augmented bacteria was less than the loss of the bacteria. Increased loss of bioaugmented biomass was also seen in nitrification bioaugmentation studies (Bouchez et al. 2000; Head and Oleszkiewicz 2005). These losses could be due to predation, differential settling of the augmented bacteria that results in loss in the effluent, or an unusually high endogenous decay rate. Addition of this loss in the model, predicted that the augmented biomass to total system VSS ratio was still less than 10% (Table 6.4).

The cost of feed stocks for bioaugmentation were determined to be practical for the predicted bioaugmentation doses (Table 6.5). While the amount of *Sphingobium* sp. BiD32 bioaugmented increased 20% using previously determined BPA degradation kinetics and increased 2000% using BPA degradation kinetics determined in the reactors with the loss of *Sphingobium* sp. BiD32 added into the model, for the worst case scenario the substrate cost was approximately $5000 per day for an 80 MGD plant using molasses as the growth substrate. These costs will depend on the feed stock chosen, the growth yield of the augmented bacteria on the feed stock, the specific degradation rate of the augmented bacteria, the specific degradation rate of the background activated sludge, and the size on the WWTP to be bioaugmented.

As BPA degradation by *Sphingobium* sp. BiD32 is partially inducible (Figure 6.7), the decrease in the BPA degradation rate should be considered when determining the amount of bacteria to augment. This result also suggests that modifications could be made to the side growth reactor to improve BPA degradation when bioaugmented, but this is not a requirement as cultures not receiving pre-conditioning were also able to rapidly degrade BPA.

6.7 Conclusions

This study investigated the bioaugmentation of the BPA-degrading bacterium *Sphingobium* sp. BiD32 in lab scale sequencing batch reactors. The main conclusions are:

- Daily bioaugmentation of *Sphingobium* sp. BiD32 resulted in enhanced BPA removal compared to the control reactor at two different SRTs (8-day and 3-day) and with two different initial BPA concentrations (100 µg/L and 10 µg/L)
- Enhanced BPA removal was lost with time from bioaugmentation
- Bioaugmentation of *Sphingobium* sp. BiD32 resulted in decreased BPA discharged with the effluent, sorbed to waste solids, and left in the reactors compared to the control reactor
- Augmented bacteria have a net loss in the reactor system
- Modeling results suggest that bioaugmentation is feasible and cost-effective
- Continuous bioaugmentation is a potential solution to achieve EBTCR in WWTPs

6.8 Acknowledgements

Funding was provided by the National Science Foundation (CBET 0829132). The King County Wastewater Treatment Division Graduate Student Research Fellowship Program provided support to Nicolette Zhou. We thank Charlton Callendar, Emily Johanning, Songlin Wang, and Peiran Zhou for their assistance in maintaining the reactors.

6.9 Supplementary Information

Table 6.6. qPCR cycling parameters for 16S rRNA gene concentration quantification

	cycles	*Sphingobium* sp. BiD32
Hot-start activation	1	95ºC for 10 min
Denaturation	50	95ºC for 15 sec
Annealing	50	65ºC for 1 min
Extension	50	60ºC for 1 min
Dissociation	1	95ºC for 15 sec

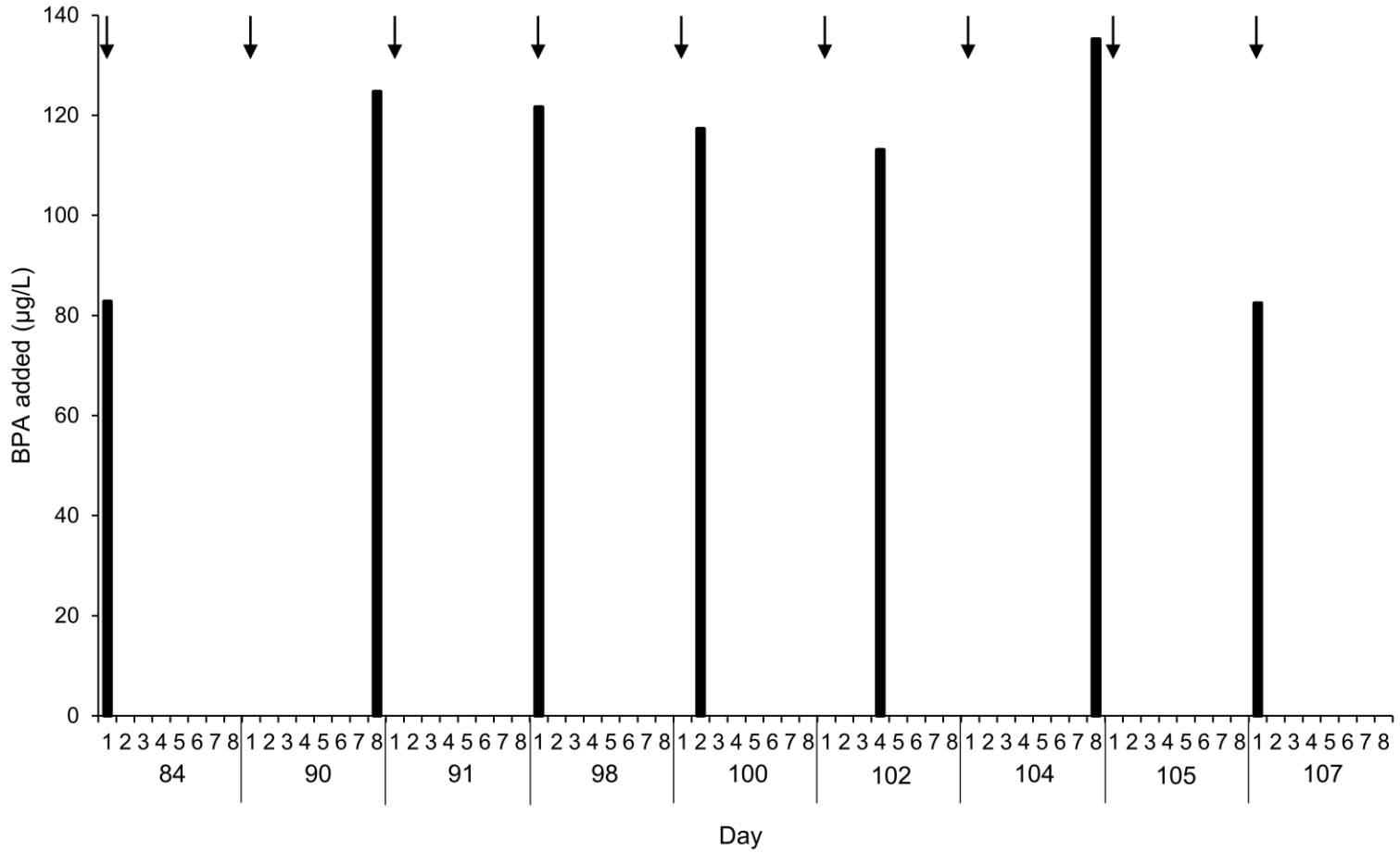

Figure 6.8. Overview of bisphenol A additions (bars) and *Sphingobium* sp. BiD32 augmentation (arrows).

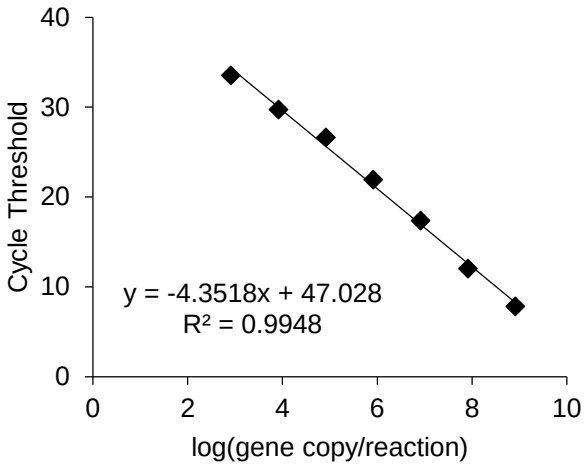

Figure 6.9. Example *Sphingobium* sp. BiD32 16S rRNA gene qPCR standard curve.

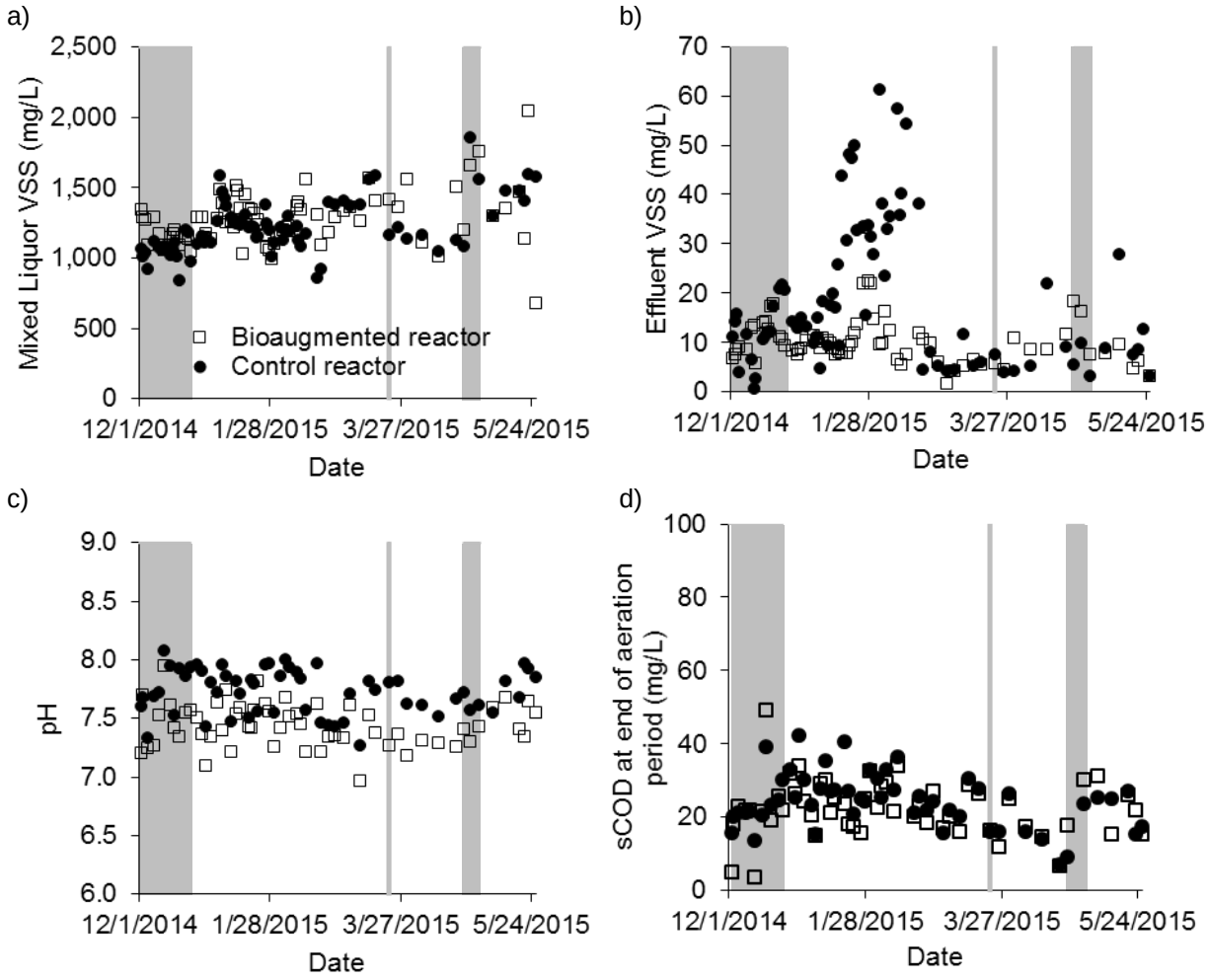

Figure 6.10. Operation during the phase I (8 day SRT) in the bioaugmented reactor (open squares) and the control reactor (closed circles). a) reactor mixed liquor VSS, b) effluent VSS, c) reactor pH, and d) sCOD at the end of the aeration period. The increase in effluent VSS around 2/1/15 was due to a bulking event and no experiments were conducted at this time. Shaded regions show when experiments where completed.

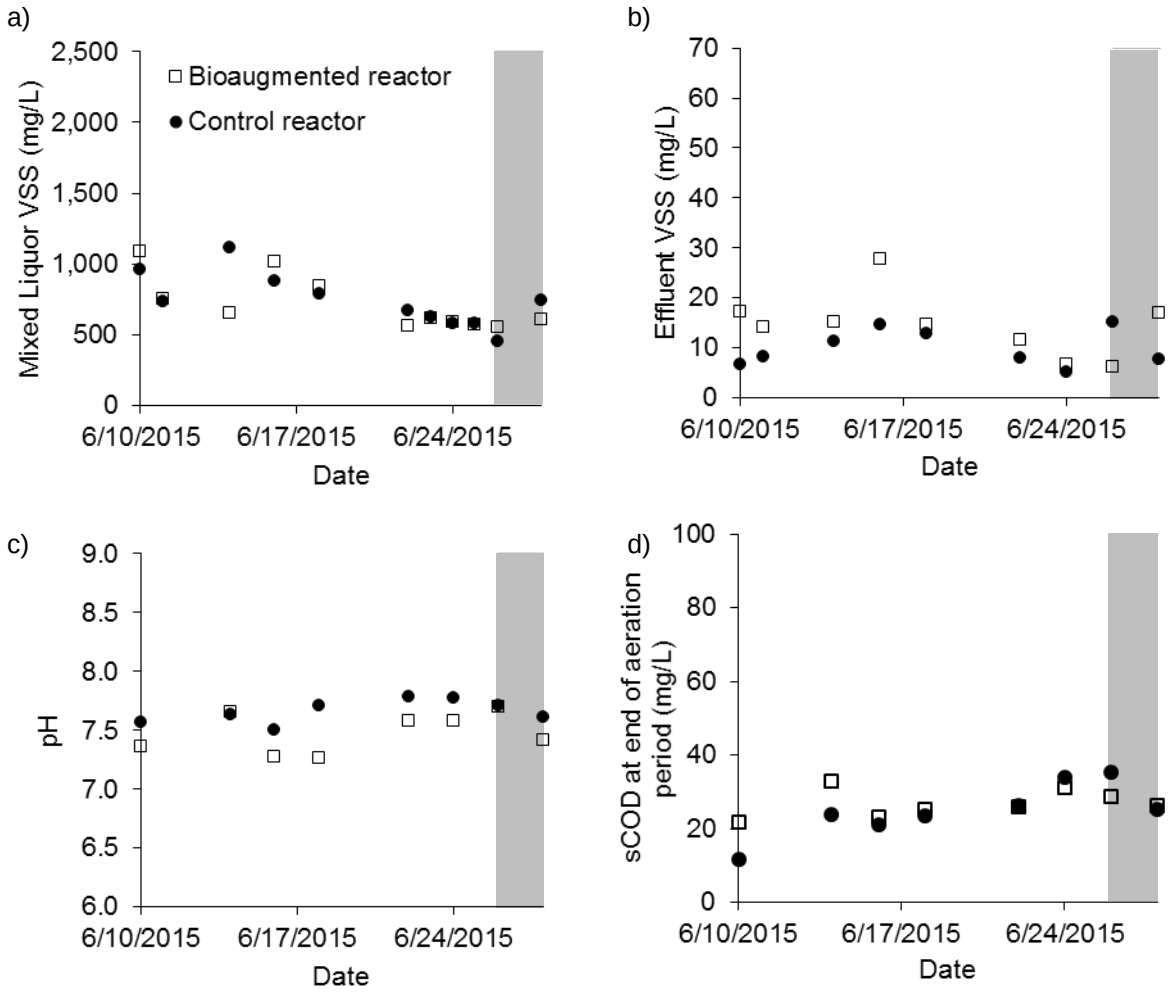

Figure 6.11. Operation during the phase II (3 day SRT) in the bioaugmented reactor (open squares) and the control reactor (closed circles). a) reactor mixed liquor VSS, b) effluent VSS, c) reactor pH, and d) sCOD at the end of the aeration period. Shaded regions show when experiments where completed.

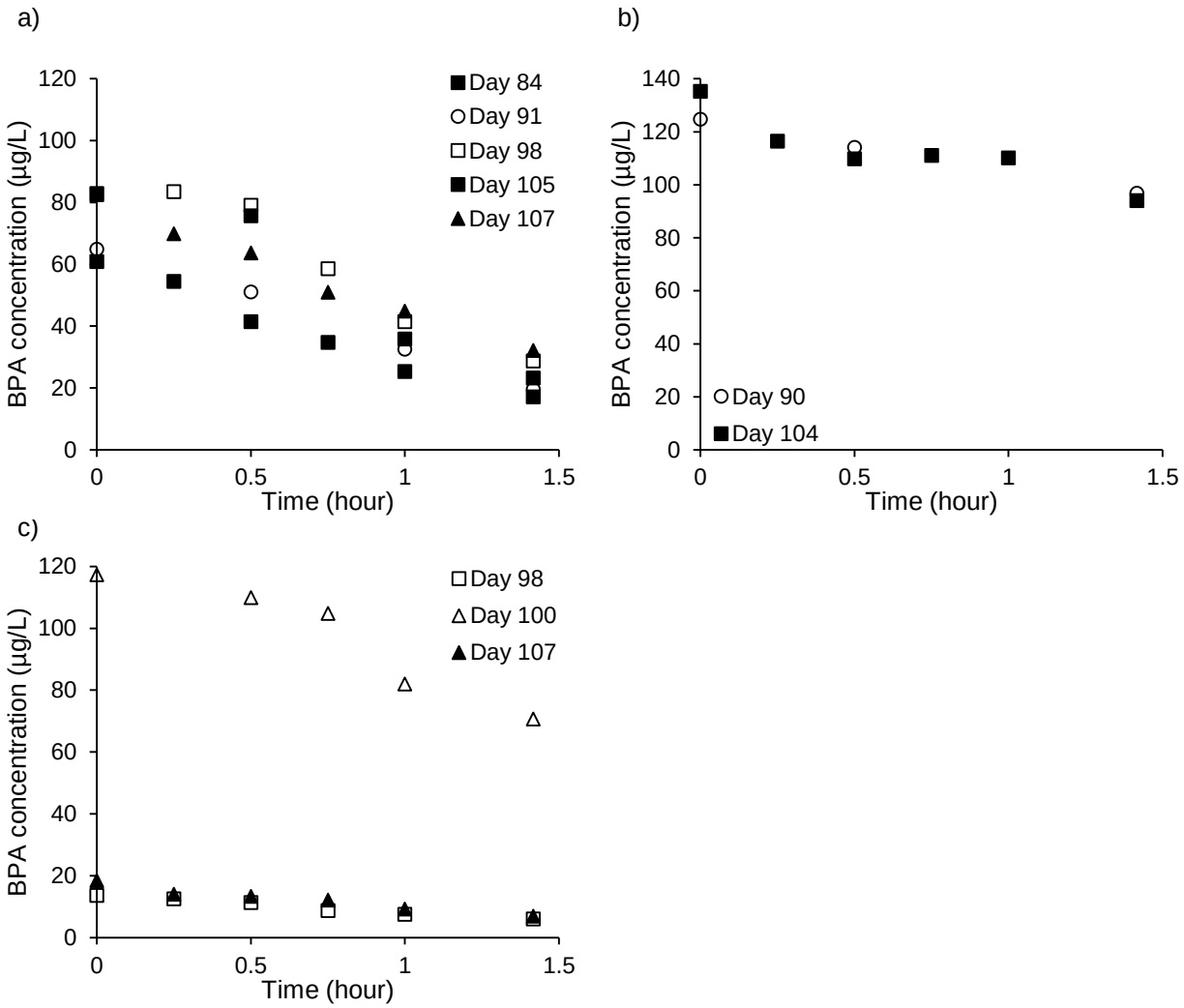

Figure 6.12. BPA degradation in the test reactor with an initial BPA concentration of approximately of 100 µg/L during a) cycle 1, b) cycle 2, and c) cycle 3.

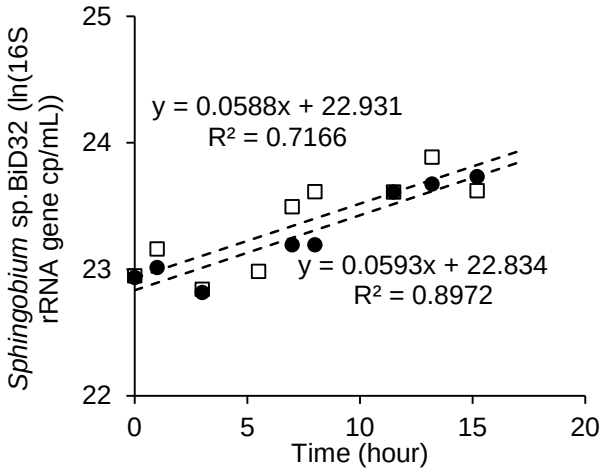

Figure 6.13. Growth of *Sphingobium* sp. BiD32 in autoclaved, sonicated, and filtered waste solids:reactor feed (3:1).

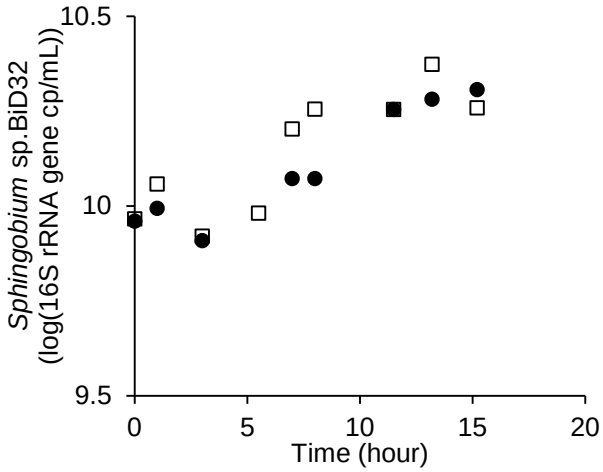

Figure 6.14. *Sphingobium* sp. BiD32 16S rRNA gene concentrations in autoclaved, sonicated, and filtered waste solids:reactor feed (3:1).

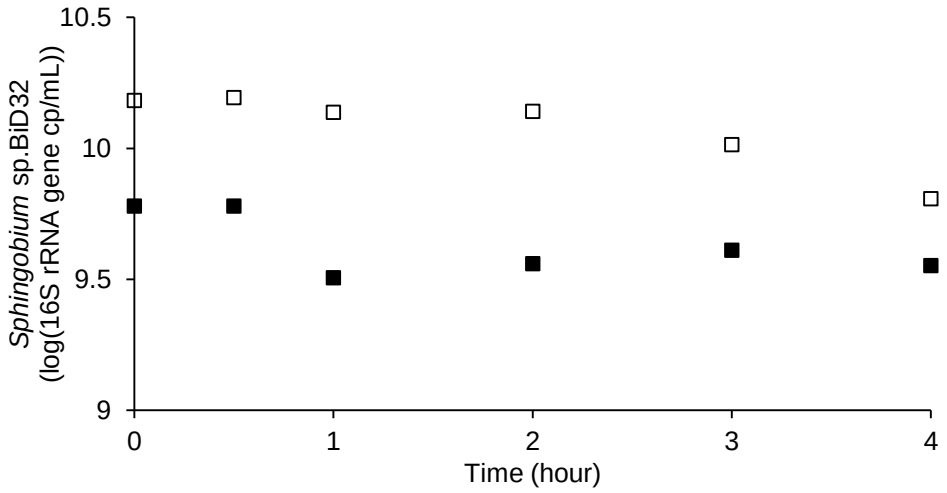

Figure 6.15. *Sphingobium* sp. BiD32 16S rRNA gene concentrations in waste solids from the control reactor when operating at an 8-day SRT.

CHAPTER 7: IDENTIFICATION OF PUTATIVE GENES INVOLVED IN BISPHENOL A DEGRADATION USING DIFFERENTIAL PROTEIN ABUNDANCE ANALYSIS OF *SPHINGOBIUM* SP. BID32

Adapted with permission from:
Zhou, Nicolette A., Henrik Kjeldal, Heidi L. Gough, and Jeppe L. Nielsen. 2015. "Identification of putative genes involved in bisphenol A degradation using differential protein abundance analysis of *Sphingobium* sp. BiD32." *Environmental Science & Technology*. doi:10.1021/acs.est.5b02987.
Copyright 2015 American Chemical Society.

7.1 Chapter summary

This chapter focuses on Objective V: identification of proteins potentially involved in trace organic contaminant degradation. Proteomics studies are important for understanding environmental degradation of TOrCs because while there are documented functional genes associated with many of the processes in wastewater and in environmental remediation, this is not the case for TOrCs removal. Therefore, tracking metabolic capabilities is not currently possible for this class of contaminants. This study used a combination of genomics, proteomics, and metabolomics to determine which proteins are likely involved in the degradation of BPA by *Sphingobium* sp. BiD32. A novel *p*-hydroxybenzoate hydroxylase enzyme was hypothesized to be involved in BPA degradation. It was upregulated in the presence of BPA and closely related to a protein involved in xenobiotics biodegradation and metabolism. The metabolomics portion of this study resulted in the identification of BPA-M, a metabolite of BPA. However, this study was conducted at higher BPA concentrations (2 mg/L), therefore the identified metabolite may not be present during degradation at environmentally relevant concentrations as the degradation pathway may be different. The identified *p*-hydroxybenzoate hydroxylase was also implicated in the metabolic pathway associated with the detected metabolite. This enzyme may serve as a future genetic marker for BPA degradation. Proteins involved in the transformation of the intermediate, protocatechuate, are also likely to be involved in the BPA degradation pathway as they were more abundant in the presence of BPA, functionally annotated to proteins involved in xenobiotics biodegradation and metabolism, and matched genes previously identified to be involved in protocatechuate degradation in a variety of organisms. *p*-hydroxybenzoate may function as future marker of BPA degradation, which would allow for monitoring of BPA-degrading organisms *in situ* and increase the understanding of microbial processing of TOrCs. This study demonstrates how proteomics can be used to inform studies in environmental engineering and wastewater treatment.

7.2 Abstract

Discharge of the endocrine disrupting compound bisphenol A (BPA) with wastewater treatment plant (WWTP) effluents into surface waters results in deleterious effects on aquatic life. *Sphingobium* sp. BiD32 was previously isolated from activated sludge based on its ability to degrade BPA. This study investigated BPA metabolism by *Sphingobium* sp. BiD32 using label-free quantitative proteomics. The genome of *Sphingobium* sp. BiD32 was sequenced to provide a species-specific platform for optimal protein identification. The bacterial proteomes of *Sphingobium* sp. BiD32 in the presence and absence of BPA were identified and quantified. A total of 2155 proteins were identified; 1174 of these proteins were quantified, and 184 of these proteins had a statistically significant change in abundance in response to the presence/absence of BPA ($p \leq 0.05$). Proteins encoded by genes previously identified to be responsible for protocatechuate degradation were upregulated in the presence of BPA. The analysis of the metabolites from BPA degradation by *Sphingobium* sp. BiD32 detected a hydroxylated metabolite. A novel *p*-hydroxybenzoate hydroxylase enzyme detected by proteomics was implicated in the metabolic pathway associated with the detected metabolite. This enzyme is hypothesized to be involved in BPA degradation by *Sphingobium* sp. BiD32, and may serve as a future genetic marker for BPA degradation.

7.3 Introduction

Wastewater treatment plants (WWTP) discharge endocrine disrupting compounds (EDC) to aquatic environments, resulting in deleterious effects on aquatic life. A common EDC detected in WWTP effluents and surface waters is bisphenol A (BPA). BPA is a widely used plasticizer for polycarbonate plastics and epoxy resins manufacturing (US EPA 2014) with 3.2 million metric tons produced globally in 2003 (Tsai 2006). BPA is an estrogen and androgen receptor agonist (Flint et al. 2012) and has negative effects on aquatic life at concentrations measured in the environment (Baek et al. 2003; Oehlmann et al. 2006; Sohoni et al. 2001). While BPA is partially removed during wastewater treatment, residual concentrations enter the receiving aquatic environments (Flint et al. 2012; Lemos et al. 2009) with BPA detected in 41.2% of US streams tested and a median and maximum concentration of 140 ng/L and 12,000 ng/L, respectively (Kolpin et al. 2002). Up to 29 ng/L BPA was detected in groundwater impacted by WWTP effluent (Rudel et al. 1998). New technologies are needed to improve the removal of EDCs, such as BPA, during wastewater treatment.

Bioaugmentation with EDC-degrading bacteria is a possible solution to improve the removal of EDCs during wastewater treatment (Zhou et al. 2014). Previous studies have isolated many bacteria capable of degrading various contaminants (Meade et al. 2001; Zhang et al. 2007; Kang and Kondo 2002; Pauwels et al. 2008; Murdoch and Hay 2005). Among these is *Sphingobium* sp. BiD32, which was isolated from

activated sludge and is capable of degrading BPA to 5 ng/L (Zhou et al. 2013). As average effluent concentrations range from 4.2 to 1600 ng/L (Ballesteros-Gomez et al. 2007; Duong et al. 2010a), bioaugmentation with these EDC-degrading bacteria can likely improve the removal of EDCs in WWTPs. Understanding how the bacteria degrade these contaminants will improve bioaugmentation techniques by potentially allowing for easier monitoring of EDC degradation.

Identifying genes that could be used as genetic indicators of BPA degradation would enable tracking of biodegradation potential in WWTPs. Proteomic studies have been effective at identifying degradation genes and pathways of other EDCs and pharmaceuticals, as demonstrated by recent work with ibuprofen (Almeida et al. 2013) and 17β-estradiol (E2) (Z. Li et al. 2012a). Previous proteomic studies have also led to the identification of gene markers for E2 exposure using label-free proteomics (Collodoro et al. 2012). However, this approach has not yet been applied for BPA degradation.

The objective of this study was to identify enzymes involved in BPA degradation by *Sphingobium* sp. BiD32 and to elucidate the degradation pathway using a combination of genomics, proteomics, and metabolite analysis. Label-free quantitative proteomics was used to investigate the effect of BPA on the proteome of *Sphingobium* sp. BiD32 and the results were used to identify candidate BPA catabolic genes in the organism's genome. Analysis of the metabolites from BPA then assisted in confirming potential genes involved and the pathway.

7.4 Materials and methods

7.4.1 Chemicals, reagents, and bacterial strain

BPA (≥99%) was obtained from Sigma Aldrich (St. Louis, MO, USA). Organic solvents and water used for BPA sample extraction and analysis were high performance liquid chromatography (HPLC) grade. A 35 mg/L BPA aqueous stock was prepared by adding BPA dissolved in acetonitrile (1000 mg/L), evaporating the acetonitrile at 60ºC, adding water, and autoclave sterilizing (121ºC, 20 min). A control of acetonitrile was prepared the same way as the BPA aqueous stock. *Sphingobium* sp. BiD32 (GenBank accession number JX87937) was previously isolated from activated sludge (Zhou et al. 2013).

7.4.2 Library preparation, genome sequencing, assembly, and analysis

The whole genome sequence of bacterial strain *Sphingobium* sp. BiD32 was prepared and completed (details in Supporting Information (SI)). The sequences were trimmed and assembled using de novo assembly by the CLC Genomics Workbench version 5.5.1 (CLC bio, Aarhus, Denmark). During trimming, the quality score limit was set at 0.05 and reads < 50 bp were discarded. Default parameters for

assembly were used with the exception of the word size (62), the minimum contig length (1000), and the similarity fraction (0.95). Assembled contigs were curated by CodonCode Aligner v 3.7 (CodonCode Corp.) and analyzed with the Rapid Annotation using Subsystem Technology (RAST) annotation server for subsystem classification and functional annotation (Overbeek et al. 2005). This whole-genome shotgun project was deposited at DDBJ/EMBL/GenBank under the accession numbers CAVK010000001 to CAVK010000262.

7.4.3 Sample preparation for proteomic analysis

Samples were prepared for proteomic analysis by growing *Sphingobium* sp. BiD32 in the presence and absence of BPA (Figure 7.1). *Sphingobium* sp. BiD32 was inoculated by transferring a single colony from solid media into R2B media (pre-inoculum culture, PIC), a carbon-rich liquid media prepared based on the composition of the solid media R2A (Reasoner and Geldreich 1979). After reaching an optical density of 0.603 at 600 nm (OD_{600}), 5 mL of *Sphingobium* sp. BiD32 was transferred into a second flask of R2B (inoculum culture, IC). When the IC reached an OD_{600} of 0.302, 8 mL was inoculated into experimental flasks containing R2B for an estimated initial volatile suspended solids (VSS) concentration of 5 mg/L. Five replicate cultures of *Sphingobium* sp. BiD32 were grown (100 rpm, 28ºC) with an initial concentration of 1.5 mg/L BPA and five replicates were grown without BPA. The BPA added to five of the replicates contributed less than 0.6% of the carbon in the media. OD_{600} was measured and samples for BPA quantification were collected every one to two hours. An HPLC instrument with ultraviolet detector (HPLC-UV) was used to quantify total BPA concentrations (sorbed and dissolved fraction) using previously reported methods (Zhou et al. 2013). BPA was re-spiked into the cultures at 7.6 hours to ensure that BPA was present and actively being degraded when the cells were harvested. *Sphingobium* sp. BiD32 cultures (with and without BPA) were harvested when reaching an OD_{600} between 0.385 and 0.412. At the point of harvest, the cultures were still in exponential growth and approximately 60% of the BPA had been degraded. Cells were harvested by washing the cell pellet twice with 20 mL phosphate-buffered saline (PBS) and collected by centrifugation (10,000 xg, 4ºC, 15 min). The proteins were extracted and digested in-solution (details in SI).

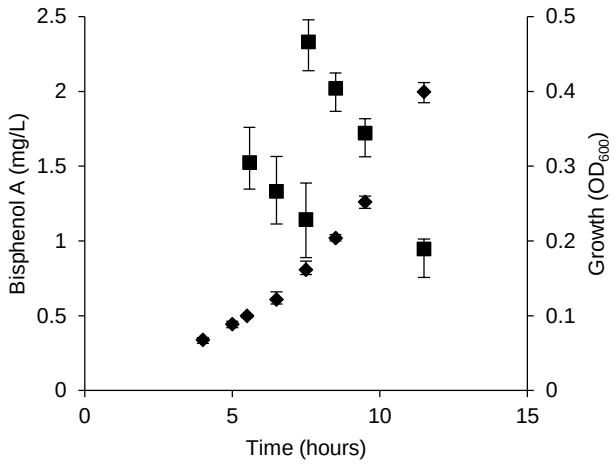

Figure 7.1. Growth and harvesting of *Sphingobium* sp. BiD32 for differential proteomics analysis. Degradation of BPA is shown as squares. Growth of *Sphingobium* sp. BiD32 both in the presence and absence of BPA is shown as diamonds; no differences were seen between the two conditions (p=0.45). BPA was respiked at 7.6 hours. Cells were harvested for protein extraction at 11.5 hours. Error bars represent the range of measurements from replicates (*n*=5).

7.4.4 LC-MS/MS analyses for proteomics

Tryptic digests from the cytosolic and membrane fractions were analyzed separately by an automated liquid chromatography electrospray ionization tandem mass spectrometer (LC-ESI-MS/MS) with an UltiMate 3000 RSLCnano system on-line coupled to a Q Exactive mass spectrometer via a Nanospray Flex ion source (Thermo Fisher Scientific, Hvidovre, Denmark) as described elsewhere (Kjeldal et al. 2014a) with the following modifications: survey scans were detected at 350-1850 m/z and a dynamic exclusion of 45 sec was used for minimizing repetitive selection of the same ions and normalized collision energy was set to 35. Peptides were eluted using 148 min linear gradient, ranging from 13-50% (v/v) of solvent consisting of 0.1% (v/v) formic acid, 0.005% (v/v) heptafluorobutyric acid, and 90% (v/v) acetonitrile.

7.4.5 Label-free quantification

Raw data files from the Q Exactive instrument were processed with MaxQuant v.1.5.1.2 (Max Planck Institute of Biochemistry, Martinsried, Germany; Cox and Mann 2008). Carboxymethylation was set as a fixed modification, oxidation of methionine was set as a variable modification, and a false discovery rate of 1% was utilized. Label-free quantification was determined using the label-free quantitation (LFQ) feature of MaxQuant. All other settings were default. The raw data was searched against a sequence database retrieved from UniProt (downloaded October 21, 2014) and was composed of the predicted open reading frames (ORFs) of *Sphingobium* sp. BiD32. Differences in protein abundances between control and treated (with BPA) were statistically evaluated using a Student's t-test with the statistical significance

set at $p \leq 0.05$. Protein abundances are represented as $\log_2$ transformed LFQ values. Identified proteins include proteins with a single peptide in at least one LC-MS run. Quantified proteins include proteins with at least two quantifiable unique peptides in at least two LC−MS runs.

7.4.6 Functional annotation of proteins

Quantified proteins more abundant in the presence of BPA were compared to a database containing all proteins with a Kyoto Encyclopedia of Genes and Genomes (KEGG) orthology (KO) identifier (downloaded from UniProt November 2, 2013) using CLC Main Workbench v 6.6.2 (CLCbio, Denmark) and The Basic Local Alignment Search Tool for proteins (BLASTp) with default settings. Quantified proteins more abundant in the presence of BPA were also compared to a database containing all proteins in the Patric database (downloaded from Patric August 16, 2015) (Wattam et al. 2013) using CLC Main Workbench v 6.6.2 (CLCbio, Denmark) and The Basic Local Alignment Search Tool for proteins (BLASTp) with default settings. Matches with the highest similarity scores and an E-value ≤ 1E-05 were recorded for each protein. Proteins were mapped using the KO identifier from the BLASTp search and the Pathway mapping feature at the KEGG (v. 68.0) website (http://www.genome.jp/KEGG/).

7.4.7 Pathway prediction of BPA

The BPA SMILES (simplified molecular-input line-entry system) line notation (Oc1ccc(cc1)C(c2ccc(O)cc2)(C)C) was submitted to the EAWAG biocatalysis/biodegradation database pathway prediction system (EAWAG-BBD PPS, http://eawag-bbd.ethz.ch/predict/) (Gao et al. 2010).

7.4.8 Sample preparation for metabolomics

Samples for metabolite analysis were collected from log-phase growth *Sphingobium* sp. BiD32 cultures that were actively degrading BPA. *Sphingobium* sp. BiD32 was inoculated into R2B containing either 0.5 or 2 mg/L BPA by transferring a single colony from solid media. The bacteria were grown at 100 rpm and 28ºC. Samples were preserved by adding an equal volume of acetonitrile, vortexing, and centrifuging (10 min, 10,000 ×g) to remove particles. Decanted samples were stored at 4ºC in glass vials until concentrated for use. Samples were prepared as described elsewhere with minor modifications (Wissenbach et al. 2011). To concentrate, 1 mL of the sample was evaporated after centrifugation at 10,000×g, under a gentle stream of nitrogen while at 60ºC. The residue was resuspended in 50 µL of mobile phase A/B (1:1;v:v (A) 10 mM ammonium formate in acetonitrile with 0.1% (v/v) formic acid and (B) acetonitrile with 0.1% (v/v) formic acid.

7.4.9 LC-MS/MS analyses for metabolomics

An Ultra High Definition (UHD) Accurate-Mass Quadrupole Time-of-Flight (Q-TOF) coupled with an ultra-HPLC system (Agilent Technologies, Inc.; Santa Clara, CA, USA) was used to determine the presence of BPA and the corresponding metabolites (details in SI).

7.5 Results

7.5.1 Whole genome sequencing

Whole genome sequencing of *Sphingobium* sp. BiD32 was completed to provide an organism-specific genomic template for the MS-based label-free quantitative proteomics. Information obtained from the assembly of the *Sphingobium* sp. BiD32 genome is summarized in Table 7.1. 169 out of 206 (82%) bacterial essential genes proposed by Gil et al. were identified in the genome, suggesting that the genome is mostly complete (Table 7.6, supplement) (Wattam et al. 2013).

Table 7.1. Sphingobium sp. BiD32 whole genome assembly.

parameter	value
contigs	262
reads	2,632,020
fold coverage	65
mean read length (bp)	118.31
N50 contig length (Kb)	33.3
draft genome size (b)	4,788,021
predicted coding sequences	4,670
GC content (%)	31.3

7.5.2 Label-free quantitative MS-based proteomics of Sphingobium sp. BiD32

Proteins extracted from five biological replicates of *Sphingobium* sp. BiD32 grown in the presence and absence of BPA were subjected to shotgun-proteomics and label-free quantification. A total of 2180 proteins were identified, corresponding to approximately 47% of the predicted CDS of *Sphingobium* sp. BiD32. The number of proteins quantified, differentially abundant in response to the presence/absence of BPA ($p \leq 0.05$), and differentially abundant by more than 2-fold ($-1.0 \leq \log_2$ (fold abundance) ≥ 1.0, $p \leq 0.05$) in response to BPA are summarized in Table 7.2. Proteins differentially abundant by more than 2-fold are shown by the shaded regions of Figure 7.2 for both the cytosolic and membrane proteins; 43 proteins were upregulated in the cells exposed to BPA, while 48 proteins were downregulated in the presence of BPA. The upregulated proteins were further evaluated to identify those potentially involved in BPA degradation.

Table 7.2. Sphingobium sp. BiD32 proteomic analysis.

proteins	value
identified[a]	2155
quantified[b]	1174
differentially abundant in response to BPA	184
differentially abundant by more than 2-fold	90

[a]identified, protein was measured in 1 of 5 replicate incubations
[b]quantified, protein was measured in 2 or more of 5 replicate incubations

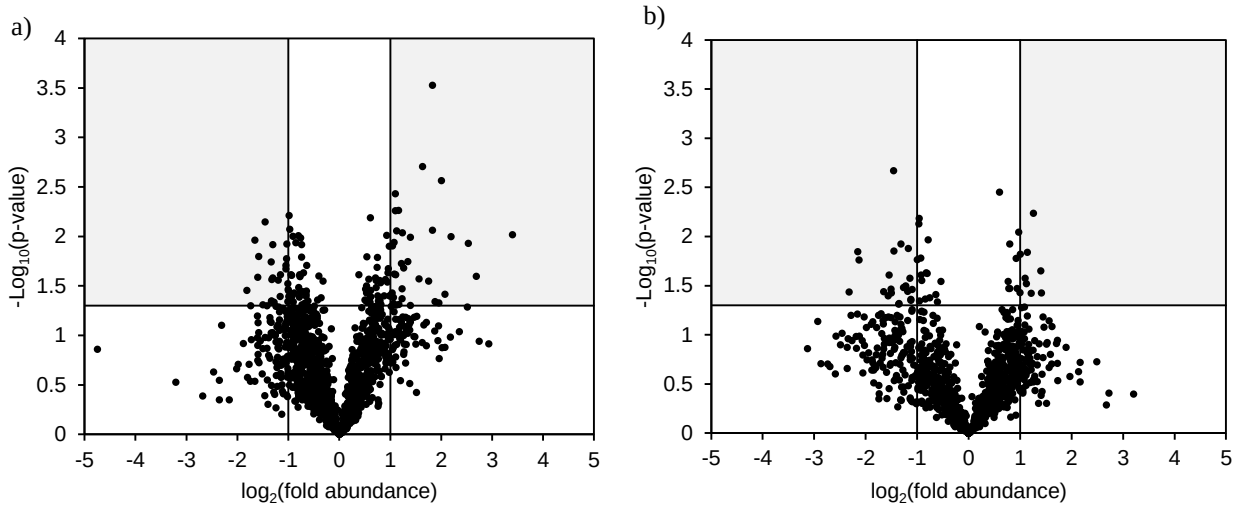

Figure 7.2. Volcano plot of a) cytosolic and b) membrane quantified proteins. Statistically significant ($p \leq 0.05$) differentially abundant proteins ($-1 \leq \log_2$ (fold abundance) ≥ 1) are shaded gray.

7.5.3 Functional annotation of proteins

Proteins were functionally annotated by comparing them to those with KO identifiers and those in the Patric database. Twenty-seven (27) of the 43 upregulated proteins matched to proteins with KO identifiers. These proteins were annotated to the following categories: metabolism, genetic information processing, environmental information processing, cellular processes, and organismal systems. Metabolism included proteins related to xenobiotics biodegradation and metabolism (N1MT47, N1MMX0, N1MNM9, N1MWA7, N1MSB0, and N1MS32), energy metabolism (N1ML71, N1MN00, N1MTK7, N1MRW4, N1MPN2, and N1MLU6), lipid metabolism (N1MTK7), amino acid metabolism (N1MF55, N1MFT4, N1MFX4, N1MK88, N1ML71, N1MMX0, N1MPU3, N1MQ53, N1MS39, N1MWX7, and N1MRW4), metabolism of other amino acids (N1MPU3), metabolism of cofactors and vitamins (N1MH82 and N1MPU3), glycan biosynthesis and metabolism (N1MQ53), biosynthesis of other secondary metabolites (N1MTJ4), metabolism of terpenoids and polyketides (N1MTK7), and carbohydrate metabolism (N1MJQ9, N1MKJ6, N1ML71, N1MN00, N1MNR5, N1MTJ4, N1MTK7, and N1MWX7). Genetic information processing included proteins related to translation (N1MH82). Environmental information processing included proteins related to membrane transport (N1MGE8) and

signal transduction (N1MTJ4). Cellular processes included transport and catabolism (N1ML71) and cell growth and death (N1MPU5). Organismal systems included endocrine system (N1MN00). Functional information for four additional proteins was determined by matching upregulated proteins to proteins in the Patric database. These proteins had Enzyme Class (EC) assignments of glycosidases (N1MKW1), enoyl-(acyl-carrier-protein) reductase (NADH) (N1MSL9), and glutamate dehydrogenase (N1MUY1). A protein without an EC assignment, had a Gene Ontology (GO) assignment of translation release factor activity and translation termination (N1MIL6).

The xenobiotic biodegradation and metabolism orthology were given particular focus as these were most likely to be involved with BPA degradation. These accounted for more of the functionally annotated upregulated proteins than any other orthology. The level of homology between the proteins annotated to xenobiotic biodegradation and metabolism and the entries in the KO database varied, ranging from moderate (44% sequence identity) to high (88% sequence identity) (Table 7.3). These proteins were characterized as dehydrogenases, a dioxygenase, a hydratase, a hydroxylase, and a cycloisomerase and were related functionally to the degradation of aromatic contaminants (Table 7.3). The presence of BPA resulted in a 3-to-6-fold increased abundance ($\log_2$ of 1.6 to 2.7) of these proteins. While two of the proteins were exclusively associated with ‘benzoate degradation’ (N1MT47 and N1MWA7), the remaining four were associated with degradation of multiple aromatic xenobiotics, including polycyclic aromatic hydrocarbons, toluene, and aminobenzoate. Additionally, the hydroxymuconate-6-semialdehyde (N1MMX0), which was almost 4-fold upregulated in samples exposed to BPA relative to the control, was found to be highly homologous (98% sequence identity, BLAST against the UniProtKB database) to a predicted oxidoreductase of the aromatic hydrocarbon degrading bacterium *Sphingobium* sp. Ant17.

Table 7.3. Proteins upregulated in response to BPA related to xenobiotic degradation and metabolism proteins.

UniProtKB accession number and gene	protein name assigned in genome annotation	log2 (Fold Abundance)	accession (Hit)	greatest identity %	greatest bit score	KEGG Orthology	benzoate degradation	aminobenzoate degradation	chlorocyclohexane and chlorobenzene degradation	toluene degradation	polycyclic aromatic hydrocarbon degradation
N1MT47 *proJ*	4-oxalomesaconate hydratase	2.5	Q2G4H3	88	638	K10220	■				
N1MMX0 *proC*	4-carboxy-2-hydroxymuconate-6-semialdehyde dehydrogenase	1.8	Q2G4H6	86	567	K10219	■	■			
N1MNM9 *proB*	Protocatechuate 4,5-dioxygenase beta chain	2.0	Q2G4H5	85	497	K04101	■	■			■
N1MWA7	*p*-hydroxybenzoate hydroxylase	2.7	B8GZG3	78	184	K00481	■				
N1MSB0 *proA*	Protocatechuate 4,5-dioxygenase alpha chain	1.6	Q2G4H4	78	225	K04100	■	■			■
N1MS32	Muconate cycloisomerase	1.6	Q39HW9	44	179	K01856	■	■	■	■	

Four (4) of the proteins categorized as xenobiotic biodegradation and metabolism (N1MMX0, N1MNM9, N1MSB0, and N1MT47) were homologous respectively to the genes *proC*, *proB, proA*, and *proJ*, which are part of a proposed protocatechuate degradation pathway for BPA (Table 7.4). Previous descriptions of the protocatechuate degradation pathway have suggested two major structural organizations of the involved genes: the *Comamonas*-type, in which the genes of the pathway are confined to a single operon, and the *Sphingobium*-type, in which the genes constitute several transcriptional units (Nojiri et al. 2013). The structural organization of the protocatechuate degradation genes of *Sphingobium* sp. BiD32 (Figure 7.3) appeared to be analogous to the *Sphingobium*-type and the genes were confined to possibly three operons: *proFNTEL*, *proCBAJXR*, and *proKUI* (Figure 7.3).

The proteins related to the *proCBAJ* operon were all highly upregulated (~4-fold) in response to BPA exposure. Genes *proB* and *proA* encode for the small and large subunit of the protocatechuate 4,5-dioxygenase, respectively. This enzyme mediates the first reaction in the protocatechuate 4,5-cleavage pathway, catalyzing the oxygenolytic fission of protocatechuate and its conversion to 4-carboxy-2-hydroxymuconate-6-semialdehyde dehydrogenase (CHMS). The *proC* gene of *Sphingobium* sp. BiD32 encoded for a protein that is highly homologous (~78-85% sequence identity) to the CHMS genes of other protocatechuate degraders (*2811*, *ligC*, and *pmdC*) (Nojiri et al. 2013). CHMS catalyzes the oxidation of

the hemiacetal form of CHMS resulting in 2-pyrone-4,6-dicarboxylate (PDC) (Nojiri et al. 2013). PDC is then converted to the kenol-enol tautomers of 4-oxalomesaconate (OMA) by the enzyme 2-pyrone-4,6-dicarboxylate hydrolase (PDC hydrolase), which is encoded for by *proI* in *Sphingobium* sp. BiD32. *proU* is believed to encode for an OMA tautomerase that catalyzes the tautomerization of the enol form of OMA to the keto form. Previous studies performed on OMA tautomerase mutants indicates that this gene is essential for OMA conversion (Kamimura et al. 2010a). OMA is then converted to 4-carboxy-4-hydroxy-2-oxoadipate (CHA) by the enzyme 4-oxalomesaconate hydratase (OMA hydratase), which is encoded for by *proJ* in *Sphingobium* sp. BiD32. *proJ* is highly homologous to *ligJ* (~85% sequence identity) from *Sphingobium* sp. strain SYK-6, an organism with the ability to grow using a wide variety of lignin-derived mono- and diaromatic compounds (Masai et al. 2012b). CHA is converted to pyruvate and oxaloacetate catalyzed by the enzyme 4-carboxy-4-hydroxy-2-oxoadipate aldolase (CHA aldolase), which is encoded for by *proK* in *Sphingobium* sp. BiD32. *proK* shows a high degree of sequence similarity (~91% sequence identity) with the CHA aldolase of *Sphingomonas* sp. LB126 (*fldZ*), an organism with the ability to grow on the polycyclic aromatic hydrocarbon fluorene as the sole source of energy and carbon (Wattiau et al. 2001). Pyruvate and oxaloacetate are then readily assimilated and used in the Krebs cycle. Upstream of *proK* in the genome of *Sphingobium* sp. BiD32 is a LysR-type transcriptional regulator (*proR*), which likely modulates transcription of the *proRKUI* operon through positive regulation (Maddocks and Oyston 2008).

Table 7.4. Gene cluster containing the protocatechuate transformation genes encoding for proteins upregulated by more than 2-fold in response to bisphenol A and close proximity genes.

gene	UniProtKB accession number	protein name assigned in genome annotation	length (bp)	log_2 (fold abundance)	p-value
EBBID32_29090 (*proF*)	N1MMW4	p-hydroxybenzoate hydroxylase	404	NQ	
EBBID32_29100 (*proN*)	N1MNM4	Uncharacterized protein	186	NQ	
EBBID32_29110 (*proT*)	N1MSA4	Major facilitator superfamily MFS_1	435	ND	
EBBID32_29120 (*proE*)	N1MT38	Transcriptional regulator, AraC family	290	ND	
EBBID32_29130 (*proL*)	N1MP91	Uncharacterized protein	75	ND	
EBBID32_29140 (*proC*)	N1MMX0	4-carboxy-2-hydroxymuconate-6-semialdehyde dehydrogenase	312	1.8	3.0E-04
EBBID32_29150 (*proB*)	N1MNM9	Protocatechuate 4,5-dioxygenase beta chain	299	2.0	2.7E-03
EBBID32_29160 (*proA*)	N1MSB0	Protocatechuate 4,5-dioxygenase alpha chain	140	1.6	2.0E-04
EBBID32_29170 (*proJ*)	N1MT47	4-oxalomesaconate hydratase	341	2.5	1.2E-02
EBBID32_29180 (*proX*)	N1MP96	3-hydroxyisobutyrate dehydrogenase and related beta-hydroxyacid dehydrogenases	315	NQ	
EBBID32_29190 (*proR*)	N1MMX5	Transcriptional regulator, LysR family	383	NQ	
EBBID32_29200 (*proK*)	N1MNN2	Putative siderophore biosynthesis protein,related to 2-demethylmenaquinone methyltransferase	224	NQ	
EBBID32_29210 (*proU*)	N1MSB6	2-methylaconitate isomerase	351	NQ	
EBBID32_29220 (*proI*)	N1MT55	2-pyrone-4,6-dicarboxylic acid hydrolase	302	NQ	
EBBID32_29230	N1MPA3	Carboxylic ester hydrolase	487	ND	
EBBID32_29240	N1MMY1	Uncharacterized protein	117	ND	
EBBID32_29250	N1MNN8	Uncharacterized protein	37	ND	

NQ, not quantified; proteins were not quantified, but were identified
ND, not detected; protein was not identified or quantified

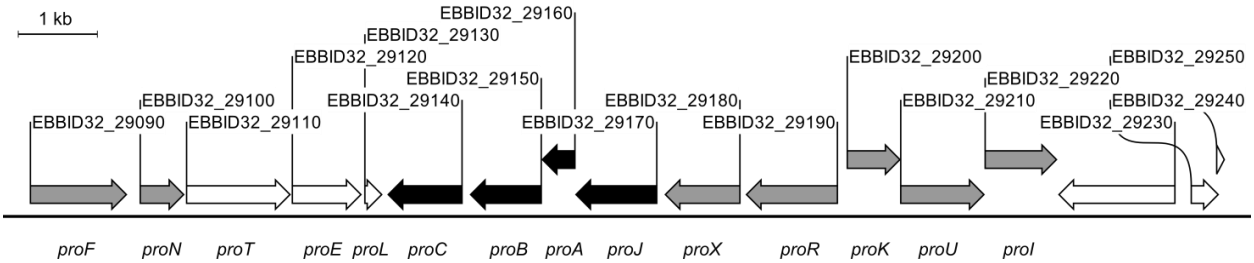

Figure 7.3. Gene organization of the proposed protocatechuate operons (*proCBAJ* and *proRKUI*) and close proximity genes on contig 143 (CAVK010000143.1) of *Sphingobium* sp. BiD32. Proposed gene names were based upon their similarity to genes of the protocatechuate pathway from other organisms. A black arrow indicates that the corresponding gene was more abundant by more than 2-fold in response to BPA exposure (Table 7.4), a grey arrow indicates that the protein was identified, but not quantified, and a white arrow indicates that the gene was identified but the protein was not present in the proteome.

Located outside the protocatechuate gene cluster, another protein (N1MN05) was functionally annotated (K00100) to bisphenol degradation. This protein was found to be more abundant in cells exposed to BPA relative to the control, though by less than 2-fold ($\log_2 = 0.72$). It was functionally annotated to the transformation of several bisphenol metabolites, including the transformation of bis(4-hydroxyphenyl)-methanol to 4,4'-dihydroxybenzophenone and transformation of 1-(4'hydroxyphenyl)-ethanol to 4'-hydroxyacetophenone.

Thirty (30) out of 48 of the downregulated proteins matched to proteins with a KO identifier. These proteins were functionally annotated to the following categories: metabolism, genetic information processing, environmental information processing, cellular processes, and human diseases. Metabolism included proteins related to carbohydrate metabolism (N1MKW5, N1MJA6, N1MGN1, N1MG01, N1MIP5, N1MKD6, N1MHY2, N1MSX0, and N1MLE2), nucleotide metabolism (N1MHY2, N1MJA6, and N1MMB5), energy metabolism (N1MKW5, N1MSC3, N1MG01, N1MIP5, N1MSX0, and N1MLE2), lipid metabolism (N1MLC6 and N1MKW5), amino acid metabolism (N1MWN4, N1MIR7, N1MKD6, N1MQT8, N1MN31, N1MS44), metabolism of other amino acids (N1MLE2), glycan biosynthesis and metabolism (N1MI43), metabolism of terpenoids and polyketides (N1MKW5), metabolism of cofactors and vitamins (N1MRQ2, N1MT40, N1MNZ6, N1MIR7, and N1MY92) and biosynthesis of other secondary metabolites (N1MPK8). Genetic information processing included proteins related to translation (N1MMK2, N1MMZ3, N1MNQ3 and N1MQ71) and folding, sorting, and degradation (N1MTE1). Environmental information processing included proteins related to membrane transport (N1MSV8), cellular processes included transport and catabolism (N1MLE2), and human diseases included drug resistance (N1MPK8 and N1MI43) and infectious diseases (N1MJ91).

7.5.4 Metabolite identification

The parent compound (BPA) and one metabolite (BPA-M; 1,2-Bis(4-hydroxyphenyl)-2-propanol) were detected during metabolite analysis (Table 7.5). BPA-M was detected in the samples with an initial BPA concentration of 2 mg/L, but not in the samples with an initial BPA concentration of 0.5 mg/L. This suggests that BPA-M did not reach concentrations above the method detection limits at the lower initial BPA concentration. Pure chemicals of the intermediate were not available so that standards for quantification could not be prepared.

Table 7.5. BPA metabolites identified during BPA degradation by *Sphingobium* sp. BiD32.

identified BPA metabolites		retention time (min)	m/z
BPA	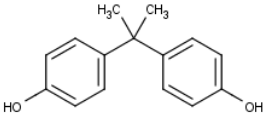	20.6	227.10775
BPA-M (1,2-Bis(4-hydroxyphenyl)-2-propanol)	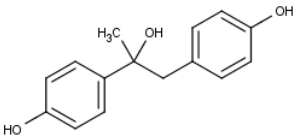	15	243.10267

7.5.5 Catabolic pathway of bisphenol A

The catabolic pathway of BPA by *Sphingobium* sp. BiD32 was predicted using the online prediction tool EAWAG-BBD PPS (Figure 7.4, BPA to BPA-M1). It was predicted that BPA-M was a potential product of the first step in BPA degradation (Figure 7.4, top panel). More than one pathway was predicted by EAWAG-BBD PPS, however metabolites and enzymes were observed only for the pathway shown in Figure 7.4. Smaller compounds predicted as intermediates are unlikely to be detected even if present as they have molecular masses too small for detection by the HPLC-TOF method used for metabolite analysis, and these metabolites are likely to be readily transformed.

Enzymes predicted to be involved in the transformation of BPA to BPA-M were compared to the proteins upregulated in *Sphingobium* sp. BiD32. This transformation involves substitution by a hydroxyl group. The top two matches to enzymes predicted by the EAWAG-BBD PPS were N1MMX0 (83% identity similarity to Q9KWL3) and N1MWA7 (68% identity similarity to Q03298). N1MWA7, identified as a *p*-hydroxybenzoate hydroxylase by genome annotation (Table 7.3), was identified as a protein likely involved in the degradation of BPA by *Sphingobium* sp. BiD32 (Figure 7.4). Following hydroxylation of BPA to BPA-M, it was predicted that BPA-M was dehydrated forming 4,4'-dihydroxy-alpha-methylstilbene (BPA-M1). No enzyme catalyzing this step is known, and hence no candidate was found

for BiD32. The middle steps (BPA-M2 to BPA-M5), suggested that BPA-M1 is broken into two aromatic constituents (BPA-M2 and BPA-M4) based upon proteomics data. BPA-M2 is oxidized to BPA-M3 and BPA-M4 is processed via the protocatechuate pathway. It remains unclear if BPA-M3 is processed by *Sphingobium* sp. BiD32, though a previous study proposed the demethylation of BPA-M3 resulting in 4-hydroxybenzaldehyde, which was further converted to benzoic acid and eventually to carbon dioxide and water (Li et al. 2012). The bottom part of the pathway (BPA-M5 to BPA-M12) represents the protocatechuate pathway described from other organisms, and the *Sphingobium* sp. BiD32 enzymes catalyzing each step.

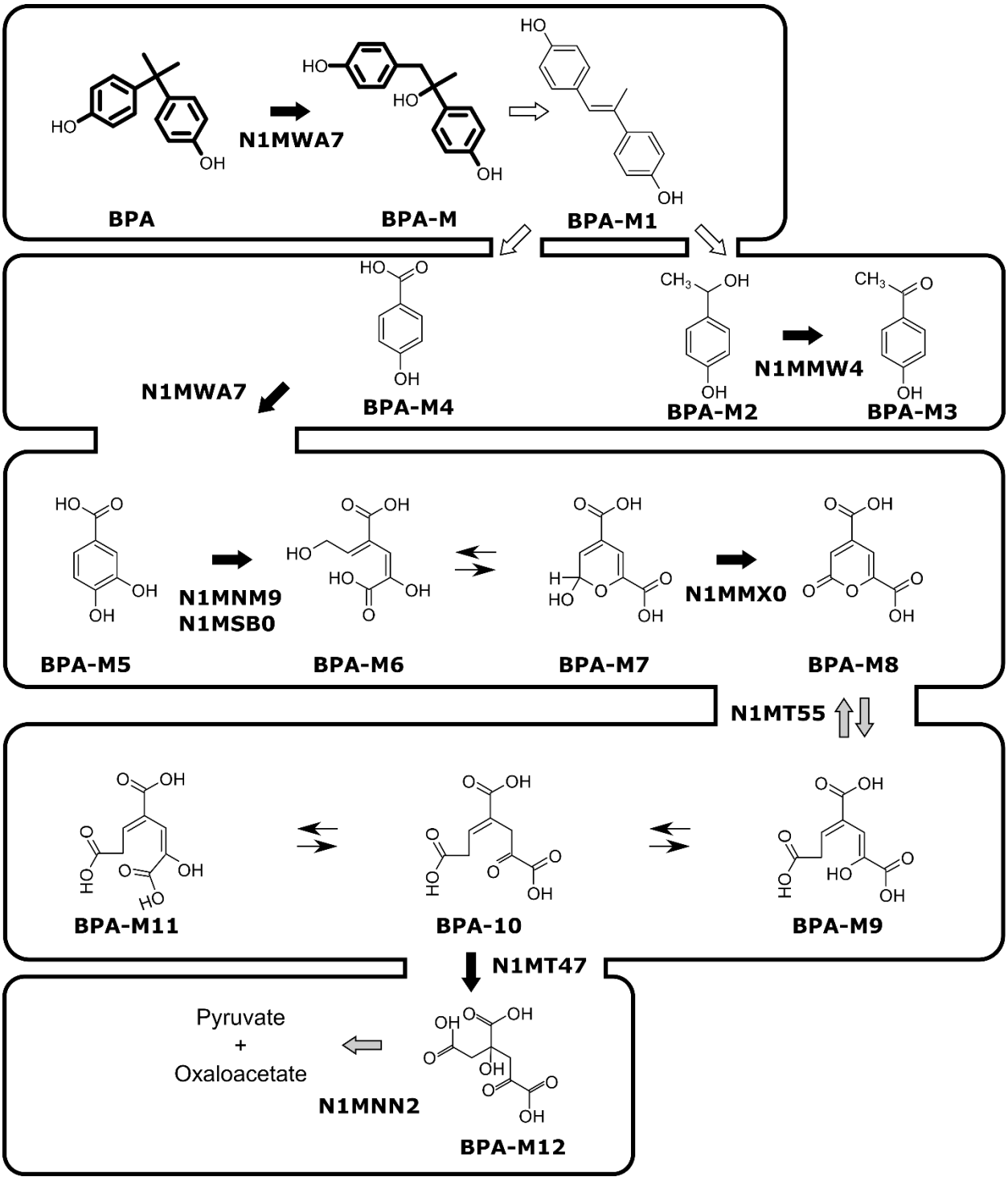

Figure 7.4. Proposed pathway for BPA degradation by *Sphingobium* sp. BiD32 based on measured metabolites (bold) and metabolites and proteins predicted to be involved in BPA degradation by the EAWAG Biocatalysis/Biodegradation Pathway Prediction System (top panel). The degradation pathway of BPA metabolites (bottom panels) was proposed based upon previous findings (Kamimura et al. 2010b). Solid arrows indicate identification of a candidate enzyme upregulated in *Sphingobium* sp. BiD32 by more than 2-fold in response to BPA relative to the control. Grey arrows indicate identification of a candidate enzyme only quantified in the proteome of BPA-exposed cells. Thin arrows indicate that the step is not catalyzed enzymatically. Metabolites are as follows: BPA, bisphenol A; BPA-M, 1,2-bis(4-hydroxyphenyl)-2-propanol; BPA-M1, 4,4'-(1E)-prop-1-ene-1,2-

diyldiphenol; BPA-M2, 1-(4'-hydroxyphenyl)-ethanol; BPA-M3, 4'-hydroxyacetophenone; BPA-M4, 4-hydroxybenzoate; BPA-M5, protocatechuate (PCA); BPA-M6, 4-carboxy-2-hydroxymuconate-6-semialdehyde (CHMS); BPA-M7, 4-carboxy-2-hydroxymuconate-6-semialdehyde (CHMS hemiacetal form); BPA-M8, 2-pyrone-4,6-dicarboxylate (PDC); BPA-M9, 4-oxalomesacconate (OMA) enol form; BPA-M10, OMA ketoform; BPA-M11, OMA ketoform; BPA-M12, 4-carboxy-4-hydroxy-2-oxoadipate (CHA).

7.6 Discussion

In this study, the metabolism of BPA by *Sphingobium* sp. BiD32 was investigated using three different tiers of biochemistry (genome, proteome, and metabolome) and was successfully employed to identify previously undocumented proteins putatively involved in bacterial BPA degradation. The overarching goal was to identify genes involved in BPA degradation for use as potential biomarkers in future work. The gene involved in the initial transformation of BPA may also enable identification of other new BPA-degrading bacteria.

A *p*-hydroxybenzoate hydroxylase (N1MWA7) was identified as involved in BPA degradation based on proteomics results and metabolite analysis. This protein was significantly more abundant in the presence of BPA (Table 7.3), was functionally annotated to proteins involved in xenobiotics biodegradation and metabolism (Table 7.3), and closely matched enzymes predicted to be involved in the transformation of BPA to BPA-M (Figure 7.4). Upregulated *Sphingobium* sp. BiD32 proteins that were functionally annotated to xenobiotics biodegradation and metabolism were distantly related to each other.

Proteins involved in protocatechuate transformation are also likely to be involved in the BPA degradation pathway (N1MMX0, N1MNM9, N1MSB0, and N1MT47). These proteins were more abundant in the presence of BPA (Table 7.4), were functionally annotated to proteins involved in xenobiotics biodegradation and metabolism (Table 7.3), and matched genes previously identified to be involved in protocatechuate degradation in a variety of organisms including *Sphingobium* sp. strain SYK-6 (Masai et al. 2012a), *Sphingomonas* sp. strain LB126 (Wattiau et al. 2001), *Novosphingobium aromaticivorans* DSM 12444 (Wattiau et al. 2001), *Comamonas* sp. strain E6 (Kamimura et al. 2010), *Comamonas testosteroni* BR6020 (Providenti et al. 2001), *Pseudomonas straminea* NGJ1 (Maruyama et al. 2001), and *Arthrobacter keyseri* 12B (Eaton 2001). The organization of the protocatechuate degradation genes in *Sphingobium* sp. BiD32 most notably resembles that of *Sphingobium* sp. strain SYK-6, a bacterium capable of degrading a wide variety of lignin-derived biaryls and monoaryls (Masai et al. 2012).

While several studies have documented microbial degradation of BPA and predicted BPA degradation pathways, few proteins involved in BPA degradation have been reported (Zhang et al. 2013). Included amongst these was a cytochrome P450 monooxygenase reported to catalyze the transformation of BPA to

BPA-M by *Sphingomonas* sp. AO1 (Sasaki et al. 2005a). This cytochrome P450 monooxygenase was found to be involved in BPA degradation by using a cytochrome P450 inhibitor (Sasaki et al. 2005b) and then confirmed by purifying the components of the cytochrome P450 monooxygenase system and testing their ability to degrade BPA (Sasaki et al. 2005a). The *Sphingomonas* sp. AO1 cytochrome P450 (B1Q2N5) was related to a *Sphingobium* sp. BiD32 putative cytochrome P450 hydroxylase (N1MI62) that was identified in the genome, but not detected based on the proteomics portion of this study (Figure 7.5, supplemental; 30% identity match; E-value = 5.1e-45). Also, a *Sphingomonas* sp. AO1 ferredoxin that is part of the cytochrome P450 monooxygenase system (B1Q2N4) was closely related to a *Sphingobium* sp. BiD32 ferredoxin gene (N1MLS9) detected in the genome and proteome (Figure 7.5, supplemental; 47% identity match; E-value = 4.4e-23), but not differentially expressed. Lack of increased proteome expression of these enzymes by *Spingobium* sp. BiD32 suggested that differing pathways may be involved in BPA degradation by these two organisms.

Other enzymes previously reported to be involved in BPA degradation included a second cytochrome P450, an ammonia monooxygenase, and an extracelluar laccase. The cytochrome P450 was reported to catalyze the ipso substitution as the initial step in BPA degradation by *Sphingomonas* sp. TTNP3 (Kolvenbach et al. 2007). An ammonia monooxygenase in *Nitrosomonas europaea* (Roh et al. 2009) and an extracellular laccase in *Pseudomonas* sp. LBC1 (Telke et al. 2009) were also reported to be involved in BPA degradation, though specific degradation steps mediated were not identified. No proteins similar to these three were identified in the proteome of *Sphingobium* sp. BiD32.

Investigation of the metabolome resulted in the identification of BPA-M (Table 7.5). BPA-M has also been detected during BPA degradation by other isolated bacteria (Zhang et al. 2013b), generally resulting in complete mineralization. For example, BPA degradation by *Sphingomonas* sp. MV1 resulted in the transformation of 85% of the BPA to BPA-M (Spivack et al. 1994). BPA-M was further degraded and finally oxidized to carbon dioxide and cell biomass, as determined by HPLC. BPA degradation by unidentified strain WH1 followed the main degradation pathway that occurred in *Sphingomonas* sp. MV1, resulting in transformation to BPA-M and, ultimately, mineralization (Ronen and Abeliovich 2000). BPA-M was also detected during BPA degradation by *Sphingomonas* sp. AO1, though in that study further investigation of the degradation products was not conducted, as it was not the focus of the study (Sasaki et al. 2005a). The current study detected BPA-M during degradation of high concentrations of BPA by *Sphingobium* sp. BiD32; other metabolites were not detected suggesting that they were either too small to be detected or they were transformed quickly, resulting in too low concentrations to be detected. While the same metabolite, BPA-M, was identified during BPA degradation by *Sphingobium* sp. BiD32

and by *Sphingomonas* sp. AO1, different enzymes were predicted to be involved in the transformation (Sasaki et al. 2005a) suggesting that the mechanisms responsible for BPA degradation by these organisms likely differ.

This is the first study using a combination of genomics, proteomics, and metabolite analysis to identify BPA metabolites and enzymes responsible for BPA degradation. Previous studies identified enzymes responsible for the initial transformation of BPA using various inhibitors. This study identified a novel enzyme responsible for the initial transformation of BPA. It also identified a novel BPA transformation pathway with the increased abundance in the protocatechuate transformation genes. The results further suggest how *Sphingobium* sp. BiD32 degrades BPA beyond 4-hydroxybenzoate. Additional research is needed to elucidate the function of multiple enzymes in BPA degradation. Identification of these enzymes may allow for future monitoring of bioaugmented bacteria in WWTPs and identifying other similar BPA-degrading bacteria.

7.7 Acknowledgements

This work was funded by the Danish Research Council for Strategic Research via the Research Centre "EcoDesign-MBR" (Grant No. 26-03-0250) and the National Science Foundation (NSF CBET-0829132). Support was provided to N.A. Zhou by the Valle Scholarship and Scandinavian Exchange and the King County Technology Transfer Fellowship Programs at the University of Washington.

7.8 Supporting information

7.8.1 Library preparation and genome sequencing

DNA extraction was performed using the FastDNA Spin Kit for Soil (MP Biomedicals, Santa Ana, CA, USA). The DNA was cleaned up by the following process: mix 100 µL of DNA 1:1 with phenol:chloroform:isoamyl alcohol (25:24:1, pH ~7.5), vortex, centrifuge (10,000 x *g*, 10 min), transfer the upper layer to a fresh tube, add 1 µL of 20 mg/mL glycogen, 10 µL of 7.5 M NH_4Ac, and 250 µL 99% (v/v) ethanol, incubate for 5 min at room temperature, centrifuge (10,000 x *g*, 15 min), discard supernatant, dry pellet 15 min, and dissolve in 100 µL water. The library for paired-end sequencing was constructed using the Nextera DNA Sample Preparation Kit (Illumina, San Diego, CA, USA. The manufacturer's instructions were followed with the following modification: the clean-up of the tagmented DNA was performed using the MinElute Reaction Cleanup Kit (Qiagen Inc., Valencia, CA, USA). The library was sequenced using an Illumina HiSeq as previously described (McIlroy et al. 2013a) generating paired-end reads of 150 bp in length.

7.8.2 Protein extraction

The cell pellet was resuspended in 10 mL PBS supplemented with protease inhibitors (Complete, Mini, EDTA-free Protease Inhibitor Cocktail Tablets; 1 Tablet in 50 mL solution; Boehringer Mannheim, Mannheim, Germany). The cells were disrupted by sonication (cycle 0.5, 10 min, 20W power output; Sonopuls HD2200, SH213G Booster Horn, TT13 sonotrode, Bandelin Electronic, Berlin, Germany), cell debris was removed by centrifugation (6000 x *g*, 4 ºC, 4 min), and the supernatant was centrifuged (30,000 x *g*, 4 ºC, 60 min). The supernatant (cytosolic fraction) was collected in a fresh tube (~10 mL). The pellet was resuspended in 10 mL PBS supplemented with protease inhibitor cocktail tablets, centrifuged (30,000 x *g*, 4 ºC, 60 min), and the supernatant was discarded. The pellet (membrane-associated fraction) was resuspended in 5 mL PBS supplemented with the protease inhibitor cocktail tablets. The proteins were concentrated by acetone precipitation. The BCA Protein Assay (Thermo Fisher Scientific) was used to quantify the protein content prior to in-solution digestion.

7.8.3 In-solution digestion

Twenty (20) µg of protein was digested for each sample as follows: digestion buffer was added 1:1 with the protein samples for a final concentration of 1% (w/v) sodium deoxycholate and 50 mM triethylammonium bicarbonate. The mixture was heated to 99 ºC for 10 minutes, then cooled to 37 ºC. Protein extracts were reduced by adding tris(2-carboxyethyl)phosphine (TCEP) (1 µg TCEP/25 µg protein) and incubating samples at 37 ºC for 30 min. Following reduction, proteins were alkylated by adding iodoacetic acid (1 µg iodoacetic acid/10 µg protein) and the proteins were incubated in the dark

(37 ºC, 20 min). Finally, proteins were mixed with trypsin in a ratio of 1:50 (w/w) and digested overnight at 37 ºC. Samples were acidified and sodium deoxycholate was pelleted by centrifugation (10,000 x *g*, 4 ºC, 10 min). The supernatant was transferred to a fresh tube, dried in a vacuum concentrator (Labconco, Buch & Holm, Herlev, Denmark), and resuspended in 0.1% (v/v) t*rifluoroacetic acid* (TFA) and 0.005% (v/v) heptafluorobutyric Acid (HFBA).

7.8.4 LC/MS analyses for metabolomics

An Ultra High Definition Accurate-Mass Quadrupole Time-of-Flight coupled with an ultra-HPLC system (Agilent Technologies, Inc.; Santa Clara, CA, USA) was used to determine the presence of BPA and corresponding metabolites. Gradient elution was performed using an ACQUITY UPLC BEH C18 column (2.1 x 100 mm, 1.7 µm; Waters Co., Milford, MA, USA). The flow rate was set to 0.4 mL/min and the gradient was programmed as follows: 0.00-5.00 2 % B, 5.00-7.00 7 % B, 7.00-9.00 15% B, 9.00-11.50 20% B, 11.50-14.00 25% B, 14.00-15.50 30 % B, 15.50-17.00 35% B, 17.00-18.50 45% B, 18.50-20.00 60 % B, 20.00-27.00 100% B. Column equilibration to starting conditions was performed after gradient elution for 3 min. The sample injection volume was set to 5 µL. A jet stream ESI source running in negative ionization mode was used with the following settings: gas temperature: 320 °C; drying gas: 8 L/min; nebulizer gas: 35 psig; sheath gas temperature: 380 °C ; sheath gas flow: 11 L/min; VCap: 3000 V; nozzle voltage: 0 V; fragmentor: 100 V; skimmer: 40 V; OCT 1 RF Vpp: 750 V. Fullscan (100-600 m/z; 4 spectra/s) data dependent MS/MS (50-600 m/z; 4 spectra/s; collision energy: 22 eV) acquisition was used for identification and relative quantification of the corresponding metabolites. Metabolites were identified after visual inspection and interpretation of the corresponding MS/MS spectra using MassHunter Workstation (Agilent Technologies, Inc.; Santa Clara, CA, USA) software Accelrys Draw Academic Version 4.1 (Accelrys, Inc.; San Diego, CA, USA). After that the corresponding metabolites were relatively quantified using full scan.

Table 7.6. Summary of essential genes in *Sphingobium* sp. BiD32

Genes from Gil et al. 2004		Genes from this study		
Gene	Protein function	UniProt accession number	Gene	UniProt protein name
dnaB	Replicative DNA helicase	N1ML46	EBBID32_4900	Replicative DNA helicase
dnaE	DNA polymerase III, alpha subunit	N1MTG1	EBBID32_46350	DNA-directed DNA polymerase (EC 2.7.7.7)
dnaG	DNA primase	N1MQY3	EBBID32_37220	DNA primase (EC 2.7.7.-)
dnaN	DNA polymerase III, beta subunit	N1MMD2	EBBID32_27170	DNA polymerase III subunit beta (EC 2.7.7.7)
dnaQ	DNA polymerase III, epsilon subunit	N1MY79	EBBID32_45620	DNA polymerase III epsilon subunit (EC 2.7.7.7)
dnaX	DNA polymerase III, gamma and tau subunits	N1MN77	EBBID32_30090	DNA polymerase III subunits gamma and tau (EC 2.7.7.7)
gyrA	DNA gyrase, A subunit	N1MF61	EBBID32_1980	DNA gyrase subunit A (EC 5.99.1.3)
gyrB	DNA gyrase, B subunit	N1MX63	EBBID32_42330	DNA gyrase subunit B (EC 5.99.1.3)
holA	DNA polymerase III, delta subunit	N1MHJ1	EBBID32_10130	DNA polymerase III delta subunit
holB	DNA polymerase III, delta prime subunit	N1MG02	EBBID32_2260	DNA polymerase III delta prime subunit (EC 2.7.7.7)
hupA	DNA binding protein	-	-	-
lig	DNA ligase (NAD dependent)	N1MTF7	EBBID32_44150	DNA ligase (EC 6.5.1.2) (Polydeoxyribonucleotide synthase [NAD(+)])
ssb	SSB	N1MS91	EBBID32_42110	Single-stranded DNA-binding protein (SSB)
		N1MI11	EBBID32_11980	Single-stranded DNA-binding protein (SSB)
		N1MKF9	EBBID32_2740	Single-stranded DNA-binding protein
		N1MNZ8	EBBID32_16910	Single-stranded DNA-binding protein
		N1MQJ0	EBBID32_35470	Single-stranded DNA-binding protein
nth	Endonuclease III	N1MQ94	EBBID32_34580	Endonuclease III (EC 4.2.99.18) (DNA-(apurinic or apyrimidinic site) lyase)
polA	5'-3' exonuclease domain of DNA polymerase I	N1MIR1	EBBID32_9920	DNA polymerase I (EC 2.7.7.7)
ung	Uracil-DNA glycosylase	N1MPC7	EBBID32_18480	Uracil-DNA glycosylase (UDG) (EC 3.2.2.27)
deaD	ATP-dependent RNA helicase	N1MWC1	EBBID32_42370	ATP-dependent helicase, DEAD/DEAH box family,associated with Flp pilus assembly
greA	Transcription elongation factor	N1MRI7	EBBID32_37150	Transcription elongation factor GreA (Transcript cleavage factor GreA)
nusA	Transcription-translation coupling	N1MHH7	EBBID32_10030	Transcription termination/antitermination protein NusA

. . . . . .

Table 7.6. (continued)

Genes from Gil et al. 2004		Genes from this study		
Gene	Protein function	UniProt accession number	Gene	UniProt protein name
nusG	Transcription antitermination protein	N1MYL4	EBBID32_46920	Transcription termination/antitermination protein NusG
rpoA	RNA polymerase, alpha subunit	N1MTL7	EBBID32_44800	DNA-directed RNA polymerase subunit alpha (RNAP subunit alpha) (EC 2.7.7.6) (RNA polymerase subunit alpha) (Transcriptase subunit alpha)
rpoB	RNA polymerase, beta subunit	N1MGG9	EBBID32_6430	DNA-directed RNA polymerase subunit beta (RNAP subunit beta) (EC 2.7.7.6) (RNA polymerase subunit beta) (Transcriptase subunit beta)
rpoC	RNA polymerase, beta prime subunit	N1MH76	EBBID32_6440	DNA-directed RNA polymerase subunit beta' (RNAP subunit beta') (EC 2.7.7.6) (RNA polymerase subunit beta') (Transcriptase subunit beta')
rpoD	RNA polymerase, major sigma subunit	N1MUQ0	EBBID32_37230	RNA polymerase sigma factor RpoD (Sigma-70)
alaS	Alanyl-tRNA synthase	N1MF76	EBBID32_2150	Alanine--tRNA ligase (EC 6.1.1.7) (Alanyl-tRNA synthetase)
argS	Arginyl-tRNA synthase	N1ML25	EBBID32_22890	Arginine--tRNA ligase (EC 6.1.1.19) (Arginyl-tRNA synthetase)
asnS	Asparaginyl-tRNA synthase	-	-	-
aspS	Aspartyl-tRNA synthase	N1MMZ3	EBBID32_24440	Aspartyl-tRNA synthetase @ Aspartyl-tRNA(Asn) synthetase (EC 6.1.1.12) (EC 6.1.1.23)
cysS	Cysteinyl-tRNA synthase	N1MI93	EBBID32_9890	Cysteine--tRNA ligase (EC 6.1.1.16) (Cysteinyl-tRNA synthetase)
glnS	Glutaminyl-tRNA synthase	-	-	-
gltX	Glutamyl-tRNA synthase	N1MMK7	EBBID32_11700	Glutamate--tRNA ligase (EC 6.1.1.17) (Glutamyl-tRNA synthetase)
		N1MQL4	EBBID32_35670	Glutamate--tRNA ligase (EC 6.1.1.17) (Glutamyl-tRNA synthetase)
glyS	Glycyl-tRNA synthase, b subunit	-	-	-
hisS	Histidyl-tRNA synthase	N1MRV5	EBBID32_40350	Histidine--tRNA ligase (EC 6.1.1.21) (Histidyl-tRNA synthetase)
ileS	Isoleucyl-tRNA synthase	N1MRC6	EBBID32_38780	Isoleucine--tRNA ligase (EC 6.1.1.5) (Isoleucyl-tRNA synthetase)
leuS	Leucyl-tRNA synthase	-	-	-
lysS	Lysyl-tRNA synthase	N1MMS3	EBBID32_28730	Lysine--tRNA ligase (EC 6.1.1.6) (Lysyl-tRNA synthetase)
metS	Methionyl-tRNA synthase	N1MF87	EBBID32_2250	Methionine--tRNA ligase (EC 6.1.1.10) (Methionyl-tRNA synthetase)

. . . . . .

Table 7.6. (continued)

Genes from Gil et al. 2004		Genes from this study		
Gene	Protein function	UniProt accession number	Gene	UniProt protein name
pheS	Phenylalanyl-tRNA synthase, a subunit	N1MMW9	EBBID32_11610	Phenylalanine--tRNA ligase alpha subunit (EC 6.1.1.20) (Phenylalanyl-tRNA synthetase alpha subunit)
pheT	Phenylalanyl-tRNA synthase, b subunit	N1MMK2	EBBID32_11600	Phenylalanine--tRNA ligase beta subunit
proS	Prolyl-tRNA synthase	N1MVW1	EBBID32_40560	Proline--tRNA ligase (EC 6.1.1.15) (Prolyl-tRNA synthetase)
serS	Seryl-tRNA synthase	N1MWF7	EBBID32_42780	Serine--tRNA ligase (EC 6.1.1.11) (Seryl-tRNA synthetase) (Seryl-tRNA(Ser/Sec) synthetase)
thrS	Threonyl-tRNA synthase	N1MQ37	EBBID32_20910	Threonine--tRNA ligase (EC 6.1.1.3) (Threonyl-tRNA synthetase)
trpS	Tryptophanyl-tRNA synthase	N1MLA8	EBBID32_20750	Tryptophanyl-tRNA synthetase (EC 6.1.1.2)
tyrS	Tyrosyl-tRNA synthase	N1MNH0	EBBID32_31200	Tyrosine--tRNA ligase (EC 6.1.1.1) (Tyrosyl-tRNA synthetase)
valS	Valyl-tRNA synthase	-	-	-
iscS	Cysteine desulfurase-NifS homolog	-	-	-
mnmA	tRNA (5-methylaminomethyl-2-thiouridylate) methyl-transferase	N1MJD7	EBBID32_12170	tRNA-specific 2-thiouridylase MnmA (EC 2.8.1.-)
mnmE	GTP binding protein involved in biosynthesis of 5-methilaminomethyl-2-thiouridine	-	-	-
mnmG	Glucose-inhibited division protein A, involved in bio-synthesis of 5-methylaminomethyl-2-thiouridine	N1MWE3	EBBID32_42620	tRNA uridine 5-carboxymethylaminomethyl modification enzyme MnmG (Glucose-inhibited division protein A)
pth	Peptidyl-tRNA hydrolase	-	-	-
rnpA	Protein component of Rna P	N1MS04	EBBID32_28250	Ribonuclease P protein component (RNase P protein) (RNaseP protein) (EC 3.1.26.5) (Protein C5)
rplA	50S ribosomal protein L1	N1MTK2	EBBID32_46900	50S ribosomal protein L1
rplB	50S ribosomal protein L2	N1MU12	EBBID32_32250	50S ribosomal protein L2
rplC	50S ribosomal protein L3	N1MNQ3	EBBID32_32220	50S ribosomal protein L3
rplD	50S ribosomal protein L4	N1MPK6	EBBID32_32230	50S ribosomal protein L4
rplE	50S ribosomal protein L5	N1MT72	EBBID32_32340	50S ribosomal protein L5
rplF	50S ribosomal protein L6	N1MNR8	EBBID32_32370	50S ribosomal protein L6
rplI	50S ribosomal protein L9	N1MH13	EBBID32_5530	50S ribosomal protein L9
rplJ	50S ribosomal protein L10	N1MM45	EBBID32_21480	50S ribosomal protein L10
rplK	50S ribosomal protein L11	N1MXT1	EBBID32_46910	50S ribosomal protein L11
rplL	50S ribosomal protein L12	N1MQV1	EBBID32_21470	50S ribosomal protein L7/L12

. . . . . .

Table 7.6. (continued)

Genes from Gil et al. 2004		Genes from this study		
Gene	Protein function	UniProt accession number	Gene	UniProt protein name
rplM	50S ribosomal protein L13	N1MKZ8	EBBID32_6050	50S ribosomal protein L13
rplN	50S ribosomal protein L14	N1MNR3	EBBID32_32320	50S ribosomal protein L14
rplO	50S ribosomal protein L15	N1MQ71	EBBID32_32410	50S ribosomal protein L15
rplP	50S ribosomal protein L16	N1MT67	EBBID32_32290	50S ribosomal protein L16
rplQ	50S ribosomal protein L17	N1MSE1	EBBID32_44810	50S ribosomal protein L17
rplR	50S ribosomal protein L18	N1MPM0	EBBID32_32380	50S ribosomal protein L18
rplS	50S ribosomal protein L19	-	-	-
rplT	50S ribosomal protein L20	N1MHX8	EBBID32_11630	50S ribosomal protein L20
rplU	50S ribosomal protein L21	N1MXS9	EBBID32_46860	50S ribosomal protein L21
rplV	50S ribosomal protein L22	N1MNQ6	EBBID32_32270	50S ribosomal protein L22
rplW	50S ribosomal protein L23	N1MT64	EBBID32_32240	50S ribosomal protein L23
rplX	50S ribosomal protein L24	N1MPL6	EBBID32_32330	50S ribosomal protein L24
rpmA	50S ribosomal protein L27	N1MTJ8	EBBID32_46850	50S ribosomal protein L27
rpmB	50S ribosomal protein L28	-	-	-
rpmC	50S ribosomal protein L29	N1MU16	EBBID32_32300	50S ribosomal protein L29
rpmE	50S ribosomal protein L31	N1MK28	EBBID32_19160	50S ribosomal protein L31
rpmF	50S ribosomal protein L32	N1MR51	EBBID32_24830	50S ribosomal protein L32
rpmG	50S ribosomal protein L33	N1MNB6	EBBID32_28140	50S ribosomal protein L33
rpmH	50S ribosomal protein L34	N1MND0	EBBID32_28240	50S ribosomal protein L34
rpmI	50S ribosomal protein L35	N1MIP7	EBBID32_11640	50S ribosomal protein L35
rpmJ	50S ribosomal protein L36	N1MVY0	EBBID32_40770	50S ribosomal protein L36
rpsB	30S ribosomal protein S2	N1MLE7	EBBID32_19050	30S ribosomal protein S2
rpsC	30S ribosomal protein S3	N1MPL1	EBBID32_32280	30S ribosomal protein S3
rpsD	30S ribosomal protein S4	N1MS81	EBBID32_39520	30S ribosomal protein S4
rpsE	30S ribosomal protein S5	N1MT75	EBBID32_32390	30S ribosomal protein S5
rpsF	30S ribosomal protein S6	N1MLB9	EBBID32_5550	30S ribosomal protein S6
rpsG	30S ribosomal protein S7	N1MPK3	EBBID32_32180	30S ribosomal protein S7
rpsH	30S ribosomal protein S8	N1MQ66	EBBID32_32360	30S ribosomal protein S8
rpsI	30S ribosomal protein S9	N1MH47	EBBID32_6040	30S ribosomal protein S9
rpsJ	30S ribosomal protein S10	N1MQ50	EBBID32_32210	30S ribosomal protein S10
rpsK	30S ribosomal protein S11	N1MXW9	EBBID32_44790	30S ribosomal protein S11
rpsL	30S ribosomal protein S12	N1MNP8	EBBID32_32170	30S ribosomal protein S12
rpsM	30S ribosomal protein S13	N1MX42	EBBID32_44780	30S ribosomal protein S13
rpsN	30S ribosomal protein S14	N1MU22	EBBID32_32350	30S ribosomal protein S14
rpsO	30S ribosomal protein S15	N1MWU7	EBBID32_44080	30S ribosomal protein S15
rpsP	30S ribosomal protein S16	-	-	-
rpsQ	30S ribosomal protein S17	N1MQ61	EBBID32_32310	30S ribosomal protein S17
rpsR	30S ribosomal protein S18	N1MKW0	EBBID32_5540	30S ribosomal protein S18

. . . . . .

Table 7.6. (continued)

Genes from Gil et al. 2004		Genes from this study		
Gene	Protein function	UniProt accession number	Gene	UniProt protein name
rpsS	30S ribosomal protein S19	N1MQ55	EBBID32_32260	30S ribosomal protein S19
rpsT	30S ribosomal protein S20	N1MLB3	EBBID32_20800	30S ribosomal protein S20
cspR	Ribosomal methytransferase	-	-	-
engA	GTP binding protein	N1ML93	EBBID32_20540	GTP-binding protein EngA
era	GTP binding protein	N1MPH8	EBBID32_29830	GTPase Era
ksgA	Dimethyladenosine transferase	N1MNJ0	EBBID32_15010	Ribosomal RNA small subunit methyltransferase A (EC 2.1.1.182) (16S rRNA (adenine(1518)-N(6)/adenine(1519)-N(6))-dimethyltransferase) (16S rRNA dimethyladenosine transferase) (16S rRNA dimethylase) (S-adenosylmethionine-6-N', N'-adenosyl(rRNA) dimethyltransferase)
obg	GTP binding protein	N1MH61	EBBID32_9070	GTPase Obg (GTP-binding protein Obg)
rbfA	Ribosome binding factor A	N1MIB5	EBBID32_10090	Ribosome-binding factor A
ychF	GTP binding protein	-	-	-
efp	Elongation factor P	N1MSN2	EBBID32_30260	Elongation factor P (EF-P)
fusA	Elongation factor G	N1MT59	EBBID32_32190	Elongation factor G (EF-G)
frr	Ribosome-recycling factor	N1MPI6	EBBID32_19080	Ribosome-recycling factor (RRF) (Ribosome-releasing factor)
hemK	N5-glutamine methyltransferase, modulation of release factor activity	-	-	-
infA	Initiation factor IF-1	N1MLI5	EBBID32_21700	Translation initiation factor 1
infB	Initiation factor IF-2	N1MMH1	EBBID32_10060	Translation initiation factor IF-2
infC	Initiation factor IF-3	N1MQQ8	EBBID32_20920	Translation initiation factor IF-3
lepA	GTP binding elongation factor	N1MPM8	EBBID32_32480	Elongation factor 4 (EF-4) (EC 3.6.5.n1) (Ribosomal back-translocase LepA)
prfA	Peptide chain release factor 1 (RF1)	N1ML74	EBBID32_7030	Peptide chain release factor 1 (RF-1)
smpB	tmRNA binding protein	N1MT03	EBBID32_28860	SsrA-binding protein
tsf	Elongation factor Ts	N1MK19	EBBID32_19060	Elongation factor Ts (EF-Ts)
tufA	Elongation factor Tu	N1MU06	EBBID32_32200	Elongation factor Tu (EF-Tu)
pnp	Polyribonucleotide nucleotidyltransferase	N1MTF1	EBBID32_44100	Polyribonucleotide nucleotidyltransferase (EC 2.7.7.8) (Polynucleotide phosphorylase)
rnc	Ribonuclease III	N1MSI7	EBBID32_29860	Ribonuclease 3 (EC 3.1.26.3) (Ribonuclease 3) (Ribonuclease III)
map	Methionine aminopeptidase	N1MNN0	EBBID32_14170	Methionine aminopeptidase (MAP) (MetAP) (EC 3.4.11.18) (Peptidase M)

. . . . . .

Table 7.6. (continued)

Genes from Gil et al. 2004		Genes from this study		
Gene	Protein function	UniProt accession number	Gene	UniProt protein name
pepA	Aminopeptidase A/I	N1MJP9	EBBID32_15050	Probable cytosol aminopeptidase (Leucine aminopeptidase) (Leucyl aminopeptidase)
dnaJ	Hsp70 cochaperone	N1MUJ9	EBBID32_36680	Chaperone protein DnaJ
dnaK	Chaperone Hsp70	N1MKR0	EBBID32_21690	Chaperone protein DnaK (HSP70) (Heat shock 70 kDa protein) (Heat shock protein 70)
groEL	Class I heat shock protein	N1MXP7	EBBID32_44190	60 kDa chaperonin (GroEL protein) (Protein Cpn60)
groES	Class I heat shock protein	N1MWW0	EBBID32_44180	10 kDa chaperonin (GroES protein) (Protein Cpn10)
grpE	Hsp70 cochaperone	N1MSJ2	EBBID32_27410	Protein GrpE (HSP-70 cofactor)
ffh	Protein component of signal recognition particle	-	-	-
ftsY	Signal recognition particle receptor	-	-	-
secA	Preprotein transloscase subunit (ATPase)	N1MJR3	EBBID32_2320	Protein translocase subunit SecA
		N1MLZ7	EBBID32_25510	Protein translocase subunit SecA
secE	Membrane-embedded preprotein translocase subunit	N1MU79	EBBID32_46930	Protein translocase subunit SecE
secY	Membrane-embedded preprotein translocase subunit	N1MNS2	EBBID32_32420	Protein translocase subunit SecY
gcp	Probable O-sialoglycoprotein endopeptidase	-	-	-
hflB	ATP-dependent protease	-	-	-
Ion	ATP-dependent protease La	N1MSL6	EBBID32_30110	Lon protease (EC 3.4.21.53) (ATP-dependent protease La)
ftsZ	Cytoskeletal cell division protein	N1MN60	EBBID32_29940	Cell division protein FtsZ
pitA	Low-affinity inorganic phosphate transporter	N1MKL0	EBBID32_18270	Probable low-affinity inorganic phosphate transporter
ptsG	PTS glucose-specific enzyme II	N1MPW1	EBBID32_36160	PTS system, N-acetylglucosamine-specific IIA component / PTS system, N-acetylglucosamine-specific IIB component / PTS system, N-acetylglucosamine-specific IIC component (EC 2.7.1.69)
ptsH	Histidine-containing phosphocarrier protein of PTS	-	-	-
ptsI	PTS enzyme I	-	-	-
eno	Enolase	N1MPM3	EBBID32_17470	Enolase (EC 4.2.1.11) (2-phospho-D-glycerate hydro-lyase) (2-phosphoglycerate dehydratase)

. . . . . .

Table 7.6. (continued)

Genes from Gil et al. 2004		Genes from this study		
Gene	Protein function	UniProt accession number	Gene	UniProt protein name
fbaA	Fructose-1,6-bisphosphate aldolase	N1MFY7	EBBID32_2110	Fructose-bisphosphate aldolase class I (EC 4.1.2.13)
gapA	Glyceraldehyde-3-phosphate dehydrogenase	N1MGI2	EBBID32_2090	Glyceraldehyde-3-phosphate dehydrogenase (EC 1.2.1.-)
gpmA	Phosphoglycerate mutase	N1MKX3	EBBID32_4340	2,3-bisphosphoglycerate-dependent phosphoglycerate mutase (BPG-dependent PGAM) (PGAM) (Phosphoglyceromutase) (dPGM) (EC 5.4.2.11)
ldh	L-lactate dehydrogenase	N1MX13	EBBID32_41730	Predicted L-lactate dehydrogenase, Iron-sulfur cluster-binding subunit YkgF
		N1MST7	EBBID32_41740	Predicted L-lactate dehydrogenase, Fe-S oxidoreductase subunit YkgE
pfkA	6-Phosphofructokinase	N1MJW0	EBBID32_13780	Phosphofructokinase
pgi	Glucose-6-phosphate isomerase	N1MN52	EBBID32_29890	Glucose-6-phosphate isomerase (GPI) (EC 5.3.1.9) (Phosphoglucose isomerase) (Phosphohexose isomerase)
pgk	Phosphoglycerate kinase	N1MF71	EBBID32_2100	Phosphoglycerate kinase (EC 2.7.2.3)
pykA	Pyruvate kinase	N1MKP8	EBBID32_21540	Pyruvate kinase (EC 2.7.1.40)
tpiA	Triose-phosphate isomerase	N1MPN0	EBBID32_19530	Triosephosphate isomerase (TIM) (EC 5.3.1.1) (Triose-phosphate isomerase)
atpA	ATP synthase alpha chai	N1MH59	EBBID32_4450	ATP synthase subunit alpha (EC 3.6.3.14) (ATP synthase F1 sector subunit alpha) (F-ATPase subunit alpha)
atpB	ATP synthase A chain	N1MU63	EBBID32_35320	ATP synthase subunit a (ATP synthase F0 sector subunit a) (F-ATPase subunit 6)
atpC	ATP synthase epsilon chain	N1MHA6	EBBID32_9420	ATP synthase epsilon chain (ATP synthase F1 sector epsilon subunit) (F-ATPase epsilon subunit)
atpD	ATP synthase beta chain	N1MGP1	EBBID32_4470	ATP synthase subunit beta (EC 3.6.3.14) (ATP synthase F1 sector subunit beta) (F-ATPase subunit beta)
atpE	ATP synthase C chain	N1MQH3	EBBID32_35310	ATP synthase C chain (EC 3.6.3.14)
atpF	ATP synthase B chain	N1MPN2	EBBID32_35300	ATP synthase subunit b (ATP synthase F(0) sector subunit b) (ATPase subunit I) (F-type ATPase subunit b)
		N1MR14	EBBID32_35290	ATP synthase subunit b (ATP synthase F(0) sector subunit b) (ATPase subunit I) (F-type ATPase subunit b)

. . . . . .

Table 7.6. (continued)

Genes from Gil et al. 2004		Genes from this study		
Gene	Protein function	UniProt accession number	Gene	UniProt protein name
atpG	ATP synthase gamma chain	N1MFW9	EBBID32_4460	ATP synthase gamma chain (ATP synthase F1 sector gamma subunit) (F-ATPase gamma subunit)
atpH	ATP synthase delta chain	N1MKY8	EBBID32_4440	ATP synthase subunit delta (ATP synthase F(1) sector subunit delta) (F-type ATPase subunit delta)
yidc	Essential for proper integration of ATPase into the membrane	N1MP13	EBBID32_28270	Membrane protein insertase YidC (Foldase YidC) (Membrane integrase YidC) (Membrane protein YidC)
rpe	Ribulose-phosphate 3-epimerase	N1MJA7	EBBID32_11920	Ribulose-phosphate 3-epimerase (EC 5.1.3.1)
rpiA	Ribose 5-phosphate isomerase	N1MNY2	EBBID32_30000	Ribose 5-phosphate isomerase B (EC 5.3.1.6)
tkt	Transketolase	N1MIJ1	EBBID32_13890	Transketolase (EC 2.2.1.1)
		N1MKB0	EBBID32_2080	Transketolase (EC 2.2.1.1)
cdsA	Phosphatidate cytidylyltransferase	N1MLF5	EBBID32_19100	Phosphatidate cytidylyltransferase (EC 2.7.7.41)
fadD	Acyl-CoA synthase	-	-	-
gpsA	*sn*-Glycerol-3-phosophate dehydrogenase	N1MMY4	EBBID32_11760	Glycerol-3-phosphate dehydrogenase [NAD(P)+] (EC 1.1.1.94) (NAD(P)H-dependent glycerol-3-phosphate dehydrogenase)
plsB	*sn*-Glycerol-3-phosophate acyltransferase	-	-	-
plsC	1-Acyl-*sn*-glycerol-3-phosphate acyltransferase	N1MQV6	EBBID32_34760	1-acyl-sn-glycerol-3-phosphate acyltransferase (EC 2.3.1.51)
		N1MLM1	EBBID32_8480	1-acyl-sn-glycerol-3-phosphate acyltransferase (EC 2.3.1.51)
psd	Phosphatidylserine decarboxylase	N1MJA8	EBBID32_550	Phosphatidylserine decarboxylase proenzyme (EC 4.1.1.65)
		N1MK16	EBBID32_19010	Phosphatidylserine decarboxylase proenzyme (EC 4.1.1.65)
pssA	Phosphatidylserine synthase	-	-	-
adk	Adenylate kinase	N1MPM4	EBBID32_32430	Adenylate kinase (AK) (EC 2.7.4.3) (ATP-AMP transphosphorylase) (ATP:AMP phosphotransferase) (Adenylate monophosphate kinase)
dcd	dCTP deaminase	N1MKN3	EBBID32_4940	Deoxycytidine triphosphate deaminase (dCTP deaminase) (EC 3.5.4.13)
gmk	Guanylate kinase	N1MQ35	EBBID32_32060	Guanylate kinase (EC 2.7.4.8) (GMP kinase)
hpt	Hypoxanthine phosphoribosyltransferase	-	-	-
ndk	Nucleoside diphosphate kinase	N1MP03	EBBID32_15070	Nucleoside diphosphate kinase (NDK) (NDP kinase) (EC 2.7.4.6) (Nucleoside-2-P kinase)

. . . . . .

Table 7.6. (continued)

Genes from Gil et al. 2004		Genes from this study		
Gene	Protein function	UniProt accession number	Gene	UniProt protein name
nrdE	Ribonucleoside diphosphate reductase (major subunit)	N1MEU4	EBBID32_480	Ribonucleoside-diphosphate reductase (EC 1.17.4.1)
nrdF	Ribonucleoside diphosphate reductase (minor subunit)	N1MK05	EBBID32_460	Ribonucleoside-diphosphate reductase subunit beta (EC 1.17.4.1)
ppa	Inorganic pyrophosphatase	N1MSH1	EBBID32_40330	Inorganic pyrophosphatase (EC 3.6.1.1) (Pyrophosphate phospho-hydrolase)
prsA	Phosphoribosylpyrophospate synthase	N1MHY2	EBBID32_11680	Ribose-phosphate pyrophosphokinase (RPPK) (EC 2.7.6.1) (5-phospho-D-ribosyl alpha-1-diphosphate) (Phosphoribosyl diphosphate synthase) (Phosphoribosyl pyrophosphate synthase)
pyrG	CTP synthase	N1MM39	EBBID32_10000	CTP synthase (EC 6.3.4.2) (CTP synthetase) (UTP--ammonia ligase)
thyA	Thymidylate synthase	N1MQ23	EBBID32_33950	Thymidylate synthase (EC 2.1.1.45)
tmk	Thymidylate kinase	N1MJR1	EBBID32_2270	Thymidylate kinase (EC 2.7.4.9) (dTMP kinase)
trxA	Thioredoxin	N1MF95	EBBID32_2350	Thioredoxin
		N1MTF3	EBBID32_46250	Thioredoxin
trxB	Thioredoxin reductase	N1MIV3	EBBID32_14840	Thioredoxin reductase (EC 1.8.1.9)
upp	Uracil phosphoribosyltransferase	-	-	-
coaA	Pantothenate kinase	-	-	-
coaD	4'-Phosphopantetheine adenylyltransferase	N1MPL5	EBBID32_19380	Phosphopantetheine adenylyltransferase (EC 2.7.7.3) (Dephospho-CoA pyrophosphorylase) (Pantetheine-phosphate adenylyltransferase)
coaE	Dephospho-CoA kinase	N1MTX4	EBBID32_45630	Dephospho-CoA kinase (EC 2.7.1.24) (Dephosphocoenzyme A kinase)
dfp	Phosphopantothenate cysteine ligase and 4'-Phosopho-pantothenyl-L-cysteine decarboxylase	N1MQ34	EBBID32_20860	Phosphopantothenoylcysteine decarboxylase / Phosphopantothenoylcysteine synthetase (EC 4.1.1.36) (EC 6.3.2.5)
folA	Dihydrofolate reductase	N1MRZ6	EBBID32_38760	Dihydrofolate reductase (EC 1.5.1.3)
glyA	Glycine hydroxymethyltransferase	N1MN65	EBBID32_29990	Serine hydroxymethyltransferase (SHMT) (Serine methylase) (EC 2.1.2.1)
metK	Methionine adenosyltransferase	N1MRL3	EBBID32_42250	S-adenosylmethionine synthase (EC 2.5.1.6)
nadR	Adenylyltransferase	-	-	-
nadV	Nicotinamide phosphoribosyltransferase	-	-	-
pdxY	Pyridoxal kinase	-	-	-

. . . . . .

Table 7.6. (continued)

Genes from Gil et al. 2004		Genes from this study		
Gene	Protein function	UniProt accession number	Gene	UniProt protein name
ribF	Riboflavin kinase	N1MQK4	EBBID32_38770	Riboflavin biosynthesis protein (EC 2.7.1.26) (EC 2.7.7.2)
yloS	Thiamine pyrophosphokinase	-	-	-
mesJ	Conserved hypothetical protein	-	-	-
mraW	Methyltransferase	-	-	-
ybeY	Conserved hypothetical protein	N1MTZ0	EBBID32_34790	Endoribonuclease YbeY (EC 3.1.-.-)
ycfF	HIT family	-	-	-
ycfH	Putative deoxyribonuclease, *tatD* family	N1MGJ8	EBBID32_2240	Putative deoxyribonuclease YcfH
yoaE	Conserved hypothetical protein	-	-	-
yqgF	Conserved hypothetical protein	-	-	-
yraL	Conserved hypothetical protein	-	-	-

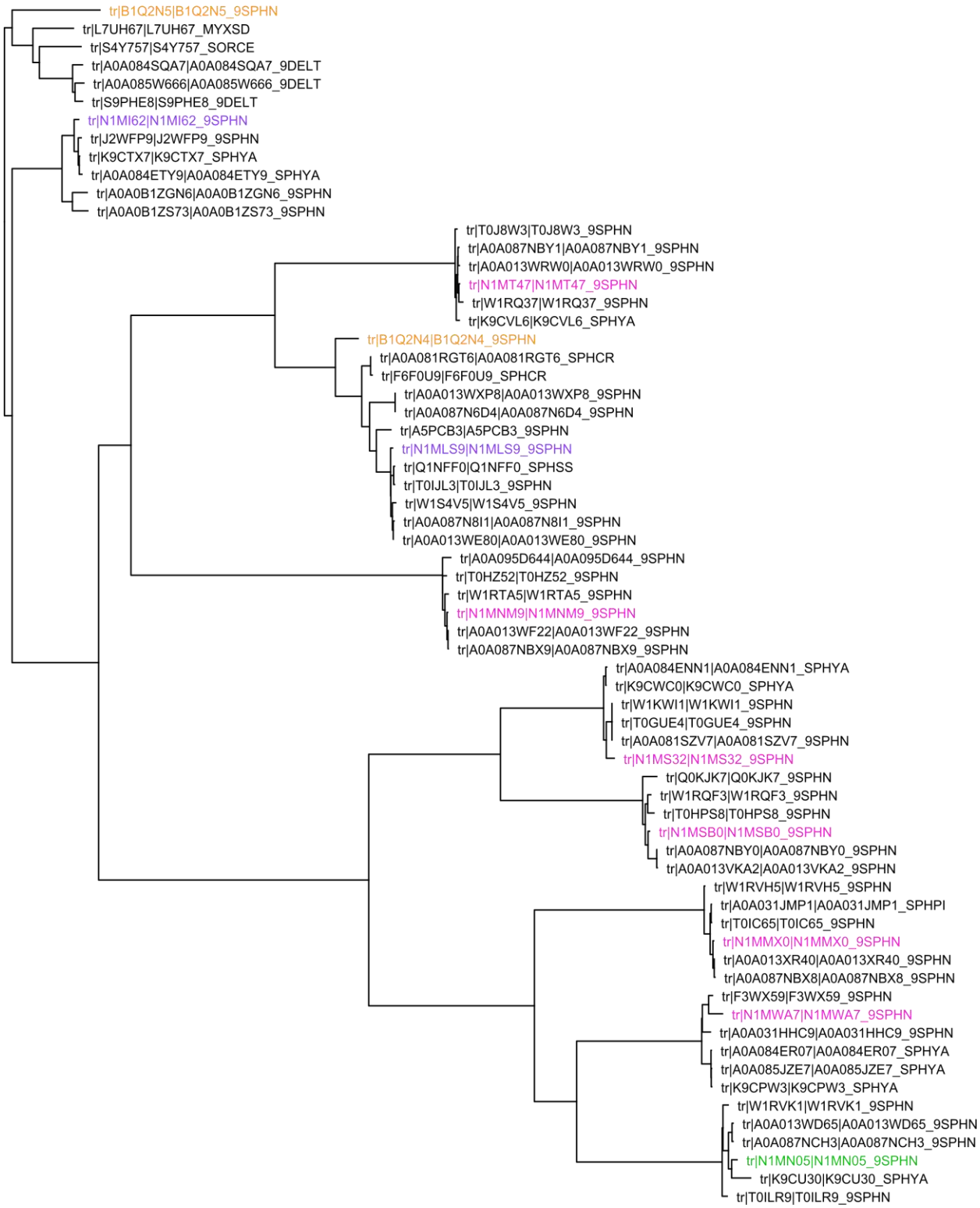

Figure 7.5. Phylogenetic relationship of *Sphingobium* sp. BiD32 proteins differentially expressed and functionally annotated to xenobiotics biodegradation and metabolism (pink), *Sphingobium* sp. BiD32 proteins functionally annotated to bisphenol degradation (green), *Sphingobium* sp. BiD32 proteins related to proteins responsible for BPA degradation by *Sphingomonas* sp. AO1 (purple), and *Sphingomonas* sp. AO1 proteins responsible for BPA degradation (orange).

CHAPTER 8: DIFFERENTIAL PROTEIN ABUNDANCE DURING 17-βESTRADIOL DEGRADATION BY *RHODOCOCCUS* SP. ESD8

8.1 Chapter summary

This chapter focuses on Objective V: identification of proteins potentially involved in trace organic contaminant degradation. This study used a combination of genomics, proteomics, and metabolomics to determine which proteins are likely involved in the transformation of E2 to E1 by *Rhodococcus* sp. EsD8. Proteins were detected in the proteome of *Rhodococcus* sp. EsD8 that were related to proteins previously identified or postulated as responsible for the transformation of E2 to E1 confirming that a similar pathway was used by this organism. These proteins include 3α-hydroxysteroid dehydrogenases, 3,17β-hydroxysteroid dehydrogenases, testosterone 17β-dehydrogenases, and 7α-hydroxysteroid dehydrogenases. These proteins were not previously identified in the *Rhodococcus* genus to the best of the author's knowledge, though they were found in a variety of organisms including humans, rats, *Pseudomonas, Stenotrophomonas,* and *Bacteroides*. Exposure of *Rhodococcus* sp. EsD8 to E2 and E1 also affected many biochemical processes, including fatty acid degradation and amino acid metabolism. Induction of genes for fatty acid degradation and amino acid metabolism have been related to cellular stress response, suggesting that E2 and/or E1 may induce a stress response on *Rhodococcus* sp. EsD8. The objective was achieved though future work should focus on knock-out experiments to confirm which of the many identified proteins are involved in E2 to E1 transformation. Identification of proteins involved in E2 degradation may lead to the ability to track degradation genes. This will assist in predicting the degradation activity of augmented bacteria rather than the microbial presence. Identification of these proteins will also potentially allow for identification of other TOrCs-degrading bacteria in activated sludge and assist in addressing fundamental questions about the evolution of these genes.

8.2 Abstract

Rhodococcus sp. strain EsD8 transforms 17β–estradiol (E2) to estrone (E1). The species was isolated from activated sludge, and can provide clues about the transformation of this contaminant during wastewater treatment. However, a model for E2 degradation for gram-positive bacteria is not yet available. This study investigated the metabolism of E2 as well as other effects of E2 and E1 on the proteome of *Rhodococcus* sp. EsD8 using label-free quantitative proteomics. The genome of *Rhodococcus* sp. EsD8 was sequenced to provide a species-specific platform for protein identification. The bacterial proteomes of *Rhodococcus* sp. EsD8 in the presence and absence of E2 and E1 were compared. A total of 2724 proteins were identified and 2186 of these proteins were quantified. Out these proteins, 964 were differentially expressed in response to the presence/absence of E2 ($p \leq 0.05$). Many genes encoding for proteins with 100% identity matches to enzymes involved in the transformation of E2 to E1 were identified in the genome and proteome. These enzyme classes include 3α-hydroxysteroid dehydrogenases, 3,17β-hydroxysteroid dehydrogenases, testosterone 17β-dehydrogenases, and 7α-hydroxysteroid dehydrogenases. Many biochemical processes were affected with exposure to E2 and E1, including fatty acid degradation and amino acid metabolism, suggesting that E2 and/or E1 may have a stress response on *Rhodococcus* sp. EsD8. This study establishes that enzymes used by other organisms for E2 degradation are also involved in activated sludge *Rhodococcus* sp. and may lead to the identification of biomarkers genes.

8.3 Introduction

Understanding how bacteria degrade endocrine disrupting compounds (EDCs) will improve techniques for enhancing their removal during wastewater treatment. EDCs discharged with wastewater treatment plant (WWTP) effluents are likely to cause negative effects on aquatic life (Baek et al. 2003; Oehlmann et al. 2006; Sohoni et al. 2001). Therefore, new technologies to improve their removal are needed such as bioaugmentation (Zhou et al. 2014). Identifying genetic indicators of EDC removal will allow for monitoring of EDC degradation activity during bioaugmentation rather than relying on secondary indicators. Also, understanding the effects these contaminants have on the augmented bacteria will be helpful, as bioaugmentation conditions or growth conditions could be modified to help prevent these negative effects.

Proteomic studies have been effective at identifying degradation genes and pathways of EDCs and pharmaceuticals, which could later be used as gene markers for EDC degradation. Identification of degradation genes and pathways using proteomics has been demonstrated by recent work with bisphenol A (Chapter 7), ibuprofen (Almeida et al. 2013) and 17β-estradiol (E2) (Li et al. 2012a). Li et al. (2012)

found that *Stenotrophomonas maltophilia* strain ZL1, isolated from activated sludge, transformed 17β-estradiol (E2) to estrone (E1) and then to tyrosine, which was used in protein biosynthesis. Previous proteomic studies have also led to the identification of gene markers for E2 exposure using label-free proteomics (Collodoro et al. 2012). In this study, three biomarkers in MCF-7/BOS cells were identified that were proposed to be used to in a rapid screening test to detect the presence of estrogens in environmental samples after further testing, demonstrating a potential use for biomarkers.

The ability of the augmented bacteria to degrade to low concentrations is important as E2 can have negative effects on aquatic life at low concentrations. E2, a potent natural hormone, is a contributor to endocrine disruption in the aquatic environment and effects from EDCs can be cumulative (Jin et al. 2012; Caliman and Gavrilescu 2009). E2 can cause a variety of negative effects on aquatic life at concentrations commonly detected in waterways, including vitellogenin induction in brown trout at 2 ng/L and fertility effects at 10 ng/L (Burkhardt-Holm et al. 2008). It caused an increase in hepatic vitellogenin in male medaka at 55.7 ng/L (Kang et al. 2002), and an increase in phenotypic female medaka resulting in many male medaka expressing intersex characteristics at 100 ng/L (Metcalfe et al. 2001).

Rhodococcus sp. EsD8 is an E2-degrading bacterium (Zhou et al. 2013) in the genus *Rhodococcus*, which is made up of high GC content, gram positive bacteria. Rhodococci are capable of degrading a variety of xenobiotics including E2 (Yoshimoto et al. 2004; Yu et al. 2007a; Kurisu et al. 2010; Zhou et al. 2013), 17α-ethinylestradiol (EE2) (Yoshimoto et al. 2004), quinoline (O'Loughlin et al. 1996), and polychlorinated biphenyls (Seto et al. 1995) amongst others. Also, large linear plasmids have been found in Rhodococci, which may contribute to their ability to degrade a variety of compounds (van der Geize and Dijkhuizen 2004). This study seeks to determine the genes and proteins involved in E2 degradation by *Rhodococcus* sp. EsD8, which was isolated from activated sludge and is capable of transforming E2 to E1 with final E2 concentrations of <6 ng/L (Zhou et al. 2013). Rhodococci typically have large genomes, and the genomes of many Rhodococci have been sequenced (Chen et al. 2014; McLeod et al. 2006; Sangal et al. 2015; Letek et al. 2010; Shields-Menard et al. 2014). Many oxidoreductases and ligases have been identified in *Rhodococcus* genomes, which are likely involved in aromatic compound degradation (McLeod et al. 2006). Proteomics studies have also been completed on Rhodococci, including *Rhodococcus jostii* RHA1 (Dávila Costa et al. 2015) and *Rhodococcus opacus* PD630 (Chen et al. 2014). Previously identified genes and proteins from other *Rhodococcus* species will allow for comparison with those identified in *Rhodococcus* sp. EsD8.

The objective of this study was to identify enzymes involved in E2 transformation to E1 by *Rhodococcus* sp. EsD8 and to study the effects of E2 and E1 exposure on the biochemical processes using a combination of genomics, proteomics, and metabolomics. Label-free quantitative proteomics was used to investigate the effect of E2 on the proteome of *Rhodococcus* sp. EsD8 and the results were used to identify candidate E2 catabolic genes in the organism's genome. Metabolomics then assisted in confirming potential genes involved and the pathway. These techniques allowed for the identification of many proteins previously predicted to be involved in E2 transformation in *Rhodococcus* sp. EsD8.

8.4 Materials and methods

8.4.1 Chemicals, reagents, and bacterial strain

Organic solvents and water used for E2 sample extraction and analysis were high pressure liquid chromatography (HPLC) grade. E2 (≥98%) was obtained from Sigma Aldrich (St. Louis, MO, USA). An aqueous stock solution (5 mg/L E2) was prepared from a concentrated (1000 mg/L E2) stock solution prepared in acetonitrile. An aliquot of the acetonitrile stock was dryed in a glass flask (60ºC); water was added to reach the aqueous stock concentration; and the flask was autoclaved (121ºC, 20 min) to ensure release of the dried E2 from the glass. A control was prepared in the same way by adding pure acetonitrile to a second empty flask, evaporating the acetonitrile at 60ºC, adding water, and autoclave sterilizing (121ºC, 20 min).

Rhodococcus sp. strain EsD8 (GenBank accession number JX87938) was previously isolated from activated sludge (Zhou et al. 2013).

8.4.2 Library preparation, genome sequencing, assembly, and analysis

The whole genome sequence of bacterial strain *Rhodococcus* sp. EsD8 was prepared and completed as previously described (Chapter 7). The sequences were trimmed and assembled using *de novo* assembly in CLC Genomics Workbench version 5.5.1 (CLC bio, Aarhus, Denmark) as previously described (Chapter 7). Assembled contigs were curated by CodonCode Aligner v 3.7 (CodonCode Corp.) and analyzed with the Rapid Annotation using Subsystem Technology (RAST) annotation server for subsystem classification and functional annotation (Aziz et al. 2008). The whole genome sequence was deposited at DDBJ/EMBL/GenBank under the accession numbers CAVJ010000001 to CAVJ010000287.

8.4.3 Sample preparation for proteomic analysis

Samples were prepared for proteomic analysis by growing *Rhodococcus* sp. EsD8 in the presence and absence of E2 (Figure 8.1). *Rhodococcus* sp. EsD8 was inoculated by transferring a single colony from

solid media into R2B media (pre-inoculum culture, PIC), a liquid media prepared based on the composition of R2A (Reasoner and Geldreich 1979). After reaching an optical density of ~0.8 at 600 nm (OD_{600}), 2 mL of *Sphingobium* sp. BiD32 was transferred into a second flask of R2B (inoculum culture, IC). When the IC reached an OD_{600} of ~0.5, 4 mL was inoculated into experimental flasks containing R2B for an estimated initial volatile suspended solids (VSS) concentration of 5.5 mg/L. Five replicate cultures of *Rhodococcus* sp. EsD8 were grown (100 rpm, 28ºC) with an initial concentration of 0.4 mg/L E2 and five replicates were grown without E2. OD_{600} was measured and samples for E2 quantification were collected every one to two hours. A high pressure liquid chromatography instrument with ultraviolet detector (HPLC-UV) was used to quantify E2 concentrations using previously reported methods (Zhou et al. 2013). E2 was re-spiked (approximately 0.5 mg/L) into the cultures every 2 hours to ensure that E2 was being actively degraded when the cells were harvested. *Rhodococcus* sp. EsD8 cultures (with and without E2) were harvested when an OD_{600} of ~0.6 was reached. At the point of harvest, the cultures were still in exponential growth and approximately 0.25 mg/L of the E2 was remaining. Cells were harvested by washing the cell pellet twice with 20 mL phosphate-buffered saline (PBS) and collected by centrifugation (10,000 xg, 4ºC, 15 min). The proteins were extracted and digested in-solution as previously described (Chapter 7).

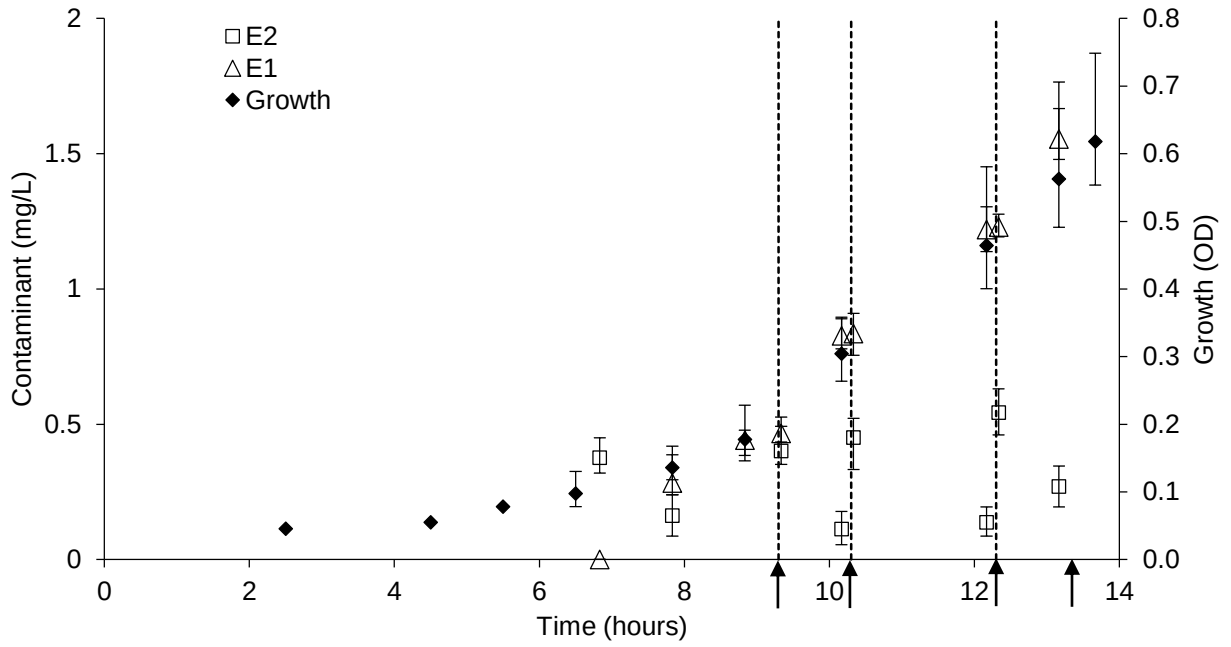

Figure 8.1. Growth and harvesting of *Rhodococcus* sp. EsD8 for differential proteomics analysis. Degradation of 17β-estradiol (E2) is shown as squares. Accumulation of estrone (E1) is shown as triangles. Growth of *Rhodococcus* sp. EsD8 in the presence and absence of E2 and E1 is shown as diamonds. E2 was re-spiked at 9.3, 10.3 and 12.3 hours (dashed lines). Cells were harvested for protein extraction at 13.1 hours. Error bars represent the range of measurements from replicates (*n*=5). The LOQ was 0.03 mg/L for E2 and 0.065 mg/L for E1.

8.4.4 LC-MS//MS analyses for proteomics

Tryptic digests were analyzed by an automated liquid chromatography electrospray ionization tandem mass spectrometer (LC-ESI-MS/MS) with an UltiMate 3000 RSLCnano system on-line coupled to a Q Exactive mass spectrometer via a Nanospray Flex ion source (Thermo Fisher Scientific, Hvidovre, Denmark) as described elsewhere (Kjeldal et al. 2014a). The following modifications were made: survey scans were measured at 350-1850 m/z and a dynamic exclusion of 45 sec was used for minimizing repetitive selection of the same ions and normalized collision energy was set to 35. Peptides were eluted using 148 minute linear gradient, ranging from 13-50% (v/v) of solvent consisting of 0.1% (v/v) formic acid, 0.005% (v/v) HFBA, and 90% (v/v) acetonitrile.

8.4.5 Label-free quantification

Raw data files from the Q Exactive instrument were processed with MaxQuant v.1.5.1.2 (Max Planck Institute of Biochemistry, Martinsried, Germany; Cox and Mann 2008) as previously described (Chapter 7). The raw data was compared to a sequence database retrieved from UniProt (downloaded October 21, 2014) which was comprised of the predicted open reading frames (ORFs) of *Rhodococcus* sp. EsD8.

Differences in protein abundances between control and treated (with E2) were statistically evaluated using a Student's t-test with the statistical significance set at $p \leq 0.05$ (n=5). Protein abundances are represented as $\log_2$ transformed LFQ values and are reported for all proteins having at least two quantifiable unique peptides in at least three LC−MS runs.

8.4.6 Functional annotation of proteins

Quantified proteins were compared to a database containing all proteins with a Kyoto Encyclopedia of Genes and Genomes (KEGG) orthology (KO) identifier as previously described (Chapter 7).

8.4.7 Pathway prediction of E2

The E2 SMILES (simplified molecular-input line-entry system) line notation (CC12CCC3C(C1CCC2O)CCC4=C3C=CC(=C4)O) was submitted to the EAWAG biocatalysis/biodegradation database pathway prediction system (EAWAG-BBD PPS, http://eawag-bbd.ethz.ch/predict/) (Gao et al. 2010).

8.4.8 Sample preparation for metabolomics

Samples for metabolomic analysis were collected from log-phase growth *Rhodococcus* sp. EsD8 cultures that were actively degrading E2. *Rhodococcus* sp. EsD8 was inoculated into R2B containing either 0.5 or 2 mg/L E2 by transferring a single colony from solid media. The bacteria were grown at 100 rpm and 28ºC. Samples were preserved by adding an equal volume of acetonitrile, vortexing, and centrifuging (10 min, 10,000 ×g) to remove particles. Decanted samples were stored at 4ºC in glass vials until concentrated for use. Samples were prepared as described elsewhere with minor modifications (Wissenbach et al. 2011). To concentrate, 1 mL of the sample was evaporated after centrifugation at 10,000×g, under a gentle stream of nitrogen while at 60ºC. The residue was resuspended in 50 µL of mobile phase A/B (1:1;v:v (A) 10 mM ammonium formate in acetonitrile with 0.1% (v/v) formic acid and (B) acetonitrile with 0.1% (v/v) formic acid.

8.4.9 LC-MS/MS analyses for metabolomics

An Ultra High Definition (UHD) Accurate-Mass Quadrupole Time-of-Flight (Q-TOF) coupled with an ultra-HPLC system (Agilent Technologies, Inc.; Santa Clara, CA, USA) was used to determine the presence of E2 and the corresponding metabolites as previously described (Chapter 7).

8.5 Results and discussion

8.5.1 Whole genome sequencing

Whole genome sequencing of *Rhodococcus* sp. EsD8 was completed to provide an organism-specific genomic template for the MS-based label-free quantitative proteomics. The assembly of the *Rhodococcus* sp. EsD8 genome yielded a total of 287 contigs with a total of 12,485,236 reads, a fold coverage of 206.7, a mean read length of 109.75 bp, and an N50 contig length of 45.5 Kb. The draft genome was incomplete, included 6,627,377 bases (6.6 Mb), and was comprised of 6200 predicted coding sequences (CDS), with a GC content of 70%. The GC content is within the expected range for high GC gram positive bacteria, and is similar to other *Rhodococcus* species. The genome size falls within the typical range for bacteria, and the number of CDS correlates well to the genome size (Madigan et al. 2012).

Out of the 6200 CDS, RAST was able to predict the function of 3872 (62%) with a variety of different functions predicted, indicating that *Rhodococcus* sp. EsD8 was a versatile bacterium. This percentage of genes with a predicted function is normal for sequenced bacteria (Madigan et al. 2012). Also, 177 out of 206 (86%) bacterial essential genes proposed by Gil et al. were identified in the genome, suggesting that the genome is mostly complete (Table 8.3, supplemental) (Gil et al. 2004). Several of the CDS of *Rhodococcus* sp. EsD8 with predicted functions encoded for proteins related to metabolism of aromatic compounds (100 genes), resistance to antibiotics and toxic compounds (63 genes), and stress response (126 genes).

8.5.2 Metabolite identification

The parent compound (E2) and one metabolite (E1; estrone) were detected during metabolite analysis (Table 8.1) based on their retention time and their mass-to-charge ratios. E1 accumulated over time (Figure 8.1) and no other metabolites were detected. When the proteins were harvested for proteome analysis the concentration of E1 present was 1.55 ± 0.06 mg/L (n=5) (Figure 8.1). Therefore, this study examined the differential protein expression of *Rhodococcus* sp. EsD8 while actively degrading E2 and exposed to E1.

Table 8.1. Identified E2 metabolites from E2 degradation by *Rhodococcus* sp. EsD8.

Identified BPA metabolites		Retention time (min)	m/z
E2	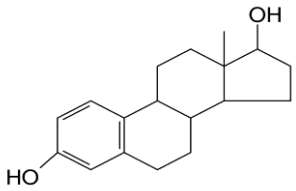	19.1	271.16980
E1 (estrone)	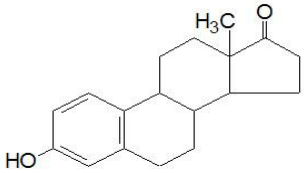	19.8	269.15415

8.5.3 Label-free quantitative MS-based proteomics of Rhodococcus sp. EsD8

Proteins extracted from the five biological replicates of *Rhodococcus* sp. EsD8 grown in the presence and absence of E2 were subjected to shotgun-up proteomics and label-free quantification. A total of 2724 proteins were identified. This corresponded to approximately 44% of the predicted CDS of *Rhodococcus* sp. EsD8. Of the 2724 proteins, 2186 were quantified and 964 had abundances that were significantly different between the E2 exposed culture and the control ($p \leq 0.05$). A total of 590 had a more than twofold (i.e. $-1.0 \leq \log_2$ (fold abundance) ≥ 1.0, $p \leq 0.05$) difference in abundance between the E2 exposed and control culture protein extracts, as shown by the shaded regions of Figure 8.2; 390 proteins were upregulated in the cells exposed to E2 and E1, while 200 proteins were downregulated in the presence of E2 and E1.

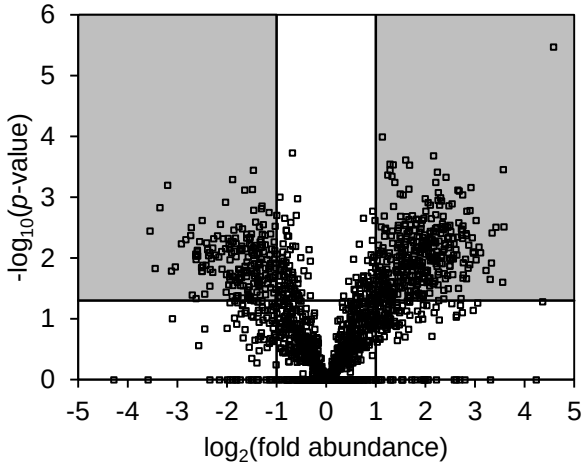

Figure 8.2. Volcano plot of cytosolic quantified proteins. Statistically significant ($p \leq 0.05$, n=5) differentially abundant proteins ($-1 \leq \log_2$ (fold abundance) ≥ 1) are shaded gray.

8.5.4 Functional annotation of proteins

Proteins were compared to all proteins with KO identifiers. 234 of the 390 upregulated proteins were similar to proteins with KO identifiers. These proteins were annotated to the following categories: metabolism, genetic information processing, environmental information processing, cellular processes, organismal systems, and human diseases (Figure 8.3). 129 of the 200 downregulated proteins matched to proteins with KO identifiers. These proteins were annotated to the following categories: metabolism, genetic information processing, environmental information processing, cellular processes, organismal systems, and human diseases (Figure 8.3).

The xenobiotic biodegradation and metabolism orthology as well as the endocrine system orthology were considered of particular relevance to elucidating genes involved with E2 degradation. The level of homology between the proteins with xenobiotic biodegradation and metabolism functions and the entries in the KO database varied, ranging from moderate (28% sequence identity) to high (95% sequence identity) (Table 8.4, supplemental). When a characterization was identified these were dehydrogenases, hydrolases, hydratases, a hydroxylase, a dioxygenase, an oxidase, an oxidoreductase, thiolases, a phosphoribosyltransferase, and an epimerase (Table 8.4, supplement). In the presence of E2, the concentrations of the proteins matched to proteins with xenobiotic biodegradation and metabolism functions were two-to-twelve-fold higher ($\log_2$ of 1.1 to 5.7) than in the unexposed control. The level of homology between the proteins annotated to endocrine system and the entries in the KO database varied, ranging from moderate (64% sequence identity) to high (92% sequence identity) (Table 8.5, supplemental). The presence of E2 resulted in a two-to-six-fold increased abundance ($\log_2$ of 1.1 to 2.9) of these proteins.

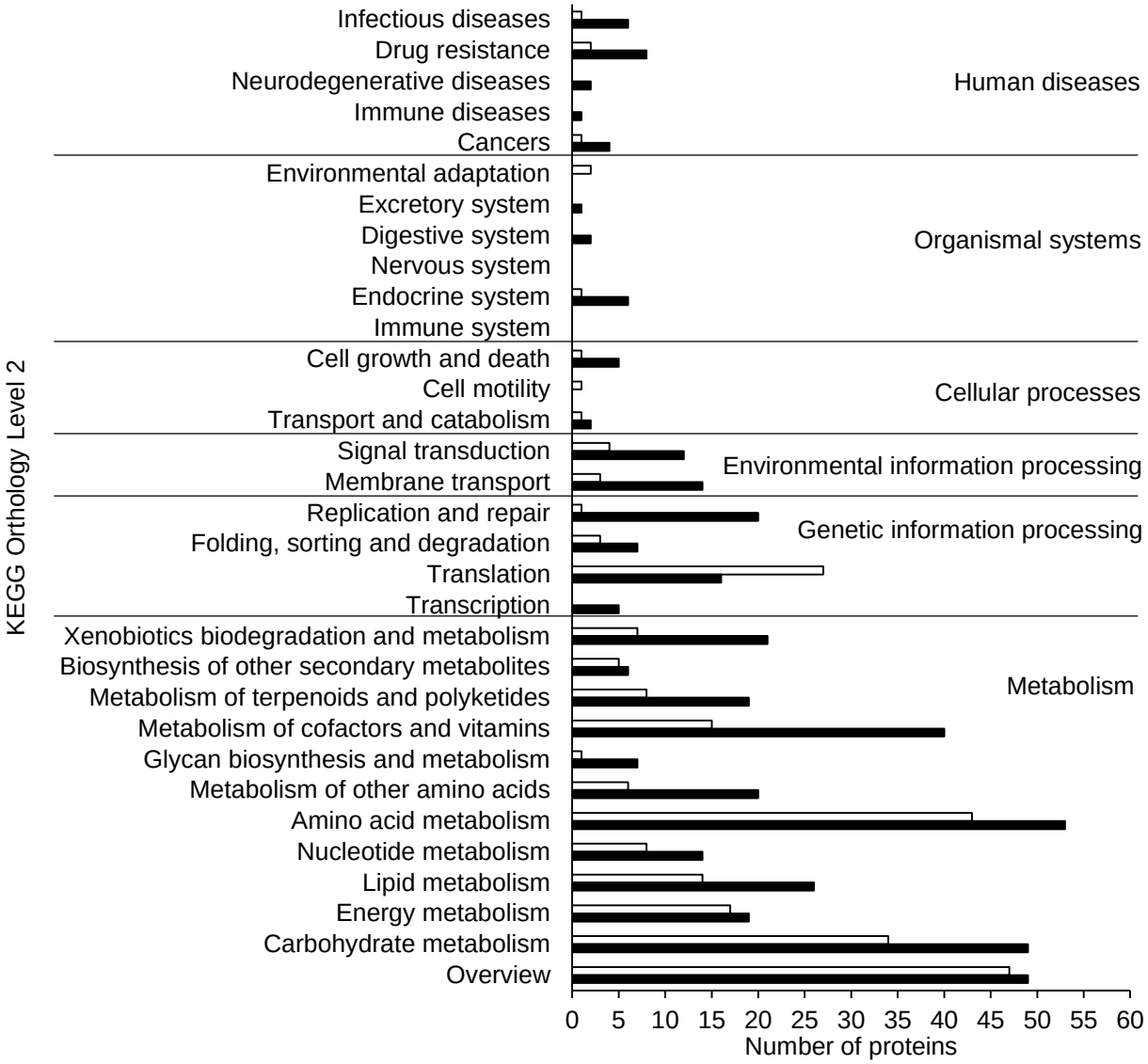

Figure 8.3. Orthological assignment of upregulated (black bars) and downregulated (white bars) proteins of *Rhodococcus* sp. EsD8 in response to 17β-estradiol.

Protein response following exposure of *Rhodococcus* sp. EsD8 to E2 and E1 suggested that multiple biochemical processes within the cell were impacted. It resulted in the upregulation of many proteins associated with amino acid metabolism (53 proteins) and carbohydrate metabolism (49 proteins, Figure 8.3). This may be a stress response of the organism to the exposure of these contaminants (Mccorquodale and Mueller 1958; Banaei-Asl et al. 2015). A protein annotated as a 'universal stress protein family' (N1MEE1) was highly upregulated ($\log_2$ of 2.6). Also, many proteins functionally annotated to fatty acid degradation were upregulated in the presence of E2 and E1 (N1M7P8, N1MEW5, N1M3N7, N1MI73, N1MBR5, N1M4Q9, N1LZP5, N1M6D1, N1LYI8, N1M624, N1M2Y7, and N1LX53). Previous studies

have found that E2 increases the abundance of acyl-CoA dehydrogenase and affects enzymes required for fatty acid beta-oxidation (Nemoto et al. 2000; Maher et al. 2010). This suggests that E2 may be partially responsible for regulating lipid metabolism in *Rhodococcus* sp. EsD8.

8.5.5 E2 transformation and associated degradation genes

The transformation pathway of E2 was predicted using the online prediction tool EAWAG-BBD PPS. The transformation of E2 to E1 involves an oxidation. Enzyme classes predicted to be involved in this transformation (EC 1.1.-.-, 1.14.13.-, and 1.14.12.12) were compared to the proteins upregulated in *Rhodococcus* sp. EsD8 (Table 8.2). One of the upregulated proteins with a high percent identity match (78%) to enzymes predicted to be involved in the transformation of E2 to E1 (N1M7J5, Table 8.2), also matched to an oxidoreductase with a KO identifier related to steroid biosynthesis (K05917).

Rhodococcus sp. EsD8 enzymes were compared to enzymes in the enzyme classes 1.1.1.50, 1.1.1.51, 1.1.1.64, and 1.1.1.159 and enzymes with 100% identity matches are reported in Table 8.6. 3α-hydroxysteroid dehydrogenases (EC 1.1.1.50) were previously identified as able to grow on steroids and aromatic hydrocarbons and may be involved in the biodegradation of these compounds (Xiong et al. 2009). The encoding gene *hsdA* was also induced several fold in the presence of steroids (Xiong et al. 2009). These proteins were identified in a variety of organisms including *Comamonas testosteroni* (Hwang et al. 2005), *Pseudomonas* sp. (Gao et al. 1998), *Eubacterium* sp. (Mallonee et al. 1995), though not in the *Rhodococcus* genus to the best of the author's knowledge. Seven genes were identified in the genome of *Rhodococcus* sp. EsD8 encoding for enzymes with 100% identity matches to the enzyme class 1.1.1.50 (Table 8.6). Four of these proteins were also detected in the proteome, and one had a statistically significant change in abundance in response to the presence/absence of E2. Two genes encoding for proteins putatively named 3α-hydroxysteroid dehydrogenase were identified in the genome and detected in the proteome (N1MC85 and N1MZ02). N1MZ02 was also statistically significant in the proteome. N1MC85 and N1MZ02 had identity matches of 36.84 and 63.7%, respectively, to proteins in the enzyme class 1.1.1.50.

3,17β-hydroxysteroid dehydrogenases (EC 1.1.1.51) were previously identified as involved in the transformation of E2 to E1. Eight genes were identified in the genome of *Rhodococcus* sp. EsD8 encoding for enzymes with 100% identity matches to the enzyme class 1.1.1.51 (Table 8.6). One of these proteins was also detected in the proteome, though none had a statistically significant change in abundance in response to the presence/absence of E2. A gene encoding for a protein putatively named 3-β hydroxysteroid dehydrogenase/isomerase family protein was identified in the genome and statistically

significant in the proteome (N1M3Q1). It had an identity match of 29.81% to proteins in the enzyme class 1.1.1.51. Five types of 17β-hydroxysteroid dehydrogenase (17β-HSD) were found in humans and monkey, with Type 1 catalyzing the formation of E2 from E1 and Type 2 responsible for the degradation of E2 to E1 (Labrie et al. 1997). 17β-HSD was also found to transform E2 to E1 in humans and rats (Biswas and Russell 1997). These proteins were identified in a variety of organisms including *Comamonas testosteroni* (Benach et al. 2002) and *Clostridium innocuum* (Stokes and Hylemon 1985), though not in the *Rhodococcus* genus to the best of the author's knowledge. A *tetR* gene was identified in *Comamonas testosteroni* downstream of the 3,17β-HSD gene and knock-out experiments determined that *tetR* was a regulator of steroid metabolism (Pan et al. 2015). Many proteins in the TetR family were identified in the proteome (62 proteins), with six statistically significant, three upregulated in the presence of E2 and E1 (N1M6X6, N1MDU8, and N1MAF0), and one downregulated (N1MBR4).

Testosterone 17β-dehydrogenase (EC 1.1.1.64) were previously identified as involved steroid degradation. These proteins were identified in a variety of organisms including humans, rats, and dogs (Poirier 2003), though not in the *Rhodococcus* genus to the best of the author's knowledge. Four genes were identified in the genome of *Rhodococcus* sp. EsD8 encoding for enzymes with 100% identity matches to the enzyme class 1.1.1.64 (Table 8.6). Two of the proteins were detected in the proteome and one had a statistically significant change in abundance in response to the presence/absence of E2.

7α-hydroxysteroid dehydrogenases (EC 1.1.1.159) were previously identified as involved in the transformation of E2 to E1. A putative 7α-HSD was identified in *Comamonas testosteroni* and reduced E2 degradation was seen in by a mutant without the 7α-HSD gene (Ji et al. 2014). These proteins were identified in a variety of organisms including *Bacteroides intestinalis* (Fukiya et al. 2009), *Stenotrophomonas maltophilia* (Pedrini et al. 2006), though not in the *Rhodococcus* genus to the best of the author's knowledge. Twenty-nine (29) genes were identified in the genome of *Rhodococcus* sp. EsD8 encoding for enzymes with 100% identity matches to the enzyme class 1.1.1.159 (Table 8.6). Twelve of the proteins were detected in the proteome, four had a statistically significant change in abundance in response to the presence/absence of E2, and three were upregulated.

Other enzymes putatively involved in E2 degradation include short-chain dehydrogenase/reductases (Zhang et al. 2015) and catechol 2,3-dioxygenases (Hu et al. 2011). Short-chain dehydrogenases/reductases are involved in metabolism of many hormones and xenobiotics and this superfamily includes 3α-hydroxysteroid dehydrogenases and 7α-hydroxysteroid dehydrogenases (Zhang et al. 2015). A gene encoding for a putative short-chain dehydrogenase/reductase was identified in the

genome (N1M3D0). It had an identity match of 31.11% to a protein in the enzyme class 1.1.1.159. A gene encoding for a catechol 2,3-dioxygenase (N1M650) was identified in the genome. Another enzyme in the catechol pathway was also detected and statistically significant in the proteome (N1M6L1, 2-keto-4-pentenoate hydratase/2-oxohepta-3-ene-1,7,dioic acid hydratase).

Table 8.2. Identification of proteins upregulated in *Rhodococcus* sp. EsD8 matching to enzymes predicted to be involved in the transformation of E2 to E1 from the EAWAG-BBD PPS in the enzyme classes 1.1.-.-., 1.14.13.- ., and 1.14.12.12.

Rhodococcus sp. EsD8 proteins			Sequence similarity		Predicted or previously identified proteins	
UniProtKB accession number	Protein name assigned in genome annotation	log2 (fold abundance)	Greatest identity %	Greatest bit score	Accession number	Functional description
Enzyme classes 1.1.-.-., 1.14.13.-., and 1.14.12.12						
N1M5S9	Glycerol-3-phosphate dehydrogenase	1.4	81	819	P64184	Glycerol-3-phosphate dehydrogenase
N1M7J5	Cytochrome P450	1.8	78	663	P0A512	Lanosterol 14-alpha demethylase

8.6 Conclusions

In this study, the transformation of E2 to E1 by *Rhodococcus* sp. EsD8 was investigated using three different tiers of biochemistry (genome, proteome, and metabolome). Insight was provided into the transformation of E2 to E1, and many genes encoding for enzymes similar to those previously determined to be responsible for E2 transformation were identified. These enzymes have not been previously identified in the *Rhodococcus* genus. This may provide insight into the evolution of these transformation genes. The impact of E2 and E1 exposure on the proteome of *Rhodococcus* sp. EsD8 also significantly impacted multiple biochemical processes within the cell, including lipid metabolism to a large degree. While removal of both E2 and E1 is desired during wastewater treatment, this study identified potential proteins involved in the transformation of E2 to E1, which could then be further degraded by other microorganisms. These proteins could also potentially be used as biomarkers to identify additional bacteria capable of transforming E2 during wastewater treatment.

8.7 Acknowledgements

This work was funded by the Danish Research Council for Strategic Research via the Research Centre "EcoDesign-MBR" (Grant No. 26-03-0250) and the National Science Foundation (NSF CBET-0829132). Support was provided to N.A. Zhou by the Valle Scholarship and Scandinavian Exchange and the King County Technology Transfer Fellowship Programs at the University of Washington.

8.8 Supplementary Information

Table 8.3. Summary of essential genes in *Rhodococcus* sp. EsD8

Genes from Gil et al. 2004		Genes from this study		
Gene	Protein function	UniProt accession number	Gene	UniProt protein name
dnaB	Replicative DNA helicase	-	-	-
dnaE	DNA polymerase III, alpha subunit	-	-	-
dnaG	DNA primase	N1MID9	EBESD8_60050	DNA primase (EC 2.7.7.-)
dnaN	DNA polymerase III, beta subunit	N1M205	EBESD8_15100	DNA polymerase III subunit beta (EC 2.7.7.7)
dnaQ	DNA polymerase III, epsilon subunit	N1LY69	EBESD8_6530	DNA polymerase III epsilon subunit (EC 2.7.7.7)
dnaX	DNA polymerase III, gamma and tau subunits	N1ME68	EBESD8_45160	DNA polymerase III subunits gamma and tau (EC 2.7.7.7)
gyrA	DNA gyrase, A subunit	N1M221	EBESD8_15250	DNA gyrase subunit A (EC 5.99.1.3)
gyrB	DNA gyrase, B subunit	N1M6Q1	EBESD8_15170	DNA gyrase subunit B (EC 5.99.1.3)
holA	DNA polymerase III, delta subunit	N1M1K2	EBESD8_12150	DNA polymerase III delta subunit (EC 2.7.7.7)
holB	DNA polymerase III, delta prime subunit	N1M7Q5	EBESD8_34460	DNA polymerase III delta prime subunit (EC 2.7.7.7)
hupA	DNA binding protein	-	-	-
lig	DNA ligase (NAD dependent)	N1MEA5	EBESD8_42360	DNA ligase (EC 6.5.1.2) (Polydeoxyribonucleotide synthase [NAD(+)])
ssb	SSB	N1M3V7	EBESD8_7450	Single-stranded DNA-binding protein (SSB)
nth	Endonuclease III	N1MBU2	EBESD8_53150	Endonuclease III (EC 4.2.99.18) (DNA-(apurinic or apyrimidinic site) lyase)
polA	5'-3' exonuclease domain of DNA polymerase I	-	-	-
ung	Uracil-DNA glycosylase	N1MAD8	EBESD8_28070	Uracil-DNA glycosylase (UDG) (EC 3.2.2.27)
deaD	ATP-dependent RNA helicase	N1M657	EBESD8_29400	ATP-dependent RNA helicase DeaD (EC 3.6.4.13) (Cold-shock DEAD box protein A)
greA	Transcription elongation factor	N1MCF5	EBESD8_35810	Transcription elongation factor GreA (Transcript cleavage factor GreA)
nusA	Transcription-translation coupling	N1M520	EBESD8_25670	Transcription termination/antitermination protein NusA
nusG	Transcription antitermination protein	N1MCF8	EBESD8_37890	Transcription termination/antitermination protein NusG

. . . . . .

Table 8.3. (continued)

Genes from Gil et al. 2004		Genes from this study		
Gene	Protein function	UniProt accession number	Gene	UniProt protein name
rpoA	RNA polymerase, alpha subunit	N1MIQ9	EBESD8_58200	DNA-directed RNA polymerase subunit alpha (RNAP subunit alpha) (EC 2.7.7.6) (RNA polymerase subunit alpha) (Transcriptase subunit alpha)
rpoB	RNA polymerase, beta subunit	N1M3H1	EBESD8_3860	DNA-directed RNA polymerase subunit beta (RNAP subunit beta) (EC 2.7.7.6) (RNA polymerase subunit beta) (Transcriptase subunit beta)
rpoC	RNA polymerase, beta prime subunit	N1M2S6	EBESD8_3850	DNA-directed RNA polymerase subunit beta' (RNAP subunit beta') (EC 2.7.7.6) (RNA polymerase subunit beta') (Transcriptase subunit beta')
rpoD	RNA polymerase, major sigma subunit	-	-	-
alaS	Alanyl-tRNA synthase	N1MD59	EBESD8_57520	Alanine--tRNA ligase (EC 6.1.1.7) (Alanyl-tRNA synthetase)
argS	Arginyl-tRNA synthase	N1MAH5	EBESD8_48730	Arginine--tRNA ligase (EC 6.1.1.19) (Arginyl-tRNA synthetase)
asnS	Asparaginyl-tRNA synthase	-	-	-
aspS	Aspartyl-tRNA synthase	N1LWS8	EBESD8_1880	Aspartyl-tRNA synthetase @ Aspartyl-tRNA(Asn) synthetase (EC 6.1.1.12) (EC 6.1.1.23)
cysS	Cysteinyl-tRNA synthase	N1MJF9	EBESD8_61200	Cysteine--tRNA ligase (EC 6.1.1.16) (Cysteinyl-tRNA synthetase)
glnS	Glutaminyl-tRNA synthase	-	-	-
gltX	Glutamyl-tRNA synthase	N1M0C9	EBESD8_14110	Glutamate--tRNA ligase (EC 6.1.1.17) (Glutamyl-tRNA synthetase)
glyS	Glycyl-tRNA synthase, b subunit	N1MBB2	EBESD8_47320	Glycine--tRNA ligase (EC 6.1.1.14) (Glycyl-tRNA synthetase)
hisS	Histidyl-tRNA synthase	N1MCI2	EBESD8_38280	Histidine--tRNA ligase (EC 6.1.1.21) (Histidyl-tRNA synthetase)
ileS	Isoleucyl-tRNA synthase	N1M5K1	EBESD8_11040	Isoleucine--tRNA ligase (EC 6.1.1.5) (Isoleucyl-tRNA synthetase)
leuS	Leucyl-tRNA synthase	N1M292	EBESD8_14680	Leucine--tRNA ligase (EC 6.1.1.4) (Leucyl-tRNA synthetase)
lysS	Lysyl-tRNA synthase	N1LWF5	EBESD8_820	Lysine--tRNA ligase (EC 6.1.1.6) (Lysyl-tRNA synthetase)
metS	Methionyl-tRNA synthase	N1MAW2	EBESD8_50390	Methionine--tRNA ligase (EC 6.1.1.10) (Methionyl-tRNA synthetase)

. . . . . .

Table 8.3. (continued)

Genes from Gil et al. 2004		Genes from this study		
Gene	Protein function	UniProt accession number	Gene	UniProt protein name
pheS	Phenylalanyl-tRNA synthase, a subunit	N1M4E1	EBESD8_22220	Phenylalanine--tRNA ligase alpha subunit (EC 6.1.1.20) (Phenylalanyl-tRNA synthetase alpha subunit)
pheT	Phenylalanyl-tRNA synthase, b subunit	N1M8Q2	EBESD8_22210	Phenylalanine--tRNA ligase beta subunit (EC 6.1.1.20) (Phenylalanyl-tRNA synthetase beta subunit)
proS	Prolyl-tRNA synthase	N1M526	EBESD8_25720	Proline--tRNA ligase (EC 6.1.1.15) (Prolyl-tRNA synthetase)
serS	Seryl-tRNA synthase	N1MAK6	EBESD8_49090	Serine--tRNA ligase (EC 6.1.1.11) (Seryl-tRNA synthetase) (Seryl-tRNA(Ser/Sec) synthetase)
thrS	Threonyl-tRNA synthase	N1MB83	EBESD8_47060	Threonine--tRNA ligase (EC 6.1.1.3) (Threonyl-tRNA synthetase)
trpS	Tryptophanyl-tRNA synthase	N1M786	EBESD8_33230	Tryptophan--tRNA ligase (EC 6.1.1.2) (Tryptophanyl-tRNA synthetase)
tyrS	Tyrosyl-tRNA synthase	N1M2S7	EBESD8_22080	Tyrosine--tRNA ligase (EC 6.1.1.1) (Tyrosyl-tRNA synthetase)
valS	Valyl-tRNA synthase	N1M542	EBESD8_24930	Valine--tRNA ligase (EC 6.1.1.9) (Valyl-tRNA synthetase)
iscS	Cysteine desulfurase-NifS homolog	-	-	-
mnmA	tRNA (5-methylaminomethyl-2-thiouridylate) methyl-transferase	N1M5B2	EBESD8_10240	tRNA-specific 2-thiouridylase MnmA (EC 2.8.1.-)
mnmE	GTP binding protein involved in biosynthesis of 5-methilaminomethyl-2-thiouridine	-	-	-
mnmG	Glucose-inhibited division protein A, involved in bio-synthesis of 5-methylaminomethyl-2-thiouridine	-	-	-
pth	Peptidyl-tRNA hydrolase	N1MAZ7	EBESD8_30370	Peptidyl-tRNA hydrolase (PTH) (EC 3.1.1.29)
rnpA	Protein component of Rna P	N1M5V7	EBESD8_15060	Ribonuclease P protein component (RNase P protein) (RNaseP protein) (EC 3.1.26.5) (Protein C5)
rplA	50S ribosomal protein L1	N1M8P0	EBESD8_37910	50S ribosomal protein L1
rplB	50S ribosomal protein L2	N1MHX6	EBESD8_57940	50S ribosomal protein L2

. . . . . .

Table 8.3. (continued)

Genes from Gil et al. 2004		Genes from this study		
Gene	Protein function	UniProt accession number	Gene	UniProt protein name
rplC	50S ribosomal protein L3	N1MEL4	EBESD8_57910	50S ribosomal protein L3
rplD	50S ribosomal protein L4	N1MDA9	EBESD8_57920	50S ribosomal protein L4
rplE	50S ribosomal protein L5	N1ME70	EBESD8_58030	50S ribosomal protein L5
rplF	50S ribosomal protein L6	N1MEM5	EBESD8_58060	50S ribosomal protein L6
rplI	50S ribosomal protein L9	N1M083	EBESD8_7470	50S ribosomal protein L9
rplJ	50S ribosomal protein L10	N1M8L9	EBESD8_37930	50S ribosomal protein L10
rplK	50S ribosomal protein L11	N1MD23	EBESD8_37900	50S ribosomal protein L11
rplL	50S ribosomal protein L12	N1MCG1	EBESD8_37940	50S ribosomal protein L7/L12
rplM	50S ribosomal protein L13	N1M2F4	EBESD8_16570	50S ribosomal protein L13
rplN	50S ribosomal protein L14	N1MeEM3	EBESD8_58010	50S ribosomal protein L14
rplO	50S ribosomal protein L15	N1MIQ3	EBESD8_58100	50S ribosomal protein L15
rplP	50S ribosomal protein L16	N1ME67	EBESD8_57980	50S ribosomal protein L16
rplQ	50S ribosomal protein L17	N1MEN8	EBESD8_58210	50S ribosomal protein L17
rplR	50S ribosomal protein L18	N1MDC2	EBESD8_58070	50S ribosomal protein L18
rplS	50S ribosomal protein L19	N1MBJ3	EBESD8_48440	50S ribosomal protein L19
rplT	50S ribosomal protein L20	N1M442	EBESD8_22240	50S ribosomal protein L20
rplU	50S ribosomal protein L21	N1M537	EBESD8_24880	50S ribosomal protein L21
rplV	50S ribosomal protein L22	N1MEL8	EBESD8_57960	50S ribosomal protein L22
rplW	50S ribosomal protein L23	N1ME65	EBESD8_57930	50S ribosomal protein L23
rplX	50S ribosomal protein L24	N1MDB7	EBESD8_58020	50S ribosomal protein L24
rpmA	50S ribosomal protein L27	N1M9F0	EBESD8_24870	50S ribosomal protein L27
rpmB	50S ribosomal protein L28	N1M4H3	EBESD8_28090	50S ribosomal protein L28
		N1MGK1	EBESD8_50820	50S ribosomal protein L28
rpmC	50S ribosomal protein L29	N1MHY0	EBESD8_57990	50S ribosomal protein L29
rpmE	50S ribosomal protein L31	N1MG03	EBESD8_48660	50S ribosomal protein L31
rpmF	50S ribosomal protein L32	N1MB06	EBESD8_50790	50S ribosomal protein L32
		N1M518	EBESD8_11630	50S ribosomal protein L32
rpmG	50S ribosomal protein L33	N1MD20	EBESD8_37850	50S ribosomal protein L33
		N1MCC8	EBESD8_50830	50S ribosomal protein L33
rpmH	50S ribosomal protein L34	N1M6P0	EBESD8_15070	50S ribosomal protein L34
rpmI	50S ribosomal protein L35	N1M7Y3	EBESD8_22250	50S ribosomal protein L35
rpmJ	50S ribosomal protein L36	N1MEN3	EBESD8_58160	50S ribosomal protein L36
rpsB	30S ribosomal protein S2	N1M5E7	EBESD8_26000	30S ribosomal protein S2
rpsC	30S ribosomal protein S3	N1MDB2	EBESD8_57970	30S ribosomal protein S3
rpsD	30S ribosomal protein S4	N1MHZ7	EBESD8_58190	30S ribosomal protein S4
rpsE	30S ribosomal protein S5	N1ME74	EBESD8_58080	30S ribosomal protein S5
rpsF	30S ribosomal protein S6	N1LZX3	EBESD8_7440	30S ribosomal protein S6

. . . . . .

Table 8.3. (continued)

Genes from Gil et al. 2004		Genes from this study		
Gene	Protein function	UniProt accession number	Gene	UniProt protein name
rpsG	30S ribosomal protein S7	N1M8B4	EBESD8_20910	30S ribosomal protein S7
rpsH	30S ribosomal protein S8	N1MIP8	EBESD8_58050	30S ribosomal protein S8
rpsI	30S ribosomal protein S9	N1M6C7	EBESD8_16580	30S ribosomal protein S9
rpsJ	30S ribosomal protein S10	N1MIN9	EBESD8_57900	30S ribosomal protein S10
rpsK	30S ribosomal protein S11	N1ME80	EBESD8_58180	30S ribosomal protein S11
rpsL	30S ribosomal protein S12	N1M7G4	EBESD8_20900	30S ribosomal protein S12
rpsM	30S ribosomal protein S13	N1MDD2	EBESD8_58170	30S ribosomal protein S13
rpsN	30S ribosomal protein S14	N1MB13	EBESD8_50840	30S ribosomal protein S14
rpsO	30S ribosomal protein S15	N1MJ27	EBESD8_62340	30S ribosomal protein S15
rpsP	30S ribosomal protein S16	N1M180	EBESD8_11920	30S ribosomal protein S16
rpsQ	30S ribosomal protein S17	N1MIP6	EBESD8_58000	30S ribosomal protein S17
rpsR	30S ribosomal protein S18	N1MC59	EBESD8_50850	30S ribosomal protein S18
		N1M4I7	EBESD8_7460	30S ribosomal protein S18
rpsS	30S ribosomal protein S19	N1MIP1	EBESD8_57950	30S ribosomal protein S19
rpsT	30S ribosomal protein S20	N1LZV3	EBESD8_12160	30S ribosomal protein S20
cspR	Ribosomal methytransferase	-	-	-
engA	GTP binding protein	-	-	-
era	GTP binding protein	N1MB94	EBESD8_47190	GTPase Era
ksgA	Dimethyladenosine transferase	N1M6N6	EBESD8_30530	Ribosomal RNA small subunit methyltransferase A (EC 2.1.1.182) (16S rRNA (adenine(1518)-N(6)/adenine(1519)-N(6))-dimethyltransferase) (16S rRNA dimethyladenosine transferase) (16S rRNA dimethylase) (S-adenosylmethionine-6-N', N'-adenosyl(rRNA) dimethyltransferase)
obg	GTP binding protein	N1M8L5	EBESD8_24860	GTPase Obg (GTP-binding protein Obg)
rbfA	Ribosome binding factor A	N1LYX2	EBESD8_2870	Ribosome-binding factor A
ychF	GTP binding protein	N1M6B2	EBESD8_16430	Ribosome-binding ATPase YchF
efp	Elongation factor P	N1M969	EBESD8_26510	Elongation factor P (EF-P)
fusA	Elongation factor G	N1M407	EBESD8_20920	Elongation factor G (EF-G)
frr	Ribosome-recycling factor	N1M556	EBESD8_25970	Ribosome-recycling factor (RRF) (Ribosome-releasing factor)

. . . . . .

Table 8.3. (continued)

Genes from Gil et al. 2004		Genes from this study		
Gene	Protein function	UniProt accession number	Gene	UniProt protein name
hemK	N5-glutamine methyltransferase, modulation of release factor activity	N1MBP3	EBESD8_48620	Release factor glutamine methyltransferase (RF MTase) (EC 2.1.1.297) (N5-glutamine methyltransferase PrmC) (Protein-(glutamine-N5) MTase PrmC) (Protein-glutamine N-methyltransferase PrmC)
infA	Initiation factor IF-1	N1MIQ5	EBESD8_58150	Translation initiation factor IF-1
infB	Initiation factor IF-2	N1LYH1	EBESD8_2890	Translation initiation factor IF-2
infC	Initiation factor IF-3	N1M8Q8	EBESD8_22260	Translation initiation factor IF-3
lepA	GTP binding elongation factor	N1M590	EBESD8_12230	Elongation factor 4 (EF-4) (EC 3.6.5.n1) (Ribosomal back-translocase LepA)
prfA	Peptide chain release factor 1 (RF1)	N1MF93	EBESD8_48650	Peptide chain release factor 1 (RF-1)
smpB	tmRNA binding protein	N1M8D5	EBESD8_36820	SsrA-binding protein (Small protein B)
tsf	Elongation factor Ts	N1M9Q7	EBESD8_25990	Elongation factor Ts (EF-Ts)
tufA	Elongation factor Tu	N1M2E2	EBESD8_20930	Elongation factor Tu (EF-Tu)
pnp	Polyribonucleotide nucleotidyltransferase	N1MEL3	EBESD8_62320	Polyribonucleotide nucleotidyltransferase (EC 2.7.7.8) (Polynucleotide phosphorylase)
rnc	Ribonuclease III	N1M1C7	EBESD8_11650	Ribonuclease 3 (EC 3.1.26.3) (Ribonuclease III)
map	Methionine aminopeptidase	N1M540	EBESD8_25820	Methionine aminopeptidase (MAP) (MetAP) (EC 3.4.11.18) (Peptidase M)
		N1M107	EBESD8_10550	Methionine aminopeptidase (MAP) (MetAP) (EC 3.4.11.18) (Peptidase M)
		N1ME77	EBESD8_58130	Methionine aminopeptidase (MAP) (MetAP) (EC 3.4.11.18) (Peptidase M)
pepA	Aminopeptidase A/I	N1MFE4	EBESD8_60820	Probable cytosol aminopeptidase (Leucine aminopeptidase) (Leucyl aminopeptidase)
dnaJ	Hsp70 cochaperone	N1MB67	EBESD8_51350	Chaperone protein DnaJ
		N1M5A0	EBESD8_12380	Chaperone protein DnaJ
dnaK	Chaperone Hsp70	N1MGQ4	EBESD8_51330	Chaperone protein DnaK (HSP70) (Heat shock 70 kDa protein) (Heat shock protein 70)
		N1LWV4	EBESD8_2080	Chaperone protein DnaK (HSP70) (Heat shock 70 kDa protein) (Heat shock protein 70)

. . . . . .

Table 8.3. (continued)

Genes from Gil et al. 2004		Genes from this study		
Gene	Protein function	UniProt accession number	Gene	UniProt protein name
groEL	Class I heat shock protein	N1M7K4	EBESD8_34380	60 kDa chaperonin (GroEL protein) (Protein Cpn60)
		N1MIV6	EBESD8_58850	60 kDa chaperonin (GroEL protein) (Protein Cpn60)
		N1M3W7	EBESD8_7600	60 kDa chaperonin (GroEL protein) (Protein Cpn60)
groES	Class I heat shock protein	N1M675	EBESD8_34370	10 kDa chaperonin (GroES protein) (Protein Cpn10)
grpE	Hsp70 cochaperone	N1LYP2	EBESD8_2070	Protein GrpE (HSP-70 cofactor)
		N1MCI7	EBESD8_51340	Protein GrpE (HSP-70 cofactor)
ffh	Protein component of signal recognition particle	N1M5V0	EBESD8_11890	Signal recognition particle protein (Fifty-four homolog)
ftsY	Signal recognition particle receptor	N1M1F6	EBESD8_11850	Signal recognition particle receptor FtsY (SRP receptor)
secA	Preprotein transloscase subunit (ATPase)	N1MA54	EBESD8_43220	Protein translocase subunit SecA
secE	Membrane-embedded preprotein translocase subunit	N1M8L6	EBESD8_37880	Protein translocase subunit SecE
secY	Membrane-embedded preprotein translocase subunit	N1MEN0	EBESD8_58110	Protein translocase subunit SecY
gcp	Probable O-sialoglycoprotein endopeptidase	-	-	-
hflB	ATP-dependent protease	-	-	-
Ion	ATP-dependent protease La	-	-	-
ftsZ	Cytoskeletal cell division protein	N1M0W9	EBESD8_10970	Cell division protein FtsZ
pitA	Low-affinity inorganic phosphate transporter	N1M202	EBESD8_19580	Probable low-affinity inorganic phosphate transporter
		N1M605	EBESD8_28030	Probable low-affinity inorganic phosphate transporter
ptsG	PTS glucose-specific enzyme II	-	-	-
ptsH	Histidine-containing phosphocarrier protein of PTS	-	-	-
ptsI	PTS enzyme I	N1M198	EBESD8_17110	Phosphoenolpyruvate-protein phosphotransferase (EC 2.7.3.9) (Phosphotransferase system, enzyme I)
eno	Enolase	N1MCE1	EBESD8_37630	Enolase (EC 4.2.1.11) (2-phospho-D-glycerate hydro-lyase) (2-phosphoglycerate dehydratase)
fbaA	Fructose-1,6-bisphosphate aldolase	N1MBI8	EBESD8_52300	Fructose-bisphosphate aldolase class II (EC 4.1.2.13)

. . . . . .

Table 8.3. (continued)

Genes from Gil et al. 2004		Genes from this study		
Gene	Protein function	UniProt accession number	Gene	UniProt protein name
gapA	Glyceraldehyde-3-phosphate dehydrogenase	N1M5N0	EBESD8_26830	Glyceraldehyde-3-phosphate dehydrogenase (EC 1.2.1.-)
		N1M8W2	EBESD8_25630	Glyceraldehyde-3-phosphate dehydrogenase (EC 1.2.1.-)
gpmA	Phosphoglycerate mutase	N1M831	EBESD8_20110	2,3-bisphosphoglycerate-dependent phosphoglycerate mutase (BPG-dependent PGAM) (PGAM) (Phosphoglyceromutase) (dPGM) (EC 5.4.2.11)
ldh	L-lactate dehydrogenase	N1M615	EBESD8_28230	L-lactate dehydrogenase (L-LDH) (EC 1.1.1.27)
pfkA	6-Phosphofructokinase	N1MDM2	EBESD8_42450	6-phosphofructokinase (EC 2.7.1.11)
pgi	Glucose-6-phosphate isomerase	-	-	-
pgk	Phosphoglycerate kinase	N1M456	EBESD8_26840	Phosphoglycerate kinase (EC 2.7.2.3)
pykA	Pyruvate kinase	N1MAX3	EBESD8_45940	Pyruvate kinase (EC 2.7.1.40)
		N1MIL8	EBESD8_57650	Pyruvate kinase (EC 2.7.1.40)
tpiA	Triose-phosphate isomerase	N1M5F9	EBESD8_26850	Triosephosphate isomerase (TIM) (EC 5.3.1.1) (Triose-phosphate isomerase)
atpA	ATP synthase alpha chai	N1MBJ9	EBESD8_48540	ATP synthase subunit alpha (EC 3.6.3.14) (ATP synthase F1 sector subunit alpha) (F-ATPase subunit alpha)
atpB	ATP synthase A chain	N1MAG1	EBESD8_48580	ATP synthase subunit a (ATP synthase F0 sector subunit a) (F-ATPase subunit 6)
atpC	ATP synthase epsilon chain	N1MFZ1	EBESD8_48510	ATP synthase epsilon chain (ATP synthase F1 sector epsilon subunit) (F-ATPase epsilon subunit)
atpD	ATP synthase beta chain	N1MBN2	EBESD8_48520	ATP synthase subunit beta (EC 3.6.3.14) (ATP synthase F1 sector subunit beta) (F-ATPase subunit beta)
atpE	ATP synthase C chain	N1MBN9	EBESD8_48570	ATP synthase subunit c
atpF	ATP synthase B chain	N1MFZ6	EBESD8_48560	ATP synthase subunit b (ATP synthase F(0) sector subunit b) (ATPase subunit I) (F-type ATPase subunit b)
atpG	ATP synthase gamma chain	N1MAF7	EBESD8_48530	ATP synthase gamma chain (ATP synthase F1 sector gamma subunit) (F-ATPase gamma subunit)
atpH	ATP synthase delta chain	N1MF85	EBESD8_48550	ATP synthase subunit delta (ATP synthase F(1) sector subunit delta) (F-type ATPase subunit delta)

. . . . . .

Table 8.3. (continued)

Genes from Gil et al. 2004		Genes from this study		
Gene	Protein function	UniProt accession number	Gene	UniProt protein name
yidc	Essential for proper integration of ATPase into the membrane	N1M0M6	EBESD8_15040	Inner membrane protein translocase component YidC, long form
rpe	Ribulose-phosphate 3-epimerase	N1M5L9	EBESD8_26730	Ribulose-phosphate 3-epimerase (EC 5.1.3.1)
		N1LXS1	EBESD8_370	Ribulose-phosphate 3-epimerase (EC 5.1.3.1)
rpiA	Ribose 5-phosphate isomerase	N1M249	EBESD8_1350	Ribose 5-phosphate isomerase B / Galactose 6-phosphate isomerase (EC 5.3.1.6)
tkt	Transketolase	N1M2Z9	EBESD8_22630	Transketolase (EC 2.2.1.1)
cdsA	Phosphatidate cytidylyltransferase	N1M3X0	EBESD8_25960	Phosphatidate cytidylyltransferase (EC 2.7.7.41)
fadD	Acyl-CoA synthase	-	-	-
gpsA	*sn*-Glycerol-3-phosophate dehydrogenase	N1M191	EBESD8_12020	Glycerol-3-phosphate dehydrogenase [NAD(P)+] (EC 1.1.1.94) (NAD(P)H-dependent glycerol-3-phosphate dehydrogenase)
		N1M8Q6	EBESD8_38200	Glycerol-3-phosphate dehydrogenase [NAD(P)+] (EC 1.1.1.94) (NAD(P)H-dependent glycerol-3-phosphate dehydrogenase)
plsB	*sn*-Glycerol-3-phosophate acyltransferase	N1MHQ7	EBESD8_57340	Glycerol-3-phosphate 1-O-acyltransferase (EC 2.3.1.15)
plsC	1-Acyl-*sn*-glycerol-3-phosphate acyltransferase	N1LZE2	EBESD8_10660	1-acyl-sn-glycerol-3-phosphate acyltransferase (EC 2.3.1.51)
		N1MIH4	EBESD8_57350	1-acyl-sn-glycerol-3-phosphate acyltransferase (EC 2.3.1.51)
		N1M0M9	EBESD8_10220	1-acyl-sn-glycerol-3-phosphate acyltransferase (EC 2.3.1.51)
		N1MBU1	EBESD8_49030	1-acyl-sn-glycerol-3-phosphate acyltransferase (EC 2.3.1.51)
psd	Phosphatidylserine decarboxylase	N1LZZ6	EBESD8_7740	Phosphatidylserine decarboxylase proenzyme (EC 4.1.1.65)
pssA	Phosphatidylserine synthase	-	-	-
adk	Adenylate kinase	N1MDC7	EBESD8_58120	Adenylate kinase (AK) (EC 2.7.4.3) (ATP-AMP transphosphorylase) (ATP:AMP phosphotransferase) (Adenylate monophosphate kinase)
dcd	dCTP deaminase	N1MF41	EBESD8_59960	Deoxycytidine triphosphate deaminase (dCTP deaminase) (EC 3.5.4.13)
gmk	Guanylate kinase	N1M9W9	EBESD8_26620	Guanylate kinase (EC 2.7.4.8) (GMP kinase)

. . . . . .

Table 8.3. (continued)

Genes from Gil et al. 2004		Genes from this study		
Gene	Protein function	UniProt accession number	Gene	UniProt protein name
hpt	Hypoxanthine phosphoribosyltransferase	N1LYA9	EBESD8_960	Hypoxanthine-guanine phosphoribosyltransferase (EC 2.4.2.8)
ndk	Nucleoside diphosphate kinase	N1M4U1	EBESD8_24900	Nucleoside diphosphate kinase (NDK) (NDP kinase) (EC 2.7.4.6) (Nucleoside-2-P kinase)
nrdE	Ribonucleoside diphosphate reductase (major subunit)	N1M897	EBESD8_36420	Ribonucleoside-diphosphate reductase (EC 1.17.4.1)
nrdF	Ribonucleoside diphosphate reductase (minor subunit)	N1MCM0	EBESD8_36410	Ribonucleoside-diphosphate reductase subunit beta (EC 1.17.4.1)
ppa	Inorganic pyrophosphatase	N1M2N4	EBESD8_1000	Inorganic pyrophosphatase (EC 3.6.1.1) (Pyrophosphate phospho-hydrolase)
prsA	Phosphoribosylpyrophospate synthase	N1MAY1	EBESD8_30220	Ribose-phosphate pyrophosphokinase (RPPK) (EC 2.7.6.1) (5-phospho-D-ribosyl alpha-1-diphosphate) (Phosphoribosyl diphosphate synthase) (Phosphoribosyl pyrophosphate synthase)
pyrG	CTP synthase	N1M360	EBESD8_23230	CTP synthase (EC 6.3.4.2) (CTP synthetase) (UTP--ammonia ligase)
thyA	Thymidylate synthase	N1M0P3	EBESD8_10320	Thymidylate synthase (TS) (TSase) (EC 2.1.1.45)
tmk	Thymidylate kinase	N1MEH8	EBESD8_43160	Thymidylate kinase (EC 2.7.4.9) (dTMP kinase)
trxA	Thioredoxin	N1LWU6	EBESD8_2030	Thioredoxin
		N1M7V9	EBESD8_22000	Thioredoxin
		N1M7M9	EBESD8_38860	Thioredoxin
		N1M6N0	EBESD8_14970	Thioredoxin
trxB	Thioredoxin reductase	N1LYN6	EBESD8_2020	Thioredoxin reductase (EC 1.8.1.9)
		N1M5U7	EBESD8_14960	Thioredoxin reductase (EC 1.8.1.9)
		N1MDT8	EBESD8_40900	Thioredoxin reductase (EC 1.8.1.9)
		N1M854	EBESD8_36020	Thioredoxin reductase (EC 1.8.1.9)
		N1M5I7	EBESD8_31900	Thioredoxin reductase (EC 1.8.1.9)
		N1M2Z1	EBESD8_2010	Thioredoxin reductase (EC 1.8.1.9)
		N1M324	EBESD8_4950	Thioredoxin reductase (EC 1.8.1.9)

. . . . . .

Table 8.3. (continued)

Genes from Gil et al. 2004		Genes from this study		
Gene	Protein function	UniProt accession number	Gene	UniProt protein name
upp	Uracil phosphoribosyltransferase	N1M772	EBESD8_32980	Uracil phosphoribosyltransferase (EC 2.4.2.9) (UMP pyrophosphorylase) (UPRTase)
coaA	Pantothenate kinase	N1MBT4	EBESD8_35900	Pantothenate kinase (EC 2.7.1.33) (Pantothenic acid kinase)
coaD	4'-Phosphopantetheine adenylyltransferase	N1M4H7	EBESD8_28140	Phosphopantetheine adenylyltransferase (EC 2.7.7.3) (Dephospho-CoA pyrophosphorylase) (Pantetheine-phosphate adenylyltransferase)
coaE	Dephospho-CoA kinase	N1MF32	EBESD8_61530	Dephospho-CoA kinase (EC 2.7.1.24)
dfp	Phosphopantothenate cysteine ligase and 4'-Phosopho-pantothenyl-L-cysteine decarboxylase	N1M434	EBESD8_26640	Phosphopantothenoylcysteine decarboxylase / Phosphopantothenoylcysteine synthetase (EC 4.1.1.36) (EC 6.3.2.5)
folA	Dihydrofolate reductase	N1LZA4	EBESD8_10310	Dihydrofolate reductase (EC 1.5.1.3)
		N1M3W3	EBESD8_5360	Dihydrofolate reductase (EC 1.5.1.3)
		N1M601	EBESD8_15480	Dihydrofolate reductase (EC 1.5.1.3)
		N1MI92	EBESD8_56650	Dihydrofolate reductase (EC 1.5.1.3)
		N1LYB2	EBESD8_2190	Dihydrofolate reductase (EC 1.5.1.3)
		N1M7A0	EBESD8_20400	Dihydrofolate reductase (EC 1.5.1.3)
		N1M086	EBESD8_7520	Dihydrofolate reductase (EC 1.5.1.3)
		N1M2G9	EBESD8_2450	Dihydrofolate reductase (EC 1.5.1.3)
		N1MGS1	EBESD8_54130	Dihydrofolate reductase (EC 1.5.1.3)
		N1M3D5	EBESD8_18670	Dihydrofolate reductase (EC 1.5.1.3)
		N1MHQ8	EBESD8_55040	Dihydrofolate reductase (EC 1.5.1.3)
glyA	Glycine hydroxymethyltransferase	N1M844	EBESD8_35920	Serine hydroxymethyltransferase (SHMT) (Serine methylase) (EC 2.1.2.1)
metK	Methionine adenosyltransferase	N1M5D2	EBESD8_26650	S-adenosylmethionine synthase (AdoMet synthase) (EC 2.5.1.6) (MAT) (Methionine adenosyltransferase)
nadR	Adenylyltransferase	-	-	-
nadV	Nicotinamide phosphoribosyltransferase	-	-	-

. . . . . .

Table 8.3. (continued)

Genes from Gil et al. 2004		Genes from this study		
Gene	Protein function	UniProt accession number	Gene	UniProt protein name
pdxY	Pyridoxal kinase	-	-	-
ribF	Riboflavin kinase	N1MFW7	EBESD8_62360	Riboflavin biosynthesis protein (EC 2.7.1.26) (EC 2.7.7.2)
yloS	Thiamine pyrophosphokinase	-	-	-
mesJ	Conserved hypothetical protein	-	-	-
mraW	Methyltransferase	-	-	-
ybeY	Conserved hypothetical protein	N1MB97	EBESD8_47170	Endoribonuclease YbeY (EC 3.1.-.-)
ycfF	HIT family	N1ME29	EBESD8_44600	HIT family protein
ycfH	Putative deoxyribonuclease, *tatD* family	N1MC80	EBESD8_50380	Putative deoxyribonuclease YcfH
yoaE	Conserved hypothetical protein	-	-	-
yqgF	Conserved hypothetical protein	-	-	-
yraL	Conserved hypothetical protein	-	-	-

Table 8.4. Proteins upregulated in response to 17β-estradiol related to xenobiotic degradation and metabolism proteins.

UniProtKB accession number and gene	Protein name assigned in genome annotation	Log2 (Fold Abundance)	Accession (Hit)	Greatest identity %	Greatest bit score	KEGG Orthology	Benzoate degradation	Fluorobenzoate degradation	Aminobenzoate degradation	Chloroalkane and chloroalkene degradation	Chlorocyclohexane and chlorobenzene degradation	Naphthalene degradation	Bisphenol degradation	Toluene degradation	Xylene degradation	Ethylbenzene degradation	Caprolactam degradation	Steroid degradation	Metabolism of xenobiotics by cytochrome P450	Drug metabolism – cytochrome P450	Drug metabolism – other enzymes	Polycyclic aromatic hydrocarbon degradation
N1M168	Uncharacterized protein	5.7	B9J937	28	45	K01053											■					
N1M7P8	Uncharacterized protein	3.2	H8MEL2	42	35	K00128				■												
N1M0E8	3-hydroxybutyryl-CoA dehydrogenase 3-hydroxyacyl-CoA dehydrogenase	2.1	V9XBW7	95	465	K00074	■															
N1M3N7	Aldehyde dehydrogenase	2.1	C1B581	75	571	K00128				■												
N1MEY8	Enoyl-CoA hydratase/3-hydroxyacyl-CoA dehydrogenase/3-hydroxybutyryl-CoA epimerase	2.0	Q0S8Z0	80	1017	K01782											■					
N1M570	Epoxide hydrolase	1.9	A4YR09	29	108	K01253													■			
N1MBR5	Alcohol dehydrogenase	1.9	V9XRY3	95	545	K13953				■		■							■	■		
N1LZQ4	Uncharacterized protein	1.8	F6G2J2	30	55	K00799													■	■		
N1M4Q9	Aldehyde-alcohol dehydrogenase	1.7	B2HR86	80	1408	K04072				■		■										
N1MI21	Dienelactone hydrolase family	1.6	V9XH60	67	281	K01061		■			■			■								

Table 8.4. (continued)

UniProtKB accession number and gene	Protein name assigned in genome annotation	Log2 (Fold Abundance)	Accession (Hit)	Greatest identity %	Greatest bit score	KEGG Orthology	Benzoate degradation	Fluorobenzoate degradation	Aminobenzoate degradation	Chloroalkane and chloroalkene degradation	Chlorocyclohexane and chlorobenzene degradation	Naphthalene degradation	Bisphenol degradation	Toluene degradation	Xylene degradation	Ethylbenzene degradation	Caprolactam degradation	Steroid degradation	Metabolism of xenobiotics by cytochrome P450	Drug metabolism – cytochrome P450	Drug metabolism – other enzymes	Polycyclic aromatic hydrocarbon degradation
N1M3V3	Uncharacterized protein	1.6	M1FIB0	29	41	K14727	■															
N1M0L0	Enoyl-CoA hydratase	1.5	V9XEF0	88	363	K01692	■		■								■					
N1MHQ3	1,2-dihydroxycyclohexa-3,5-diene-1-carboxylate dehydrogenase	1.5	V9XGV7	81	395	K05783	■	■							■							
N1M6D1	3-ketoacyl-CoA thiolase @ acetyl-CoA acetyltransferase	1.4	E4WF67	80	607	K00632	■									■						
N1LYA9	Hypoxanthine-guanine phosphoribosyltransferase	1.4	V9XKE1	92	313	K00760														■		
N1M4P5	Putative cytochrome P450 hydroxylase	1.3	Q0SDD0	39	260	K00517			■				■									■
N1MCB5	Benzoate 1,2-dioxygenase alpha subunit	1.2	V9XHZ8	91	866	K05549	■	■							■							
N1M754	Cholesterol oxidase	1.2	V9XF97	86	976	K03333												■				
N1M624	3-ketoacyl-CoA thiolase	1.2	Q0S1G1	93	761	K00632	■									■						
N1LYW6	Probable phenylacetic acid degradation NADH oxidoreductase paaE	1.2	V9XFJ4	85	594	K15983												■				
N1LX53	Alcohol dehydrogenase	1.1	A8MAG5	33	164	K13953				■		■							■	■		

Table 8.5. Proteins upregulated in response to 17β-estradiol related to endocrine system proteins.

UniProtKB accession number and gene	Protein name assigned in genome annotation	Log2 (Fold Abundance)	Accession (Hit)	Greatest identity %	Greatest bit score	KEGG Orthology	Glucagon signaling pathway	Adipocytokine signaling pathway	PPAR signaling pathway	Thyroid hormone synthesis
N1MEW5	Butyryl-CoA dehydrogenase	2.9	C7Q8L2	72	554	K00249			■	
N1MI73	FadE30	2.0	Q0SC74	64	471	K00249			■	
N1M831	2,3-bisphosophoglycerate-dependent phosphoglycerate mutase	1.5	V9XET6	92	446	K01834	■			
N1MCE9	Glutathione peroxidase	1.3	E4WDD2	84	293	K00760				■
N1LYI8	Isovaleryl-CoA dehydrogenase	1.2	D2Q523	74	570	K00249			■	
N1M2Y7	Long-chain-fatty-acid--CoA	1.1	V9XJM5	75	961	K01897		■		

Table 8.6. *Rhodococcus* sp. EsD8 proteins with 100% identity match to enzyme classes 1.1.1.50, 1.1.1.51, 1.1.1.64, and 1.1.1.159.

Rhodococcus sp. EsD8 proteins		sequence similarity		predicted or previously identified proteins		detected in genome	identified in proteome	statistically significant in proteome	upregulated in response to E2	downregulated in response to E2
UniProtKB accession number	protein name assigned in genome annotation	greatest identity %	greatest bit score	accession number	functional description					
				EC 1.1.1.50						
N1LYF8	NADH-quinone oxidoreductase subunit K	100	16.16	Q3IEQ7	HsdA protein	x				
N1M2U8	Uncharacterized protein	100	16.16	C0VPW7	Type I restriction modification DNA specificity domain protein	x	x			
N1MDK6	Uncharacterized protein	100	20.4	A0A0E8YID6	Short-chain dehydrogenase/reductas	x	x	x		
N1M9D7	Putative ATP/GTP-binding protein protein	100	20.79	L8FA20	3 alpha-hydroxysteroid dehydrogenase/carbonyl reductase	x	x			
N1MA23	Uncharacterized protein	100	17.7	E8M6U0	HsdA	x	x			
N1MFY9	Uncharacterized protein	100	16.16	C0VPW7	Type I restriction modification DNA specificity domain protein	x				
N1M9T9	Uncharacterized protein	100	16.16	G0A7T4	Restriction modification system DNA specificity domain protein	x				
N1MB50	Transcriptional regulator, IclR family	100	18.86	D5RHP7	Oxidoreductase, short chain dehydrogenase/reductase family protein	x				

Table 8.6. (continued)

Rhodococcus sp. EsD8 proteins		sequence similarity		predicted or previously identified proteins		detected in genome	identified in proteome	statistically significant in proteome	upregulated in response to E2	downregulated in response to E2
UniProtKB accession number	protein name assigned in genome annotation	greatest identity %	greatest bit score	accession number	functional description					
				EC 1.1.1.51						
N1M3T5	Uncharacterized protein	100	19.25	O18404	3-hydroxyacyl-CoA dehydrogenase type-2	x				
N1M6A3	Fatty acid hydroxylase FAH1P, putative	100	19.63	A0A088TQ85	3-beta-hydroxysteroid dehydrogenase	x				
N1M7E6	Butyryl-CoA dehydrogenase	100	22.33	Q0K3I5	H16_B0642 protein	x				
N1M7K7	Uncharacterized protein	100	23.1	Q7LZT0	3(or 17)beta-hydroxysteroid dehydrogenase I	x				
N1M8H3	Uncharacterized protein	100	18.86	P37058	Testosterone 17-beta-dehydrogenase 3	x				
N1MB50	Transcriptional regulator, IclR family	100	18.86	D5RHP7	Oxidoreductase, short chain dehydrogenase/reductase family protein	x				
N1MDC9	Uncharacterized protein	100	15.39	P37058	Testosterone 17-beta-dehydrogenase 3	x				
N1MJH1	Uncharacterized protein	100	21.17	O08756	3-hydroxyacyl-CoA dehydrogenase type-2	x	x			

Table 8.6. (continued)

Rhodococcus sp. EsD8 proteins		sequence similarity		predicted or previously identified proteins		detected in genome	identified in proteome	statistically significant in proteome	upregulated in response to E2	downregulated in response to E2
UniProtKB accession number	protein name assigned in genome annotation	greatest identity %	greatest bit score	accession number	functional description					
				EC 1.1.1.64						
N1M689	Short-chain type dehydrogenase/ reductase	100	514.61	W4A6S2	Estradiol 17-beta-dehydrogenase	x	x	x		
N1M5W5	Uncharacterized protein	100	17.32	W4AA75	Estradiol 17-beta-dehydrogenase	x				
N1M099	3-oxoacyl-[acyl-carrier protein] reductase	100	105.53	Q92506	Estradiol 17-beta-dehydrogenase 8	x				
N1MDH4	Short chain dehydrogenase	100	617.46	W3ZXT1	Estradiol 17-beta-dehydrogenase	x	x			
				EC 1.1.1.159						
N1M8L7	Uncharacterized protein	100	18.09	P0AET9	7-alpha-hydroxysteroid dehydrogenase	x				
N1M3E7	Uncharacterized protein	100	14.24	P0AET9	7-alpha-hydroxysteroid dehydrogenase	x				
N1MF28	Ferredoxin, 2Fe-2S	100	15.39	P0AET9	7-alpha-hydroxysteroid dehydrogenase	x				
N1MCT5	Uncharacterized protein	100	15.01	P0AET9	7-alpha-hydroxysteroid dehydrogenase	x				
N1LWZ9	Uncharacterized protein	100	13.47	P0AET9	7-alpha-hydroxysteroid dehydrogenase	x				
N1M2J9	Uncharacterized protein	100	16.55	P0AET9	7-alpha-hydroxysteroid dehydrogenase	x	x			

Table 8.6. (continued)

Rhodococcus sp. EsD8 proteins		sequence similarity		predicted or previously identified proteins						
UniProtKB accession number	protein name assigned in genome annotation	greatest identity %	greatest bit score	accession number	functional description	detected in genome	identified in proteome	statistically significant in proteome	upregulated in response to E2	downregulated in response to E2
				EC 1.1.1.159						
N1MD08	Uncharacterized protein	100	15.39	P0AET9	7-alpha-hydroxysteroid dehydrogenase	x	x			
N1M8S4	UvrABC system protein A	100	20.02	P0AET9	7-alpha-hydroxysteroid dehydrogenase	x	x	x	x	
N1M3P6	Aromatic amino acid transport protein AroP	100	16.16	P0AET9	7-alpha-hydroxysteroid dehydrogenase	x	x			
N1M716	Uncharacterized protein	100	14.24	P0AET9	7-alpha-hydroxysteroid dehydrogenase	x				
N1LZE1	Uncharacterized protein	100	13.85	P0AET9	7-alpha-hydroxysteroid dehydrogenase	x	x			
N1MC95	3-oxoacyl-[acyl-carrier protein] reductase	100	100.14	P0AET9	7-alpha-hydroxysteroid dehydrogenase	x	x	x	x	
N1M976	Uncharacterized protein	100	14.62	P0AET9	7-alpha-hydroxysteroid dehydrogenase	x	x			
N1M3B1	Sigma factor, sigma 70 type, group 4 (ECF)	100	18.48	P0AET9	7-alpha-hydroxysteroid dehydrogenase	x	x	x		
N1MBW0	Uncharacterized protein	100	13.85	P0AET9	7-alpha-hydroxysteroid dehydrogenase	x				
N1M424	Aspartate carbamoyltransferase	100	20.02	P0AET9	7-alpha-hydroxysteroid dehydrogenase	x	x	x	x	

Table 8.6. (continued)

Rhodococcus sp. EsD8 proteins		sequence similarity		predicted or previously identified proteins		detected in genome	identified in proteome	statistically significant in proteome	upregulated in response to E2	downregulated in response to E2
UniProtKB accession number	protein name assigned in genome annotation	greatest identity %	greatest bit score	accession number	functional description					
				EC 1.1.1.159						
N1M557	Flavin reductase-like, FMN-binding	100	15.39	P0AET9	7-alpha-hydroxysteroid dehydrogenase	x				
N1MDX4	FMN reductase	100	18.09	P0AET9	7-alpha-hydroxysteroid dehydrogenase	x	x			
N1M515	Putative quinone oxidoreductase	100	15.78	P0AET9	7-alpha-hydroxysteroid dehydrogenase	x				
N1M872	Uncharacterized protein	100	14.62	P0AET9	7-alpha-hydroxysteroid dehydrogenase	x				
N1M6X3	Putative cytochrome P450 hydroxylase	100	20.02	P0AET9	7-alpha-hydroxysteroid dehydrogenase	x				
N1LX22	Mycofactocin radical SAM maturase	100	18.86	P0AET9	7-alpha-hydroxysteroid dehydrogenase	x	x			
N1MBP9	Transcription termination factor Rho	100	16.16	P0AET9	7-alpha-hydroxysteroid dehydrogenase	x	x			
N1M8G6	Long-chain-fatty-acid--CoA ligase	100	14.62	P0AET9	7-alpha-hydroxysteroid dehydrogenase	x				
N1MIT0	Uncharacterized protein	100	16.16	P0AET9	7-alpha-hydroxysteroid dehydrogenase	x				
N1M311	Uncharacterized protein	100	15.39	P0AET9	7-alpha-hydroxysteroid dehydrogenase	x				

Table 8.6. (continued)

Rhodococcus sp. EsD8 proteins		sequence similarity		predicted or previously identified proteins		detected in genome	identified in proteome	statistically significant in proteome	upregulated in response to E2	downregulated in response to E2
UniProtKB accession number	protein name assigned in genome annotation	greatest identity %	greatest bit score	accession number	functional description					
				EC 1.1.1.159						
N1MCL3	Transcriptional regulator/sugar kinase	100	16.93	P0AET9	7-alpha-hydroxysteroid dehydrogenase	x				
N1M7W9	Uncharacterized protein	100	13.85	P0AET9	7-alpha-hydroxysteroid dehydrogenase	x				
N1M1V3	Uncharacterized protein	100	12.7	P0AET9	7-alpha-hydroxysteroid dehydrogenase	x				

CHAPTER 9: CONCLUSIONS

One of the listed grand challenges by the National Academy of Engineering it to provide access to clean water. This is becoming more difficult even in developed countries due to extreme weather changes, resulting in increased water reclamation. While TOrCs in drinking water are not currently known to be a human health concern and the effects of many TOrCs on aquatic life are as yet unknown, increased public awareness of TOrCs is influencing the acceptance of water reuse and the beneficial use of biosolids. This study proposes a new technology to reduce the concentrations of TOrCs in wastewater. Therefore, when it is determined which TOrCs are an environmental or human health concern, a technical solution will already have been designed. The approach studied here is capable of improving TOrCs removal without significant modifications to existing WWTPs, large capital costs, or large energy requirements. This will make the technology meet the concerns of the general public and make it more practical for the utilities potentially implementing bioaugmentation.

This study hypothesized that *bioaugmentation of TOrC-degrading bacteria into the activated sludge portion of a WWTP can improve the removal efficiencies of the TOrC*. Previously identified TOrC-degrading bacteria have not been tested for their suitability for bioaugmentation, and the few studies that previously considered bioaugmentation for improved TOrCs removal found rapid loss of the augmented bacteria. This study addressed the following questions:

(1) Can bacteria be identified that meet the requirements of bioaugmentation?
(2) Is bioaugmentation a feasible option to improve TOrCs removal during wastewater treatment?
(3) Is TOrCs degradation achieved through activity of specialized enzymes and degradation pathways?

The first question was addressed by isolating and characterizing eleven bacteria that degraded triclosan, BPA, ibuprofen, E2, and gemfibrozil (Chapter 4). An enrichment process was designed to isolate TOrCs-degrading bacteria from activated sludge based on the assumptions that the targeted bacteria were of extreme low abundance in the initial activated sludge inoculum, they could use the TOrC as a carbon source (no other carbon source was added, including severely limiting or removing vitamins), they may grow slower than other populations (the enrichments were transferred when the TOrC was degraded rather than when growth was observed), and they grew slower than nitrifiers (the ammonia was removed or severely limited in the media). This enrichment process could be used to isolate bacteria that degrade other TOrCs, depending on the specific WWTP needs and the end use of the water to be treated. Seven of the eleven bacteria met all criteria identified as critical for successful bioaugmentation; specifically they *(1)* degraded to low ng/L concentrations, *(2)* grew using a variety of carbon sources especially protein-

rich carbon sources while maintaining the ability to degrade the TOrC, *(3)* preferentially degraded the TOrC in the presence of higher concentrations of other carbon sources, and *(4)* degraded at rates that made them practical for use in WWTP. As ecotoxicology and human health impacts are identified, it may not be necessary for the bacteria to degrade to low ng/L concentrations.

The second question was addressed by generating a model simulating bioaugmentation in full scale activated sludge processes (Chapter 5) and by studying bioaugmentation in lab scale reactors (Chapter 6). The full scale models predicted that bioaugmentation was a feasible technology for enhanced TOrC removal in a 4-stage activated sludge process. It also demonstrated that sorption had a large influence on TOrCs degradation, when assuming that only non-sorbed TOrCs were biologically available. This suggested that TOrCs with lower sorption partitioning coefficients would require a lower bioaugmentation dose to achieve similar residual chemical concentrations.

The lab scale reactor study demonstrated the ability of bioaugmentation to improve the degradation of TOrCs (Chapter 6). Bioaugmentation improved BPA removal with a less than 2% increase in total system VSS, and decreased the BPA in the effluent, sorbed to the waste solids, and left in the reactors. These results support bioaugmentation as a useful technique to implement at WWTPs, especially because it prevents TOrCs from transfer to biosolids (as seen by the reduced mass in the wasted solids) in addition to removing it from the effluent. Bioaugmentation also resulted in a greater enhancement in BPA removal at a low SRT compared to a high SRT, due to the inherently lower removal efficiencies with a low SRT without bioaugmentation. This suggested that bioaugmentation may be useful for WWTPs that have low TOrC removal efficiencies, including WWTPs that operate at low SRTs.

Bacterial growth and loss kinetics were determined to see how they affect the long-term applicability of measured degradation kinetics. The bacteria was found to have a net loss under lab scale reactors conditions. This suggests that augmented bacteria will not accumulate in the system as was predicted in the full scale model. Therefore, determined kinetics need to be applied to the full scale model to more accurately predicted required bioaugmentation doses. Also, because the bacteria was lost from the reactors rapidly, an increase in SRT will not result in lower bioaugmentation doses due to accumulation of the augmented biomass. However, a lower bioaugmentation doses would be required due to the higher activated sludge biomass concentrations.

The third question was addressed by using a combination of genomics, proteomics, and metabolomics to identified proteins likely involved the degradation of specific TOrCs. If it can be determined if TOrCs

degradation is achieved through activity of specialized enzymes and degradation pathways, then biomarkers could potentially be created to monitor for the degradation genes of the augmented bacteria rather than just the presence of the bacteria. This approach resulted in the identification of novel enzymes involved in the degradation of BPA (Chapter 7) and gemfibrozil (Appendix B), and identified known E2 degradation genes in a new organism (Chapter 8). Also, the previously unknown degradation pathway of one TOrC (gemfibrozil) was predicted, and the initial degradation pathway of BPA was confirmed and later degradation steps were identified.

Many practical implications arise from this study, specifically because cultured bacteria were used for bioaugmentation. Other approaches often rely on an in-line selection process, so that the process cannot be transferred to other treatment processes where the same in-line selection may not be possible. However, here bioaugmentation with the bacterial cultures could be applied to wastewater treatment processes including conventional activated sludge processes, membrane bioreactors, and moving bed biofilm reactors, amongst others. This application would improve the quality of the biosolids, potentially allowing them to be reclassified in the future. Continuous bioaugmentation could also be applied to other waste streams such as hospital or pharmaceutical manufacturing wastes that have high concentrations of these contaminants. This application may allow for growth of the bacteria on the waste stream, which would reduce operating costs and allow for use of bacteria that are not able to maintain the ability to degrade the TOrC when grown in the absence of the TOrC. Bioaugmentation may also useful for treating landfill leachate when added to the activated sludge portion of the treatment system. Bioaugmentation for TOrCs removal could also make direct potable reuse easier when used as a pretreatment technology before reverse osmosis, which would reduce the contaminants in the retentate. Wetlands have also recently been evaluated as a possible solution to treat wastewater for reuse purposes and TOrC-degrading bacteria could be augmented in this situation. Finally, bioaugmentation of sand filters in drinking water treatment plants has recently been studied, and bacteria with the identified characteristics may be appropriate for this situation.

Before application of bioaugmentation to full-scale WWTPs, future work should focus on optimizing the bioaugmentation process. This includes continuous bioaugmentation studies at the pilot-scale with automated bioaugmentation and a continuously stirred tank reactor design instead of a sequencing batch reactor. This will help demonstrate its applicability to full-scale systems. Techniques for maintaining the degradation activity in the system after bioaugmentation should also be tested. If the loss of degradation activity is due to loss of the augmented bacteria, techniques for protecting the augmented bacteria from predators should be explored, as well as options to delay when endogenous respiration occurs. For

example, bacteria to be augmented could be grown on solid media, pre-flocculated, or grown on primary effluent in dialysis tubing. This last option would also have the benefit of exposing the augmented bacteria to the TOrC during growth, to reduce lag prior at the start of degradation. Experiments should be conducted to test if early, mid, or late growth phase of the bacteria is best to maintain the bacteria in the system longer without sacrificing the degradation ability. However, if the loss of degradation was due to the loss of the degradation activity from the augmented bacteria, experiments should be conducted to determine if the degradation activity was lost due to activated sludge conditions, growth phase, etc. or if the degradation activity was transferred to another organism.

Future work should also focus on confirming genes and proteins responsible for the degradation. Confirmation of TOrCs degradation genes will allow for monitoring of the TOrC degradation activity of the bacteria augmented in pilot-scale studies or when implemented at full-scale treatment plants, instead of relying on the bacterial signature. The location of the degradation genes should also be determined to see if they are on plasmids. This will reveal insight into the adaption of these bacteria for their ability to remove TOrCs. It may also lead to future research directions including introduction of the degradation genes into other bacteria. A bacterium that meets all the bioaugmentation criteria could be modified to contain a variety of TOrCs degradation genes, allowing for ease of bioaugmentation, removal of more TOrCs, and decreased operating costs. The bacteria would be selected for its ability to grow to high biomass concentrations quickly on an inexpensive substrate. This bacteria could then be used as a "starter kit" for WWTPs looking to improve the removal of TOrCs in general, and other bacteria could be added if they want to remove a specific TOrC. Alternatively, the enzymes responsible for the degradation could be isolated and these could be directly added to the WWTPs. This would allow for direct bioaugmentation of the degradation ability, rather than bioaugmentation with a bacteria that may be rapidly lost due to predation or may lose its degradation ability over time.

The primary achievement of this study was the establishment of a biological approach to improve the removal efficiencies of TOrCs during wastewater treatment. This will be helpful as new information is known about the environmental and human health effects of TOrCs in our wastewater and drinking water. This research could be applied to assist in direct potable reuse efforts, and it has provided valuable information regarding the genes responsible for the removal of these contaminants, which could lead to new technologies that improve upon this approach for TOrCs removal.

REFERENCES

Abllah, Nfn, and Ah Lee. 1991. "A Batch Activated-Sludge Study of Pineapple Waste-Water Using a Bioaugmentation Process." *Water Science and Technology* 24 (5): 233–40.

Almeida, B., H. Kjeldal, I. Lolas, A. D. Knudsen, G. Carvalho, K. L. Nielsen, M. T. Barreto Crespo, A. Stensballe, and J. L. Nielsen. 2013. "Quantitative Proteomic Analysis of Ibuprofen-Degrading Patulibacter Sp Strain I11." *Biodegradation* 24 (5): 615–30. doi:10.1007/s10532-012-9610-5.

Almeida, B., A. Oehmen, R. Marques, D. Brito, G. Carvalho, and M. T. Barreto Crespo. 2013. "Modelling the Biodegradation of Non-Steroidal Anti-Inflammatory Drugs (NSAIDs) by Activated Sludge and a Pure Culture." *Bioresource Technology* 133 (April): 31–37. doi:10.1016/j.biortech.2013.01.035.

Amann, R. I., B. J. Binder, R. J. Olson, S. W. Chisholm, R. Devereux, and D. A. Stahl. 1990. "Combination of 16S rRNA-Targeted Oligonucleotide Probes with Flow Cytometry for Analyzing Mixed Microbial Populations." *Applied and Environmental Microbiology* 56 (6): 1919–25.

Anari, M. R., R. Bakhtiar, B. Zhu, S. Huskey, R. B. Franklin, and D. C. Evans. 2002. "Derivatization of Ethinylestradiol with Dansyl Chloride to Enhance Electrospray Ionization: Application in Trace Analysis of Ethinylestradiol in Rhesus Monkey Plasma." *Analytical Chemistry* 74 (16): 4136–44. doi:10.1021/ac025712h.

Annweiler, E., H. H. Richnow, G. Antranikian, S. Hebenbrock, C. Garms, S. Franke, W. Francke, and W. Michaelis. 2000. "Naphthalene Degradation and Incorporation of Naphthalene-Derived Carbon into Biomass by the Thermophile Bacillus Thermoleovorans." *Applied and Environmental Microbiology* 66 (2): 518–23.

AWWA. 1998. *Standard Methods for the Examination of Water and Wastewater*. New York: American Water Works Association.

Aylward, Frank O., Bradon R. McDonald, Sandra M. Adams, Alejandra Valenzuela, Rebeccah A. Schmidt, Lynne A. Goodwin, Tanja Woyke, Cameron R. Currie, Garret Suen, and Michael Poulsen. 2013. "Comparison of 26 Sphingomonad Genomes Reveals Diverse Environmental Adaptations and Biodegradative Capabilities." *Applied and Environmental Microbiology* 79 (12): 3724–33. doi:10.1128/AEM.00518-13.

Aziz, Ramy K, Daniela Bartels, Aaron A Best, Matthew DeJongh, Terrence Disz, Robert A Edwards, Kevin Formsma, et al. 2008. "The RAST Server: Rapid Annotations Using Subsystems Technology." *BMC Genomics* 9: 75. doi:10.1186/1471-2164-9-75.

Badiefar, Leila, Bagher Yakhchali, Susana Rodriguez-Couto, Antonio Veloso, Jose Ma Garcia-Arenzana, Yoshinobu Matsumura, and Mahvash Khodabandeh. 2015. "Biodegradation of Bisphenol A by the Newly-Isolated Enterobacter Gergoviae Strain BYK-7 Enhanced Using Genetic Manipulation." *Rsc Advances* 5 (37): 29563–72. doi:10.1039/c5ra01818h.

Baek, H. J., M. H. Park, Y. D. Lee, and H. B. Kim. 2003. "Effect of in Vitro Xenoestrogens on Steroidogenesis in Mature Female Fish, Chasmichthys Dolichognathus." *Fish Physiology and Biochemistry* 28 (1-4): 413–14. doi:10.1023/B:FISH.0000030609.71170.f9.

Ballesteros-Gomez, Ana, Francisco-Javier Ruiz, Soledad Rubio, and Dolores Perez-Bendito. 2007. "Determination of Bisphenols A and F and Their Diglycidyl Ethers in Wastewater and River Water by Coacervative Extraction and Liquid Chromatography-Fluorimetry." *Analytica Chimica Acta* 603 (1): 51–59. doi:10.1016/j.aca.2007.09.048.

Banaei-Asl, Farzad, Ali Bandehagh, Ebrahim Dorani Uliaei, Davoud Farajzadeh, Katsumi Sakata, Ghazala Mustafa, and Setsuko Komatsu. 2015. "Proteomic Analysis of Canola Root Inoculated with Bacteria under Salt Stress." *Journal of Proteomics* 124 (June): 88–111. doi:10.1016/j.jprot.2015.04.009.

Baronti, C, R Curini, G D'Ascenzo, A Di Corcia, A Gentili, and R Samperi. 2000. "Monitoring Natural and Synthetic Estrogens at Activated Sludge Sewage Treatment Plants and in a Receiving River Water." *Environmental Science & Technology* 34 (24): 5059–66. doi:10.1021/es001359q.

Bartrolí, Albert, Julián Carrera, and Julio Pérez. 2011. "Bioaugmentation as a Tool for Improving the Start-up and Stability of a Pilot-Scale Partial Nitrification Biofilm Airlift Reactor." *Bioresource Technology* 102 (6): 4370–75. doi:10.1016/j.biortech.2010.12.084.

Benach, Jordi, Charlotta Filling, Udo C. T. Oppermann, Pietro Roversi, Gérard Bricogne, Kurt D. Berndt, Hans Jörnvall, and Rudolf Ladenstein. 2002. "Structure of Bacterial 3beta/17beta-Hydroxysteroid Dehydrogenase at 1.2 A Resolution: A Model for Multiple Steroid Recognition." *Biochemistry* 41 (50): 14659–68.

Benner, Jessica, Damian E. Helbling, Hans-Peter E. Kohler, Janneke Wittebol, Elena Kaiser, Carsten Prasse, Thomas A. Ternes, et al. 2013. "Is Biological Treatment a Viable Alternative for Micropollutant Removal in Drinking Water Treatment Processes?" *Water Research* 47 (16): 5955–76. doi:10.1016/j.watres.2013.07.015.

Bester, K. 2005. "Fate of Triclosan and Triclosan-Methyl in Sewage Treatment Plants and Surface Waters." *Archives of Environmental Contamination and Toxicology* 49 (1): 9–17. doi:10.1007/s00244-004-0155-4.

"Bisphenol A (BPA) Action Plan Summary | Existing Chemicals | OPPT | US EPA." 2014. Accessed April 28. http://www.epa.gov/oppt/existingchemicals/pubs/actionplans/bpa.html.

Biswas, M. G., and D. W. Russell. 1997. "Expression Cloning and Characterization of Oxidative 17beta- and 3alpha-Hydroxysteroid Dehydrogenases from Rat and Human Prostate." *The Journal of Biological Chemistry* 272 (25): 15959–66.

Bouchez, Patureau, Dabert, Juretschko, Doré, Delgenès, Moletta, and Wagner. 2000. "Ecological Study of a Bioaugmentation Failure." *Environmental Microbiology* 2 (2): 179–90. doi:10.1046/j.1462-2920.2000.00091.x.

Brausch, John M., and Gary M. Rand. 2011. "A Review of Personal Care Products in the Aquatic Environment: Environmental Concentrations and Toxicity." *Chemosphere* 82 (11): 1518–32. doi:10.1016/j.chemosphere.2010.11.018.

Bulloch, Daryl N., Ramon Lavado, Kristy L. Forsgren, Szabolcs Beni, Daniel Schlenk, and Cynthia K. Larive. 2012. "Analytical and Biological Characterization of Halogenated Gemfibrozil Produced through Chlorination of Wastewater." *Environmental Science & Technology* 46 (10): 5583–89. doi:10.1021/es3006173.

Burkhardt-Holm, Patricia, Helmut Segner, Richard Burki, Armin Peter, Sara Schubert, Marc J.-F. Suter, and Mark E. Borsuk. 2008. "Estrogenic Endocrine Disruption in Switzerland: Assessment of Fish Exposure and Effects." *Chimia* 62 (5): 376–82. doi:10.2533/chimia.2008.376.

Caliman, Florentina Anca, and Maria Gavrilescu. 2009. "Pharmaceuticals, Personal Care Products and Endocrine Disrupting Agents in the Environment - A Review." *Clean-Soil Air Water* 37 (4-5): 277–303. doi:10.1002/clen.200900038.

Carballa, M., F. Omil, and J. M. Lema. 2005. "Removal of Cosmetic Ingredients and Pharmaceuticals in Sewage Primary Treatment." *Water Research* 39 (19): 4790–96. doi:10.1016/j.watres.2005.09.018.

Carballa, M, F Omil, JM Lema, M Llompart, C Garcia-Jares, I Rodriguez, M Gomez, and T Ternes. 2004. "Behavior of Pharmaceuticals, Cosmetics and Hormones in a Sewage Treatment Plant." *Water Research* 38 (12): 2918–26. doi:10.1016/j.watres.2004.03.029.

Cardinal, Lynne J., and Michael K. Stenstrom. 1991. "Enhanced Biodegradation of Polyaromatic Hydrocarbons in the Activated Sludge Process." *Water Environment Federation* 63 (7): 950–57.

Chen, Yj, and Jpn Rosazza. 1994. "Microbial Transformation of Ibuprofen by a Nocardia Species." *Applied and Environmental Microbiology* 60 (4): 1292–96.

Chen, Yong, Yunfeng Ding, Li Yang, Jinhai Yu, Guiming Liu, Xumin Wang, Shuyan Zhang, et al. 2014. "Integrated Omics Study Delineates the Dynamics of Lipid Droplets in Rhodococcus Opacus PD630." *Nucleic Acids Research* 42 (2): 1052–64. doi:10.1093/nar/gkt932.

Chimchirian, Robert F., Rominder P. S. Suri, and Hongxiang Fu. 2007. "Free Synthetic and Natural Estrogen Hormones in Influent and Effluent of Three Municipal Wastewater Treatment Plants." *Water Environment Research* 79 (9): 969–74. doi:10.2175/106143007X175843.

Clara, M., B. Strenn, O. Gans, E. Martinez, N. Kreuzinger, and H. Kroiss. 2005. "Removal of Selected Pharmaceuticals, Fragrances and Endocrine Disrupting Compounds in a Membrane Bioreactor and Conventional Wastewater Treatment Plants." *Water Research* 39 (19): 4797–4807. doi:10.1016/j.watres.2005.09.015.

Collodoro, Mike, Pascale Lemaire, Gauthier Eppe, Virginie Bertrand, Rowan Dobson, Gabriel Mazzucchelli, Joelle Widart, Edwin De Pauw, and Marie-Claire De Pauw-Gillet. 2012. "Identification and Quantification of Concentration-Dependent Biomarkers in MCF-7/BOS Cells Exposed to 17 Beta-Estradiol by 2-D DIGE and Label-Free Proteomics." *Journal of Proteomics* 75 (14): 4555–69. doi:10.1016/j.jprot.2012.04.032.

Coogan, Melinda A., Regina E. Edziyie, Thomas W. La Point, and Barney J. Venables. 2007. "Algal Bioaccumulation of Triclocarban, Triclosan, and Methyl-Triclosan in a North Texas Wastewater, Treatment Plant Receiving Stream." *Chemosphere* 67 (10): 1911–18. doi:10.1016/j.chemosphere.2006.12.027.

Corcoran, Jenna, Matthew J. Winter, and Charles R. Tyler. 2010. "Pharmaceuticals in the Aquatic Environment: A Critical Review of the Evidence for Health Effects in Fish." *Critical Reviews in Toxicology* 40 (4): 287–304. doi:10.3109/10408440903373590.

Cox, Jürgen, and Matthias Mann. 2008. "MaxQuant Enables High Peptide Identification Rates, Individualized P.p.b.-Range Mass Accuracies and Proteome-Wide Protein Quantification." *Nature Biotechnology* 26 (12): 1367–72. doi:10.1038/nbt.1511.

Cui, Di, Ang Li, Tian Qiu, Rui Cai, Changlong Pang, Jihua Wang, Jixian Yang, Fang Ma, and Nanqi Ren. 2014. "Improvement of Nitrification Efficiency by Bioaugmentation in Sequencing Batch Reactors at Low Temperature." *Frontiers of Environmental Science & Engineering* 8 (6): 937–44. doi:10.1007/s11783-014-0668-7.

Dann, Andrea B., and Alice Hontela. 2011. "Triclosan: Environmental Exposure, Toxicity and Mechanisms of Action." *Journal of Applied Toxicology* 31 (4): 285–311. doi:10.1002/jat.1660.

Daughton, Cg, and Ta Ternes. 1999. "Pharmaceuticals and Personal Care Products in the Environment: Agents of Subtle Change?" *Environmental Health Perspectives* 107 (December): 907–38. doi:10.2307/3434573.

Daughton, Christian G. 2007. "Pharmaceuticals in the Environment: Sources and Their Management." In *Analysis, Fate and Removal of Pharmaceuticals in the Water Cycle*, edited by M. Petrovic and D. Barcelo, 50:1–58.

Dávila Costa, José Sebastián, O. Marisa Herrero, Héctor M. Alvarez, and Lars Leichert. 2015. "Label-Free and Redox Proteomic Analyses of the Triacylglycerol-Accumulating Rhodococcus Jostii RHA1." *Microbiology (Reading, England)* 161 (Pt 3): 593–610. doi:10.1099/mic.0.000028.

de Kermoysan, Goulwen, Sandrine Joachim, Patrick Baudoin, Matthieu Lonjaret, Cleo Tebby, François Lesaulnier, François Lestremau, et al. 2013. "Effects of Bisphenol A on Different Trophic Levels in a Lotic Experimental Ecosystem." *Aquatic Toxicology* 144–145 (November): 186–98. doi:10.1016/j.aquatox.2013.09.034.

Delong, Ef. 1992. "Archaea in Coastal Marine Environments." *Proceedings of the National Academy of Sciences of the United States of America* 89 (12): 5685–89. doi:10.1073/pnas.89.12.5685.

Dickenson, Eric R. V., Shane A. Snyder, David L. Sedlak, and Joerg E. Drewes. 2011. "Indicator Compounds for Assessment of Wastewater Effluent Contributions to Flow and Water Quality." *Water Research* 45 (3): 1199–1212. doi:10.1016/j.watres.2010.11.012.

Drewes, J. E., J. Hemming, S. J. Ladenburger, J. Schauer, and W. Sonzogni. 2005. "An Assessment of Endocrine Disrupting Activity Changes during Wastewater Treatment through the Use of Bioassays and Chemical Measurements." *Water Environment Research* 77 (1): 12–23. doi:10.2175/106143005X41573.

Du, Dijun, Zhao Wang, Nathan R. James, Jarrod E. Voss, Ewa Klimont, Thelma Ohene-Agyei, Henrietta Venter, Wah Chiu, and Ben F. Luisi. 2014. "Structure of the AcrAB-TolC Multidrug Efflux Pump." *Nature* 509 (7501): 512–15. doi:10.1038/nature13205.

Duong, Cuong N., Jin Sung Ra, Jaeweon Cho, Sang D. Kim, Hoon K. Choi, Ji-Hyung Park, Kyoung W. Kim, Edu Inam, and Sang Don Kim. 2010a. "Estrogenic Chemicals and Estrogenicity in River Waters of South Korea and Seven Asian Countries." *Chemosphere* 78 (3): 286–93. doi:10.1016/j.chemosphere.2009.10.048.

Eaton, R. W. 2001. "Plasmid-Encoded Phthalate Catabolic Pathway in Arthrobacter Keyseri 12B." *Journal of Bacteriology* 183 (12): 3689–3703. doi:10.1128/JB.183.12.3689-3703.2001.

Engst, W, R Landsiedel, H Hermersdörfer, J Doehmer, and H Glatt. 1999. "Benzylic Hydroxylation of 1-Methylpyrene and 1-Ethylpyrene by Human and Rat Cytochromes P450 Individually Expressed in V79 Chinese Hamster Cells." *Carcinogenesis* 20 (9): 1777–85.

"Estradiol - PubChem." 2014. Accessed June 19. http://pubchem.ncbi.nlm.nih.gov/summary/summary.cgi?cid=5757.

Fair, Patricia A., Hing-Biu Lee, Jeff Adams, Colin Darling, Grazina Pacepavicius, Mehran Alaee, Gregory D. Bossart, Natasha Henry, and Derek Muir. 2009. "Occurrence of Triclosan in Plasma of Wild Atlantic Bottlenose Dolphins (Tursiops Truncatus) and in Their Environment." *Environmental Pollution* 157 (8-9): 2248–54. doi:10.1016/j.envpol.2009.04.002.

Fang, Yu, Adcharee Karnjanapiboonwong, Darcy A. Chase, Jiafan Wang, Audra N. Morse, and Todd A. Anderson. 2012. "Occurrence, Fate, and Persistence of Gemfibrozil in Water and Soil." *Environmental Toxicology and Chemistry* 31 (3): 550–55. doi:10.1002/etc.1725.

Federle, TW, SK Kaiser, and BA Nuck. 2002. "Fate and Effects of Triclosan in Activated Sludge." *Environmental Toxicology and Chemistry* 21 (7): 1330–37. doi:10.1897/1551-5028(2002)021<1330:FAEOTI>2.0.CO;2.

Fiehn, Oliver. 2002. "Metabolomics — the Link between Genotypes and Phenotypes." In *Functional Genomics*, edited by Chris Town, 155–71. Springer Netherlands. http://link.springer.com/chapter/10.1007/978-94-010-0448-0_11.

Fischer, Janett, Uwe Kappelmeyer, Matthias Kastner, Frieder Schauer, and Hermann J. Heipieper. 2010. "The Degradation of Bisphenol A by the Newly Isolated Bacterium Cupriavidus Basilensis JF1 Can Be Enhanced by Biostimulation with Phenol." *International Biodeterioration & Biodegradation* 64 (4): 324–30. doi:10.1016/j.ibiod.2010.03.007.

Flint, Shelby, Tricia Markle, Sarah Thompson, and Elizabeth Wallace. 2012. "Bisphenol A Exposure, Effects, and Policy: A Wildlife Perspective." *Journal of Environmental Management* 104 (August): 19–34. doi:10.1016/j.jenvman.2012.03.021.

Flippin, Jennifer L., Duane Huggett, and Christy M. Foran. 2007. "Changes in the Timing of Reproduction Following Chronic Exposure to Ibuprofen in Japanese Medaka, Oryzias Latipes." *Aquatic Toxicology* 81 (1): 73–78. doi:10.1016/j.aquatox.2006.11.002.

Foster, Adam Lloyd. 2007. "Occurrence and Fate of Endocrine Disruptors through the San Marcos Wastewater Treatment Plant," August. https://digital.library.txstate.edu/handle/10877/3880.

Fraker, SL, and GR Smith. 2004. "Direct and Interactive Effects of Ecologically Relevant Concentrations of Organic Wastewater Contaminants on Rana Pipiens Tadpoles." *Environmental Toxicology* 19 (3): 250–56. doi:10.1002/tox.20017.

Froehner, Sandro, Willian Piccioni, Karina Scurupa Machado, and Miguel Mansur Aisse. 2011. "Removal Capacity of Caffeine, Hormones, and Bisphenol by Aerobic and Anaerobic Sewage Treatment." *Water Air and Soil Pollution* 216 (1-4): 463–71. doi:10.1007/s11270-010-0545-3.

Frothingham, R., Rl Allen, and Kh Wilson. 1991. "Rapid 16s Ribosomal Dna Sequencing from a Single Colony Without Dna Extraction or Purification." *Biotechniques* 11 (1): 40 – &.

Fry, N. K., J. K. Fredrickson, S. Fishbain, M. Wagner, and D. A. Stahl. 1997. "Population Structure of Microbial Communities Associated with Two Deep, Anaerobic, Alkaline Aquifers." *Applied and Environmental Microbiology* 63 (4): 1498–1504.

Fuchs, B. M., G. Wallner, W. Beisker, I. Schwippl, W. Ludwig, and R. Amann. 1998. "Flow Cytometric Analysis of the in Situ Accessibility of Escherichia Coli 16S rRNA for Fluorescently Labeled Oligonucleotide Probes." *Applied and Environmental Microbiology* 64 (12): 4973–82.

Fujii, K., S. Kikuchi, M. Satomi, N. Ushio-Sata, and N. Morita. 2002. “Degradation of 17 Beta-Estradiol by a Gram-Negative Bacterium Isolated from Activated Sludge in a Sewage Treatment Plant in Tokyo, Japan.” *Applied and Environmental Microbiology* 68 (4): 2057–60. doi:10.1128/AEM.68.4.2057-2060.2002.

Fukiya, Satoru, Miki Arata, Hiroko Kawashima, Daisuke Yoshida, Maki Kaneko, Kimiko Minamida, Jun Watanabe, et al. 2009. “Conversion of Cholic Acid and Chenodeoxycholic Acid into Their 7-Oxo Derivatives by Bacteroides Intestinalis AM-1 Isolated from Human Feces.” *FEMS Microbiology Letters* 293 (2): 263–70. doi:10.1111/j.1574-6968.2009.01531.x.

Gao, Junfeng, Lynda B. M. Ellis, and Lawrence P. Wackett. 2010a. “The University of Minnesota Biocatalysis/Biodegradation Database: Improving Public Access.” *Nucleic Acids Research* 38 (January): D488–91. doi:10.1093/nar/gkp771.

Gao, X., J. Liu, and G. Li. 1998. “Purification and Properties of 3 Alpha-Hydroxysteroid Dehydrogenase and 3-Keto-5 Beta-Steroid-Delta 4-Dehydrogenase.” *Annals of the New York Academy of Sciences* 864 (December): 383–92.

Gedalanga, Phillip B., Peerapong Pornwongthong, Rebecca Mora, Sheau-Yun Dora Chiang, Brett Baldwin, Dora Ogles, and Shaily Mahendra. 2014. “Identification of Biomarker Genes To Predict Biodegradation of 1,4-Dioxane.” *Applied and Environmental Microbiology* 80 (10): 3209–18. doi:10.1128/ABM.04162-1.

Gentry, T. J., C. Rensing, and I. L. Pepper. 2004. “New Approaches for Bioaugmentation as a Remediation Technology.” *Critical Reviews in Environmental Science and Technology* 34 (5): 447–94. doi:10.1080/10643380490452362.

Gil, Rosario, Francisco J. Silva, Juli Peretó, and Andrés Moya. 2004. “Determination of the Core of a Minimal Bacterial Gene Set.” *Microbiology and Molecular Biology Reviews* 68 (3): 518–37. doi:10.1128/MMBR.68.3.518-537.2004.

Gough, Heidi L., Diane Nelsen, Christopher Muller, and John Ferguson. 2013. “Enhanced Methane Generation During Theromophilic Co-Digestion of Confectionary Waste and Grease-Trap Fats and Oils with Municipal Wastewater Sludge.” *Water Environment Research* 85 (2): 175–83. doi:10.2175/106143012X13418552642128.

Gross, B., J. Montgomery-Brown, A. Naumann, and M. Reinhard. 2004. “Occurrence and Fate of Pharmaceuticals and Alkylphenol Ethoxylate Metabolites in an Effluent-Dominated River and Wetland.” *Environmental Toxicology and Chemistry* 23 (9): 2074–83. doi:10.1897/03-606.

Guerra, P., M. Kim, S. Teslic, M. Alaee, and S. A. Smyth. 2015. “Bisphenol-A Removal in Various Wastewater Treatment Processes: Operational Conditions, Mass Balance, and Optimization.” *Journal of Environmental Management* 152 (April): 192–200. doi:10.1016/j.jenvman.2015.01.044.

Hamilton, Andrea, David L. Popham, David J. Carl, Xavier Lauth, Victor Nizet, and Amanda L. Jones. 2006. “Penicillin-Binding Protein 1a Promotes Resistance of Group B Streptococcus to Antimicrobial Peptides.” *Infection and Immunity* 74 (11): 6179–87. doi:10.1128/IAI.00895-06.

Hanson, Jessica R., Corinne E. Ackerman, and Kate M. Scow. 1999. “Biodegradation of Methyl Tert-Butyl Ether by a Bacterial Pure Culture.” *Applied and Environmental Microbiology* 65 (11): 4788–92.

Hartmann, Erica M., and Jean Armengaud. 2014. “Shotgun Proteomics Suggests Involvement of Additional Enzymes in Dioxin Degradation by Sphingomonas Wittichii RW1.” *Environmental Microbiology* 16 (1): 162–76. doi:10.1111/1462-2920.12264.

Hashimoto, T., K. Onda, T. Morita, B. Luxmy, K. Tada, A. Miya, and T. Murakami. 2010. “Contribution of the Estrogen-Degrading Bacterium Novosphingobium Sp. Strain JEM-1 to Estrogen Removal in Wastewater Treatment.” *Journal of Environmental Engineering* 136 (9): 890–96. doi:10.1061/(ASCE)EE.1943-7870.0000218.

Hay, AG, PM Dees, and GS Sayler. 2001. “Growth of a Bacterial Consortium on Triclosan.” *Fems Microbiology Ecology* 36 (2-3): 105–12. doi:10.1111/j.1574-6941.2001.tb00830.x.

Hayter, Anthony. 1996. *Probability and Statistics for Engineers and Scientists*. Boston, MA: International Thomson Publishing.

Head, M. A., and J. A. Oleszkiewicz. 2005. "Bioaugmentation with Nitrifying Bacteria Acclimated to Different Temperatures." *Journal of Environmental Engineering-Asce* 131 (7): 1046–51. doi:10.1061/(ASCE)0733-9372(2005)131:7(1046).

Heidler, Jochen, and Rolf U. Halden. 2007. "Mass Balance Assessment of Triclosan Removal during Conventional Sewage Treatment." *Chemosphere* 66 (2): 362–69. doi:10.1016/j.chemosphere.2006.04.066.

Helander, Anders, Ingrid Olsson, and Helen Dahl. 2007. "Postcollection Synthesis of Ethyl Glucuronide by Bacteria in Urine May Cause False Identification of Alcohol Consumption." *Clinical Chemistry* 53 (10): 1855–57. doi:10.1373/clinchem.2007.089482.

Holland, Herbert L, and Hedda K Weber. 2000. "Enzymatic Hydroxylation Reactions." *Current Opinion in Biotechnology* 11 (6): 547–53. doi:10.1016/S0958-1669(00)00142-7.

Huang, Qiuxin, Yiyi Yu, Caiming Tang, Kun Zhang, Jianlan Cui, and Xianzhi Peng. 2011. "Occurrence and Behavior of Non-Steroidal Anti-Inflammatory Drugs and Lipid Regulators in Wastewater and Urban River Water of the Pearl River Delta, South China." *Journal of Environmental Monitoring* 13 (4): 855–63. doi:10.1039/c1em10015g.

Hu, Anyi, Jibing He, Kung-Hui Chu, and Chang-Ping Yu. 2011. "Genome Sequence of the 17β-Estradiol-Utilizing Bacterium Sphingomonas Strain KC8." *Journal of Bacteriology* 193 (16): 4266–67. doi:10.1128/JB.05356-11.

Hung, Yung-Tse, Frank L. Horsfall, John M. Wong, and Don R. Coker. 1986. "Bio-conversion of Accumulated Sludge with Bacterial Augmentation Process in Aerated Lagoons for Municipal Wastewater Treatment." *International Journal of Environmental Studies* 28 (1): 41–56. doi:10.1080/00207238608710306.

Hwang, Chi-Ching, Yi-Hsun Chang, Chao-Nan Hsu, Hsien-Hua Hsu, Chen-Wei Li, and Hwa-I. Pon. 2005. "Mechanistic Roles of Ser-114, Tyr-155, and Lys-159 in 3alpha-Hydroxysteroid Dehydrogenase/carbonyl Reductase from Comamonas Testosteroni." *The Journal of Biological Chemistry* 280 (5): 3522–28. doi:10.1074/jbc.M411751200.

Iasur-Kruh, Lilach, Yitzhak Hadar, and Dror Minz. 2011. "Isolation and Bioaugmentation of an Estradiol-Degrading Bacterium and Its Integration into a Mature Biofilm." *Applied and Environmental Microbiology* 77 (11): 3734–40. doi:10.1128/AEM.00691-11.

"Ibuprofen Uses, Dosage & Side Effects - Drugs.com." 2014. Accessed June 19. http://www.drugs.com/ibuprofen.html.

Ifelebuegu, A. O. 2011. "The Fate and Behavior of Selected Endocrine Disrupting Chemicals in Full Scale Wastewater and Sludge Treatment Unit Processes." *International Journal of Environmental Science and Technology* 8 (2): 245–54.

Ike, M, C Jin, and M Fujita. 1995. "Isolation and Characterization of a Novel Bisphenol A-Degrading Bacterium Pseudomonas Paucimobilis Strain FJ-4." *Japanese Journal of Water Treatment Biology* 31 (3): 203–12.

Il Kim, Seung, Jong-Soon Choi, and Hyung-Yeel Kahng. 2007. "A Proteomics Strategy for the Analysis of Bacterial Biodegradation Pathways." *Omics-a Journal of Integrative Biology* 11 (3): 280–94. doi:10.1089/omi.2007.0019.

Isabelle, Martine, Richard Villemur, Pierre Juteau, and Francois Lepine. 2011. "Isolation of Estrogen-Degrading Bacteria from an Activated Sludge Bioreactor Treating Swine Waste, Including a Strain That Converts Estrone to Beta-Estradiol." *Canadian Journal of Microbiology* 57 (7): 559–68. doi:10.1139/W11-051.

Jackevicius, Cynthia A., Jack V. Tu, Joseph S. Ross, Dennis T. Ko, Daniel Carreon, and Harlan M. Krumholz. 2011. "Use of Fibrates in the United States and Canada." *Jama-Journal of the American Medical Association* 305 (12): 1217–24.

Jiang, Liying, Jun Yang, and Jianmeng Chen. 2010. “Isolation and Characteristics of 17 Beta-Estradiol-Degrading Bacillus Spp. Strains from Activated Sludge.” *Biodegradation* 21 (5): 729–36. doi:10.1007/s10532-010-9338-z.

Jin, Shiwei, Fangxing Yang, Tao Liao, Yang Hui, Sheng Wen, and Ying Xu. 2012. “Enhanced Effects by Mixtures of Three Estrogenic Compounds at Environmentally Relevant Levels on Development of Chinese Rare Minnow (Gobiocypris Rarus).” *Environmental Toxicology and Pharmacology* 33 (2): 277–83. doi:10.1016/j.etap.2011.12.016.

Jin, Yuanxiang, Rujia Chen, Weiping Liu, and Zhengwei Fu. 2010. “Effect of Endocrine Disrupting Chemicals on the Transcription of Genes Related to the Innate Immune System in the Early Developmental Stage of Zebrafish (Danio Rerio).” *Fish & Shellfish Immunology* 28 (5-6): 854–61. doi:10.1016/j.fsi.2010.02.009.

Ji, Wei, Yuanan Chen, Hao Zhang, Xiao Zhang, Ziyi Li, and Yuanhua Yu. 2014. “Cloning, Expression and Characterization of a Putative 7alpha-Hydroxysteroid Dehydrogenase in Comarnonas Testosteroni.” *Microbiological Research* 169 (2-3): 148–54. doi:10.1016/j.micres.2013.07.009.

Joss, A., H. Andersen, T. Ternes, P. R. Richle, and H. Siegrist. 2004. “Removal of Estrogens in Municipal Wastewater Treatment under Aerobic and Anaerobic Conditions: Consequences for Plant Optimization.” *Environmental Science & Technology* 38 (11): 3047–55. doi:10.1021/es0351488.

Kagle, Jeanne, Abigail W. Porter, Robert W. Murdoch, Giomar Rivera-Cancel, and Anthony G. Hay. 2009. “Biodegradation of Pharmaceutical and Personal Care Products.” In *Advances in Applied Mircobiology, Vol 67*, edited by AI Laskin, 67:65–108. San Diego: Elsevier Academic Press Inc.

Kamaraj, M., Rajeshwari Sivaraj, and R. Venckatesh. 2014. “Biodegradation of Bisphenol A by the Tolerant Bacterial Species Isolated from Coastal Regions of Chennai, Tamil Nadu, India.” *International Biodeterioration & Biodegradation* 93 (September): 216–22. doi:10.1016/j.ibiod.2014.02.014.

Kamimura, Naofumi, Taichi Aoyama, Rieko Yoshida, Kenji Takahashi, Daisuke Kasai, Tomokuni Abe, Kohei Mase, Yoshihiro Katayama, Masao Fukuda, and Eiji Masai. 2010a. “Characterization of the Protocatechuate 4,5-Cleavage Pathway Operon in Comamonas Sp. Strain E6 and Discovery of a Novel Pathway Gene.” *Applied and Environmental Microbiology* 76 (24): 8093–8101. doi:10.1128/AEM.01863-10.

Kang, IJ, H Yokota, Y Oshima, Y Tsuruda, T Yamaguchi, M Maeda, N Imada, H Tadokoro, and T Honjo. 2002. “Effect of 17 Beta-Estradiol on the Reproduction of Japanese Medaka (Oryzias Latipes).” *Chemosphere* 47 (1): 71–80. doi:10.1016/S0045-6535(01)00205-3.

Kang, J. H., and F. Kondo. 2002. “Bisphenol a Degradation by Bacteria Isolated from River Water.” *Archives of Environmental Contamination and Toxicology* 43 (3): 265–69. doi:10.1007/s00244-002-1209-0.

Kang, J. H., N. Ri, and F. Kondo. 2004. “Streptomyces Sp Strain Isolated from River Water Has High Bisphenol A Degradability.” *Letters in Applied Microbiology* 39 (2): 178–80. doi:10.1111/j.1472-765X.2004.01562.x.

Karickhoff, Sw, Ds Brown, and Ta Scott. 1979. “Sorption of Hydrophobic Pollutants on Natural Sediments.” *Water Research* 13 (3): 241–48. doi:10.1016/0043-1354(79)90201-X.

Karnjanapiboonwong, Adcharee, Jamie G. Suski, Ankit A. Shah, Qingsong Cai, Audra N. Morse, and Todd A. Anderson. 2011. “Occurrence of PPCPs at a Wastewater Treatment Plant and in Soil and Groundwater at a Land Application Site.” *Water Air and Soil Pollution* 216 (1-4): 257–73. doi:10.1007/s11270-010-0532-8.

Ke, Jinxia, Weiqin Zhuang, Karina Yew-Hoong Gin, Martin Reinhard, Lim Tok Hoon, and Joo-Hwa Tay. 2007. “Characterization of Estrogen-Degrading Bacteria Isolated from an Artificial Sandy Aquifer with Ultrafiltered Secondary Effluent as the Medium RID A-1006-2008.” *Applied Microbiology and Biotechnology* 75 (5): 1163–71. doi:10.1007/s00253-007-0923-y.

Khan, S.J., and J.E. Ongerth. 2005. “Occurrence and Removal of Pharmaceuticals at an Australian Sewage Treatment Plant.” *Water* 32 (4): 80–85.

Kim, Jeong Myeong, and Che Ok Jeon. 2009. “Isolation and Characterization of a New Benzene, Toluene, and Ethylbenzene Degrading Bacterium, Acinetobacter Sp. B113.” *Current Microbiology* 58 (1): 70–75. doi:10.1007/s00284-008-9268-8.

Kim, Joon-Woo, Hyo-Sang Jang, Jong-Gu Kim, Hiroshi Ishibashi, Masashi Hirano, Kazuaki Nasu, Nobuhiro Ichikawa, Yuji Takao, Ryota Shinohara, and Koji Arizono. 2009. “Occurrence of Pharmaceutical and Personal Care Products (PPCPs) in Surface Water from Mankyung River, South Korea.” *Journal of Health Science* 55 (2): 249–58. doi:10.1248/jhs.55.249.

Kim, Sang D., Jaeweon Cho, In S. Kim, Brett J. Vanderford, and Shane A. Snyder. 2007. “Occurrence and Removal of Pharmaceuticals and Endocrine Disruptors in South Korean Surface, Drinking, and Waste Waters.” *Water Research* 41 (5): 1013–21. doi:10.1016/j.watres.2006.06.034.

Kim, Seong-Jae, Ohgew Kweon, and Carl E. Cerniglia. 2009. “Proteomic Applications to Elucidate Bacterial Aromatic Hydrocarbon Metabolic Pathways.” *Current Opinion in Microbiology* 12 (3): 301–9. doi:10.1016/j.mib.2009.03.006.

Kimura, K., H. Hara, and Y. Watanabe. 2010. “Elimination of Selected Pharmaceuticals by Biosolids from Municipal Wastewater Treatment Plants: Importance of Modest pH Change and Degree of Mineralization.” *Water Science and Technology* 62 (5): 1084–89. doi:10.2166/wst.2010.356.

Kim, Young-Mo, Kumarasamy Murugesan, Stefan Schmidt, Varima Bokare, Jong-Rok Jeon, Eun-Ju Kim, and Yoon-Seok Chang. 2011. “Triclosan Susceptibility and Co-Metabolism - A Comparison for Three Aerobic Pollutant-Degrading Bacteria.” *Bioresource Technology* 102 (3): 2206–12. doi:10.1016/j.biortech.2010.10.009.

Kjeldal, H., L. Pell, A. Pommerening-Röser, and J. L. Nielsen. 2014a. “Influence of P-Cresol on the Proteome of the Autotrophic Nitrifying Bacterium Nitrosomonas Eutropha C91.” *Archives of Microbiology* 196 (7): 497–511. doi:10.1007/s00203-014-0985-z.

Kleywegt, Sonya, Vince Pileggi, Paul Yang, Chunyan Hao, Xiaoming Zhao, Carline Rocks, Serei Thach, Patrick Cheung, and Brian Whitehead. 2011. “Pharmaceuticals, Hormones and Bisphenol A in Untreated Source and Finished Drinking Water in Ontario, Canada — Occurrence and Treatment Efficiency.” *Science of The Total Environment* 409 (8): 1481–88. doi:10.1016/j.scitotenv.2011.01.010.

Kolpin, Dana W., Edward T. Furlong, Michael T. Meyer, E. Michael Thurman, Steven D. Zaugg, Larry B. Barber, and Herbert T. Buxton. 2002. “Pharmaceuticals, Hormones, and Other Organic Wastewater Contaminants in U.S. Streams, 1999−2000: A National Reconnaissance.” *Environ. Sci. Technol.* 36 (6): 1202–11. doi:10.1021/es011055j.

Kolvenbach, B., N. Schlaich, Z. Raoui, J. Prell, S. Zuehlke, A. Schaeffer, F. P. Guengerich, and P. F. X. Corvini. 2007. “Degradation Pathway of Bisphenol A: Does Ipso Substitution Apply to Phenols Containing a Quaternary Alpha-Carbon Structure in the Para Position?” *Applied and Environmental Microbiology* 73 (15): 4776–84. doi:10.1128/AEM.00329-07.

Kosma, Christina I., Dimitra A. Lambropoulou, and Triantafyllos A. Albanis. 2014. “Investigation of PPCPs in Wastewater Treatment Plants in Greece: Occurrence, Removal and Environmental Risk Assessment.” *Science of the Total Environment* 466 (January): 421–38. doi:10.1016/j.scitotenv.2013.07.044.

Kostich, Mitchell S., Angela L. Batt, and James M. Lazorchak. 2014. “Concentrations of Prioritized Pharmaceuticals in Effluents from 50 Large Wastewater Treatment Plants in the US and Implications for Risk Estimation.” *Environmental Pollution* 184 (January): 354–59. doi:10.1016/j.envpol.2013.09.013.

Kurisu, Futoshi, Maki Ogura, Satoshi Saitoh, Atsushi Yamazoe, and Osami Yagi. 2010. “Degradation of Natural Estrogen and Identification of the Metabolites Produced by Soil Isolates of Rhodococcus Sp and Sphingomonas Sp.” *Journal of Bioscience and Bioengineering* 109 (6): 576–82. doi:10.1016/j.jbiosc.2009.11.006.

Labrie, F., V. Luu-The, S. X. Lin, C. Labrie, J. Simard, R. Breton, and A. Bélanger. 1997. “The Key Role of 17 Beta-Hydroxysteroid Dehydrogenases in Sex Steroid Biology.” *Steroids* 62 (1): 148–58.

Layton, A. C., B. W. Gregory, J. R. Seward, T. W. Schultz, and G. S. Sayler. 2000. “Mineralization of Steroidal Hormones by Biosolids in Wastewater Treatment Systems in Tennessee USA.” *Environmental Science & Technology* 34 (18): 3925–31. doi:10.1021/es9914487.

Lee, Do Gyun, Kun-Ching Cho, and Kung-Hui Chu. 2015. “Removal of Triclosan in Nitrifying Activated Sludge: Effects of Ammonia Amendment and Bioaugmentation.” *Chemosphere* 125 (April): 9–15. doi:10.1016/j.chemosphere.2014.12.085.

Lee, Do Gyun, Fuman Zhao, Yohannes H. Rezenom, David H. Russell, and Kung-Hui Chu. 2012. “Biodegradation of Triclosan by a Wastewater Microorganism.” *Water Research* 46 (13): 4226–34. doi:10.1016/j.watres.2012.05.025.

Lemos, Marco F. L., Cornelis A. M. van Gestel, and Amadeu M. V. M. Soares. 2009. “Endocrine Disruption in a Terrestrial Isopod under Exposure to Bisphenol A and Vinclozolin.” *Journal of Soils and Sediments* 9 (5): 492–500. doi:10.1007/s11368-009-0104-y.

Letek, Michal, Patricia González, Iain MacArthur, Héctor Rodríguez, Tom C. Freeman, Ana Valero-Rello, Mónica Blanco, et al. 2010. “The Genome of a Pathogenic Rhodococcus: Cooptive Virulence Underpinned by Key Gene Acquisitions.” *PLoS Genet* 6 (9): e1001145. doi:10.1371/journal.pgen.1001145.

Leu, Shao-Yuan, and Michael K. Stenstrom. 2010. “Bioaugmentation to Improve Nitrification in Activated Sludge Treatment.” *Water Environment Research* 82 (6): 524–35. doi:10.2175/106143009X12487095237071.

Li, Guiying, Lei Zu, Po-Keung Wong, Xinping Hui, Yu Lu, Jukun Xiong, and Taicheng An. 2012. “Biodegradation and Detoxification of Bisphenol A with One Newly-Isolated Strain Bacillus Sp GZB: Kinetics, Mechanism and Estrogenic Transition.” *Bioresource Technology* 114 (June): 224–30. doi:10.1016/j.biortech.2012.03.067.

Lin, Angela Yu-Chen, Yu-Ting Tsai, Tsung-Hsien Yu, Xiao-Huan Wang, and Cheng-Fang Lin. 2011. “Occurrence and Fate of Pharmaceuticals and Personal Care Products in Taiwan's Aquatic Environment.” *Desalination and Water Treatment* 32 (1-3): 57–64. doi:10.5004/dwt.2011.2678.

Lin, A. Y. C., and M. Reinhard. 2005. “Photodegradation of Common Environmental Pharmaceuticals and Estrogens in River Water.” *Environmental Toxicology and Chemistry* 24 (6): 1303–9. doi:10.1897/04-236R.1.

Lishman, Lori, Shirley Anne Smyth, Kurtis Sarafin, Sonya Kleywegt, John Toito, Thomas Peart, Bill Lee, Mark Servos, Michel Beland, and Peter Seto. 2006. “Occurrence and Reductions of Pharmaceuticals and Personal Care Products and Estrogens by Municipal Wastewater Treatment Plants in Ontario, Canada.” *Science of the Total Environment* 367 (2-3): 544–58. doi:10.1016/j.scitotenv.2006.03.021.

Li, Zhongtian, Renu Nandakumar, Nandakumar Madayiputhiya, and Xu Li. 2012a. “Proteomic Analysis of 17 Beta-Estradiol Degradation by Stenotrophomonas Maltophilia.” *Environmental Science & Technology* 46 (11): 5947–55. doi:10.1021/es300273k.

Lobos, Jh, Tk Leib, and Tm Su. 1992. “Biodegradation of Bisphenol-a and Other Bisphenols by a Gram-Negative Aerobic Bacterium.” *Applied and Environmental Microbiology* 58 (6): 1823–31.

Lozano, Nuria, Clifford P. Rice, Mark Ramirez, and Alba Torrents. 2013. “Fate of Triclocarban, Triclosan and Methyltriclosan during Wastewater and Biosolids Treatment Processes.” *Water Research* 47 (13): 4519–27. doi:10.1016/j.watres.2013.05.015.

Ludwig, W., O. Strunk, R. Westram, L. Richter, H. Meier, Yadhukumar, A. Buchner, et al. 2004. “ARB: A Software Environment for Sequence Data.” *Nucleic Acids Research* 32 (4): 1363–71. doi:10.1093/nar/gkh293.

Luo, Yunlong, Wenshan Guo, Huu Hao Ngo, Long Duc Nghiem, Faisal Ibney Hai, Jian Zhang, Shuang Liang, and Xiaochang C. Wang. 2014. “A Review on the Occurrence of Micropollutants in the Aquatic Environment and Their Fate and Removal during Wastewater Treatment.” *Science of the Total Environment* 473 (March): 619–41. doi:10.1016/j.scitotenv.2013.12.065.

Maddocks, Sarah E., and Petra C. F. Oyston. 2008. “Structure and Function of the LysR-Type Transcriptional Regulator (LTTR) Family Proteins.” *Microbiology* 154 (12): 3609–23. doi:10.1099/mic.0.2008/022772-0.

Madigan, Michael, John Martinko, David Stahl, and David Clark. 2012. *Brock Biology of Microorganisms*. 13th ed. San Francisco, CA: Benjamin Cummings.

Maere, Steven, Karel Heymans, and Martin Kuiper. 2005. “BiNGO: A Cytoscape Plugin to Assess Overrepresentation of Gene Ontology Categories in Biological Networks.” *Bioinformatics (Oxford, England)* 21 (16): 3448–49. doi:10.1093/bioinformatics/bti551.

Maher, Amy C., Mahmood Akhtar, and Mark A. Tarnopolsky. 2010. “Men Supplemented with 17beta-Estradiol Have Increased Beta-Oxidation Capacity in Skeletal Muscle.” *Physiological Genomics* 42 (3): 342–47. doi:10.1152/physiolgenomics.00016.2010.

Mallonee, D. H., M. A. Lijewski, and P. B. Hylemon. 1995. “Expression in Escherichia Coli and Characterization of a Bile Acid-Inducible 3 Alpha-Hydroxysteroid Dehydrogenase from Eubacterium Sp. Strain VPI 12708.” *Current Microbiology* 30 (5): 259–63.

Martin, J., D. Camacho-Munoz, J. L. Santos, I. Aparicio, and E. Alonso. 2012. “Occurrence of Pharmaceutical Compounds in Wastewater and Sludge from Wastewater Treatment Plants: Removal and Ecotoxicological Impact of Wastewater Discharges and Sludge Disposal.” *Journal of Hazardous Materials* 239 (November): 40–47. doi:10.1016/j.jhazmat.2012.04.068.

Maruyama, K., M. Miwa, N. Tsujii, T. Nagai, N. Tomita, T. Harada, H. Sobajima, and H. Sugisaki. 2001. “Cloning, Sequencing, and Expression of the Gene Encoding 4-Hydroxy-4-Methyl-2-Oxoglutarate Aldolase from Pseudomonas Ochraceae NGJ1.” *Bioscience, Biotechnology, and Biochemistry* 65 (12): 2701–9.

Masai, Eiji, Naofumi Kamimura, Daisuke Kasai, Akio Oguchi, Akiho Ankai, Shigehiro Fukui, Mikio Takahashi, et al. 2012a. “Complete Genome Sequence of Sphingobium Sp. Strain SYK-6, a Degrader of Lignin-Derived Biaryls and Monoaryls.” *Journal of Bacteriology* 194 (2): 534–35. doi:10.1128/JB.06254-11.

Masuda, Midori, Yoshiki Yamasaki, Shun Ueno, and Akira Inoue. 2007. “Isolation of Bisphenol A-Tolerant/degrading Pseudomonas Monteilii Strain N-502.” *Extremophiles* 11 (2): 355–62. doi:10.1007/s00792-006-0047-9.

Matsumura, Yoshinobu, Chiemi Hosokawa, Miho Sasaki-Mori, Ayako Akahira, Kenji Fukunaga, Toshihiko Ikeuchi, Ko-Ichi Oshiman, and Tetsuaki Tsuchido. 2009. “Isolation and Characterization of Novel Bisphenol - A-Degrading Bacteria from Soils.” *Biocontrol Science* 14 (4): 161–69.

Mccorquodale, Dj, and Gc Mueller. 1958. “Effect of Estradiol on the Level of Amino Acid-Activating Enzymes in the Rat Uterus.” *Journal of Biological Chemistry* 232 (1): 31–42.

McIlroy, Simon Jon, Rikke Kristiansen, Mads Albertsen, Søren Michael Karst, Simona Rossetti, Jeppe Lund Nielsen, Valter Tandoi, Robert James Seviour, and Per Halkjær Nielsen. 2013a. “Metabolic Model for the Filamentous ‘Candidatus Microthrix Parvicella’ Based on Genomic and Metagenomic Analyses.” *The ISME Journal* 7 (6): 1161–72. doi:10.1038/ismej.2013.6.

McLeod, Michael P., René L. Warren, William W. L. Hsiao, Naoto Araki, Matthew Myhre, Clinton Fernandes, Daisuke Miyazawa, et al. 2006. “The Complete Genome of Rhodococcus Sp. RHA1 Provides Insights into a Catabolic Powerhouse.” *Proceedings of the National Academy of Sciences of the United States of America* 103 (42): 15582–87. doi:10.1073/pnas.0607048103.

Meade, M. J., R. L. Waddell, and T. M. Callahan. 2001. “Soil Bacteria Pseudomonas Putida and Alcaligenes Xylosoxidans Subsp Denitrificans Inactivate Triclosan in Liquid and Solid Substrates.” *Fems Microbiology Letters* 204 (1): 45–48. doi:10.1111/j.1574-6968.2001.tb10860.x.

Melcer, Henryk, and Gary Klecka. 2011a. “Treatment of Wastewaters Containing Bisphenol A: State of the Science Review.” *Water Environment Research* 83 (7): 650–66. doi:10.2175/106143010X12851009156925.

Metcalfe, CD, TL Metcalfe, Y Kiparissis, BG Koenig, C Khan, RJ Hughes, TR Croley, RE March, and T Potter. 2001. "Estrogenic Potency of Chemicals Detected in Sewage Treatment Plant Effluents as Determined by in Vivo Assays with Japanese Medaka (Oryzias Latipes)." *Environmental Toxicology and Chemistry* 20 (2): 297–308. doi:10.1897/1551-5028(2001)020<0297:EPOCDI>2.0.CO;2.

Metcalf & Eddy, G. Tchobanoglous, F.L. Burton, and H.D. Stensel. 2003. *Wastewater Engineering: Treatment and Reuse*. 4th ed. Boston: McGraw-Hill.

Mimeault, C., A. Woodhouse, X. S. Miao, C. D. Metcalfe, T. W. Moon, and V. L. Trudeau. 2005. "The Human Lipid Regulator, Gemfibrozil Bioconcentrates and Reduces Testosterone in the Goldfish, Carassius Auratus." *Aquatic Toxicology* 73 (1): 44–54. doi:10.1016/j.aquatox.2005.01.009.

Monard, Cecile, Fabrice Martin-Laurent, Oscar Lima, Marion Devers-Lamrani, and Francoise Binet. 2013. "Estimating the Biodegradation of Pesticide in Soils by Monitoring Pesticide-Degrading Gene Expression." *Biodegradation* 24 (2): 203–13. doi:10.1007/s10532-012-9574-5.

Mrozik, A., Z. Piotrowska-Seget, and S. Labuzek. 2003. "Bacterial Degradation and Bioremediation of Polycyclic Aromatic Hydrocarbons." *Polish Journal of Environmental Studies* 12 (1): 15–25.

Munoz, Ivan, Nuria Tomas, Jordi Mas, Juan Fracisco Garcia-Reyes, Antonio Molina-Diaz, and Amadeo R. Fernandez-Alba. 2010. "Potential Chemical and Microbiological Risks on Human Health from Urban Wastewater Reuse in Agriculture. Case Study of Wastewater Effluents in Spain." *Journal of Environmental Science and Health Part B-Pesticides Food Contaminants and Agricultural Wastes* 45 (4): 300–309. doi:10.1080/03601231003704648.

Murdoch, Robert W., and Anthony G. Hay. 2013. "Genetic and Chemical Characterization of Ibuprofen Degradation by Sphingomonas Ibu-2." *Microbiology (Reading, England)* 159 (Pt 3): 621–32. doi:10.1099/mic.0.062273-0.

———. 2015. "The Biotransformation of Ibuprofen to Trihydroxyibuprofen in Activated Sludge and by Variovorax Ibu-1." *Biodegradation* 26 (2): 105–13. doi:10.1007/s10532-015-9719-4.

Murdoch, RW, and AG Hay. 2005. "Formation of Catechols via Removal of Acid Side Chains from Ibuprofen and Related Aromatic Acids." *Applied and Environmental Microbiology* 71 (10): 6121–25. doi:10.1128/AEM.71.10.6121-6125.2005.

Nakada, Norihide, Toshikatsu Tanishima, Hiroyuki Shinohara, Kentaro Kiri, and Hideshige Takada. 2006. "Pharmaceutical Chemicals and Endocrine Disrupters in Municipal Wastewater in Tokyo and Their Removal during Activated Sludge Treatment." *Water Research* 40 (17): 3297–3303. doi:10.1016/j.watres.2006.06.039.

Nakagawa, A., A. Shigeta, H. Iwabuchi, M. Horiguchi, K. Nakamura, and H. Takahagi. 1991. "Simultaneous Determination of Gemfibrozil and Its Metabolites in Plasma and Urine by a Fully Automated High Performance Liquid Chromatographic System." *Biomedical Chromatography: BMC* 5 (2): 68–73. doi:10.1002/bmc.1130050205.

Nakamura, Hakobu. 1968. "Genetic Determination of Resistance to Acriflavine, Phenethyl Alcohol, and Sodium Dodecyl Sulfate in Escherichia Coli." *Journal of Bacteriology* 96 (4): 987–96.

Nemoto, Y., K. Toda, M. Ono, K. Fujikawa-Adachi, T. Saibara, S. Onishi, H. Enzan, T. Okada, and Y. Shizuta. 2000. "Altered Expression of Fatty Acid-Metabolizing Enzymes in Aromatase-Deficient Mice." *The Journal of Clinical Investigation* 105 (12): 1819–25. doi:10.1172/JCI9575.

Nie, Yafeng, Zhimin Qiang, Heqing Zhang, and Weiwei Ben. 2012. "Fate and Seasonal Variation of Endocrine-Disrupting Chemicals in a Sewage Treatment Plant with A/A/O Process." *Separation and Purification Technology* 84 (January): 9–15. doi:10.1016/j.seppur.2011.01.030.

Nocker, Andreas, Ching-Ying Cheung, and Anne K. Camper. 2006. "Comparison of Propidium Monoazide with Ethidium Monoazide for Differentiation of Live vs. Dead Bacteria by Selective Removal of DNA from Dead Cells." *Journal of Microbiological Methods* 67 (2): 310–20. doi:10.1016/j.mimet.2006.04.015.

Nojiri, Hideaki, Masataka Tsuda, Masao Fukuda, and Yoichi Kamagata. 2013. *Biodegradative Bacteria: How Bacteria Degrade, Survive, Adapt, and Evolve*. Springer Science & Business Media.

Oehlmann, Jorg, Ulrike Schulte-Oehlmann, Jean Bachmann, Matthias Oetken, Ilka Lutz, Werner Kloas, and Thomas A. Ternes. 2006. "Bisphenol A Induces Superfeminization in the Ramshorn Snail Marisa Cornuarietis (Gastropoda : Prosobranchia) at Environmentally Relevant Concentrations." *Environmental Health Perspectives* 114 (April): 127–33. doi:10.1289/ehp.8065.

Ogilvie, Brian W., Donglu Zhang, Wenying Li, A. David Rodrigues, Amy E. Gipson, Jeff Holsapple, Paul Toren, and Andrew Parkinson. 2006. "Glucuronidation Converts Gemfibrozil to a Potent, Metabolism-Dependent Inhibitor of Cyp2c8: Implications for Drug-Drug Interactions." *Drug Metabolism and Disposition* 34 (1): 191–97. doi:10.1124/dmd.105.007633.

O'Loughlin, Edward J., Staci R. Kehrmeyer, and Gerald K. Sims. 1996. "Isolation, Characterization, and Substrate Utilization of a Quinoline Degrading Bacterium." *International Biodeterioration & Biodegradation* 38 (2): 107–18.

Onesios, Kathryn M., Jim T. Yu, and Edward J. Bouwer. 2009. "Biodegradation and Removal of Pharmaceuticals and Personal Care Products in Treatment Systems: A Review RID A-3287-2010." *Biodegradation* 20 (4): 441–66. doi:10.1007/s10532-008-9237-8.

Oshiman, Ko-ichi, Yuji Tsutsumi, Tomoaki Nishida, and Yoshinobu Matsumura. 2007. "Isolation and Characterization of a Novel Bacterium, Sphingomonas Bisphenolicum Strain AO1, That Degrades Bisphenol A." *Biodegradation* 18 (2): 247–55. doi:10.1007/s10532-006-9059-5.

Oulton, Rebekah L., Tamar Kohn, and David M. Cwiertny. 2010. "Pharmaceuticals and Personal Care Products in Effluent Matrices: A Survey of Transformation and Removal during Wastewater Treatment and Implications for Wastewater Management RID H-1430-2011." *Journal of Environmental Monitoring* 12 (11): 1956–78. doi:10.1039/c0em00068j.

Overbeek, R., T. Begley, R. M. Butler, J. V. Choudhuri, H. Y. Chuang, M. Cohoon, V. de Crecy-Lagard, et al. 2005. "The Subsystems Approach to Genome Annotation and Its Use in the Project to Annotate 1000 Genomes." *Nucleic Acids Research* 33 (17): 5691–5702. doi:10.1093/nar/gki866.

Panneerselvam, R. 2004. *Research Methodology*. New Delhi: Prentice-Hall.

Pan, Tianyuan, Pu Huang, Guangming Xiong, and Edmund Maser. 2015. "Isolation and Identification of a Repressor TetR for 3,17β-HSD Expressional Regulation in Comamonas Testosteroni." *Chemico-Biological Interactions* 234 (June): 205–12. doi:10.1016/j.cbi.2014.12.034.

Patel, Vibhuti J., Konstantinos Thalassinos, Susan E. Slade, Joanne B. Connolly, Andrew Crombie, J. Colin Murrell, and James H. Scrivens. 2009. "A Comparison of Labeling and Label-Free Mass Spectrometry-Based Proteomics Approaches." *Journal of Proteome Research* 8 (7): 3752–59. doi:10.1021/pr900080y.

Pauwels, Bram, Klaas Wille, Herlinde Noppe, Hubert De Brabander, Tom van de Wiele, Willy Verstraete, and Nico Boon. 2008. "17 Alpha-Ethinylestradiol Cometabolism by Bacteria Degrading Estrone, 17 Beta-Estradiol and Estriol." *Biodegradation* 19 (5): 683–93. doi:10.1007/s10532-007-9173-z.

Paxeus, N. 2004. "Removal of Selected Non-Steroidal Anti-Inflammatory Drugs (NSAIDs), Gemfibrozil, Carbamazepine, Beta-Blockers, Trimethoprim and Triclosan in Conventional Wastewater Treatment Plants in Five EU Countries and Their Discharge to the Aquatic Environment." *Water Science and Technology* 50 (5): 253–60.

Pedrini, Paola, Elisa Andreotti, Alessandra Guerrini, Mariangela Dean, Giancarlo Fantin, and Pier Paolo Giovannini. 2006. "Xanthomonas Maltophilia CBS 897.97 as a Source of New 7beta- and 7alpha-Hydroxysteroid Dehydrogenases and Cholylglycine Hydrolase: Improved Biotransformations of Bile Acids." *Steroids* 71 (3): 189–98. doi:10.1016/j.steroids.2005.10.002.

Peng, Xianzhi, Yiyi Yu, Caiming Tang, Jianhua Tan, Qiuxin Huang, and Zhendi Wang. 2008. "Occurrence of Steroid Estrogens, Endocrine-Disrupting Phenols, and Acid Pharmaceutical Residues in Urban Riverine Water of the Pearl River Delta, South China." *Science of The Total Environment* 397 (1–3): 158–66. doi:10.1016/j.scitotenv.2008.02.059.

Perez, Angela L., Marianna Anderle De Sylor, Andrew J. Slocombe, Mindy G. Lew, Ken M. Unice, and Ellen P. Donovan. 2013. "Triclosan Occurrence in Freshwater Systems in the United States

(1999-2012): A Meta-Analysis." *Environmental Toxicology and Chemistry* 32 (7): 1479–87. doi:10.1002/etc.2217.

Petersen, Karina, Eva Fetter, Olivier Kah, Francois Brion, Stefan Scholz, and Knut Erik Tollefsen. 2013. "Transgenic (cyp19a1b-GFP) Zebrafish Embryos as a Tool for Assessing Combined Effects of Oestrogenic Chemicals." *Aquatic Toxicology* 138 (August): 88–97. doi:10.1016/j.aquatox.2013.05.001.

Petrović, Mira, Susana Gonzalez, and Damià Barceló. 2003. "Analysis and Removal of Emerging Contaminants in Wastewater and Drinking Water." *TrAC Trends in Analytical Chemistry* 22 (10): 685–96. doi:10.1016/S0165-9936(03)01105-1.

Piwoni, Marvin, and Jack Keeley. 1990. "Basic Concepts of Contaminant Sorption at Hazardous Waste Sites." United States Environmental Protection Agency.

Poirier, Donald. 2003. "Inhibitors of 17 Beta-Hydroxysteroid Dehydrogenases." *Current Medicinal Chemistry* 10 (6): 453–77.

Providenti, M. A., J. Mampel, S. MacSween, A. M. Cook, and R. C. Wyndham. 2001. "Comamonas Testosteroni BR6020 Possesses a Single Genetic Locus for Extradiol Cleavage of Protocatechuate." *Microbiology (Reading, England)* 147 (Pt 8): 2157–67.

Qasim, Sr, and Ml Stinehelfer. 1982. "Effect of a Bacterial Culture Product on Biological Kinetics." *Journal Water Pollution Control Federation* 54 (3): 255–60.

Quintana, Jb, S Weiss, and T Reemtsma. 2005. "Pathway's and Metabolites of Microbial Degradation of Selected Acidic Pharmaceutical and Their Occurrence in Municipal Wastewater Treated by a Membrane Bioreactor." *Water Research* 39 (12): 2654–64. doi:10.1016/j.watres.2005.04.068.

Ramirez, Alejandro J., Richard A. Brain, Sascha Usenko, Mohammad A. Mottaleb, John G. O'Donnell, Leanne L. Stahl, John B. Wathen, et al. 2009. "Occurrence of Pharmaceuticals and Personal Care Products in Fish: Results of a National Pilot Study in the United States." *Environmental Toxicology and Chemistry* 28 (12): 2587–97.

Rappsilber, Juri, Matthias Mann, and Yasushi Ishihama. 2007. "Protocol for Micro-Purification, Enrichment, Pre-Fractionation and Storage of Peptides for Proteomics Using StageTips." *Nature Protocols* 2 (8): 1896–1906. doi:10.1038/nprot.2007.261.

Reasoner, D.J., and E.E. Geldreich. 1979. "A New Medium for the Enumeration and Sub Culture of Bacteria from Potable Water." *Abstracts of the Annual Meeting of the American Society for Microbiology*, no. 79: 180.

Reich-Slotky, Ronit, Christina A. Kabbash, Phyllis Della-Latta, John S. Blanchard, Steven J. Feinmark, Sherry Freeman, Gilla Kaplan, Howard A. Shuman, and Samuel C. Silverstein. 2009. "Gemfibrozil Inhibits Legionella Pneumophila and Mycobacterium Tuberculosis Enoyl Coenzyme A Reductases and Blocks Intracellular Growth of These Bacteria in Macrophages." *Journal of Bacteriology* 191 (16): 5262–71. doi:10.1128/JB.00175-09.

Roh, Hyungkeun, and Kung-Hui Chu. 2010. "A 17 Beta-Estradiol-Utilizing Bacterium, Sphingomonas Strain KC8: Part I - Characterization and Abundance in Wastewater Treatment Plants." *Environmental Science & Technology* 44 (13): 4943–50. doi:10.1021/es1001902.

———. 2011. "Effects of Solids Retention Time on the Performance of Bioreactors Bioaugmented with a 17β-Estradiol-Utilizing Bacterium, Sphingomonas Strain KC8." *Chemosphere* 84 (2): 227–33. doi:10.1016/j.chemosphere.2011.04.029.

Roh, Hyungkeun, Nethra Subramanya, Fuman Zhao, Chang-Ping Yu, Justin Sandt, and Kung-Hui Chu. 2009. "Biodegradation Potential of Wastewater Micropollutants by Ammonia-Oxidizing Bacteria." *Chemosphere* 77 (8): 1084–89. doi:10.1016/j.chemosphere.2009.08.049.

Ronen, Z., and A. Abeliovich. 2000. "Anaerobic-Aerobic Process for Microbial Degradation of Tetrabromobisphenol A." *Applied and Environmental Microbiology* 66 (6): 2372–77. doi:10.1128/AEM.66.6.2372-2377.2000.

Rosal, Roberto, Antonio Rodríguez, José Antonio Perdigón-Melón, Alice Petre, Eloy García-Calvo, María José Gómez, Ana Agüera, and Amadeo R. Fernández-Alba. 2010. "Occurrence of

Emerging Pollutants in Urban Wastewater and Their Removal through Biological Treatment Followed by Ozonation." *Water Research* 44 (2): 578–88. doi:10.1016/j.watres.2009.07.004.
Rudel, R. A., S. J. Melly, P. W. Geno, G. Sun, and J. G. Brody. 1998. "Identification of Alkylphenols and Other Estrogenic Phenolic Compounds in Wastewater, Septage, and Groundwater on Cape Cod, Massachusetts." *Environmental Science & Technology* 32 (7): 861–69. doi:10.1021/es970723r.
Saiyood, S., A. S. Vangnai, P. Thiravetyan, and D. Inthorn. 2010. "Bisphenol A Removal by the Dracaena Plant and the Role of Plant-Associating Bacteria." *Journal of Hazardous Materials* 178 (1–3): 777–85. doi:10.1016/j.jhazmat.2010.02.008.
Sakai, Kiyofumi, Hayato Yamanaka, Kunihiko Moriyoshi, Takashi Ohmoto, and Tatsuhiko Ohe. 2007. "Biodegradation of Bisphenol A and Related Compounds by Sphingomonas Sp Strain BP-7 Isolated from Seawater." *Bioscience Biotechnology and Biochemistry* 71 (1): 51–57. doi:10.1271/bbb.60351.
Salem, S., D. H. J. G. Berends, J. J. Heijnen, and M. C. M. Van Loosdrecht. 2003. "Bio-Augmentation by Nitrification with Return Sludge." *Water Research* 37 (8): 1794–1804. doi:10.1016/S0043-1354(02)00550-X.
Samaras, Vasilios G., Athanasios S. Stasinakis, Daniel Mamais, Nikolaos S. Thomaidis, and Themistokles D. Lekkas. 2013a. "Fate of Selected Pharmaceuticals and Synthetic Endocrine Disrupting Compounds during Wastewater Treatment and Sludge Anaerobic Digestion." *Journal of Hazardous Materials* 244 (January): 259–67. doi:10.1016/j.jhazmat.2012.11.039.
Sanderson, H., D. J. Johnson, C. J. Wilson, R. A. Brain, and K. R. Solomon. 2003. "Probabilistic Hazard Assessment of Environmentally Occurring Pharmaceuticals Toxicity to Fish, Daphnids and Algae by ECOSAR Screening." *Toxicology Letters* 144 (3): 383–95. doi:10.1016/S0378-4274(03)00257-1.
Sangal, Vartul, Amanda L. Jones, Michael Goodfellow, Paul A. Hoskisson, Peter Kämpfer, and Iain C. Sutcliffe. 2015. "Genomic Analyses Confirm Close Relatedness between Rhodococcus Defluvii and Rhodococcus Equi (Rhodococcus Hoagii)." *Archives of Microbiology* 197 (1): 113–16. doi:10.1007/s00203-014-1060-5.
Santos, J. L., I. Aparicio, and E. Alonso. 2007. "Occurrence and Risk Assessment of Pharmaceutically Active Compounds in Wastewater Treatment Plants. A Case Study: Seville City (Spain)." *Environment International* 33 (4): 596–601. doi:10.1016/j.envint.2006.09.014.
Sasaki, M., A. Akahira, K. I. Oshiman, T. Tsuchido, and Y. Matsumura. 2005. "Purification of Cytochrome P450 and Ferredoxin, Involved in Bisphenol A Degradation, from Sphingomonas Sp Strain AO1." *Applied and Environmental Microbiology* 71 (12): 8024–30. doi:10.1128/AEM.71.12.8024-8030.2005.
Sasaki, M., J. Maki, K. Oshiman, Y. Matsumura, and T. Tsuchido. 2005. "Biodegradation of Bisphenol A by Cells and Cell Lysate from Sphingomonas Sp Strain AO1." *Biodegradation* 16 (5): 449–59. doi:10.1007/s10532-004-5023-4.
Sauvage, Eric, Frédéric Kerff, Mohammed Terrak, Juan A. Ayala, and Paulette Charlier. 2008. "The Penicillin-Binding Proteins: Structure and Role in Peptidoglycan Biosynthesis." *FEMS Microbiology Reviews* 32 (2): 234–58. doi:10.1111/j.1574-6976.2008.00105.x.
Scheytt, T., P. Mersmann, R. Lindstadt, and T. Heberer. 2005. "1-Octanol/water Partition Coefficients of 5 Pharmaceuticals from Human Medical Care: Carbamazepine, Clofibric Acid, Diclofenac, Ibuprofen, and Propyphenazone." *Water Air and Soil Pollution* 165 (1-4): 3–11. doi:10.1007/s11270-005-3539-9.
Schmidt, Wiebke, Kathleen O'Rourke, Robert Hernan, and Brian Quinn. 2011. "Effects of the Pharmaceuticals Gemfibrozil and Diclofenac on the Marine Mussel (Mytilus Spp.) and Their Comparison with Standardized Toxicity Tests." *Marine Pollution Bulletin* 62 (7): 1389–95. doi:10.1016/j.marpolbul.2011.04.043.
Schwarzenbach, René P., Beate I. Escher, Kathrin Fenner, Thomas B. Hofstetter, C. Annette Johnson, Urs von Gunten, and Bernhard Wehrli. 2006. "The Challenge of Micropollutants in Aquatic Systems." *Science* 313 (5790): 1072–77. doi:10.1126/science.1127291.

Semrany, Samer, Lidia Favier, Hayet Djelal, Samir Taha, and Abdeltif Amrane. 2012. "Bioaugmentation: Possible Solution in the Treatment of Bio-Refractory Organic Compounds (Bio-ROCs)." *Biochemical Engineering Journal* 69 (December): 75–86. doi:10.1016/j.bej.2012.08.017.

Seo, Jong-Su, Young-Soo Keum, and Qing X. Li. 2009. "Bacterial Degradation of Aromatic Compounds." *International Journal of Environmental Research and Public Health* 6 (1): 278–309. doi:10.3390/ijerph6010278.

Servos, M. R., D. T. Bennie, B. K. Burnison, A. Jurkovic, R. McInnis, T. Neheli, A. Schnell, P. Seto, S. A. Smyth, and T. A. Ternes. 2005. "Distribution of Estrogens, 17 Beta-Estradiol and Estrone, in Canadian Municipal Wastewater Treatment Plants." *Science of the Total Environment* 336 (1-3): 155–70. doi:10.1016/j.scitotenv.2004.05.025.

Seto, M., K. Kimbara, M. Shimura, T. Hatta, M. Fukuda, and K. Yano. 1995. "A Novel Transformation of Polychlorinated Biphenyls by Rhodococcus Sp. Strain RHA1." *Applied and Environmental Microbiology* 61 (9): 3353–58.

Shannon, Paul, Andrew Markiel, Owen Ozier, Nitin S. Baliga, Jonathan T. Wang, Daniel Ramage, Nada Amin, Benno Schwikowski, and Trey Ideker. 2003. "Cytoscape: A Software Environment for Integrated Models of Biomolecular Interaction Networks." *Genome Research* 13 (11): 2498–2504. doi:10.1101/gr.1239303.

Shevchenko, A., O. N. Jensen, A. V. Podtelejnikov, F. Sagliocco, M. Wilm, O. Vorm, P. Mortensen, A. Shevchenko, H. Boucherie, and M. Mann. 1996. "Linking Genome and Proteome by Mass Spectrometry: Large-Scale Identification of Yeast Proteins from Two Dimensional Gels." *Proceedings of the National Academy of Sciences of the United States of America* 93 (25): 14440–45. doi:10.1073/pnas.93.25.14440.

Shields-Menard, Sara A., Steven D. Brown, Dawn M. Klingeman, Karl Indest, Dawn Hancock, Jayani J. Wewalwela, W. Todd French, and Janet R. Donaldson. 2014. "Draft Genome Sequence of Rhodococcus Rhodochrous Strain ATCC 21198." *Genome Announcements* 2 (1): e00054–14. doi:10.1128/genomeA.00054-14.

Shi, J., S. Fujisawa, S. Nakai, and M. Hosomi. 2004. "Biodegradation of Natural and Synthetic Estrogens by Nitrifying Activated Sludge and Ammonia-Oxidizing Bacterium Nitrosomonas Europaea." *Water Research* 38 (9): 2323–30. doi:10.1016/j.watres.2004.02.022.

Smith, G. R., and A. A. Burgett. 2005. "Effects of Three Organic Wastewater Contaminants on American Toad, Bufo Americanus, Tadpoles." *Ecotoxicology* 14 (4): 477–82. doi:10.1007/s10646-004-1352-7.

Snyder, Shane A., Samer Adham, Adam M. Redding, Fred S. Cannon, James DeCarolis, Joan Oppenheimer, Eric C. Wert, and Yeomin Yoon. 2007. "Role of Membranes and Activated Carbon in the Removal of Endocrine Disruptors and Pharmaceuticals." *Desalination* 202 (1-3): 156–81. doi:10.1016/j.desa1.2005.12.052.

Sohoni, P., C. R. Tyler, K. Hurd, J. Caunter, M. Hetheridge, T. Williams, C. Woods, et al. 2001. "Reproductive Effects of Long-Term Exposure to Bisphenol a in the Fathead Minnow (Pimephales Promelas)." *Environmental Science & Technology* 35 (14): 2917–25. doi:10.1021/es000198n.

Solyanikova, I., and L. Golovleva. 2011. "Biochemical Features of the Degradation of Pollutants by Rhodococcus as a Basis for Contaminated Wastewater and Soil Cleanup." *Microbiology* 80 (5): 591–607. doi:10.1134/S0026261711050158.

Spivack, J, T K Leib, and J H Lobos. 1994. "Novel Pathway for Bacterial Metabolism of Bisphenol A. Rearrangements and Stilbene Cleavage in Bisphenol A Metabolism." *The Journal of Biological Chemistry* 269 (10): 7323–29.

Spongberg, Alison L., Jason D. Witter, Jenaro Acuña, José Vargas, Manuel Murillo, Gerardo Umaña, Eddy Gómez, and Greivin Perez. 2011. "Reconnaissance of Selected PPCP Compounds in Costa Rican Surface Waters." *Water Research* 45 (20): 6709–17. doi:10.1016/j.watres.2011.10.004.

Stasinakis, Athanasios S., Georgia Gatidou, Daniel Mamais, Nikolaos S. Thomaidis, and Themistokles D. Lekkas. 2008. "Occurrence and Fate of Endocrine Disrupters in Greek Sewage Treatment Plants." *Water Research* 42 (6-7): 1796–1804. doi:10.1016/j.watres.2007.11.003.

Stephenson, Dianne, and Tom Stephenson. 1992. "Bioaugmentation for Enhancing Biological Wastewater Treatment." *Biotechnology Advances* 10 (4): 549–59. doi:10.1016/0734-9750(92)91452-K.

Stokes, N. A., and P. B. Hylemon. 1985. "Characterization of Delta 4-3-Ketosteroid-5 Beta-Reductase and 3 Beta-Hydroxysteroid Dehydrogenase in Cell Extracts of Clostridium Innocuum." *Biochimica Et Biophysica Acta* 836 (2): 255–61.

Stolz, Andreas. 2009. "Molecular Characteristics of Xenobiotic-Degrading Sphingomonads." *Applied Microbiology and Biotechnology* 81 (5): 793–811. doi:10.1007/s00253-008-1752-3.

Stringfellow, W. T., and L. Alvarez-Cohen. 1999. "Evaluating the Relationship between the Sorption of PAHs to Bacterial Biomass and Biodegradation." *Water Research* 33 (11): 2535–44. doi:10.1016/S0043-1354(98)00497-7.

Stumpf, Marcus, Thomas A Ternes, Rolf-Dieter Wilken, Silvana Vianna Rodrigues, and Wolfram Baumann. 1999. "Polar Drug Residues in Sewage and Natural Waters in the State of Rio de Janeiro, Brazil." *Science of The Total Environment* 225 (1–2): 135–41. doi:10.1016/S0048-9697(98)00339-8.

Sumpter, John P. 2005. "Endocrine Disrupters in the Aquatic Environment: An Overview." *Acta Hydrochimica et Hydrobiologica* 33 (1): 9–16. doi:10.1002/aheh.200400555.

Sumpter, J P, and S Jobling. 1995. "Vitellogenesis as a Biomarker for Estrogenic Contamination of the Aquatic Environment." *Environmental Health Perspectives* 103 (Suppl 7): 173–78.

Tanner, R.S. 1997. *Manual of Environmental Microbiology*. Washington, D.C.: ASM Press.

Tauxe-Wuersch, A., L. F. De Alencastro, D. Grandjean, and J. Tarradellas. 2005. "Occurrence of Several Acidic Drugs in Sewage Treatment Plants in Switzerland and Risk Assessment." *Water Research* 39 (9): 1761–72. doi:10.1016/j.watres.2005.03.003.

Tchobanoglous, George, H. David Stensel, Ryujiro Tsuchihashi, Franklin Burton, Mohammad Abu-Orf, Gregory Bowden, and William Pfrang. 2014. *Wastewater Engineering: Treatment and Resource Recovery*. 5th ed. New York: McGraw-Hill.

Telke, Amar A., Dayanand C. Kalyani, Umesh U. Jadhav, Ganesh K. Parshetti, and Sanjay P. Govindwar. 2009. "Purification and Characterization of an Extracellular Laccase from a Pseudomonas Sp LBC1 and Its Application for the Removal of Bisphenol A." *Journal of Molecular Catalysis B-Enzymatic* 61 (3-4): 252–60. doi:10.1016/j.molcatb.2009.08.001.

Ternes, T. A., M. Stumpf, J. Mueller, K. Haberer, R. D. Wilken, and M. Servos. 1999. "Behavior and Occurrence of Estrogens in Municipal Sewage Treatment Plants - I. Investigations in Germany, Canada and Brazil (vol 225, Pg 81, 1999)." *Science of the Total Environment* 228 (1): 87–87.

Ternes, Thomas A. 1998. "Occurrence of Drugs in German Sewage Treatment Plants and Rivers." *Water Research* 32 (11): 3245–60. doi:10.1016/S0043-1354(98)00099-2.

Teske, A., P. Sigalevich, Y. Cohen, and G. Muyzer. 1996. "Molecular Identification of Bacteria from a Coculture by Denaturing Gradient Gel Electrophoresis of 16S Ribosomal DNA Fragments as a Tool for Isolation in Pure Cultures." *Applied and Environmental Microbiology* 62 (11): 4210–15.

Thompson, A., P. Griffin, R. Stuetz, and E. Cartmell. 2005. "The Fate and Removal of Triclosan during Wastewater Treatment." *Water Environment Research* 77 (1): 63–67. doi:10.2175/106143005X41636.

Thorpe, Karen L., Gerd Maack, Rachel Benstead, and Charles R. Tyler. 2009. "Estrogenic Wastewater Treatment Works Effluents Reduce Egg Production in Fish." *Environmental Science & Technology* 43 (8): 2976–82. doi:10.1021/es803103c.

Topp, Edward, Sara C Monteiro, Andrew Beck, Bonnie Ball Coelho, Alistair B A Boxall, Peter W Duenk, Sonya Kleywegt, et al. 2008. "Runoff of Pharmaceuticals and Personal Care Products

Following Application of Biosolids to an Agricultural Field." *The Science of the Total Environment* 396 (1): 52–59. doi:10.1016/j.scitotenv.2008.02.011.

Toyama, Tadashi, Yusuke Sato, Daisuke Inoue, Kazunari Sei, Young-Cheol Chang, Shintaro Kikuchi, and Michihiko Ike. 2009. "Biodegradation of Bisphenol A and Bisphenol F in the Rhizosphere Sediment of Phragmites Australis." *Journal of Bioscience and Bioengineering* 108 (2): 147–50. doi:10.1016/j.jbiosc.2009.03.011.

Tsai, Wen-Tien. 2006. "Human Health Risk on Environmental Exposure to Bisphenol-A: A Review." *Journal of Environmental Science and Health Part C-Environmental Carcinogenesis & Ecotoxicology Reviews* 24 (2): 225–55. doi:10.1080/10590500600936482.

Tyagi, Meenu, M. Manuela R. da Fonseca, and Carla C. C. R. de Carvalho. 2011. "Bioaugmentation and Biostimulation Strategies to Improve the Effectiveness of Bioremediation Processes." *Biodegradation* 22 (2): 231–41. doi:10.1007/s10532-010-9394-4.

Urlacher, Vlada B, and Marco Girhard. 2012. "Cytochrome P450 Monooxygenases: An Update on Perspectives for Synthetic Application." *Trends in Biotechnology* 30 (1): 26–36. doi:10.1016/j.tibtech.2011.06.012.

U.S. EPA. 2010. "Nutrient Control Design Manual, EPA/600/R-10/100." Office of Research and Development/National Risk Management Research Laboratory, U.S. Environmental Protection Agency, Cincinnati, OH.

van der Geize, Robert, and Lubbert Dijkhuizen. 2004. "Harnessing the Catabolic Diversity of Rhodococci for Environmental and Biotechnological Applications." *Current Opinion in Microbiology* 7 (3): 255–61. doi:10.1016/j.mib.2004.04.001.

van der Linde, K., B. T. Lim, J. M. Rondeel, L. P. Antonissen, and G. M. de Jong. 1999. "Improved Bacteriological Surveillance of Haemodialysis Fluids: A Comparison between Tryptic Soy Agar and Reasoner's 2A Media." *Nephrology, Dialysis, Transplantation: Official Publication of the European Dialysis and Transplant Association - European Renal Association* 14 (10): 2433–37.

Van Limbergen, H., E. M. Top, and W. Verstraete. 1998. "Bioaugmentation in Activated Sludge: Current Features and Future Perspectives." *Applied Microbiology and Biotechnology* 50 (1): 16–23.

Wang, L. Y., X. H. Zhang, and N. F. Y. Tam. 2010. "Analysis and Occurrence of Typical Endocrine-Disrupting Chemicals in Three Sewage Treatment Plants." *Water Science and Technology* 62 (11): 2501–9. doi:10.2166/wst.2010.533.

Wattam, Alice R., David Abraham, Oral Dalay, Terry L. Disz, Timothy Driscoll, Joseph L. Gabbard, Joseph J. Gillespie, et al. 2013. "PATRIC, the Bacterial Bioinformatics Database and Analysis Resource." *Nucleic Acids Research*, November, gkt1099. doi:10.1093/nar/gkt1099.

Wattiau, P., L. Bastiaens, R. van Herwijnen, L. Daal, J. R. Parsons, M. E. Renard, D. Springael, and G. R. Cornelis. 2001. "Fluorene Degradation by Sphingomonas Sp. LB126 Proceeds through Protocatechuic Acid: A Genetic Analysis." *Research in Microbiology* 152 (10): 861–72.

Westerhoff, P., Y. Yoon, S. Snyder, and E. Wert. 2005a. "Fate of Endocrine-Disruptor, Pharmaceutical, and Personal Care Product Chemicals during Simulated Drinking Water Treatment Processes." *Environmental Science & Technology* 39 (17): 6649–63. doi:10.1021/es0484799.

Wett, B., J. A. Jimenez, I. Takács, S. Murthy, J. R. Bratby, N. C. Holm, and S. G. E. Rönner-Holm. 2011. "Models for Nitrification Process Design: One or Two AOB Populations?" *Water Science and Technology: A Journal of the International Association on Water Pollution Research* 64 (3): 568–78.

"What Are Endocrine Disruptors?| Endocrine Disruptor Screening Program | US EPA." 2014. Accessed April 28. http://www.epa.gov/endo/pubs/edspoverview/whatare.htm.

Wilderer, Pa, Ma Rubio, and L. Davids. 1991. "Impact of the Addition of Pure Cultures on the Performance of Mixed Culture Reactors." *Water Research* 25 (11): 1307–13. doi:10.1016/0043-1354(91)90108-3.

Wilson, BA, VH Smith, F Denoyelles, and CK Larive. 2003. "Effects of Three Pharmaceutical and Personal Care Products on Natural Freshwater Algal Assemblages." *Environmental Science & Technology* 37 (9): 1713–19. doi:10.1021/es0259741.

Wissenbach, Dirk K., Markus R. Meyer, Daniela Remane, Armin A. Weber, and Hans H. Maurer. 2011. "Development of the First Metabolite-Based LC-MS N Urine Drug Screening Procedure-Exemplified for Antidepressants." *Analytical and Bioanalytical Chemistry* 400 (1): 79–88. doi:10.1007/s00216-010-4398-9.

Wu, Chenxi, Xiaolong Huang, Jason D. Witter, Alison L. Spongberg, Kexiong Wang, Ding Wang, and Jiantong Liu. 2014. "Occurrence of Pharmaceuticals and Personal Care Products and Associated Environmental Risks in the Central and Lower Yangtze River, China." *Ecotoxicology and Environmental Safety* 106 (August): 19–26. doi:10.1016/j.ecoenv.2014.04.029.

Xia, K., A. Bhandari, K. Das, and G. Pillar. 2005. "Occurrence and Fate of Pharmaceuticals and Personal Care Products (PPCPs) in Biosolids." *Journal of Environmental Quality* 34 (1): 91–104.

Xiong, Guangming, Yijing Luo, Saihong Jin, and Edmund Maser. 2009. "Cis- and Trans-Regulatory Elements of 3alpha-Hydroxysteroid Dehydrogenase/carbonyl Reductase as Biosensor System for Steroid Determination in the Environment." *Chemico-Biological Interactions* 178 (1-3): 215–20. doi:10.1016/j.cbi.2008.10.012.

Yamanaka, Hayato, Kunihiko Moriyoshi, Takashi Ohmoto, Tatsuhiko Ohe, and Kiyofumi Sakai. 2007. "Degradation of Bisphenol A by Bacillus Pumilus Isolated from Kimchi, a Traditionally Fermented Food." *Applied Biochemistry and Biotechnology* 136 (1): 39–51. doi:10.1007/BF02685937.

———. 2008. "Efficient Microbial Degradation of Bisphenol a in the Presence of Activated Carbon." *Journal of Bioscience and Bioengineering* 105 (2): 157–60. doi:10.1263/jbb.105.157.

Yang, Xin, Riley C. Flowers, Howard S. Weinberg, and Philip C. Singer. 2011. "Occurrence and Removal of Pharmaceuticals and Personal Care Products (PPCPs) in an Advanced Wastewater Reclamation Plant." *Water Research* 45 (16): 5218–28. doi:10.1016/j.watres.2011.07.026.

Yan, Qing, Xu Gao, You-Peng Chen, Xu-Ya Peng, Yi-Xin Zhang, Xiu-Mei Gan, Cheng-Fang Zi, and Jin-Song Guo. 2014. "Occurrence, Fate and Ecotoxicological Assessment of Pharmaceutically Active Compounds in Wastewater and Sludge from Wastewater Treatment Plants in Chongqing, the Three Gorges Reservoir Area." *Science of the Total Environment* 470 (February): 618–30. doi:10.1016/j.scitotenv.2013.09.032.

Ye, Lin, and Tong Zhang. 2013. "Bacterial Communities in Different Sections of a Municipal Wastewater Treatment Plant Revealed by 16S rDNA 454 Pyrosequencing." *Applied Microbiology and Biotechnology* 97 (6): 2681–90. doi:10.1007/s00253-012-4082-4.

Ying, Guang-Guo, and Rai S. Kookana. 2007. "Triclosan in Wastewaters and Biosolids from Australian Wastewater Treatment Plants." *Environment International* 33 (2): 199–205. doi:10.1016/j.envint.2006.09.008.

Yoshimoto, T, F Nagai, J Fujimoto, K Watanabe, H Mizukoshi, T Makino, K Kimura, H Saino, H Sawada, and H Omura. 2004. "Degradation of Estrogens by Rhodococcus Zopfii and Rhodococcus Equi Isolates from Activated Sludge in Wastewater Treatment Plants." *Applied and Environmental Microbiology* 70 (9): 5283–89. doi:10.1128/AEM.70.9.5283-5289.2004.

Yu, Chang-Ping, Hyungkeun Roh, and Kung-Hui Chu. 2007a. "17 Beta-Estradiol-Degrading Bacteria Isolated from Activated Sludge." *Environmental Science & Technology* 41 (2): 486–92. doi:10.1021/es060923f.

Yu, Jimmy C., T. Y. Kwong, Q. Luo, and Zongwei Cai. 2006. "Photocatalytic Oxidation of Triclosan." *Chemosphere* 65 (3): 390–99. doi:10.1016/j.chemosphere.2006.02.011.

Yu Yeh, R. -Li, and Yung-Tse Hung. 1988. "Bio-Augmented Activated Sludge Treatment of Potato Wastewaters." *Acta Hydrochimica et Hydrobiologica* 16 (2): 213–20. doi:10.1002/aheh.19880160214.

Yu, Yiyi, Qiuxin Huang, Zhifang Wang, Kun Zhang, Caiming Tang, Jianlan Cui, Jialiang Feng, and Xianzhi Peng. 2011. "Occurrence and Behavior of Pharmaceuticals, Steroid Hormones, and Endocrine-Disrupting Personal Care Products in Wastewater and the Recipient River Water of the Pearl River Delta, South China." *Journal of Environmental Monitoring* 13 (4): 871–78. doi:10.1039/C0EM00602E.

Zhang, Chang, Guangming Zeng, Li Yuan, Jian Yu, Jianbing Li, Guohe Huang, Beidou Xi, and Hongliang Liu. 2007. "Aerobic Degradation of Bisphenol A by Achromobacter Xylosoxidans Strain B-16 Isolated from Compost Leachate of Municipal Solid Waste." *Chemosphere* 68 (1): 181–90. doi:10.1016/j.chemosphere.2006.12.012.

Zhang, Hao, Ye Ji, Yan Wang, Xiao Zhang, and Yuanhua Yu. 2015. "Cloning and Characterization of a Novel Beta-Ketoacyl-ACP Reductase from Comamonas Testosteroni." *Chemico-Biological Interactions* 234 (June): 213–20. doi:10.1016/j.cbi.2015.01.003.

Zhang, Weiwei, Kun Yin, and Lingxin Chen. 2013a. "Bacteria-Mediated Bisphenol A Degradation." *Applied Microbiology and Biotechnology* 97 (13): 5681–89. doi:10.1007/s00253-013-4949-z.

Zhang, Yingying, Cong Yuan, Guojun Hu, Meng Li, Yao Zheng, Jiancao Gao, Yanping Yang, Ying Zhou, and Zaizhao Wang. 2013. "Characterization of Four nr5a Genes and Gene Expression Profiling for Testicular Steroidogenesis-Related Genes and Their Regulatory Factors in Response to Bisphenol A in Rare Minnow Gobiocypris Rarus." *General and Comparative Endocrinology* 194 (December): 31–44. doi:10.1016/j.ygcen.2013.08.014.

Zhang, Zhaohan, Yujie Feng, Peng Gao, Ce Wang, and Nanqi Ren. 2011. "Occurrence and Removal Efficiencies of Eight EDCs and Estrogenicity in a STP." *Journal of Environmental Monitoring* 13 (5): 1366–73. doi:10.1039/c0em00597e.

Zhou, Nicolette A., Henrik Kjeldal, Heidi L. Gough, and Jeppe L. Nielsen. 2015. "Identification of Putative Genes Involved in Bisphenol A Degradation Using Differential Protein Abundance Analysis of Sphingobium Sp. BiD32." *Environmental Science & Technology* 49 (20): 12232–41. doi:10.1021/acs.est.5b02987.

Zhou, Nicolette A., April C. Lutovsky, Greta L. Andaker, John F. Ferguson, and Heidi L. Gough. 2014. "Kinetics Modeling Predicts Bioaugmentation with Sphingomonad Cultures as a Viable Technology for Enhanced Pharmaceutical and Personal Care Products Removal during Wastewater Treatment." *Bioresource Technology* 166 (August): 158–67. doi:10.1016/j.biortech.2014.05.028.

Zhou, Nicolette A, April C Lutovsky, Greta L Andaker, Heidi L Gough, and John F Ferguson. 2013. "Cultivation and Characterization of Bacterial Isolates Capable of Degrading Pharmaceutical and Personal Care Products for Improved Removal in Activated Sludge Wastewater Treatment." *Biodegradation* 24 (6): 813–27. doi:10.1007/s10532-013-9630-9.

Zhou, Yiqi, Jinmiao Zha, and Zijian Wang. 2012. "Occurrence and Fate of Steroid Estrogens in the Largest Wastewater Treatment Plant in Beijing, China." *Environmental Monitoring and Assessment* 184 (11): 6799–6813. doi:10.1007/s10661-011-2459-y.

Zhu, Wenhong, Jeffrey W. Smith, and Chun-Ming Huang. 2010. "Mass Spectrometry-Based Label-Free Quantitative Proteomics." *Journal of Biomedicine and Biotechnology*. doi:10.1155/2010/840518.

Zorita, Saioa, Lennart Martensson, and Lennart Mathiasson. 2009. "Occurrence and Removal of Pharmaceuticals in a Municipal Sewage Treatment System in the South of Sweden." *Science of the Total Environment* 407 (8): 2760–70. doi:10.1016/j.scitotenv.2008.12.030.

APPENDIX A: PERSISTENCE OF *SPHINGOBIUM* SP. BID32 BIOAUGMENTED IN LABORATORY REACTORS

10.1 Chapter summary

This chapter focuses on exploring observations made while testing Objective III: testing the feasibility of bioaugmentation to improve TOrC removal in lab scale reactors. As reported in Chapter 6, BPA degradation activity was lost over time, though *Sphingobium* sp. BiD32 16S rRNA gene were observed to persist over the long-term. *Sphingobium* sp. BiD32 16S rRNA gene concentrations were monitored in the lab scale reactors and *Sphingobium* sp. BiD32 was found to accumulate in the bioaugmented reactor following two weeks of daily bioaugmentation. Therefore, this study examines the loss of *Sphingobium* sp. BiD32 and the viability of *Sphingobium* sp. BiD32 remaining in the test reactor at the end of cycle 8. Viable *Sphingobium* sp. BiD32 were detected in the test reactor at the end of cycle 8 (23 hours after bioaugmentation; 30% of the detected *Sphingobium* sp. BiD32 were viable and 0.04% of the *Sphingobium* sp. BiD32 at the beginning of cycle 1). As *Sphingobium* sp. BiD32 was still present in the reactor, the hypothesis was tested that *Sphingobium* sp. BiD32 was incorporated into the activated sludge flocs, which may result in diffusion limitation of the BPA. However, disrupting the activated sludge flocs did not result in improved BPA removal, in disagreement with this hypothesis. Using the information from this study, it is now hypothesized that the *Sphingobium* sp. BiD32 remaining in the reactor at the end of cycle 8 may still be capable of degrading BPA, however the percent remaining is too low to improve the BPA removal. Understanding the fate of the augmented bacteria would be important when implementing bioaugmentation at WWTPs, to ensure that enough bacteria is present in the system to achieve desired TOrC effluent concentrations, but not too much bacteria is augmented that it affects the operation of the plant.

10.2 Introduction

Enhanced Biological TOrC Removal (EBTCR) has been proposed as a technological approach to improve trace organic contaminant (TOrC) removal efficiencies in wastewater treatment plants (WWTP) (Zhou et al. 2014, Chapter 6). These contaminants enter surface waters through discharge of WWTP effluents, and can negative effects on aquatic life (Zhang et al. 2013; Baek et al. 2003; Oehlmann et al. 2006; Sohoni et al. 2001). TOrCs are partially removed using traditional secondary wastewater treatment (Samaras et al. 2013b; Snyder et al. 2007; Nakada et al. 2006; Ternes et al. 1999), however new technologies must be developed to improve the removal of TOrCs. During EBTCR, bacteria with known TOrCs degradation capabilities are continuously bioaugmented from a side growth reactor into the activated sludge process. As TOrCs are biologically removed, bioaugmentation seems to be a low-impact approach for increasing their removal. Modeling has previously documented the potential effectiveness of EBTCR using known TOrCs-degrading pure cultures (Zhou et al. 2014) and Chapter 6 demonstrated the potential of EBTCR in a lab-scale reactor study. However, questions remain about the fate of the bacteria augmented into the reactors.

Success of bioaugmentation relies both on survival of bioaugmented bacteria, and expression of degradation genes. While early bioaugmentation studies showed improved TOrCs removal, they also found rapid loss of the augmented bacteria and/or TOrC degradation activity (Hashimoto et al. 2010; Roh and Chu 2011, Chapter 6). While these studies suggested that continuous bioaugmentation is necessary to maintain improved TOrCs removal, it is also important to understand the loss of the augmented bacteria and its associated TOrCs degradation activity. Bacteria may be consumed by rotifiers and protozoa or may die through endogenous decay. Even when the host bacteria persists, the TOrCs degradation activity may be lost due to loss of the degradation genes, gene inactivation, or cell dormancy. Understanding the loss of the bacteria and the degradation activity will allow improved determination of bioaugmention doses required to achieve desired TOrCs removal.

The objective of this study was to investigate two potential mechanisms that might explain why enhanced BPA removal was lost with time in bioaugmented lab-scale reactors when *Sphingobium* sp. BiD32 was still detected. First, the viability of *Sphingobium* sp. BiD32 was assessed by comparing detected 16S rRNA gene concentrations monitored using qPCR and to the signal from intact cells using propidium monoazide (PMA)-qPCR. PMA is a cell membrane-impermeable dye, allowing one to measure DNA from viable bacteria only when combined with qPCR (Nocker et al. 2006). Second, the potential for *Sphingobium* sp. BiD32 incorporation into flocs limiting access to BPA in the bulk liquid was tested by evaluating BPA degradation capacity when the bacteria were released from the flocs, and by developing

fluorescent in situ hybridization (FISH) protocols to visualize the association between *Sphingobium* sp. BiD32 and the activated sludge flocs. The study results showed that a small percentage of the augmented *Sphingobium* sp. BiD32 remained viable at the end of cycle 8, and refinement of the FISH method is required to further assess if the *Sphingobium* sp. BiD32 has been incorporated into the flocs; however, releasing bacteria from flocs did not improve their ability to degrade BPA and the remaining *Sphingobium* sp. BiD32 was likely at too low of a concentration to improve BPA removal.

10.3 Materials and methods

10.3.1 Laboratory reactor operation

Two (2) lab scale sequencing batch reactors (SBR) operated as part of studies in Chapter 6 were used as test materials for this study. The SBRs were had 3-hour cycles consisting of the following steps: Step 1 feeding (5 minute), Step 2 anoxic mixing (25 minutes), Step 3 aerated reaction (90 minutes), Step 4 settling (45 minutes), and Step 5 decanting (15 minutes). The SBRs were manually wasted at the end of an aeration period once each day to maintain an 8 day or 3 day solids retention time (SRT). *Sphingobium* sp. BiD32 was bioaugmented into the test reactor and *Sphingopyxis* sp. TrD1 was bioaugmented into the control reactor each day at the start of cycle 1 as previously described (Chapter 6) resulting in a concentration of 15.1 mg/L ± 2.7 (n=76) of *Sphingobium* sp. BiD32 and 17.5 mg/L ± 3.7 (n=75) *Sphingopyxis* sp. TrD1.

10.3.2 Bacterial concentrations

10.3.2.1.1 qPCR

Sphingobium sp. BiD32 16S rRNA gene concentrations were measured by qPCR. DNA was extracted using the MO BIO UltraClean Microbial DNA Isolation Kit (MO BIO Laboratories, Inc., Carlsbad, CA, USA). The manufacturer's instructions were followed with two modifications: the samples were heated (65ºC, 10 min) to increase the yield (an optional step suggested by the manufacturer) and the samples were agitated for 20 seconds at speed 4.0 in a cell homogenizer (FastPrep®-24 Instrument; MP Biomedicals, Inc, Solon, OH, USA). Extracts were evaluated using a NanoDrop 1000 spectrophotometer (NanoDrop Technologies, Wilmington, DE, USA) to determine the quality and concentration of the DNA. A 260:280 ratio between 1.7 and 1.9 was considered to be acceptable, and the concentration was determined at 260 nm.

Primers for detection of *Sphingobium* sp. BiD32 16S rRNA gene concentrations were designed using NCBI Primer-BLAST (http://www.ncbi.nlm.nih.gov/tools/primer-blast/) and purchased from Invitrogen (Invitrogen, Carlsbad, CA, USA). The primers are summarized in Table 10.1. The primers matched 100%

to *Sphingobium* sp. BiD32 and to five closely related sequences including uncultured soil bacterium clones, *Sphingomonas* sp. B1-105, and *Sphingomonas* sp. A1-13. The forward primer had greater than 6 mismatches, insertions, or deletions compared to *Sphingopyxis* sp. TrD1 and the reverse primer had one mismatch.

Table 10.1. Primers used for PCR reactions

Target Organisms	Primer	Sequence	Tm	GC (%)
Primers used for qPCR				
Sphingobium sp. BiD32[1]	65F	5'-AACGATCCCTTCGGGGATA-3'	60.2	52.6
	268R	5'-TAAGGATCGTTGCCTTGGTGA-3'	60.6	47.6
Primers used for cloning reactions				
Bacteria[2]	8F	5'-AGAGTTTGATCCTGGCTAG-3'		
	1492R	5'-TTCCGGTTGATCCYGCCGGA-3'		

[1]These primers were designed for this study

[2] Delong, EF. 1992. "Archaea in Coastal Marine Environments." *Proceedings of the National Academy of Sciences of the United States of America* 89 (12): 5685–89. doi:10.1073/pnas.89.12.5685.

Standards for *Sphingobium* sp. BiD32 qPCR and *Sphingobium* sp. BiD32 and *Sphingopyxis* sp. TrD1 negative controls were prepared using the PCR product of their 16S rRNA genes, which were generated using Bacterial primers 8F and 1492R. The PCR product was cloned using a TOPO TA Cloning Kit (Invitrogen Molecular Probes, Grand Island, NY, USA). Plasmids were isolated by QIAprep Spin Miniprep Kit (Qiagen, Valencia, CA, USA), quantified using a NanoDrop 1000 spectrophotometer (NanoDrop Technologies, Wilmington, DE, USA), and linearized by the restriction enzyme EcoRI (R6011, Promega Corporation, Madison, WI, USA).

qPCR analysis was performed using an Eppendorf MasterCycler Realplex (Eppendorf North America, Inc., Westbury, NY, USA) and GoTaq qPCR Master Mix (Promega Corporation, Madison, WI, USA). The PCR program was as follows: hot-start activation (95ºC for 10 minutes), 50 cycles of denaturation (95ºC for 15 seconds), annealing (65ºC for 1 minute), and extension (60ºC for 1 minute), and dissociation (95ºC for 15 seconds). Each DNA extract was processed at a tenfold and hundredfold dilution to evaluate for potential PCR inhibition.

A standard curve was generated using tenfold dilutions of the linearized plasmids (linearized using EcoRI). A representative standard curve is shown as Supplemental Figure 10.9. The resulting standard curve for *Sphingobium* sp. BiD32 had an average efficiency of 0.70 (R^2=0.958) with a method detection limit of 8.18×10^3 16S rRNA gene copies per PCR reaction (i.e. the lowest standard applied, which amplified circa cycle ~31.5, n=15). Negative controls included the closely related organisms *Sphingobium* sp. BiD10 (7.5×10^7 16S rRNA gene copies added per PCR reaction, cycle threshold ~32.3,

n=17), *Sphingopyxis* sp. TrD1 ($6.7x10^7$ 16S rRNA gene copies added per PCR reaction, cycle threshold ~31.7, n=14), and a water blank (rarely amplified, cycle threshold ~38.1, n=8).

10.3.2.1.2 Propidium monoazide-qPCR

PMA-qPCR was used to determine if augmented biomass was alive at the end of 8 cycles, using previously described methods (Nocker et al. 2006). Two (2) mL samples were collected at the end of the eighth cycle and processed as follows: samples were centrifuged (10,000 ×g, 10 minutes), decanted, washed with 1.8 mL phosphate buffered saline (PBS), centrifuged (10,000 ×g, 10 minutes), decanted, resuspended in 1.8 mL PBS (mixed by pipetting), and split into two tubes. Half of the sample was centrifuged (10,000 ×g, 10 minutes), decanted, and stored at -20ºC until DNA extraction. 50 µM PMA was added to the other half of the sample to destroy extracellular DNA or DNA in cells with permeable membranes. The samples with PMA were incubated while shaking in the dark for 15 minutes. They were then incubated shaking, on ice, 20 cm away from a 650 W halogen light for 15 minutes to destroy the PMA. The samples were then centrifuged (10,000 ×g, 10 minutes), decanted, and stored at -20ºC until DNA extraction. DNA extraction and qPCR were completed as described above. Controls measuring the total Bacteria 16S rRNA gene by qPCR with the primers 8F and 1492R were completed with 100% autoclaved activated sludge, 50% autoclaved/50% fresh activated sludge, and 100% fresh activated sludge. Controls measuring the *Sphingobium* sp. BiD32 16S rRNA gene were completed with fresh *Sphingobium* sp. BiD32 inoculated into fresh activated sludge and autoclaved *Sphingobium* sp. BiD32 inoculated into fresh activated sludge.

10.3.3 Kinetics of augmented bacteria

The rate of change in augmented bacterial concentrations was calculated as:

$$\frac{dX}{dt} = -k_X X \qquad \text{(Eq 10.1)}$$

where dX/dt was the rate of change of the augmented bacteria (mg/L-hr), k_X was the net loss rate (hr^{-1}), and X was the augmented bacterial concentration (mg/L). The net loss includes growth, endogenous decay, and predation.

Sphingobium sp. BiD32 concentrations were monitored in the bioaugmented reactor using qPCR. Eq 10.1 was integrated and linearized as:

$$lnX = -k_X t + lnX_0 \qquad \text{(Eq 10.2)}$$

The equation was solved graphically and the y-intercept was $\ln X_0$ and the slope was k_X.

10.3.4 Prediction of Sphingobium sp. BiD32 and BPA concentrations in reactors

Loss of *Sphingobium* sp. BiD32 in the bioaugmented reactor was predicted using Eqs 10.3 and 10.4 for each cycle. The rate of bacterial loss was calculated using Eq 10.1. Eq 10.1 was then integrated and linearized as:

$$lnX_{1,1} = -k_X t + lnX_{1,0} \quad \text{(Eq 10.3)}$$

where $X_{1,0}$ was the *Sphingobium* sp. BiD32 concentration at the beginning of cycle 1 (mg/L), $X_{1,1}$ was the *Sphingobium* sp. BiD32 concentration at the end of cycle 1 reaction period (mg/L), and t was reaction time (hr). Using the k_X calculated above and the known $X_{1,0}$ in the bioaugmented reactor (14.8 mg/L), $X_{1,1}$ was calculated over the period of a single cycle (t=1.5 hr).

The loss of *Sphingobium* sp. BiD32 due to wasting and decanting was calculated by:

$$X_{2,0} = X_{1,1} - X_{1,1}\frac{V_w}{V} - X_{1,1}\frac{VSS_e}{VSS}\frac{V_e}{V} \quad \text{(Eq 10.4)}$$

where $X_{2,0}$ was the *Sphingobium* sp. BiD32 concentration at the beginning of cycle 2 (mg/L), V_w was the volume wasted (12.5 mL), V was the total volume (950 mL), VSS_e was the biomass in the effluent (9 mg/L), VSS was the biomass in the reactor (1270 mg/L), and V_e was the effluent volume (225 mL).

The BPA concentrations in the bioaugmented reactor were then predicted using the calculated *Sphingobium* sp. BiD32 concentrations (Eq 10.3 and 10.4) for each cycle by:

$$\frac{c_T}{c_{T,0}} = exp(-k_{cT}t) \quad \text{(Eq 10.5)}$$

where c_T was the total BPA concentration (µg/L), $c_{T,0}$ was the initial BPA concentration (µg/L), k_{cT} was the total degradation rate (hr^{-1}), and t was the reaction time (1.5 hr).

k_{cT} was calculated by:

$$k_{cT} = (k_c'X + k_{AS}'VSS)f_L \quad \text{(Eq 10.6)}$$

where k_c' was the specific BPA degradation rate by *Sphingobium* sp. BiD32 (0.06 L/mg-hr), X was the *Sphingobium* sp. BiD32 biomass predicted for each cycle (mg/L) from Eq 10.4, k_{AS}' was the specific BPA degradation rate by the background activated sludge (0.00023 L/mg-hr), and VSS was the activated sludge biomass (1270 mg/L), and f_L was the BPA in the liquid fraction (calculated as $1/(1+K_P(VSS+X))$ (Zhou et al. 2014)).

10.3.5 Disruption of flocs

Activated sludge flocs were disrupted to determine if release from flocs would improve BPA removal activity. Waste activated sludge was collected from the bioaugmented and control reactors at the end of

cycle 8. Half of the collected waste sludge was blended for 5 minutes in a standard kitchen blender on high. Disruption of the flocs was confirmed visually and microscopically. Approximately 100 µg/L BPA was spiked into the blended and untreated sludge from both reactors. Experimental flasks were aerated and mixed using a magnetic stir bar. BPA concentrations were monitored over 1.5 hours using an LC-MS/MS (method described in Chapter 4).

10.3.6 FISH

Fluorescent in-situ hybridization (FISH) methods were developed to test if *Sphingobium* sp. BiD32 was incorporating into activated sludge flocs. Two test probes specific to *Sphingobium* sp. BiD32 were designed using NCBI/Primer-BLAST (http://www.ncbi.nlm.nih.gov/tools/primer-blast/). These probes targeted regions of the 16S rRNA previously identified as best for FISH hybridization (Fuchs et al. 1998). Designed probes are shown in Table 10.2 and labeled with CY3. Probes used to measure Bacteria were EUB338, EUB338II, and EUB338III labeled with CY5 (Amann et al. 1990).

Table 10.2. FISH probes for *Sphingobium* sp. BiD32

E. Coli position	Sequence	GC content (%)	Tm (ºC)	$[FA]_m$[a]	HE[a]
40	5'-TCGTTCGACTGCATGTATTAGG-3'	45.5	60.8	28.1	0.9998
1412	5'-GCGAATCCAAATGGAGCG-3'	55.6	59.9	15.3	0.9629

$[FA]_m$, Melting formamide concentration where half of the target molecules are hybridized at Tm
HE, Hybridization efficiency with no formamide
[a] Calculate from mathfish.cee.wisc.edu

The FISH protocol was as follows: wasted sludge from the SBR was allowed to settle by gravity for 45 minutes, 0.5 mL of settled flocs were fixed by washing twice with 9 mL of PBS, adding 9 mL of 4.4% paraformaldehyde in PBS, incubating for 2 hours, washing three times with 9 mL PBS, and washing with 30% ethanol, 50% ethanol, and 70% ethanol. When washing, samples were gently centrifuged as to not disturb the flocs (750 ×g, 2 minutes). Samples were stored in 70% ethanol at -20ºC. Hybridization was completed by evaporating approximately 10 µL of the samples in each well of a multi-well slide, adding 10 µL of hybridization buffer with 0.83 pmol probe into each well, placing the slides into humidity chambers, and incubating for 1.5 hours at 46ºC. The slides were then washed for 20 minutes at 48ºC, rinsed in MilliQ water, and had Vectashield (Vector Laboratories, Inc., Burlingame, CA, USA) applied to each well.

10.4 Results and discussion

10.4.1 Persistence of Sphingobium sp. BiD32 in lab scale reactors

Sphingobium sp. BiD32 concentrations increased in the bioaugmented reactor by 1000x over approximately two weeks after the start of bioaugmentation (Figure 10.1). *Sphingobium* sp. BiD32 remained below detection in the control reactor. While *Sphingobium* sp. BiD32 was still detected in the test reactor at the end of the 8th cycle (Figure 10.1, open circles), it was 2.3% of the amount measured after augmentation at the beginning of cycle 1 (Figure 10.1, closed squares). Persistence of *Sphingobium* sp. BiD32 in the bioaugmented reactor was not an expected outcome.

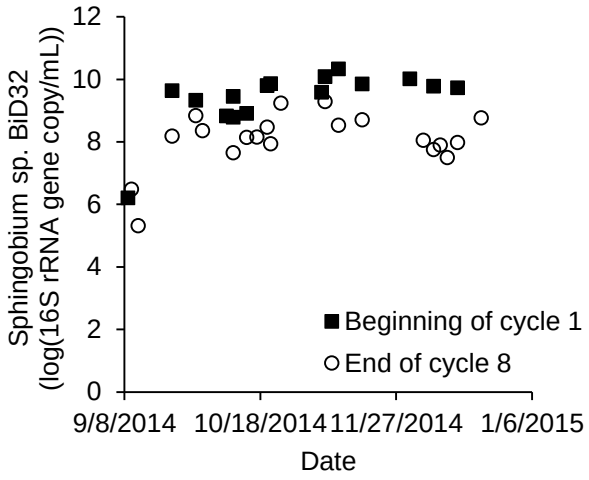

Figure 10.1. Log of *Sphingobium* sp. BiD32 16S rRNA gene concentrations in the bioaugmented reactor after bioaugmenting (cycle 1; closed squares) and at the end of the cycle prior to bioaugmentation (cycle 8; open circles) when operating at an 8-day SRT.

On the first day of bioaugmentation, *Sphingobium* sp. BiD32 16S rRNA gene concentrations decreased after bioaugmentation (as expected) by two orders of magnitude (Figure 10.2, closed circles). However, after three weeks of daily bioaugmentation with *Sphingobium* sp. BiD32, the concentrations of the 16S rRNA gene remaining in the system were too high and obscured attempts to visualize the fate of recently augmented bacteria (Figure 10.2, open markers). The concentrations may be high due to DNA remaining in the system from dead *Sphingobium* sp. BiD32 or from accumulation of *Sphingobium* sp. BiD32 after weeks of bioaugmentation.

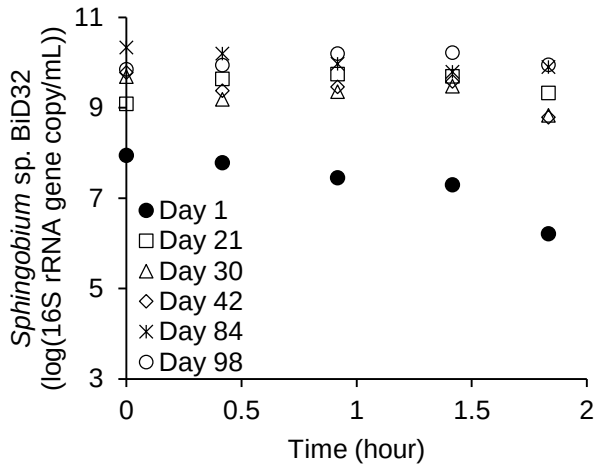

Figure 10.2. Log of *Sphingobium* sp. BiD32 16S rRNA gene concentrations versus time during cycle 1 after daily feeding of *Sphingobium* sp. BiD32 beginning on Day 1. Subsequent days represent other experimental periods.

Sphingobium sp. BiD32 16S rRNA gene concentrations were measured using PMA-qPCR to determine if the persistence of *Sphingobium* sp. BiD32 was due to residual DNA present in the reactor rather than due to persistence of viable *Sphingobium* sp. BiD32. To validate the PMA-qPCR method, *Sphingobium* sp. BiD32 16S rRNA gene concentrations were measured in samples from the control reactor (no *Sphingobium* sp. BiD32 present) with autoclaved and viable *Sphingobium* sp. BiD32 augmented into replicates. In the sample with autoclaved *Sphingobium* sp. BiD32, the 16S rRNA gene was not amplified by PMA-qPCR (amplified at cycle 31). In the sample with the viable *Sphingobium* sp. BiD32, the 16S rRNA gene was amplified at expected concentrations.

The PMA-qPCR method was applied to samples drawn from the test reactor at the end of cycle 8. Viable *Sphingobium* sp. BiD32 was detected at the end of cycle 8 (Figure 10.3). The 16S rRNA gene concentration from all *Sphingobium* sp. BiD32 (measured by qPCR) was statistically different from the 16S rRNA gene concentration from viable *Sphingobium* sp. BiD32 (measured by PMA-qPCR) (p=0.002, t-test, n=5). This confirmed that some of the signal detected by qPCR in Figure 10.2 was not viable *Sphingobium* sp. BiD32. 29.7% of *Sphingobium* sp. BiD32 as measured by qPCR at the end of cycle 8 was determined to be viable by PMA-qPCR at the end of cycle 8. Also, 0.14% of the *Sphingobium* sp. BiD32 measured after augmentation at the beginning of cycle 1 was determined to be viable at the end of cycle 8.

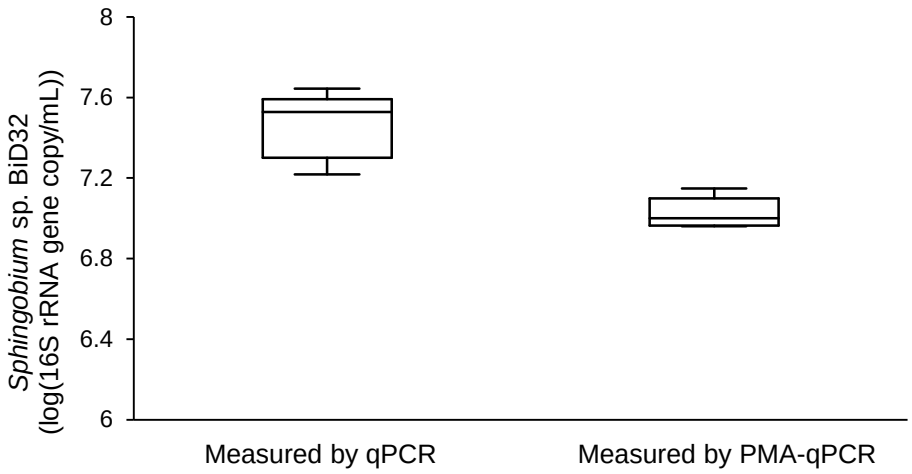

Figure 10.3. *Sphingobium* sp. BiD32 16S rRNA gene concentrations at the end of cycle 8 on day 185 (n=5). The middle line shows the median concentration, the box shows the first through third quartile, and the errors bars show the range of the concentrations.

10.4.2 Predicted Sphingobium sp. BiD32 and BPA concentrations in reactors

To determine if the loss of *Sphingobium* sp. BiD32 due to predation could explained the loss of enhanced BPA removal, the loss rates determined during batch experiments (Figure 10.4a; 0.16 hr^{-1}) and from the first day of bioaugmentation (Figure 10.2 with linearized data shown in Figure 10.4b; 1.94 hr^{-1}) were used to predict the *Sphingobium* sp. BiD32 concentration (Figure 10.5a) and BPA removal (Figure 10.5b) for 24 hours after bioaugmentation. The *Sphingobium* sp. BiD32 concentration at the beginning of each cycle was predicted using Eq 10.3 through Eq 10.6 and the bacterial loss rates (Figure 10.5a, gray and white bars). Based on these predictions, the loss of *Sphingobium* sp. BiD32 as measured during the batch experiment (Figure 10.5a, white bars) matched most closely to the *Sphingobium* sp. BiD32 concentrations predicted based on the actual BPA degradation (Figure 10.5a, black bars), suggesting that a loss rate of 0.16 hr^{-1} is most applicable for this system. The removal of BPA in the reactors was also predicted using the predicted *Sphingobium* sp. BiD32 concentrations based off of the first day of bioaugmentation (Figure 10.5b, gray bars) and the batch experiment (Figure 10.5b, white bars). Again, the removal of BPA

predicted based off of the batch experiment results (Figure 10.5b, white bars) matched most closely to the actual removal of BPA in the bioaugmented reactor (Figure 105.b, black bars).

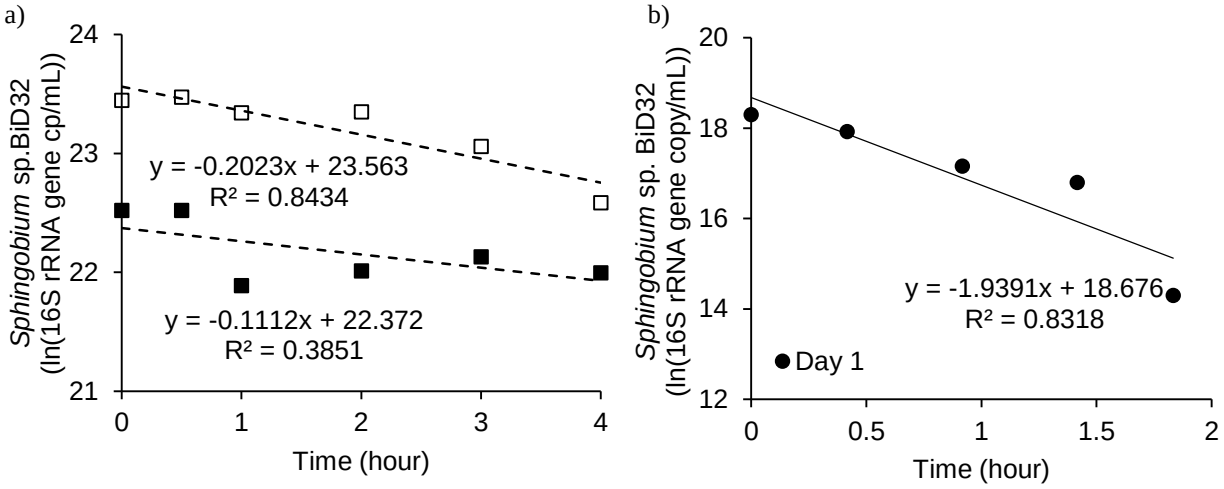

Figure 10.4. Natural log of S*phingobium* sp. BiD32 16S rRNA gene versus time. Shows loss of *Sphingobium* sp. BiD32 a) in waste solids (same data as shown in Figure 6.6) and b) during the bioaugmentation cycle on the first day of bioaugmentation when operating at an 8-day SRT (same data as shown in Figure 10.2 from Day 1). Line fit using Eq 10.2.

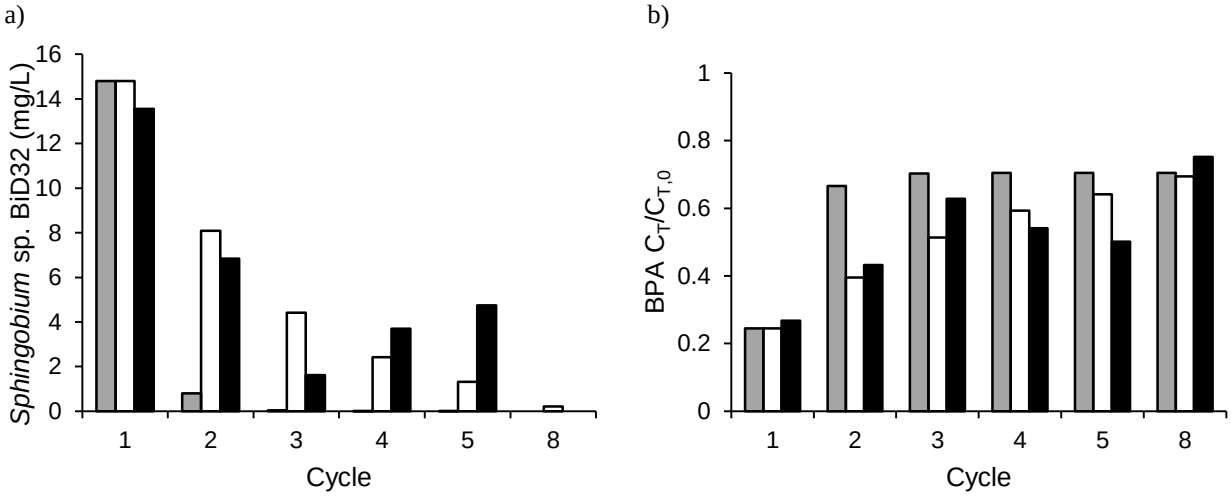

Figure 10.5. Comparison of predicted bacterial concentrations, and measured and predicted bisphenol A (BPA) removal. Concentrations during 8-cycles (24 hours) in the bioaugmented reactor of a) *Sphingobium* sp. BiD32 and b) BPA in the reactor at the end of a cycle. Gray bars represent concentrations predicted based on the first day of bioaugmentation. White bars represent concentrations predicted based on the batch experiment based on the loss rate 0.16 hr^{-1}). Black bars represent a) *Sphingobium* sp. BiD32 concentrations predicted based on the measured BPA degradation and b) BPA removal measured in the test reactor.

These predictions show a loss of 86.5% of the augmented *Sphingobium* sp. BiD32 using a loss rate of 0.16 hr^{-1}, which matches well to the qPCR results seen (Figure 10.1) that show a removal of 97.7%. These predictions suggest that *Sphingobium* sp. BiD32 was lost at a rapid rate from the test reactor, potentially due to predation, a high endogeneous decay rate, or loss in the effluent due to differential settling. High

concentrations of rotifers and protozoa were measured in the lab scale reactors and in the batch experiment used to measure *Sphingobium* sp. BiD32 loss (Figure 10.6).

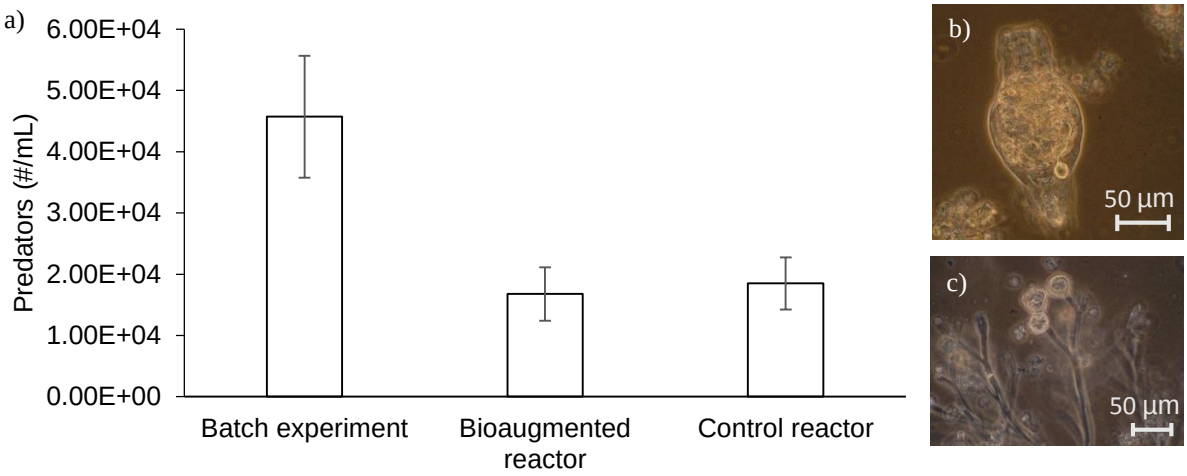

Figure 10.6. Predators in reactor activated sludge. a) Number of predators per mL, b and c) typical predators seen in reactor activated sludge.

10.4.3 Disruption of flocs

To test the hypothesis that the loss of enhanced BPA removal was due to diffusion limitations if *Sphingobium* sp. BiD32 was incorporated into activated sludge flocs, the activated sludge flocs from the reactors were disrupted. No improvement in BPA removal was seen (Figure 10.7). The removal of BPA in the untreated and blended waste solids from the bioaugmented and control reactor were not significantly different (p=0.66). The removal of BPA during this experiment was statistically different from the removal of BPA during cycle 1 in the test reactor (p<0.001). If the loss of the enhanced BPA removal was due to inhibition of BPA removal by the activated sludge flocs, the BPA removal with disrupted flocs (Figure 10.7, open circles) would be more similar to the BPA removal during cycle 1 in the test reactor (Figure 10.7, closed triangles) than to the BPA removal in untreated waste solids (Figure 10.7, closed circles and squares), however the removals were not similar. The total degradation rates (k_{cT}) are summarized in Table 10.3. The degradation rates were statistically equivalent for blended and untreated sludge from the bioaugmented and control reactors. Lack of improved degradation following disruption of flocs in the bioaugmentation reactor suggests that diffusion limitation of BPA was not the cause of the decrease in BPA removal.

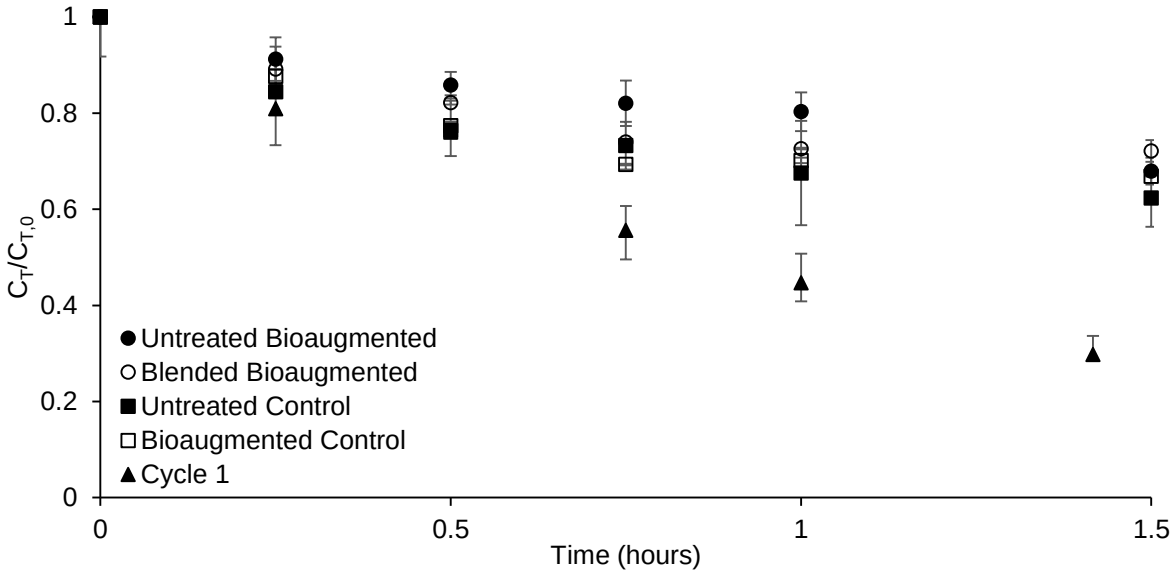

Figure 10.7. Bisphenol A concentrations in untreated waste solids and blended waste solids from both the bioaugmented and control reactors, and during cycle 1 in the bioaugmented reactor (data from Figure 6.2). Error bars show the average deviation of the replicates (n=2).

Table 10.3. Total bisphenol A degradation rates in untreated and blended waste solids

	Waste solids from bioaugmented reactor		Waste solids from control reactor	
	Untreated	Blended	Untreated	Blended
k_{cT} (hr^{-1})	0.24 ± 0.03	0.22 ± 0.003	0.30 ± 0.09	0.32 ± 0.07

Error represents the average deviation of the replicates k_{cT} (n=2)
All conditions are statistically equivalent (p-values range from 0.27 to 0.90, t-test)

10.4.4 FISH method development for visualizing flocs

FISH was used to attempt to identify where *Sphingobium* sp. BiD32 was located in the activated sludge matrix of the bioaugmented reactor. Bacteria were visualized in reactor activated sludge flocs (Figure 10.8) and in *Sphingobium* sp. BiD32 pure culture samples using previously established FISH probes. FISH probes designed to target *Sphingobium* sp. BiD32 were used to visualize *Sphingobium* sp. BiD32 in the activated sludge flocs. However, this method was not optimized and therefore, *Sphingobium* sp. BiD32 could not be located in the flocs or in pure culture tests. A formamide concentration of 35% was tested initially. Future work to optimize the primers to visualize *Sphingobium* sp. BiD32 should focus on different formamide concentrations (Table 10.2) and hybridization temperatures.

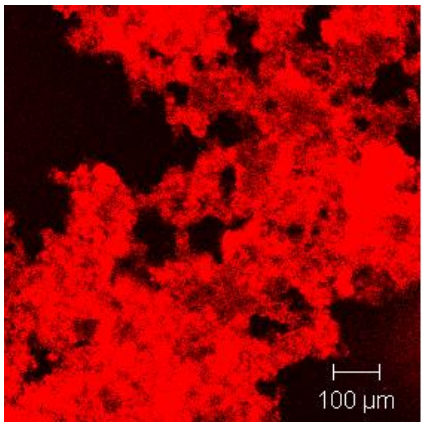

Figure 10.8. Activated sludge floc from the test reactor using Bacterial FISH probes.

10.5 Conclusions

This study tested two potential hypotheses for why the enhanced BPA degradation seen in the bioaugmented reactor was lost following more than 5 cycles after bioaugmentation. *Sphingobium* sp. BiD32 was detected in the reactors at the end of cycle 8 (23 hours after bioaugmentation) using qPCR (2.3% of the augmented bacteria remaining) and PMA-qPCR (0.14% of the augmented bacteria remaining). Also, predictions of the *Sphingobium* sp. BiD32 and BPA concentrations in the bioaugmented reactor suggest that less than 13.5% of the augmented bacteria were remaining at the end of the 8th cycle. It was hypothesized that *Sphingobium* sp. BiD32 was incorporated into activated sludge flocs and, therefore, BPA was diffusion limited. However, disrupting the activated sludge flocs taken from the reactors during cycle 8 did not result in improved BPA removal. These results suggest that the augmented bacteria may have lost their ability to degrade BPA over the course of the day or that the remaining amount of *Sphingobium* sp. BiD32 was too low to enhance BPA removal. Future work should focus on confirming a role of the degradation genes identified in Chapter 7 and designing qPCR methods to monitor them instead of the 16S rRNA gene. This would allow assessment of whether the degradation genes were lost or suppressed in activated sludge.

10.6 Supplementary Information

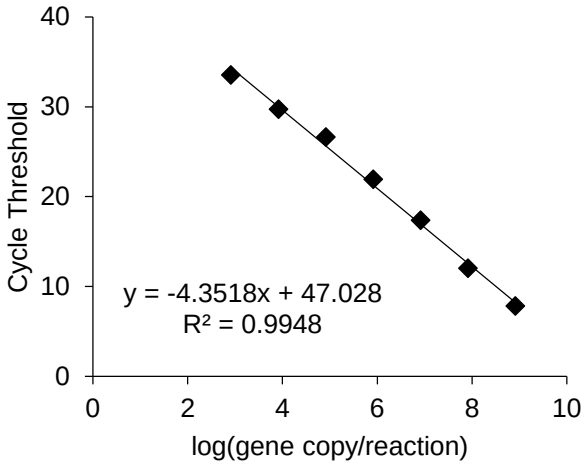

Figure 10.9. Example Sphingobium sp. BiD32 16S rRNA gene qPCR standard curve.

APPENDIX B: PROTEOMIC AND METABOLOMIC ANALYSIS REVEALS INSIGHT INTO THE DEGRADATION OF GEMFIBROZIL BY *BACILLUS* SP. GED10

This chapter is under review for Environmental Science and Technology.

Henrik Kjeldal (HK) is first author of this manuscript. HK and NAZ contributed equally for completing experiments, and HK took the lead on data analysis and writing. NAZ consulted during interpretation of data analysis, and contributed extensively to editing of early and final drafts.

11.1 Chapter summary

This chapter focuses on Objective V: identification of proteins potentially involved in trace organic contaminant degradation. The bacterial species used (*Bacillus* sp. GeD10) was the first organism reported to degrade gemfibrozil (see description in Chapter 4). Gemfibrozil is a lipid regulator. This study used a combination of genomics, proteomics, and metabolomics to determine proteins that are likely involved in the degradation of gemfibrozil by *Bacillus* sp. GeD10 and its metabolic intermediates. Two hydroxylated intermediates and a glucuronidated hydroxyl-metabolite were identified by metabolomic analysis. The degradation of gemfibrozil was predicted to involve hydroxylation catalyzed by enzymes of the Cytochromes P450 protein family and subsequent extradiol ring cleavage catalyzed by a catechol-2,3-dioxygenase. Cytochromes P450 are well known for being involved in xenobiotic degradation, and are one of the most abundant groups of enzymes responsible for biodegradation. They make up a broad class of enzymes, so cytochromes P450 generally could not be used as biomarkers of gemfibrozil degradation. However, each enzyme has a unique function, so the specific cytochrome P450 identified in this study may function as a future marker of gemfibrozil degradation. This would allow for monitoring of gemfibrozil-degrading organisms *in situ* and increase the understanding of microbial processing of TOrCs.

11.2 Abstract

Gemfibrozil is a widely used hypolipidemic and triglyceride lowering drug. Excess of the drug is excreted and discharged into the environment primarily via wastewater treatment plant effluents. *Bacillus* sp. GeD10, a gemfibrozil-degrader, was previously isolated from activated sludge. It is the first identified bacterium capable of degrading gemfibrozil. Gemfibrozil degradation by *Bacillus* sp. GeD10 was here studied through genome sequencing, quantitative proteomics and metabolite analysis. From the bacterial proteome of *Bacillus* sp. GeD10 1974 proteins were quantified, of which 284 proteins were differentially expressed by more than twofold (FDR corrected p-value ≤ 0.032, fold abundance (log2) ≥ 1) in response to gemfibrozil exposure. Metabolomic analysis identified two hydroxylated intermediates as well as a glucuronidated hydroxyl-metabolite of gemfibrozil. Overall, the presence of gemfibrozil had a major impact on the proteome of *Bacillus* sp. GeD10. Several potential enzymes and metabolites involved in gemfibrozil degradation in *Bacillus* sp. GeD10. The potential catabolic pathway/modification included ring-hydroxylation preparing the substrate for subsequent ring cleavage by a meta-cleaving enzyme. The identified genes may allow for monitoring of potential gemfibrozil-degrading organisms *in situ* and increase the understanding of microbial processing of trace level contaminants. This study represents the first omics study on a gemfibrozil-degrading bacterium.

11.3 Introduction

Gemfibrozil (5-(2,5-dimethylphenoxy)-2,2-dimethyl-pentanoic acid) is a lipid regulator widely used for the treatment of hypertriglyceridemia and hypercholesterolemia. It was prescribed over 500,000 times in North America during 2009 and excess of the compound is regularly found in the environment (Jackevicius et al. 2011). The pharmaceutical adversely affects aquatic life, such as small freshwater animals (Mimeault et al. 2005). Gemfibrozil has been shown to accumulate in goldfish, *Carassius auratus*, exposed to environmentally relevant concentrations (Mimeault et al. 2005), and has been detected in the livers of common carp, *Cyprinus carpio*, and White sucker, *Catostomus commersonii* (Ramirez et al. 2009). Evidence has associated gemfibrozil has with endocrine disrupting activity and exposure can lead to reduced testosterone levels in *Carassius auratus* (Mimeault et al. 2005). The adverse effects of gemfibrozil combined with its potential for bioaccumulation (due to its high partitioning coefficient) makes gemfibrozil a compound of concern (Sanderson et al. 2003).

Gemfibrozil is partially removed during wastewater treatment and the residual enters aquatic environments through effluent discharge and runoff from land application of biosolids (Xia et al. 2005; Stumpf et al. et al. 1999; Fang et al. 2012). Wastewater treatment plant (WWTP) influent concentrations range from 350 to 2640 ng/L (Ternes 1998; Stumpf et al. 1999; Martin et al. 2012) and effluent

concentrations range from 4 to 2300 ng/L (Martin et al. 2012; Gross et al. 2004; Kostich et al. 2014). Gemfibrozil has been detected in 3.6% of the US streams tested with a median concentration of 48 ng/L and a maximum concentration of 790 ng/L (Kolpin et al. 2002). Other studies have reported up to 1500 ng/L gemfibrozil in European and North American surface waters (Sanderson et al. 2003), and up to 6860 ng/L in groundwater below a land application site receiving biosolids (Fang et al. 2012).

Despite the low average removal efficiencies of gemfibrozil in WWTPs (Petrović et al. 2003), a gemfibrozil degrading bacterium, *Bacillus* sp. GeD10, was recently isolated from activated sludge (Zhou et al. 2013). This bacterium was isolated using gemfibrozil as the sole source of carbon and energy, yet degradation of gemfibrozil has only been documented in nutrient rich medium. In nutrient rich medium *Bacillus* sp. GeD10 is capable of degrading gemfibrozil to concentrations < 60 ng/L, and has been characterized for its bioaugmentation potential (Zhou et al. 2013).

In-depth quantitative mass spectrometry-based proteomics analysis has become an important tool for characterizing bacterial metabolism, and allows for prediction and identification of networks and cellular mechanisms (Almeida et al. 2013; Li et al. 2012; Collodoro et al. 2012; Hartmann and Armengaud 2014). This approach has been demonstrated by recent work with ibuprofen and 17β-estradiol (E2). The effect of ibuprofen on the proteome of an ibuprofen degrading bacterium, *Patulibacter* sp. I11, was previously studied, and candidate enzymes for ibuprofen degradation were identified (Almeida et al. 2013). A quantitative label-free mass-spectrometry (MS)-based proteomic study on the E2 degrading bacterium, *Stenotrophomonas maltophilia*, identified proteins likely involved in the degradation of E2. This lead to the hypothesis that *S. maltophilia* converted E2 to estrone (E1) and that E1 was subsequently converted to the amino acid tyrosine, which can be readily used in protein biosynthesis (Li et al. 2012).

MS-based proteomics analyses, if applied standalone, can provide information on the realized gene potential of an organism under defined conditions and facilitate the prediction and identification of novel catabolic pathways. However, if linked together with information about the end products of the cellular regulatory processes (metabolites), predicted pathways may be validated (Fiehn 2002). Hence, the combined use of proteomics and metabolomics serves as a powerful tool box for probing bacterial catabolic pathways. Recent studies have acknowledged the importance of characterizing the metabolism of xenobiotic degraders that do not necessarily utilize the xenobiotic as the sole source of energy and carbon (Almeida et al. 2013; Zhou et al. 2015; Kjeldal et al. 2014b), something which many previous studies have been restricted to (Annweiler et al. 2000; Hanson et al. 1999).

In this study the potential metabolic functions of various gene products involved in the modification of gemfibrozil by the gemfibrozil degrading bacterium *Bacillus* sp. GeD10 was evaluated. The genome of *Bacillus* sp. GeD10 was determined to facilitate the subsequent MS-based label-free quantitative proteomics analysis used to investigate the effect of gemfibrozil on its proteome. Lastly, the metabolites of gemfibrozil of *Bacillus* sp. GeD10 during gemfibrozil degradation were characterized. This study is the first to provide insight into the metabolism of gemfibrozil by a gemfibrozil-degrading organism.

11.4 Materials and methods

11.4.1 Chemicals, reagents, and bacterial strain

Gemfibrozil was obtained from Sigma Aldrich (St. Louis, MO, USA). Organic solvents and water used for gemfibrozil sample extraction and analysis were high pressure liquid chromatography (HPLC) grade. A 5 mg/L gemfibrozil aqueous stock was prepared by adding gemfibrozil dissolved in acetonitrile (1000 mg/L), evaporating the acetonitrile at 60 ºC overnight, adding water, and autoclave sterilizing (121ºC, 20 min). A control of evaporated acetonitrile was prepared the same way as the gemfibrozil aqueous stock. *Bacillus* sp. GeD10 (GenBank accession PRJNA201979) was previously isolated from activated sludge (Zhou et al. 2013).

11.4.2 Library preparation, genome sequencing, assembly, and analysis

DNA extraction was performed using the FastDNA Spin Kit for Soil (MP Biomedicals, Santa Ana, CA, USA) and the Nextera DNA Sample Preparation Kit (Illumina, San Diego, CA, USA) was used to construct a library for paired-end sequencing as previously described (Zhou et al. 2015). An Illumina HiSeq was used for sequencing the library as previously described (McIlroy et al. 2013) generating paired-end reads of 150 bp in length.

The sequences were trimmed and assembled using *de novo* assembly by the CLC Genomics Workbench version 5.5.1 (CLC bio, Aarhus, Denmark) using settings as described elsewhere (Zhou et al. 2015). The assembled contigs were then curated by CodonCode Aligner v 3.7 (CodonCode Corp.) and analyzed with the Rapid Annotation using Subsystem Technology (RAST) annotation server for subsystem classification and functional annotation (Overbeek et al. 2005). This Whole-genome Shotgun project was deposited at DDBJ/EMBL/GenBank under the accession CAVI000000000.1.

11.4.3 Sample preparation for proteomic analysis

Samples were prepared for proteomic analysis by growing *Bacillus* sp. GeD10 in the presence and absence of gemfibrozil. *Bacillus* sp. GeD10 was inoculated by transferring a single colony from solid

media (pre-inoculum culture) into R2B, a liquid media prepared based on the composition of R2A (Reasoner and Geldreich 1979; van der Linde et al. 1999). When the inoculum culture reached an optical density, measured at 600 nm (OD_{600}), of 0.5, 5 mL was inoculated into experimental flasks containing R2B for an estimated initial volatile suspended solids (VSS) concentration of 5 mg/L. Quintuplicate cultures of *Bacillus* sp. GeD10 were grown in the presence of 0.6 mg/L gemfibrozil (added by spiking known volume of gemfibrozil stock solution to the flasks) and the absence of gemfibrozil (with known volume of evaporated acetonitrile controls spiked into flasks). The bacteria were grown at 100 rpm and 28 ºC. OD_{600} was measured and samples for quantification with a HPLC instrument with ultraviolet detector (HPLC-UV) were collected every one to two hours. An HPLC-UV was used to quantify gemfibrozil concentrations using previously reported methods (Zhou et al. 2013). *Bacillus* sp. GeD10 cultures were harvested when an OD_{600} of ~0.8 was reached. Cells were harvested by washing the cell pellet twice with 20 mL phosphate-buffered saline (PBS) and collecting through centrifugation (10,000 x *g*, 4 ºC, 15 min).

Protein extraction was performed as described elsewhere (Zhou et al. 2015). Briefly, the cell pellet was resuspended in PBS supplemented with protease inhibitors and subjected to sonication. Cell debris was removed by centrifugation and proteins were pelleted by acetone precipitation. Protein content was assessed using the BCA Protein Assay (Thermo Fisher Scientific) prior to in-gel digestion.

11.4.4 In-gel digestion

For each sample 40 µg of total protein was resuspended in SDS-sample buffer containing dithiothreitol (DTT) to a final concentration of 40 mM DTT and denatured at 95ºC for 5 min. Samples were loaded onto a 4-20% (w/v) precast SDS-gel (Bio-Rad, USA) and proteins were separated at 160V for 45 min. Following separation, each lane was cut into four pieces, each piece being further excised prior to the proteins being in-gel digested using a modified version of the previously described in-gel digestion protocol (Shevchenko et al. 1996). Briefly, proteins were reduced with DTT and alkylated with iodoacetamide before being digested in-gel with trypsin. Peptides were extracted from the gel matrix and micro-purified using StageTips as previously described (Rappsilber et al. 2007). Eluted peptides were dried in a vacuum concentrator (Labconco, Buch & Holm, Herlev, Denmark), and resuspended in 0.1% (v/v) Trifluoroacetic acid (TFA) and 0.005% (v/v) Heptafluorobutyric Acid (HFBA).

11.4.5 LC-MS/MS analyses for proteomics

Tryptic digests were analyzed by an Ultimate 3000 RSLnano system (Thermo Scientific) coupled with a Q Exactive mass spectrometer (Thermo Scientific) as described elsewhere (Kjeldal et al. 2014b) using modifications related MS parameters as elution gradient as previously described (Zhou et al. 2015).

11.4.6 Data analysis

The RAW files from the Q Exactive instrument were analyzed using MaxQuant (v. 1.5.1.2) (Cox and Mann 2008b), setting carboxymethylation as a fixed modification and oxidation of methionine as a variable modification. A false discovery rate (FDR) of 1% was utilized and label-free quantification was determined using the label-free quantitation (LFQ) feature of MaxQuant. All other settings were default. The data was searched against a sequence database comprised of the predicted open reading frames (ORFs) of *Bacillus* sp. GeD10 retrieved from UniProt (downloaded the 21st of October 2014). The statistical analysis of the MaxQuant output was performed with Perseus (v. 1.5.0.31). A two-tail Student's t-test was performed and the statistical significance was set at p-value ≤ 0.05. Multiple testing correction was applied using a permutation-based FDR strategy at a FDR of 5%. Protein abundances are represented as $\log_2$ transformed LFQ values and are reported for all proteins having at least two quantifiable unique peptides.

11.4.7 Functional annotation of proteins

Overrepresentation of gene ontology (GO) categories of the proteins found to be differentially over- or underexpressed in response to gemfibrozil were assessed using Biological Network Gene Ontology Tool (BiNGO v. 2.44) (Maere et al. 2005) and visualized in Cytoscape (Shannon et al. 2003). The hypergeometric test used for the enrichment analysis in BiNGO was performed using a FDR-corrected p-value cutoff of 0.05 and the entire set of GO annotated genes of *Bacillus* sp. GeD10 (downloaded from UniProt the 21st of October 2014) was used as a reference set for the analysis (background).

In addition, for those proteins that did not have an associated GO, proteins were instead functionally annotated against proteins with an associated Kyoto Encyclopedia of Genes and Genomes (KEGG) identifier (database downloaded from UniProt the 21st of October 2014). The annotation was done using CLC Main Workbench v 6.6.2 (CLCbio, Denmark) using The Basic Local Alignment Search Tool for proteins (BLASTp) with default settings. Matches with the highest similarity scores and an E-value $\leq$ 1E-05 were recorded for each protein. Proteins were subsequently mapped using the KEGG Orthology (KO) identifier retrieved from the BLASTp search and the Pathway mapping feature at the KEGG (v. 68.0) website (http://www.genome.jp/KEGG/).

11.4.8 Aerobic pathway prediction of gemfibrozil

For prediction of gemfibrozil degradation the simplified molecular input line entry system (SMILES) line annotation of gemfibrozil (O=C(O)C(C)(C)CCCOc1cc(ccc1C)C) was submitted to the EAWAG-

Biocatalysis\Biodegradation Database (EAWAG-BBD, http://eawag-bbd.ethz.ch/, (Gao et al. 2010) choosing aerobic degradation of the compound in the prediction tool (PPS).

11.4.9 Sample preparation for metabolite identification

Samples were prepared for metabolomic analysis by degrading gemfibrozil using *Bacillus* sp. GeD10. *Bacillus* sp. GeD10 was inoculated into R2B containing 2 ppm gemfibrozil. The bacteria were grown at 100 rpm and 28 ºC. Samples were collected from log-phase growth of *Bacillus* sp. GeD10 and treated as described elsewhere (Zhou et al. 2015). Prior to LC/MS analysis, samples were resuspended in mixture of mobile phase A/B (1:1;v:v; (A) 10 mM ammonium formate with 0.1% (v/v) formic acid and (B) acetonitrile with 0.1% (v/v) formic acid).

11.4.10 LC/MS analyses for metabolite identification

Samples were analyzed on an Ultra High Definition Accurate-Mass Quadrupole Time-of-Flight coupled with an ultra-HPLC system (Agilent Technologies, Inc.; Santa Clara, CA, USA) to determine the presence of gemfibrozil and corresponding metabolites. The settings used in the setup are described elsewhere (Zhou et al. 2015).

Visual inspection and interpretation of the corresponding MS/MS spectra using MassHunter Workstation (Agilent Technologies, Inc.; Santa Clara, CA, USA) software Accelrys Draw Academic Version 4.1 (Accelrys, Inc.; San Diego, CA, USA) was used for metabolite identification. After that the corresponding metabolites were relatively quantified using full scan.

11.5 Results

11.5.1 Genome sequencing

Whole-genome sequencing of *Bacillus* sp. GeD10 was completed to provide an organism-specific genomic template for the MS-based label-free quantitative proteomics analysis (Fig. 11.1). The assembly of the *Bacillus* sp. GeD10 genome yielded a total of 327 contigs with 31,966,298 reads, a depth of coverage of 669 fold, a mean read length of 122.72 bp, and an N50 contig length of 37.2 Kb. The uncompleted draft genome included 5,865,695 bases (5.9 Mb) with a GC content of 35.1 % and was comprised of 6,156 predicted open reading frames ORFs. Out of the 6,156 ORFs 3,342 (54%) could be functionally annotated in RAST (Figure 11.6). Several of the predicted ORFs of *Bacillus* sp. GeD10 encoded for proteins related to resistance towards antibiotics and toxic compounds (72 genes) including proteins involved in resistance to tetracycline and vancomycin, as well as multidrug resistance efflux pumps. A total of 1787 hypothetical proteins (~29%) were predicted for *Bacillus* sp. GeD10.

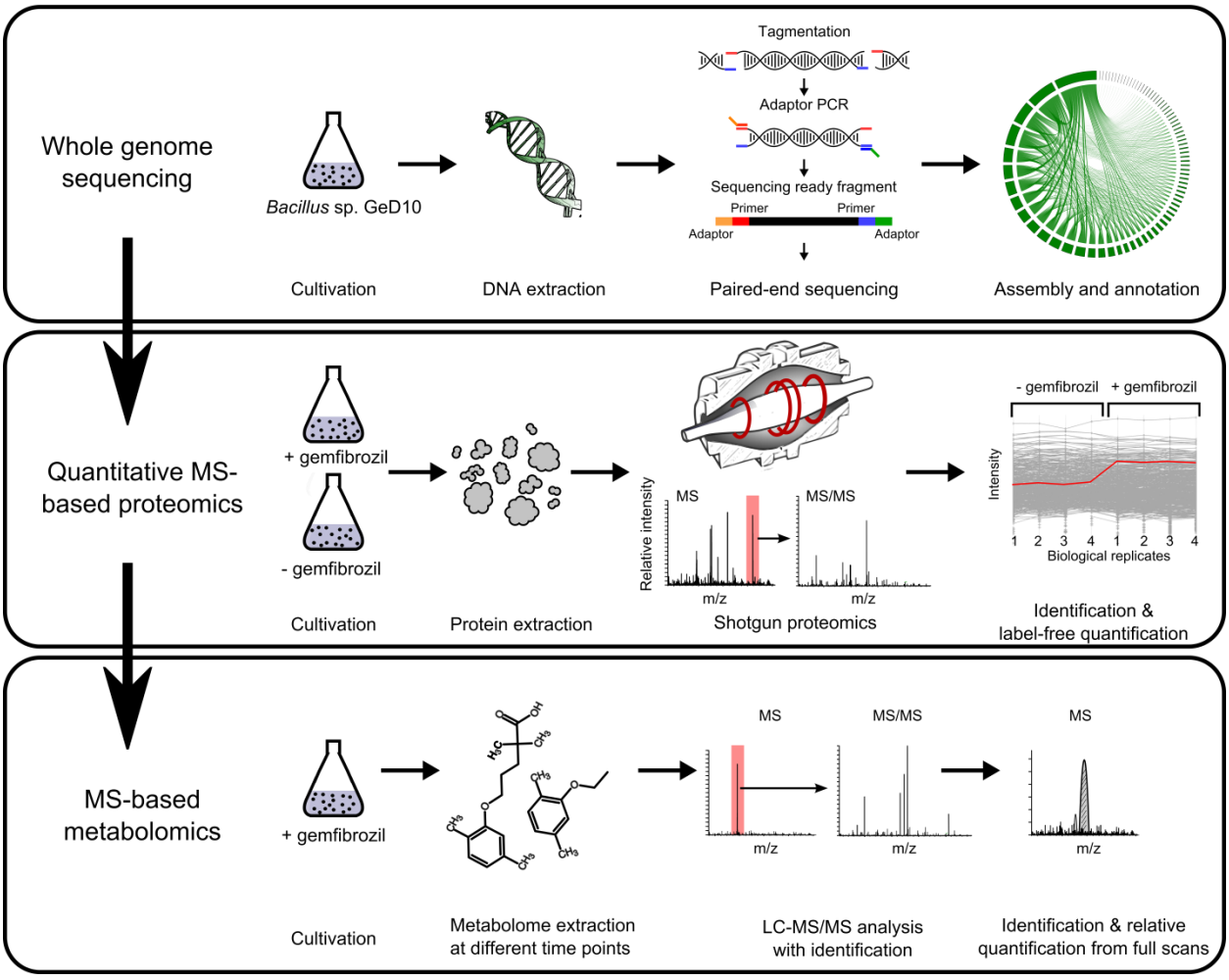

Figure 11.1. Workflow for the determination of expressed proteins during gemfibrozil degradation by Bacillus sp. GeD10. The genome of Bacillus sp. GeD10 was sequenced, and the proteome and metabolome during gemfibrozil degradation were extracted and analyzed.

11.5.2 Cell cultures for MS-based proteomics analysis

Biological quintuplicates of *Bacillus* sp. GeD10 were grown in the presence/absence of gemfibrozil in low-nutrient medium (R2B), while gemfibrozil degradation was monitored (Fig. 11.2a). Regardless of exposure to 2 mg/L gemfibrozil, *Bacillus* sp. GeD10 had a doubling time of approximately 1.15 hrs. At the point of harvest, the culture was still in exponential growth and approximately 50% of the gemfibrozil had been degraded.

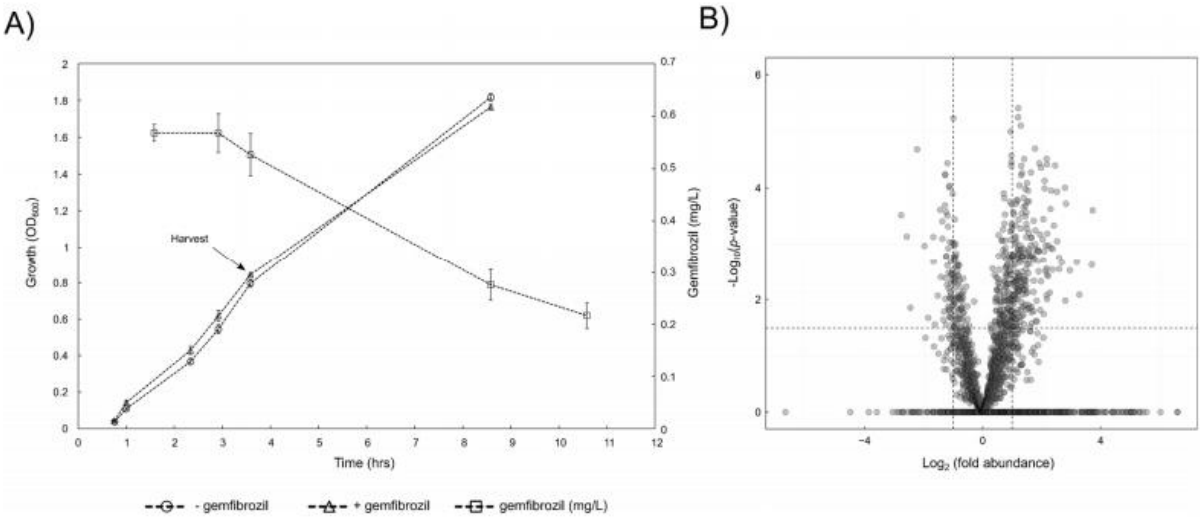

Figure 11.2. a) Degradation of gemfibrozil (squares) and growth of *Bacillus* sp. GeD10 in R2B medium in the absence (circles) and presence (triangles) of gemfibrozil. Samples for quantitative MS-based proteomics analysis were taken during logarithmic growth (OD_{600} ~ 0.8). Error bars indicate standard deviation (n = 5). b) Volcano plot of quantified proteins. The horizontal dash line indicates the threshold for statistically significant differentially expressed proteins (FDR corrected *p*-value of $-\log_{10}(0.032)$) while a minimum of a twofold change in protein abundance is indicated by vertical dash line ($-1 \leq$ fold abundance $(\log_2) \geq 1$).

11.5.3 Label-free quantitative MS-based proteomics of Bacillus sp. GeD10

Proteins were extracted from five biological replicates of *Bacillus* sp. GeD10 grown in the absence/presence of gemfibrozil and analyzed by shotgun proteomics and label-free quantification (Figure 11.1). A total of 2210 proteins could be identified, corresponding to approximately 36% of all predicted ORFs of *Bacillus* sp. GeD10. Out of the 2210 identified proteins, 1974 could be quantified with two or more unique peptides. 482 proteins were differentially expressed (FDR corrected *p*-value ≤ 0.032) of which a total of 355 were differentially overexpressed and 127 were differentially underexpressed as a result of gemfibrozil exposure (Figure 11.2b).

11.5.4 Functional annotation of proteins

The overrepresentation of GO categories among the 482 proteins that were differentially expressed (FDR corrected p-value ≤ 0.032) in response to gemfibrozil was assessed using BiNGO. The presence of gemfibrozil most notably modulated the expression of proteins functionally related to transcription, translation and various metabolic processes related to small molecules, including glucose metabolism and RNA processing, and formation of small molecules (e.g. low molecular weight monomeric molecules such as monosaccharides). The presence of gemfibrozil also resulted in the overrepresentation of reactive oxygen species-response genes (N1LTD9, N1LWV7, and N1LN68) and proteins related to energy derivation through oxidation of organic compounds (N1LU19, N1LLI2, N1LHK1, N1LKT8, N1LLL5,

N1LJW7, N1LG99, N1LRJ4, and N1LS64). A total of 17 proteins that were overexpressed by more than twofold could not be assigned any function (N1LR65, N1LJ73, N1LN71, N1M181, N1LNI9, N1LLA4, N1LS89, N1LM80, 240 N1LTU2, N1LR22, N1LPJ6, N1LUE5, N1LEA2, N1LRT9, N1LRP4, N1LN30, and N1LZ70).

As for the 127 proteins that were differentially underexpressed in response to gemfibrozil overrepresentation analysis indicated that primarily processes related to cellular macromolecule metabolic processes (30 proteins) and gene expression and translation (31 proteins) were affected. A total of 19 proteins (N1LH40, N1LSB8, N1LMV3, N1LYX5, 246 N1LV73, N1LHN4, N1LXP6, N1LXI4, N1LQQ8, N1LN26, N1LML2, N1LH85, N1LP36, 247 N1LMH1, N1LKN2, N1LHQ0, N1LVZ1, N1LKJ4, and N1LH86) that were underexpressed by more than twofold in response to gemfibrozil could not be assigned any function.

11.5.5 Proteins related to xenobiotic degradation

From the functional annotation against KO annotated genes, several proteins that were differentially overexpressed were functionally annotated to the degradation of other well-known non-chlorinated xenobiotics including benzoate (N1LNZ5, N1LRP7, and N1LW14), bisphenol (N1LX98, and N1LR96), and naphthalene (N1LUK0) (Table 11.1). Enzymes N1LNZ5, N1LRP7, and N1LW14 were implicated in benzoate degradation via a CoA-dependent beta-oxidation pathway (fatty acid metabolism).

The putative cytochrome P450 hydroxylase (N1LX98), which was functionally annotated to Bisphenol degradation, was overexpressed by more than twofold in response to gemfibrozil exposure. This protein was found to be highly homologues to other proteins of the cytochromes P450 protein family (sequence identity ~ 95%) and contains a conserved domain characteristic for enzymes of this family (InterPro domain IPR001128). It was functionally annotated to the degradation of several aromatic and polycyclic compounds (including bisphenol A), acting upon paired donors with the incorporation of oxygen (e.g. a monooxygenase). The gene encoding for the putative cytochrome P450 hydroxylase (*EBGED10_46120*) was found in a cluster with 2 hypothetical proteins (N1LXZ4 and N1LTC5) in the genome of *Bacillus* sp. GeD10. Of these two other ORFs, only one (N1LTC5) could be confirmed at the proteome level in this study. The expression of this protein remained unaltered in response to gemfibrozil exposure. No function could be assigned to the two ORFs.

The other enzyme implicated in bisphenol degradation (N1LR96) was mapped to dehydrogenation of different metabolites of bisphenol. The enzyme implicated in naphthalene degradation (N1LUK0),

catalyzes the oxidation of 2-hydroxymethylnapthalene to 2-naphthaldehyde. A total of six proteins were functionally annotated to beta-lactam resistance (N1M1I9, N1LXC8, N1LVF6, N1M122, N1LS58, and N1LVV3). These proteins were implicated in binding of the beta-lactams, such as penicillin, as well as being involved peptidoglycan biosynthesis based upon KO annotation (corresponding KO numbers are seen in Table 11.1).

Finally several proteins related to multidrug efflux (N1LUI4, N1LP52, and N1LNI7) were identified in the proteome of *Bacillus* sp. GeD10. Two of the three proteins were differentially overexpressed in response to gemfibrozil (N1LUI4 and N1LP52) (Table 11.1) while the latter protein (N1LNI7) (Table 11.2) was only identified in the proteome of gemfibrozil-exposed *Bacillus* sp. GeD10. One protein was functionally annotated to multidrug resistance being a transcriptional regulator (K18907), while the remaining two proteins (N1LP52 an N1LNI7) were both related to acriflavin resistance containing AcrB domains of the Resistance Nodulation cell Division (RND) family (IPR027463 accessible via the Uniprot accession number). The genes encoding for these three proteins were not closely associated in the genome of *Bacillus* sp. GeD10.

Among the proteins, that did not change in expression in response to gemfibrozil, were a total of 11 proteins (N1LT94, N1LWF2, N1LT34, N1LFP8, N1LM47, N1LN62, N1LR04, N1LS72, N1LLI8, N1LLT4, and N1M169) that were functionally characterized to the degradation of various xenobiotic compounds (Table 11.2). These proteins included most notably a dioxygenase (N1LT94), increasing the expression of this protein by almost twofold in 4 out of 5 replicates. No increase in the expression of this protein was observed in the fifth replicate (Table 11.2). This protein, a 302 amino acids long glyoxalase family protein (N1LT94) contains motifs characteristic of enzymes catalyzing amongst other extradiol ring-cleavage of aromatic compounds (Interpro domains IPR029068, IPR004360, IPR025870 and PFAM domains PF00903 and PF12681; accessible at UniProt using entry N1LT94) and was implicated in benzoate degradation based upon the KO annotation. The enzyme (N1LLT4) catalyzing the subsequent step following dearomatization of benzoate was also found among the non-differentially expressed proteins.

11.5.6 Metabolite identification

Metabolomics resulted in the detection of gemfibrozil and two hydroxylated gemfibrozil metabolites, M1 (5-[5-(hydroxymethyl)-2-methylphenoxy]-2,2-dimethylpentanoic acid) and M2 (5-(2,5-dimethylphenoxy)-4-hydroxy-2,2-dimethylpentanoic acid) (Figure 11.3). Additionally a glucuronic acid conjugate of a hydroxy-metabolite (Gem-glu) of gemfibrozil was also identified (Figure 11.3). M1, M2

and Gem-glu increased in abundance (relative to the initial concentration of gemfibrozil) during incubation with gemfibrozil. Given that the metabolite signal intensity is not only dependent on metabolite concentration but also the chemical structure of the metabolite, the abundance of the structurally different metabolites relative to each other could not be determined. Even so, it should be noted that the metabolite Gem-glu, as the only metabolite, was detected in trace amounts.

Table 11.1. Subset of proteins differentially expressed in response to gemfibrozil

Accession[1]	Description	Gene[2]	KO[3]	Unique peptides[4]	Mol. weight [kDa]	Sequence coverage [%]	Fold abundance [log_2][5]	FDR-corrected *p*-value
N1LHK1	AA3-600 quinol oxidase subunit I	EBGED10_15380	K02827	8	72.7	12	3.7	2.4E-03
N1LR96	Oxidoreductase, aldo/keto reductase family	EBGED10_39810	K00100	6	34.1	39.7	3.2	2.1E-03
N1LVF6	Oligopeptide transport system permease protein OppC (TC 3.A.1.5.1)	EBGED10_59350	K15582	15	37.9	34.6	2.8	1.9E-04
N1LR65	Uncharacterized protein	EBGED10_44200		3	47.6	15.6	2.8	1.0E-02
N1LXC8	Oligopeptide transport system permease protein OppB (TC 3.A.1.5.1)	EBGED10_59340	K15581	5	33.9	20.1	2.8	9.9E-05
N1LJ73	Uncharacterized protein	EBGED10_20830		8	19.7	54.8	2.7	2.2E-03
N1LN71	Hypothetical DUF1027 domain protein	EBGED10_14000		7	12.0	81	2.5	4.0E-05
N1LS50	Uracil-DNA glycosylase	ung	K03648	6	26.0	40	2.3	1.1E-04
N1LFG5	Alpha-1,4 glucan phosphorylase	EBGED10_2340	K00688	36	93.1	64.3	2.3	2.4E-04
N1LJW7	1,4-alpha-glucan branching enzyme GlgB	glgB	K00700	23	75.9	63.6	2.2	1.0E-03
N1M181	Uncharacterized protein	EBGED10_60220		4	19.0	33.3	2.2	3.8E-03
N1LP52	RND multidrug efflux transporter Acriflavin resistance protein	EBGED10_17350	K03296	20	112.4	22.4	2.1	1.3E-03
N1LNI9	Uncharacterized protein	EBGED10_35200	K11030	8	108.9	11.3	2.1	1.0E-03
N1LNZ5	Enoyl-CoA hydratase [isoleucine degradation] / 3-hydroxyacyl-CoA dehydrogenase	EBGED10_13610	K07516	44	87.4	61	2.1	3.6E-04
N1LS64	Aspartate ammonia-lyase	EBGED10_41990	K01744	11	52.5	34.2	1.9	1.2E-03
N1LVV3	Multimodular transpeptidase-transglycosylase / Penicillin-binding protein 1A/1B (PBP1)	EBGED10_38280	K05366	12	98.4	22.9	1.8	1.2E-03
N1LLA4	Uncharacterized protein	EBGED10_27640		5	96.7	10.8	1.8	1.0E-03
N1LS89	Uncharacterized protein	EBGED10_28260	K03628	8	16.5	67.6	1.7	2.6E-02
N1LLL5	2-oxoglutarate dehydrogenase E1 component	odhA	K00164	51	106.4	73.3	1.6	6.2E-04
N1LM80	Uncharacterized protein	EBGED10_7740		6	14.8	66.9	1.4	1.2E-02
N1LS58	Penicillin-binding protein 3	EBGED10_42810	K18149	16	72.9	30.9	1.3	8.3E-03
N1LG99	Glycogen biosynthesis protein GlgD,glucose-1-phosphate adenylyltransferase family	EBGED10_2320	K00975	17	38.6	67.2	1.3	2.8E-04
N1LWV7	Catalase	EBGED10_59160	K03781	19	55.9	54.3	1.3	1.0E-03
N1LTU2	Uncharacterized protein	EBGED10_33670		13	47.9	57.1	1.3	3.8E-03
N1LLI2	Succinate dehydrogenase iron-sulfur protein	EBGED10_23380	K00240	9	28.3	50.6	1.2	2.8E-02
N1LR22	Uncharacterized protein Bsub YpbR	EBGED10_37990		53	140.7	51	1.2	4.5E-03
N1LPJ6	Uncharacterized protein	EBGED10_15860		6	28.2	27.1	1.2	6.3E-03
N1LUE5	Uncharacterized protein	EBGED10_50260		6	25.8	32.3	1.1	2.3E-02
N1LV47	Glycosyl transferase, group 1 family protein	EBGED10_38420	K00754	8	42.9	43.6	1.1	9.9E-03
N1LX98	Putative cytochrome P450 hydroxylase	EBGED10_46120	K00517	20	47.1	60.6	1.1	2.9E-04
N1LKT8	Glucose-1-phosphate adenylyltransferase	glgC	K00975	22	41.1	75.2	1.0	2.1E-02
N1LEA2	Uncharacterized protein	EBGED10_5150	K14060	4	26.5	24.4	1.0	8.3E-03
N1M122	Oligopeptide ABC transporter, periplasmic oligopeptide-binding	EBGED10_57530	K15580	25	63.5	45	1.0	2.7E-04

	protein OppA (TC 3.A.1.5.1)							
N1LRJ4	Probable malate:quinone oxidoreductase	mqo	K00116	28	55.2	74.8	1.0	1.6E-02
N1LN68	Thioredoxin reductase	EBGED10_11350	K00384	22	34.7	79.2	1.0	1.8E-03
N1LUK0	Aldehyde-alcohol dehydrogenase	EBGED10_50340	K04072	53	95.2	72.7	0.9	1.5E-03
N1LRT9	Uncharacterized protein	EBGED10_23650		10	23.7	59.3	0.9	2.3E-02
N1LUI4	Transcriptional regulator, GntR family domain / Aspartate aminotransferase	EBGED10_36370	K18907	4	54.1	12.9	0.9	1.9E-02
N1LRP7	Enoyl-CoA hydratase	EBGED10_23300	K13767	14	27.9	70.5	0.9	3.6E-03
N1LU19	Isocitrate dehydrogenase [NADP]	EBGED10_48640	K00031	39	47.0	75.1	0.9	3.1E-02
N1LHR9	Trehalose-6-phosphate hydrolase	EBGED10_16130	K01226	33	65.5	63.3	0.8	2.8E-02
N1LRP4	Uncharacterized protein	EBGED10_26410		10	25.8	42.5	0.8	3.9E-03
N1LN30	Uncharacterized protein	EBGED10_10950		14	41.9	45.1	0.8	1.1E-02
N1LZ70	Uncharacterized protein	EBGED10_50530	K02204	8	37.6	37.2	0.7	9.2E-03
N1LTD9	Alkyl hydroperoxide reductase protein F	EBGED10_46860	K03387	29	54.8	77.2	0.6	2.5E-02
N1LLV5	50S ribosomal protein L1	rplA	K02863	19	24.5	75.2	-0.5	2.9E-02
N1LT29	Putative pyruvate, phosphate dikinase regulatory protein	EBGED10_51200	K09773	12	30.3	55.2	-0.8	1.5E-02
N1LKU9	10 kDa chaperonin	groS	K04078	10	10.1	76.6	-0.8	2.3E-03
N1LLB1	50S ribosomal protein L6	rplF	K02933	16	19.5	72.6	-0.8	2.5E-03
N1M0Y8	30S ribosomal protein S15	rpsO	K02956	7	10.6	65.2	-0.9	1.6E-03
N1LQ39	30S ribosomal protein S6	rpsF	K02990	16	11.3	89.6	-0.9	9.9E-03
N1LQR2	30S ribosomal protein S11	rpsK	K02948	7	13.8	63.6	-0.9	1.2E-02
N1LLA6	50S ribosomal protein L14	rplN	K02874	11	13.1	64.8	-0.9	1.9E-02
N1LQM9	50S ribosomal protein L4	rplD	K02926	12	22.5	68.1	-1.0	1.6E-03
N1LM05	50S ribosomal protein L17	rplQ	K02879	7	13.4	45.8	-1.0	1.2E-02
N1LJS3	50S ribosomal protein L10	rplJ	K02864	14	18.0	67.5	-1.0	2.7E-02
N1LH40	N-acetylmuramoyl-L-alanine amidase	EBGED10_8120	K19223	6	48.3	15.6	-1.0	3.1E-02
N1LSB8	Uncharacterized protein	EBGED10_28510		3	12.0	29.2	-1.0	1.2E-02
N1LJU7	30S ribosomal protein S17	rpsQ	K02961	10	10.2	70.1	-1.0	1.3E-04
N1LMF8	Peptidyl-prolyl cis-trans isomerase	EBGED10_24230	K03768	9	15.8	84.1	-1.0	4.3E-03
N1LMV3	Uncharacterized protein	EBGED10_13000		9	16.2	63	-1.0	3.7E-03
N1LYX5	Uncharacterized protein	EBGED10_52170		5	9.6	80.5	-1.0	2.1E-02
N1LV73	Uncharacterized protein	EBGED10_58650		6	11.1	88.7	-1.1	5.0E-03
N1LRJ7	30S ribosomal protein S5	rpsE	K02988	13	17.5	77.1	-1.1	8.4E-03
N1LHN4	Conserved hypothetical conserved protein in Tn5401	EBGED10_15730		10	10.0	78.8	-1.1	9.8E-03
N1LXP6	Uncharacterized protein	EBGED10_60850		3	13.2	31.9	-1.1	9.0E-04
N1LXI4	Endo/excinuclease amino terminal domain protein	EBGED10_61820	K03703	10	14.8	74.2	-1.1	9.9E-05
N1LJT4	30S ribosomal protein S10	rpsJ	K02946	9	11.7	65.7	-1.2	3.3E-03
N1LQQ8	Uncharacterized protein YpbS	EBGED10_37960		5	10.0	55.6	-1.2	3.7E-05
N1LR80	50S ribosomal protein L23	rplW	K02892	10	11.1	62.5	-1.2	3.1E-04
N1LLA0	50S ribosomal protein L22	rplV	K02890	11	12.5	69	-1.2	5.4E-03
N1LRF8	50S ribosomal protein L11	rplK	K02867	9	15.0	56	-1.2	1.6E-03
N1LN26	Uncharacterized protein	EBGED10_10900		4	12.1	52.4	-1.2	2.8E-02
N1LJV1	30S ribosomal protein S8	rpsH	K02994	13	14.9	79.5	-1.3	4.1E-03

N1LML2	Uncharacterized protein	EBGED10_8890		2	8.9	16.4	-1.3	9.8E-03
N1LJV7	50S ribosomal protein L15	rplO	K02876	15	15.5	63.7	-1.3	5.9E-05
N1LH85	PhaP protein	EBGED10_8520		12	20.3	75.3	-1.3	2.0E-04
N1LP36	Uncharacterized protein	EBGED10_32360		7	17.7	58.7	-1.3	1.6E-02
N1LMH1	Polyhydroxyalkanoate synthesis repressor PhaR	EBGED10_8540		6	18.5	47.5	-1.3	2.3E-02
N1LKN2	Uncharacterized protein	EBGED10_18010		2	11.1	44.2	-1.4	7.9E-04
N1LHQ0	Uncharacterized protein	EBGED10_15930		8	18.9	60.6	-1.5	8.6E-03
N1LVZ1	UPF0354 protein EBGED10	EBGED10_41620		10	31.9	44	-1.7	7.4E-04
N1LKJ4	Uncharacterized protein	EBGED10_4570		3	7.1	78.3	-2.0	1.1E-03
N1LH86	Uncharacterized protein	EBGED10_14030		5	10.4	75	-2.2	2.1E-05

[1] UniProt accession, [2] Gene identifier, [3] KEGG Orthology identifier, [4] Number of peptides used for quantification, [5] Quantitative value.

Table 11.2. Subset of proteins with no change in expression in response to gemfibrozil

Accession	Description	Gene	KO	Unique peptides	Mol. weight [kDa]	Sequence coverage [%]	Fold abundance [$\log_2$]	FDR-corrected *p*-value
N1M119	Penicillin-binding protein	EBGED10_61580	K01467	3	38.7	14.2	4.1	1.0E+00
N1M169	Uncharacterized protein	EBGED10_60020	K01055	2	33.5	8.6	3.6	1.0E+00
N1LLT4	Hydrolase, alpha/beta fold family	EBGED10_29050	K10216	2	31.4	17.7	1.9	1.0E+00
N1LTC5	Uncharacterized protein	EBGED10_46140	K06950	5	39.1	25.1	1.3	1.4E-01
N1LLI8	Acid phosphatase	EBGED10_23430	K01078	3	31.1	18.9	1.1	1.0E+00
N1LS72	Tautomerase	EBGED10_28110	K01821	1	6.7	41	0.7	1.0E+00
N1LT94	Glyoxalase family protein	EBGED10_32020	K07104	17	33.9	64.9	0.7	6.9E-02
N1LW14	3-ketoacyl-CoA thiolase @ Acetyl-CoA acetyltransferase	EBGED10_54890	K00626	26	41.9	72.4	0.5	8.6E-02
N1LMT9	Similar to eukaryotic Peptidyl prolyl 4-hydroxylase, alpha subunit	EBGED10_25980	K00472	9	24.7	62	0.4	3.9E-01
N1LR04	Fumarylacetoacetase	EBGED10_21060	K16171	6	35.5	24.2	0.2	1.0E+00
N1LDG6	Sulfate adenylyltransferase	sat	K00958	30	42.8	72.8	0.1	6.0E-01
N1LWF2	Alcohol dehydrogenase	EBGED10_43070	K13953	24	36.8	86.7	0.0	8.2E-01
N1LM47	CBS domain containing protein	EBGED10_30200	K00760	29	24.7	86.5	-0.2	5.9E-01
N1LFP8	Hypoxanthine-guanine phosphoribosyltransferase	EBGED10_3240	K00760	20	20.3	95	-0.5	1.4E-01
N1LT34	Cytidine deaminase	EBGED10_51250	K01489	10	14.4	85.6	-0.6	9.1E-02
N1LN62	Transcriptional regulator, AraC family	EBGED10_27330	K18199	4	22.1	30.8	-2.4	1.0E+00
N1LNI7	RND multidrug efflux transporter Acriflavin resistance protein	EBGED10_15200	K03296	4	111.1	5.2	-	-

[1] UniProt accession, [2] Gene identifier, [3] KEGG Orthology identifier, [4] Number of peptides used for quantification, [5] Quantitative value.

11.5.7 Catabolic pathway of gemfibrozil

The pathway of gemfibrozil modification by *Bacillus* sp. GeD10 was predicted using the online prediction tool EAWAG-BBD PPS. The number of pathways predicted was reduced to those containing the detected metabolites. Among these, two equally likely pathways were predicted, involving hydroxylation of gemfibrozil to M1 or M2. Based upon the identification of enzymes in the proteome analysis these pathways were further reduced to the pathway involving aromatic hydroxylation (hence going through M2) (Figure 11.3). The hydroxylation is predicted catalyzed by the putative P450 hydroxylase (N1LX98) found to be overexpressed by more than twofold in the proteome of *Bacillus* sp. GeD10 exposed to gemfibrozil.

Following the predicted hydroxylation of the methyl group on the aromatic ring of gemfibrozil by an oxidoreductase (step 1 to 2) it was predicted that this formed primary alcohol was oxidized to an aldehyde (step 2 to 3), and further oxidized to a carboxylic acid (step 3-4) possibly mediated by an oxidoreductase. The expression of an oxidoreductase functionally annotated to the degradation of naphthalene (N1LR96) was found to be highly overexpressed in response to gemfibrozil (Table 11.1). The oxidation of the primary alcohol to an aldehyde (step 2 to 3) is similar to the oxidation of naphthalene a reaction to which one of the enzymes identified in the proteome analysis of *Bacillus* sp. GeD10 (N1LWF2) was functionally annotated (K13953).

Further degradation was predicted to continue through side-chain cleavage (step 5b and 6b) and subsequent cleavage of the aromatic ring (step 5a to 7a). For both steps predictions in the PPS were based upon previously documented reactions catalyzed by oxygenases. The side-chain cleavage predicted by the EAWAG-BBD PPS was among others based upon the 2,4-cleavage of dichlorophenoxyacetic acid into glyxoylate and 2,4-dichlorphenol by catalyzed 2,4-dichlorophenoxyacetate alpha-ketoglutarate dioxygenase (*TfdA*). The closest homologue of the *TfdA* gene in the proteome of *Bacillus* sp. GeD10 was the protein sulfate adenylyltransferase (N1LDG6) (sequence identity ~30%), which was not differentially expressed in response to gemfibrozil (Table 11.2). Another protein with the features of a catechol dioxygenase (N1LT94) was found to be overexpressed in response to gemfibrozil, however not statistical significant, as it was only overexpressed in 4 out of 5 replicates (Table 11.2). This protein was annotated to the degradation of 4-methylcatechol (K07104) to 2-hydroxymuconate semialdehyde. 2-hydroxymuconate semialdehyde is then further degraded to cis-2-hydroxy-penta-2,4-dienoate catalyzed. One of the enzymes present both in the presence and absence of gemfibrozil and which did not change in expression was a hydrolase (N1LLT4) which was functionally annotated to this particular degradation of 2-hydroxymuconate semialdehyde to cis-2-hydroxy-penta-2,4-dienoate (K10216).

Besides hydroxylation, glucuronidation of the gemfibrozil metabolite was also observed. Glucuronidation is a chemical reaction catalyzed by glycosyl transferases. Several hexosyl transferases were identified in the proteome of *Bacillus* sp. GeD10 and were found to be differentially overexpressed (N1LFG5, N1LJW7, N1LV47 and N1LVV3) in response to gemfibrozil exposure (Table 11.1). Also two enzymes catalyzing the breakdown of glucuronic acid conjugates (glycosidases) were found to be differentially overexpressed (N1LHR9 and N1LS50) in response to gemfibrozil (Table 11.1).

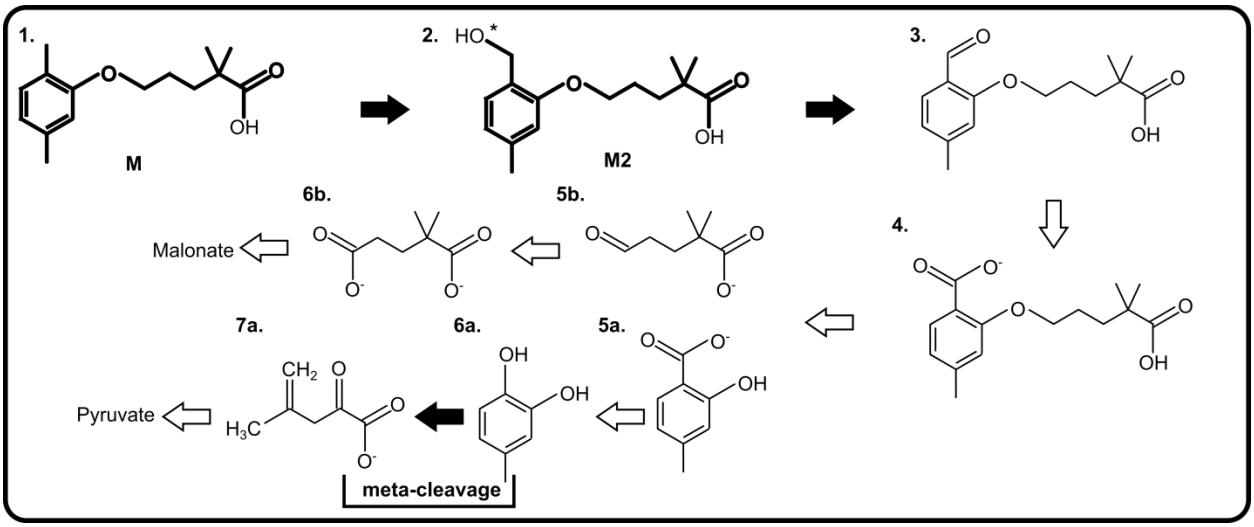

Figure 11.3. Proposed catabolic pathway for gemfibrozil by *Bacillus* sp. GeD10. Metabolites that were identified during gemfibrozil degradation have been bolded, while the other intermediate metabolites were predicted by the EAWAG-BBD PPS. Solid arrows indicate that a candidate enzyme catalyzing the reaction was identified in the quantitative MS-based proteome analysis. IUPAC nomenclature for metabolites of all steps in the pathway (1-7) can be found in the supplementary data (dataset S3). *For clarity only one of the possible isomers has been depicted.

11.6 Discussion

Even though several studies have documented that microbes are capable of degrading gemfibrozil, the metabolism of this compound remains unresolved. *Bacillus* sp. GeD10, a bacterium recently isolated and characterized for its ability to degrade gemfibrozil to low ng/L concentrations (Zhou et al. 2013), was used to gain insight into the metabolism of gemfibrozil. The approach involved three different tiers of biology, allowing for a proposed pathway of degradation for gemfibrozil. The impact of gemfibrozil exposure on the proteome of *Bacillus* sp. GeD10, despite not being the sole source of energy and carbon, was major and influenced multiple biochemical processes within the cell. The presence of gemfibrozil positively modulated the expression of a wide variety of enzymes related to energy production and turnover of organic carbon at the apparent cost of under expressing genes related to the transcriptional and translational machinery and turnover of other macromolecules. Based on the growth in this study *Bacillus*

sp. GeD10 did not utilize gemfibrozil as the sole source of energy and carbon, and more likely it seems that *Bacillus* sp. GeD10 provides an incomplete breakdown of gemfibrozil.

The combined investigations of the genome, the differentially regulated proteome, and the metabolome suggest that the initial step in gemfibrozil degradation involves hydroxylation of the aromatic ring (or the acyl side chain). Hydroxylation is well-known as a key reaction in the oxidative metabolism of organic compounds, including other xenobiotics and chemicals with structures similar to gemfibrozil (Holland and Weber 2000). Besides bisphenol, hydroxylation similar to the M2 and M1, has also previously been demonstrated for the structural homologues, methylpyrene and ethyl pyrene. The hydroxylation of gemfibrozil-analogous compounds such as bisphenol, methylpyrene and ethyl pyrene is catalyzed by proteins of the Cytochromes P450 protein superfamily (Engst et al. 1999).

The Cytochromes P450 superfamily of monooxygenases (CYPs) is a family of versatile biocatalysts, responsible for catalyzing a variety of reactions (including aromatic hydroxylation, activation of sp^3 hybridized C atoms, epoxidation of C=C double bonds, N-oxidation, N-, O-, and S-dealkylation) on a variety of substrates (Urlacher and Girhard 2012). The suggested degradation of gemfibrozil in *Bacillus* sp. GeD10 is thus similar to the aerobic degradation of bisphenol, benzene, toluene, ethylbenzene, and *o*-, *m*-, and *p*-xylenes as described in other organisms in which the aromatic ring is prepared for cleavage by the introduction of one or more hydroxyl groups (Kim and Jeon 2009). Follow hydroxylation, the newly formed hydroxyl group is oxidized to an aldehyde, likely catalyzed by an alcohol dehydrogenase (N1LWF2). The micropollutant is then converted to catechol and subsequently cleaved by a catechol-2,3-dioxygenase similar to other aromatic compounds (Seo et al. 2009). The differential overexpression of the P450 hydroxylase in the presence of gemfibrozil, may be due to gemfibrozil not only being a substrate of the P450 cytochromes as previously described, but also as an inhibitor of them. The putative cytochrome P450 hydroxylase (N1LX98) and the cluster of uncharacterized genes (N1LXZ4 and N1LTC5) and their possible involvement in xenobiotic degradation warrants further investigation.

The upregulation (in four out of five replicates) of a glyoxalase which has the domain-based features of catechol dioxygenase suggests that gemfibrozil is processed until dearomatization. Though, the apparent accumulation of M1 and M2 indicates that one or both metabolites are side products of gemfibrozil degradation or dead-end metabolites, the identification of a downstream candidate enzyme catalyzing their further degradation suggests otherwise. Incomplete degradation of gemfibrozil leading to a subsequent accumulation of M1 and M2, may explain the observed presence of these metabolites. Also

the enzyme catalyzing the subsequent step after dearomatization was observed, producing cis-2-hydroxy-penta-2,4-dienoate as a potential end metabolite.

Besides M1 and M2, a glucuronidated hydroxy-metabolite of gemfibrozil (Gem-glu) was identified, although it was detected only in trace amounts. Glucuronidation is a wide spread conjugation reaction known from human metabolism of xenobiotic compounds typically catalyzed by glycosyltransferases (Ogilvie et al. 2006). Though several glycosyltransferases were identified in the proteome of *Bacillus* sp. GeD10, no previous study has documented glucuronidation as a microbial conjugation mechanism of micropollutants. Yet several studies have documented the opposite reaction, the ability of bacteria to degrade glucuronidated micropollutants using ß-glucuronidases (Helander et al. 2007).

Several glycosidases were in fact identified in the proteome of *Bacillus* sp. GeD10. The detection of trace amounts of glucuronidated gemfibrozil may be a consequence of the concentration of the gemfibrozil used in this study. Given the high concentration of gemfibrozil the kinetic equilibrium between glycoside and non-glycoside, may in fact be driven towards the glycoside. Overall the detection of the gemfibrozil hydroxy-metabolites and glucuronidated hydroxy-metabolites in *Bacillus* sp. GeD10 resembles metabolites what has previously been detected in human plasma (Nakagawa et al. 1991).

Gemfibrozil is a known inhibitor of the enoyl reductase and have been shown to inhibit the growth of *Legionella pneumophila* but not the growth of *Listeria monocytogenes* (Reich-Slotky et al. 2009). The activity of the enoyl reductase is intimately linked with fatty acid biosynthesis and membrane composition (Reich-Slotky et al. 2009) and an inhibition of the enoyl reductase would be expected to be associated with a differential change in expression of enzymes related to fatty acid synthesis. Quite drastically, the expression of all penicillin-binding proteins of *Bacillus* sp. GeD10 was differentially overexpressed in response to gemfibrozil. Penicillin-binding proteins are amongst other responsible for the final stages of peptidoglycan synthesis (Sauvage et al. 2008). The involvement of Penicillin binding protein 1A has previously been shown to increase resistance of streptococcus towards penicillin by inactivation through binding (Hamilton et al. 2006).

Besides the already reviewed proteins, several other proteins with functions related to xenobiotic degradation were identified and some of them also found to be overexpressed in response to gemfibrozil. Although these proteins are associated with xenobiotic degradation, they also all participate in normal growth, development, and reproduction. More likely than catalyzing xenobiotic degradation, these proteins are most likely related to primary metabolism. Three proteins related to multidrug resistance in

bacteria through drug disposition were also stimulated by the presence of gemfibrozil. Two of these proteins belonged to the RND efflux family containing domains of the secondary transporter AcrB, known from efflux of a variety of hydrophobic compounds, including acriflavine in *E.coli* (Du et al. 2014; Nakamura 1968). AcrB in *E.coli* is a part of a tripartite pump, with the remaining two components being AcrA, the periplasmic component of the pump, and TolC being the outer membrane channel. Unlike, the AcrAB-TolC efflux pump in *E.coli* which comprises an operon (Du et al. 2014; Nakamura 1968), only two proteins resembling AcrB could be identified in *Bacillus* sp. GeD10 and these were not closely associated in the genome. The exact function of AcrB in *Bacillus* sp. GeD10 remains unclear, and warrants further study. As does the function of the relatively large number of uncharacterized proteins found to be differentially overexpressed in *Bacillus* sp. GeD10 in response to gemfibrozil exposure.

The initial steps have been taken in understanding the degradation of gemfibrozil and similar xenobiotics, though not all observations made in this study are accounted for. Identification of genes involved in the degradation or other specific genes involved in uptake of gemfibrozil may allow for the development of highly sensitive molecular tools for monitoring bioaugmented bacteria, diversity, and ecophysiological studies of xenobiotic degrading microorganisms. Furthermore such tools can help explain the degradation of gemfibrozil and other similar compounds in natural as well as engineered systems.

The physiological response of gemfibrozil on the metabolism of *Bacillus* sp. GeD10 was studied. Using a combination of genomics, proteomics, and metabolite analysis, a partial pathway for the degradation of gemfibrozil by *Bacillus* sp. GeD10 was proposed, including enzymes involved and metabolites produced. Indications of other cellular responses, such as inhibition effects of gemfibrozil on the metabolism were also observed. The putative cytochrome P450 hydroxylase along with an alcohol dehydrogenase and a potential catechol-2,3-dioxygenase were identified as candidate enzymes participating in the transformation of gemfibrozil. These enzymes may function as future markers of gemfibrozil degradation.

11.7 Conclusion

The physiological response of gemfibrozil on the metabolism of *Bacillus* sp. GeD10 was studied. Using a combination of genomics, proteomics, and metabolomics, a partial pathway for the degradation of gemfibrozil by *Bacillus* sp. GeD10 was established, including enzymes involved and metabolites produced. Indications of other cellular responses, especially oxidative stress conditions were confirmed through the induction of oxidative stress-related proteins. The putative cytochrome P450 hydroxylase along with a catechol-2,3-dioxygenase were identified as participating in the transformation of gemfibrozil. These enzymes may function as future markers of gemfibrozil degradation.

11.8 Acknowledgements

This study was funded by the Danish Research Council for Strategic Research via the Research Centre "EcoDesign-MBR" (Grant No. 26-03-0250) and the National Science Foundation (NSF CBET-0829132). Support was provided to Nicolette Angela Zhou by the Valle Scholarship and Scandinavian Exchange and the King County Technology Transfer Fellowship Program at the University of Washington.

APPENDIX C: GROWTH OF *SPHINGOBIUM* SP. BID32 ON BISPHENOL A

12.1 Chapter summary

This chapter documents testing to determine if *Sphingobium* sp. BiD32 grows using bisphenol A (BPA) and therefore incorporates BPA into its biomass. During this experiment *Sphingobium* sp. BiD32 (described in Chapter 4) was inoculated into experimental flasks containing a high concentration of BPA (10 mg/L). A control flask with no BPA and a control flask with 10 mg/L BPA in nutrient-rich broth were inoculated with *Sphingobium* sp. BiD32. *Sphingobium* sp. BiD32 grew using BPA, and the control confirmed that it did not grow without BPA present. This suggests that at least some of the BPA degraded by *Sphingobium* sp. BiD32 is fully degraded, as it is incorporating into *Sphingobium* sp. BiD32 biomass.

12.2 Objective

The objective of this experiment was to test if *Sphingobium* sp. BiD32 can grow using bisphenol A (BPA) as a sole carbon and energy source. This will help to determine if BPA is fully degraded by *Sphingobium* sp. BiD32, and not being transformed into products more toxic than the parent compound. In Chapter 7, an intermediate was identified during BPA degradation by *Sphingobium* sp. BiD32 when using a high concentration of BPA (2 mg/L), but not when using a lower BPA concentration (0.5 mg/L). This could be due to a low intermediate concentration when starting with a lower BPA concentration, so it is not measurable. It could also be that BPA is degraded by a different pathway at different concentrations. Therefore, since it is not known if BPA is fully mineralized during degradation by *Sphingobium* sp. BiD32, this experiment tested if *Sphingobium* sp. BiD32 grows on BPA.

12.3 Materials and methods

12.3.1 Chemicals, reagents, and bacterial strain

BPA (≥99%) was obtained from Sigma Aldrich (St. Louis, MO, USA). A 20 mg/L BPA aqueous stock was prepared by adding BPA dissolved in acetonitrile (1000 mg/L), evaporating the acetonitrile at 105ºC, adding water, and autoclave sterilizing (121ºC, 20 min). Stocks were stored in amber glass bottles to minimize potential photodegradation (Yu et al. 2006; Lin and Reinhard 2005). Aqueous stocks were stored at room temperature. *Sphingobium* sp. BiD32 (GenBank accession number JX87937) was previously isolated from activated sludge (Zhou et al. 2013).

12.3.2 Experimental media

Mineral medium consisted of mineral solution (Tanner 1997) modified to decrease the ammonia (0.2 g/L) and with potassium phosphate (2 mM) and sodium bicarbonate (2 mM) added as pH buffer and sodium nitrate (5 mg/L) as a nitrogen source. Potassium phosphate and sodium nitrate stock solutions were autoclaved. Other mineral salts and sodium bicarbonate stock solutions were filter sterilized (0.22 µm surfactant-free cellulose acetate membrane; Nalgene, Rochester, NY, USA), as was the final mineral medium. Mineral medium stock was made at 5x concentration and stored at 4ºC.

R2A broth (autoclave sterilized) was made based on the composition of R2A agar (Reasoner and Geldreich 1979) and contained 0.5 g/L yeast extract, 0.5 g/L proteose peptone, 0.5 g/L casamino acid, 0.5 g/L sucrose, 0.5 g/L soluble starch, 0.3 g/L pyruvic acid, 0.3 g/L dipotassium phosphate, and 0.05 g/L magnesium sulfate.

R2A agar was purchased commercially (BD Difco R2A Agar; Franklin Lakes, NJ, USA) and prepared according to manufacturer instructions.

12.3.3 Experimental method

It was tested if *Sphingobium* sp. BiD32 grows using BPA by inoculating *Sphingobium* sp. BiD32 into experimental flasks containing BPA as the sole carbon and energy source. *Sphingobium* sp. BiD32 was initially grown by transferring a single colony from solid R2A media into R2B. After reaching an optical density of 0.978 at 600 nm (OD_{600}), 0.5 mL of *Sphingobium* sp. BiD32 was transferred into a second flask of R2B. After reaching an OD_{600} of 0.924, 15 µL was inoculated into experimental flasks containing mineral medium and 10 mg/L BPA for an estimated colony forming unit (CFU) concentration of $3x10^6$ CFU/mL and a VSS concentrations of 0.041 mg/L. Duplicate cultures of *Sphingobium* sp. BiD32 were grown (100 rpm, 28ºC). *Sphingobium* sp. BiD32 concentrations were monitored by spread plates (Standard Method 9215C (AWWA 1998)). Controls included *(1)* 15 µL *Sphingobium* sp. BiD32 inoculated into mineral medium with no BPA present to confirm that the cells were not dividing due to stress, *(2)* 15 µL *Sphingobium* sp. BiD32 inoculated into R2B with 10 mg/L BPA to confirm that the high concentration of BPA did not prevent growth of *Sphingobium* sp. BiD32, and *(3)* 500 µL *Sphingobium* sp. BiD32 inoculated into R2B with 10 mg/L BPA to confirm that *Sphingobium* sp. BiD32 was still viable and that if there was no growth, it was due to the small inoculation volume. OD_{600} was measured for control flasks with R2B.

12.4 Results and conclusions

Sphingobium sp. BiD32 grew using BPA as a sole carbon and energy source (Figure 12.1, open markers). Controls showed that *Sphingobium* sp. BiD32 cell counts did not increase in mineral media with no BPA present (Figure 12.1, closed triangles). Controls in R2B media showed that *Sphingobium* sp. BiD32 grew in the presence of 10 mg/L BPA and that the small inoculation volume was sufficient for growth, with an OD_{600} of 0.472 and 0.482 reached in 56.5 hours for control 2 and 3, respectively.

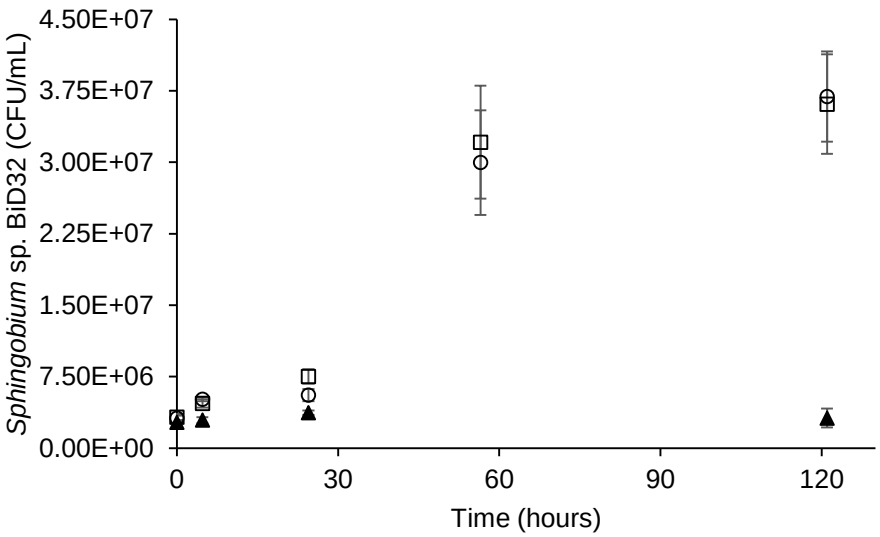

Figure 12.1. Growth of *Sphingobium* sp. BiD32 on 10 mg/L bisphenol A in mineral media (open markers). Error bars show the average deviation of the replicate spread plates. Closed triangles show *Sphingobium* sp. BiD32 in mineral media with no bisphenol A present.

Growth of *Sphingobium* sp. BiD32 on BPA demonstrates that BPA can be incorporated into the bacteria. This suggests that degradation of BPA by *Sphingobium* sp. BiD32 can result in mineralization and, therefore, a reduction in the endocrine disruption effect by BPA. Further work should focus on completing BPA degradation experiments with ^{14}C-labeled BPA to determine the fraction of BPA incorporated into *Sphingobium* sp. BiD32, mineralized, and transformed into intermediates.

VITA

Nicolette Angela Zhou (Corbin)

Born on December 28, 1989 in Seattle, WA (USA)

Citizen of the United States of America

2006-2008	Studies in Chemical Engineering, University of Alabama
2008-2009	Studies in Chemical Engineering, University of Maine
2009	Research experience in Environmental Engineering, University of California Los Angeles
2009-2010	Studies in Chemical Engineering, University of Alabama
2010-2012	Master's studies in Environmental Engineering, University of Washington
2012-2013	Visiting PhD student, Aalborg University
2013-2015	PhD studies in Environmental Engineering, University of Washington